

Risk Assessment of Mildly Flammable Refrigerants

2013 Progress Report

April 2014



The Japan Society of Refrigerating and
Air Conditioning Engineers

Copyright © 2014 by the authors and JSRAE

All rights reserved. This report or any portion thereof may not be reproduced or used in any manner whatsoever without the express written permission of JSRAE except for the use of brief quotations in a book review.

Although the authors and JSRAE have made every effort to ensure that the information in this report was correct at press time, the authors and JSRAE do not assume and hereby disclaim any liability to any party for any loss, damage, or disruption caused by errors or omissions, whether such errors or omissions result from negligence, accident, or any other cause.

The Japan Society of Refrigerating and Air Conditioning Engineers, JSRAE

Nihonbashi-Otomi Bldg. 5F

13-7 Nihon-bashi Odenma-cho

Chuo-ku, Tokyo, 103-0011 Japan

TEL +81-3-5623-3223, FAX +81-3-5623-3229

Foreword

While great successes have been achieved in climate change mitigation, global emissions of greenhouse gases continue to rise. Greenhouse gas emissions from fossil fuels are the main issue, but emissions of fluorocarbon refrigerants from refrigeration and air conditioning appliances should not be ignored because of the large global warming potential (GWP) of fluorocarbons.

The progressively more severe impact of fluorocarbon refrigerants makes the need for urgent action abundantly clear. The basic measure to reduce the impact of refrigerants is the replacement of conventional hydrofluorocarbons (HFCs) with low-GWP refrigerants. Low-GWP refrigerants are not very stable in atmosphere and thus are sometimes flammable. According to Japan's High Pressure Gas Safety Act, the use of flammable refrigerants in refrigeration and air conditioning equipment is restricted in practice. For the safe use of flammable refrigerants and relaxation of the regulation, a risk assessment needs to be performed; only a scientific risk assessment can provide a sound basis for judgment and change in regulation.

The Ministry of Economy, Trade and Industry (METI) and the New Energy and Industrial Technology Development Organization (NEDO) have been subsidizing research to obtain basic information on mildly flammable refrigerants since 2011. In addition, a research committee was set up by the Japan Society of Refrigerating and Air Conditioning Engineers to assess the risks associated with mildly flammable refrigerants. The Japan Refrigerating and Air Conditioning Industry Association and the Japan Automobile Manufacturers Association are presently conducting very definitive risk assessments, and the results are being discussed by the research committee.

This 2013 progress report provides state-of-the-art information concerning the risk of mildly flammable refrigerants. I am sure that its information will be of much interest for the risk assessment. I thank all the members and observers of the committee who helped produce this progress report. I hope that you will find it a useful and stimulating summary of the ever-sustainable story at the heart of human progress.

Chairperson of the Committee
Professor at the University of Tokyo
Eiji HIHARA
April 2014

Table of Contents

1	Introduction	<i>Eiji HIHARA</i>	1 ~ 5
2	Legal Issues with Mildly Flammable Refrigerant		
2.1	Explanation of High Pressure Gas Safety Law and Legal Issues with Mildly Flammable Refrigerant	<i>Jun ICHIOKA and Kenji TSUJI</i>	6 ~ 11
2.2	Situation for Overseas Laws, Standards, and Regulations: Current International Trends Regarding Refrigerant	<i>Satoru FUJIMOTO</i>	12 ~ 18
3	Progress at the University of Tokyo	<i>Eiji HIHARA, Chaobin DANG, Hiroaki OKAMOTO, Makoto ITO, and Tomohiro HIGASHI</i>	19 ~ 36
4	Progress at Kyushu University	<i>Shigeru KOYAMA, Yukihiro HIGASHI, Akio MIYARA, and Ryo AKASAKA</i>	37 ~ 47
5	Physical Hazard Evaluation of A2L Refrigerants Based on Several Conceivable Accident Scenarios	<i>Tomohiko IMAMURA and Osami SUGAWA</i>	48 ~ 57
6	Progress Report of Research Institute for Innovation in Sustainable Chemistry, AIST	<i>Kenji TAKIZAWA and Masanori TAMURA</i>	58 ~ 71
7	Physical Hazard Assessment on Explosion and Combustion of A2L Class Refrigerants	<i>Tei SABURI and Yuji WADA</i>	72 ~ 81
8	Efforts of the Japan Refrigeration and Air Conditioning Industry Association (JRAIA)		
8.1	Progress by Mini-Split Risk Assessment SWG	<i>Kenji TAKAICHI, Shigeharu TAIRA, and Takeshi WATANABE</i>	82 ~ 94
8.2	Progress of SWG for VRF System Risk Assessment	<i>Ryuzaburo YAJIMA</i>	95 ~ 106
8.3	Chiller SWG: Chiller Risk Assessment and Guideline Establishment	<i>Kenji UEDA</i>	107 ~ 119
9	Deregulation Activities in Japan for the Introduction of Mobile Air Conditioning Refrigerant R1234yf	<i>Japan Automobile Manufacturers Association, Inc. Vehicle Maintenance Subcommittee</i>	120 ~ 130
	Member List		131 ~ 132

1. Introduction

The use of chlorofluorocarbons (CFCs) and hydrochlorofluorocarbons (HCFCs) has been widely restricted, and to protect the ozone layer, they have been replaced with hydrofluorocarbons (HFCs). However, leakage of the refrigerant into the air from active or end-of-life air conditioners is a serious environmental issue owing to its high global warming potential (GWP). Therefore, it has been widely recognized that the replacement of HFCs with low-GWP refrigerants is important for solving this problem. The numbers of room, package, and mobile air conditioners shipped from Japan in 2013 were 90.1 million, 0.8 million, and 5 million, respectively. These are the main types of air-conditioning equipment produced in Japan. With mobile air conditioners, there is high potential for the conventional refrigerant to be replaced with R1234yf. However, studies have been conducted over the last several years on the use of lower-GWP refrigerants for stationary air conditioners. To prevent global warming, regulations have been imposed in Japan and overseas regarding the use of high-GWP refrigerants such as HFCs.

1.1 Trends in Refrigerant Regulation

The EU protocol 2006/40/EC for mobile air-conditioning refrigerants, effective from January 1, 2011, prohibits the release of new cars using refrigerants with a GWP over 150. Furthermore, starting from January 1, 2017, it prohibits the release of any new car using such refrigerants. In 2009, the automobile industry decided to replace the conventional refrigerant, R134a, with the low-GWP refrigerant, R1234yf. However, in April 2012, the EU Commission temporarily permitted the continued use of R134a owing to a supply shortage of R1234yf. The release of new model cars using refrigerants with a GWP over 150 has been prohibited since January 1, 2013.

The regulation regarding the use of stationary air conditioners is known as F-gas Regulation (EC) No. 842/2006. The present regulation focuses on reducing refrigerant leakage from air conditioners and requires proper management, instructional courses for operators, labeling of equipment containing F-gas, and reports by producers, importers, and exporters of F-gas. In November 2012, the EU Commission proposed to enhance the existing regulations. The new proposal aims to reduce the leakage of F-gas to two-thirds of the present level and prohibit the release of equipment using F-gas in fields where an environmentally friendly refrigerant has been developed. To achieve this, a phase-down schedule has been proposed that assumes that the annual amount of HFCs sold in the EU in 2015 has been reduced to one-fifth. In December 2013, the European Parliament and Council reached a trilogue agreement. The main points of the agreement are as follows:

- The “phase-down” schedule remains as initially proposed by the Commission;
- F-gases with GWPs above 2500 will be banned in stationary refrigeration systems from 2020, and those with GWPs above 750 will be banned in stationary air conditioners from 2025; and
- The issue of pricing or auctioning quotas is addressed through a review clause that empowers the Commission to assess a method for allocating quotas.

At the Conference of Parties, which aims to abolish practices that damage the ozone layer, three North American countries (US, Canada, and Mexico) submitted a proposal to revise the Montreal Protocol to restrict production and sales of HFCs. HFCs do not damage the ozone layer. The global warming issue was caused by the replacement of prohibited CFCs and HCFCs, which damage the ozone layer, with HFCs, which have high GWPs. The proposal suggests restricting the distribution of HFCs in the framework of the Montreal Protocol.

Table 1.1 and Fig. 1.1 compare the proposals and schedules of the three North American countries with those of the EU Commission.

Table 1.1 Summary of the proposed regulation of HFCs

	Proposal by three North American countries	EU Agreement
Proposal date	25th meeting of the High Contracting Parties, October 2013	December 2013
Evidential law	Montreal Protocol	Revised edition of Regulation (EC) No. 842/2006
Target refrigerants	19 types of HFCs (R1234yf and R1234ze not included)	HFCs (R1234yf and R1234ze not included)
Baselines of HFC phase-down	Average value between 2008 and 2010 Developed countries: HFCs and 85% of HCFCs Developing countries: 90% of HCFCs	Average value between 2009 and 2012
Final values of HFC phase-down	Developed countries: 15% of the 2033 baseline Developing countries: 15% of the 2043 baseline	21% of the 2030 baseline
Other restrictions		(1) Single split air-conditioning systems containing less than 3 kg of fluorinated greenhouse gases with a GWP of 750 or more shall be prohibited from 1 January 2025. (2) The use of fluorinated greenhouse gases with a GWP of 2500 or more to service or maintain refrigeration equipment with a charge size of 40 tons of CO2 equivalent or more shall be prohibited from 1 January 2020. (3) From 1 January 2017 refrigeration, air-conditioning, and heat pump equipment charged with HFCs shall not be permitted on the market unless the HFCs charged into this equipment are accounted for within the quota system.

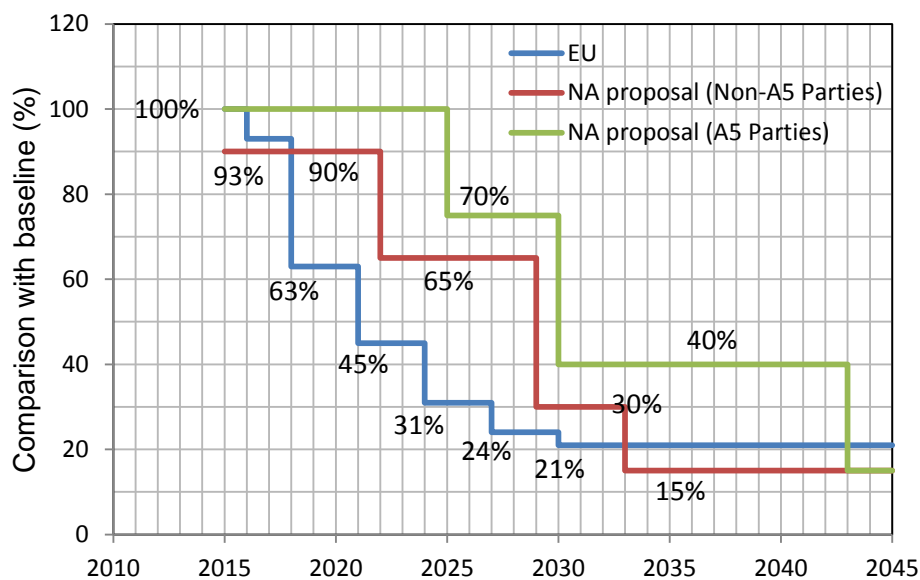


Fig. 1.1 Proposed HFC reduction stages

In Japan, the Global Environment Sub-Committee of the Central Environment Council and the Chemical and Biotechnology Sub-Committee of the Industrial Structure Council jointly created a task force and compiled an outline for the regulation of HFCs. The document released by the task force indicated that if no additional measures are taken, the emission of HFCs will double by 2020, and the emission from the air-conditioning sector will account for 80% of total emissions. It highlighted the importance of integrating appropriate measures in the air-conditioning sector. Approximately 60% of leakages in the air-conditioning sector occur during operation; the remainder is from uncollected refrigerant from end-of-life equipment. Approximately 40% of all leakage during operation is from separate-type display cases. Conventionally, it is thought that the most important alleviatory measure is the recovery of refrigerants from end-of-life refrigerators and air conditioners. However, this is inadequate.

Based on these discussions, the "Law on regulation of management and rational use of fluorocarbons" was established at the National Parliament on June 5, 2013. The name of the law was changed from the "Law for ensuring the implementation of the recovery and destruction of fluorocarbons concerning specific products." The new law requires following the replacement of high-GWP HFCs, refrigerant management and refrigerant recovery to reduce leakage of HFCs.

- (1) Fluorocarbon manufacturers, through technology development and manufacturing of lower-GWP refrigerants, should reduce the environmental impact.
- (2) Refrigeration and air-conditioning equipment manufacturers should achieve the goal of replacing high-GWP refrigerants with low-GWP refrigerants by the target year for each product sector.
- (3) For users of commercial refrigeration and air-conditioning equipment, proper management, installation, inspection, and repair is required.
- (4) For collection and destruction traders, a registration system of charging fluorocarbons for commercial refrigeration and air-conditioning equipment will be introduced, and a permit system for recovery of fluorocarbons will also be introduced.

1.2 Research trends on the Safety of Mildly Flammable Refrigerants

The development of environmentally friendly refrigerants for room and package air conditioners is imperative to the growth of air-conditioning technology. The low-GWP refrigerants R1234yf and R32 are promising candidates for replacing conventional HFC refrigerants. However, these refrigerants are not very stable in air and are flammable. Therefore, it is essential to collect basic data about the flammability of low-GWP refrigerants and research their safety for practical use. The integration of basic information about refrigerant physical properties, cycle performance, life cycle climate performance (LCCP), flammability, and risk assessment will simplify their selection for practical use. These efforts are expected to contribute to the advancement of the global air-conditioning industry.

R1234yf and R32 are less flammable than propane and R152, and are therefore classified as mildly flammable refrigerants. In ASHRAE Standard 34, the rank 2L was set for mildly flammable refrigerants with burning heats lower than 19 MJ/kg and burning velocities lower than 10 cm/s. Together with ammonia, R1234yf and R32 are classified as 2L. The characteristics of flammable refrigerants are presented in Table 1.2, where LFL, UFL, BV, and MIE denote lower flammability limit, upper flammability limit, burning velocity, and minimum ignition energy, respectively. Compared to propane, which is highly flammable, the other refrigerants have low BVs and high MIEs.

Table 1.2 Burning characteristics of flammable refrigerants

Refrigerant	GWP	LFL [vol%]	UFL [vol%]	BV [cm/s]	MIE [mJ]
R290 (Propane)	<3	1.8	9.5	38.7	0.246
R717 (Ammonia)	<1	15	28	7.2	21
R32	675	13.3	29.3	6.7	15
R1234yf	4	6.2	12.3	1.5	500

As illustrated in Fig. 1.2, the following conditions must be satisfied by an ignitable refrigerant that leaks from an appliance near an ignition source:

- (1) The refrigerant concentration must be within the required flammability range.
- (2) The energy of the ignition source must be higher than the MIE.
- (3) The air velocity adjacent to the ignition source must be lower than the BV.

If the air velocity adjacent to the ignition source is higher than the BV, burning will not occur because fire cannot propagate against the airflow.

Rank 2L on ASHRAE Standard 34 changed the restriction on refrigerants regarding their flammability and allows for the practical use of low-flammability refrigerants. However, in Japan, only the classifications “non-flammable” and “flammable” are recognized in the High Pressure Gas Safety Act and the Ordinance on the Security of Safety at Refrigeration. With the objective of gathering essential data for the risk assessment of mildly flammable refrigerants, safety studies are being conducted by project teams from the Tokyo University of Science at Suwa, Kyusyu University, University of Tokyo, and the National Institute of Advanced Industrial Science and Technology. Since 2011, they have been sponsored by the project “Development on Highly Efficient and Non-Freon Air Conditioning Systems” of the New Energy and Industrial Technology Development Organization (NEDO).

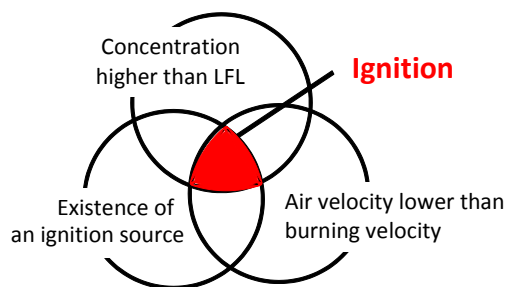


Fig. 1.2 Ignition mechanism

In addition, a research committee was created by the Japan Society of Refrigerating and Air Conditioning Engineers to assess the risks associated with mildly flammable refrigerants. The Japan Refrigerating and Air Conditioning Industry Association and the Japan Automobile Manufacturers Association are presently undertaking risk assessments and the results are being discussed by the research committee. The 2013 activities of the committee to assess the risks associated with mildly flammable refrigerants are compiled in this report. The committee members would be pleased if this report is helpful for people working in associated fields.

References

Directive 2006/40/EC of the European Parliament, 17 May, 2006.

Regulation (EC) No. 842/2006 of the European Parliament, 17 May, 2006.

Proposal for a Regulation of the European Parliament and the Council on Fluorinated Greenhouse Gases, 7 November, 2012.

Proposal for a Regulation of the European Parliament and of the Council on fluorinated greenhouse gases, 6 January 2014

Summary: North American 2013 HFC Submission to the Montreal Protocol, EPA, US, 2013.

Kenji TAKIZAWA et al., "Flammability properties of 2L refrigerants", The International Symposium on New Refrigerants and Environmental Technology, 2012.

2. Legal Issues with Mildly Flammable Refrigerant

2.1 Explanation of High Pressure Gas Safety Law and Legal Issues with

Mildly Flammable Refrigerant

2.1.1 Introduction

The present Refrigeration Safety Regulations recognize four classifications: inactive gases, active gases, toxic gases, and fluorocarbons other than inactive gases. The first three types of gases are defined by listing of those names and are demanded for an operation. An outline of the regulatory system is provided in Fig. 2.1.2.

Given the high probability that refrigerant gases with low global warming potential (GWP) will be needed in the future for a low-carbon society, after confirming the safety of a mildly flammable gas (A2L of ISO/FDIS 817), it seems that the correspondence which cooperated with foreign countries is also required. However, we are now having discussions with administrative authorities to clarify whether a mildly flammable gas can be used as an inactive gas (A1) to maintain the normal state of operation.

2.1.2 Outline of High Pressure Gas Safety Law

We have some laws and regulations about a pressure to keep safety or prevent any risks, and those are operated depending on usage. Because these laws are binding, incorrect operation is accompanied by government punishment. Although the regulatory restrictions are based on the laws, they are basically arbitrary. We should operate without confusing the laws and regulations.

Japanese regulations on pressure (i.e. for machine safety) contain the following typical laws: 1. the High Pressure Gas Safety Law, 2. Industrial Safety and Health Law, 3. Gas Business Law, and 4. Electricity Business Law. These laws are collectively called the four safety laws. The High Pressure Gas Safety Law widely regulates the manufacture, operation, maintenance of package air conditioners, chilling units, and turbo refrigerant (these are called refrigeration equipment), which are used to maintain a comfortable daily lifestyle and environment. An outline of the High Pressure Gas Safety Law is provided in the following.

(a) System of High Pressure Gas Safety Law High-pressure gas safety is mainly specified by laws, government ordinances, ministerial ordinances, and ministerial notifications. Based on the laws, the technical standards, application procedures, inspection procedures are minutely specified by ministerial ordinances. Government ordinances have specified exemptions to the laws, permissions for production and storage, values that require notification reports and high pressure gases that do not require notification reports on their sales. Ministerial ordinances are divided into several types depending on the type of business category and object of the regulation. In a ministerial ordinance regarding refrigerant equipment, the performance was specified by Refrigeration Safety Regulations in 2001.

Law	:High Pressure Gas Safety Law.
Government ordinance	:Order for Enforcement of High Pressure Gas Safety Law.
Ministerial ordinance	:1. Refrigeration Safety Regulations—regulations on production, sale, etc. of refrigerant equipment. 2. General High Pressure Gas Safety Regulations—regulations on production, sale, etc. of high-pressure gas equipment. 3. Container Safety Regulations—regulations on cylinders containing high-pressure gases.
Ministerial notification	:1. High Pressure Gas Safety Law enforcement ordinance related notification. 2. Location of production facility notification defining the details of technical standards regarding the structure, facility, and production method.

(b)Related Exemplified Standard and Operating Interpretation Internal regulations are defined for the interpretation, operation, and individual items related to the law, government ordinances, ministerial ordinances, and ministerial notifications. The related exemplified standard of the ministerial ordinances described above is included in this internal regulation. The standard regarding refrigerant equipment is called the related exemplified standard of the Refrigeration Safety Regulations. It exemplifies the technical factors of the performance-specified ministerial ordinance in as much detail as possible and provides a specification regulation. Examples are as follows.

(Examples)

1. Safe measures against fire.
2. Structure to prevent the accumulation of refrigerant gases.
3. Pressure test, airtight test.
4. Safety apparatus that can be returned to a level below the allowable pressure.
5. Gas leak detection equipment and its installation location.
6. Materials used for refrigerant equipment.
7. Design pressure.
8. Application of standard for refrigerant equipment container.
9. Welding standard.
10. Mechanical test of weld zone.
11. Non-destructive inspection of weld zone, etc.

(c)Operation Regarding Production and Sale In relation to the production and sale (including exports) of refrigerant equipment, operations are regulated based on the laws (government ordinances, ministerial ordinances, ministerial notifications, etc.). These require attention because an incorrect operation is accompanied by government punishment.

2.1.3 Daily Issue with Use of Mildly Flammable Refrigerant (example)

To use a room air conditioner, package air conditioner, or turbo refrigerating machine (hereafter called a refrigeration apparatus), the treatment of three fundamental elements, “operation,” “charging,” and “recovery,” must be considered in daily action, and these elements are difficult to understand. Moreover, regarding the law and its response (notification report, etc.) to each operation, all parties are involved, especially the builders, producers, and users.

(a)Operation and Applicable Law Although the law for a refrigeration apparatus has been adapted from the Refrigeration Safety Regulations, it treats only “the act where a gas for refrigeration is compressed or liquefied to produce a high pressure gas.” Other acts are regulated by other rule such as the General High Pressure Gas Safety Regulations.

(b)Charging or Recovery, and Applicable Law When the refrigerant gas of a refrigeration apparatus has leaked, charging is an act that produces a high pressure gas. The related law is based on the General High Pressure Gas Safety Regulations, and a notification report is required for every installation location. Charging with an inactive fluorocarbon or the act of recovery performed with a recovery subsystem is excluded^{*1}.

^{*1}The 2nd article 3rd clause No.6 of the High Pressure Gas Safety Law enforcement ordinance, and 2nd article of the High Pressure Gas Safety Law enforcement ordinance-related notification.

(c)Sale and Applicable Law The act of charging a refrigeration apparatus during an installation or repair service is not only an act of producing, but also one of selling (whether with or without compensation) the high-pressure gas. Therefore, it is necessary to follow the General High Pressure Gas Safety Regulations for commercial sales (or to include a type change notification for the high-pressure gas regarding sales). However, because an act that uses a small container (this is called a cylinder and the internal volume is less than 1 liter)^{*2} is excluded from the High Pressure Gas Safety Law, it is also exempted from the notification report on producing and selling the high-pressure gas. Moreover, when selling a class 1 refrigeration apparatus, a separate notification report on high-pressure gas dealer is also needed,

according to the Refrigeration Safety Regulations.

*2 The 2nd article 3rd clause No. 8 of the High Pressure Gas Safety Law enforcement ordinance, and 4th article of the High Pressure Gas Safety Law enforcement ordinance-related notification.

2.1.4 Legal Treatment of R1234yf, R1234ze(E), R32, etc.

(a) Treatment by Refrigeration Safety Regulations Although “flammable gases,” “toxic gases,” and “inactive gases” are defined by the second article of the Refrigeration Safety Regulations, and each refrigerant name is listed, the definition standard is not clear. Of course, there is no definition for “mildly flammable.” At present, R1234yf, R1234ze(E), and R32 are listed neither as the inactive gases nor as flammable gases. In this case, the easing of various regulations is not applied to R1234yf, R1234ze(E) and R32.

(b) Treatment by General High Pressure Gas Safety Regulations “Flammable gases,” “toxic gases,” and “inactive gases” are defined by the second article of the General High Pressure Gas Safety Regulations, and the names of these gases are listed for each category. In contrast to the Refrigeration Safety Regulations, fluorocarbons (except for flammable gases) are described under “inactive gases”, and gases (except for listed gases) with the following properties are described under “flammable gases.”

1. The lower limit for an explosion is less than 10%.
2. The difference between the higher limit and the lower limit for an explosion is more than 20%.

Figure 2.1.1 shows these types, along with where R1234yf, R1234ze(E), R32, and R717 would fall. The shaded and white parts indicate “flammable” and “non-flammable,” respectively.

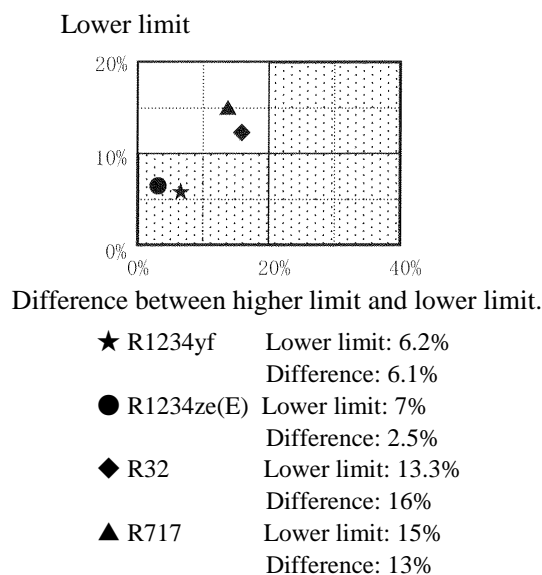


Fig. 2.1.1 Measurement results based on General High Pressure Gas Safety Regulations (JFMA, 2012)

(c) ASHRAE (American Society of Heating, Refrigerating and Air-Conditioning Engineers) Standard In ASHRAE, although R1234yf, R1234ze(E), R32, and R717 were defined as “2L” by “ASHRAE standards 34” in 2010, their treatment was not clearly defined.

(d) Recovery of R1234yf, R1234ze(E), and R32 Based on a related notification from the High Pressure Gas Safety Law enforcement ordinances, because the fluorocarbon (only an inactive gas) in the recovery equipment is being contracted out of law, R32 correspond to it. However, R1234yf and R1234ze(E) in recovery equipment are handled based on the General High Pressure Gas Safety Regulations.

2.1.5 Issues with High Pressure Gas Safety Law regarding mildly flammable refrigerant

(a)Revision of listing name principle Although “flammable gases,” “toxic gases,” and “inactive gases” are defined by the second article of the Refrigeration Safety Regulations and each refrigerant name is listed, the definition standard is not indicated. It is doubtful that R413A which is classified as “A2” (mildly flammable) in “ASHRAE standard 34” (ASHRAE 34:2013) is listed as an inactive gas. Because the treatment of a new refrigerant gas (particularly a mildly flammable gas) or a mixed gas cannot presently be determined from the viewpoint of global warming prevention, it is tackled each time while asking to Commercial Affairs Circulation Preservation Group High Pressure Gas Preservation Section, Ministry of Economy, Trade and Industry. The “flammable” number concepts of the Refrigeration Safety Regulations should be consistent with the General High Pressure Gas Safety Regulations.

(b)Recovery and Legislation of Refrigerant Gas That Is Not Treated As Inactive Gas Even when classified as flammable, gases should not be regulated uniformly. In particular, regarding a flammable gas close to an inactive gas (A2L of the mildly flammable gases), discussions are needed to ease the regulations. Moreover, it is necessary to inquire about the establishment of technical standards for the recovery subsystem.

(Draft proposal)

1. In principle, internal fittings are restricted to welded or brazed fittings. However, if welding or brazing is not appropriate, it can be replaced by the use of flange joints, which possess the strength required for safety (a threaded joint is inappropriate).
2. External connections are required for secure joinable coupling.

(c)Easing Requirements for Specified Equipment Even though the refrigerant that can be used by a specified piece of equipment is limited to only an inactive fluorocarbon by a High Pressure Gas Safety Law enforcement ordinances-related notification^{*3}, discussions are also expected in relation to the application range of fluorocarbons that are not flammable gases.

Present state) fluorocarbon (only an inactive gas)

Draft proposal) only a fluorocarbon that is not flammable gas

*3 Ministry of International Trade and Industry notification No. 139, 6th article, 2nd clause No. 2, March 24, 1997.

2.1.6 Issues with Mildly Flammable Refrigerants from Foreign Countries

From the safety administration perspective, it is desirable to clarify several issues from a professional standpoint.

1. If R32 is listed as an inactive gas, close attention must be given to foreign countries because they might interpret the listing differently.
2. We should clarify what is eased or changed by changing from A2 to A2L.
3. An explanation of the activities of many foreign countries is needed in the legislation.

Refrigerant	Classification	Outline of the regulatory system.
Fluorocarbon [Inactive gas]	Normal	
	Unit type Listed as inactive gasses in the second article of a frozen security rule	
	Specified equipment	
Ammonia Fluorocarbon [except inactive gas]	Normal	
	Unit type	
Other gasses [CO2, Helium, Propane]		

Fig. 2.1.2 Outline of regulation system in Refrigeration Safety Regulations (Akatsuka, 2010)

References

- Japan Fluorocarbon Manufacturers Association (JFMA), 2012, Table of environment and safety data of specific Freon (CFC/HCFC) and fluorocarbon, <http://www.jfma.org/database/table.html>.
- Akatsuka, H., 2010, Accidents and its lessons occurred in refrigeration and air conditioning equipments, *Journal of The High Pressure Gas Safety Institute of Japan.*, Vol. 47, 11: p.29-45.

2.2 Situation for Overseas Laws, Standards, and Regulations:

Current Global Refrigerant Trends

The following describes global regulatory trends for refrigerants. Please be advised that this information may be limited in its scope and is in no way a comprehensive account of all perspectives.

2.2.1 Trends in Japan

The Japanese government revised the current Law Concerning the Recovery and Destruction of Fluorocarbons and promulgated the new Act on June 12, 2013. Preparations, including governmental and ministerial ordinances, are underway toward full legal enforcement beginning on April 1, 2015. The first meeting was held on August 1, and a joint session of the Central Environment Council and the Industrial Structure Council deliberated upon governmental and ministerial ordinances. Currently, there is a plan to promulgate, around the spring of 2014, the “guidelines for the rational use of fluorocarbons” along with a “ministerial ordinance for the decision criteria of managers of refrigeration and air conditioning equipment” and similar ordinances. In addition, a cabinet decision concerning and subsequent promulgation of “directives relating to designated products, etc.” are expected in 2014 in the period from the summer to autumn. Ministerial ordinances and notifications are also scheduled for announcement during the same period. Here, the country sets GWP-based numerical values that take safety into account for the “designated products,” and numerical targets are imposed on product classifications for manufacturers and importers to achieve in a specified year.

A kick-off meeting of the Industrial Structure Council, Manufacturing Industry Committee, and Chemical Policy Subcommittee was held on November 30, 2013, and a “WG on measures to deal with Fluorocarbons” was established to deliberate on specific areas as described below. At these meetings, the efforts made until now and the current statuses were presented. The details are as follows.

- (1) Concerning the current status of efforts for independent action plans for the industry for fiscal year 2012, projections of CO₂ conversion values for the amounts of HFC emissions were released, and the amount of emissions for 2012 for the field of refrigeration and air conditioning equipment was 2.2 million tons. Moreover, in regard to the outlook for 2020, the emissions for HFCs used in refrigeration and air conditioning equipment are rapidly increasing and expected to reach twice the amount of current emissions.
- (2) In regard to efforts for improving refrigerant recovery, the refrigerant recovery ratio such as at the time of equipment disposal remained stagnant at about 30%.
- (3) According to a 2009 METI survey, large-scale leakage during equipment use was ascertained, and commercial-use freezing and refrigeration equipment, in particular, had an annual leakage of 13%–17%.
- (4) However, equipment developments for lower-GWP products or non-fluorocarbon products in Japan have advanced and are partially being implemented.
- (5) There is even a worldwide movement toward tightening the regulations for products with a high GWP, including the F-gas Regulation in Europe and the North American proposals presented to the Montreal Protocol conferences.

Furthermore, because these affect the direction of fluorocarbon countermeasures, the following four countermeasures are being proposed to span the entire fluorocarbon lifecycle from production to destruction, adding to existing laws for fluorocarbon recovery and destruction.

- (1) Promotion of a lower GWP for products using fluorocarbons or non-fluorocarbons (conversion by manufacturers of equipment and products)
 - Designation of special products that use fluorocarbons (air conditioners, freezers and refrigerators, blowers, etc.)
 - Decision criteria related to lower GWP concerned with designated products/promotion of non-fluorocarbons
- (2) Promotion of reuse of recovered refrigerant for actual phase-down of fluorocarbons (efforts by gas manufacturers)
 - Establishment of decision criteria related to the efforts (lower GWP, curbs on the manufacture and import, and recovery/reuse) of gas manufacturers to reduce the environmental impact from fluorocarbons
- (3) Prevention of fluorocarbon leaks when using commercial-use refrigeration and air conditioning equipment (refrigerant management by user)

- Establishment of decision criteria related to efforts for appropriate equipment management (periodic inspection) by user
 - Refrigerant leakage amount report by user
- (4) Charge by registered contractor and reuse by licensed contractor

2.2.2 Trends in Europe

The existing F-gas Regulation in Europe was established in 2005 and came into effect in 2007. A review for a revised proposal was scheduled in 2011. The EU Commission began an investigation for a revision in 2009, and although there was a slight delay, a revised proposal centering on an HFC phase-down came out on November 7, 2012. For this, the European Parliament Committee submitted an amendment on June 19, 2013. The details were extremely strict and included details that prohibited the use of HFCs in stationary-type freezers and refrigerators, along with air conditioners, in 2020. For this, the same EU Council came out with an HFC phase-down amendment that was close to the proposal of the EU Commission. From this, a tripartite meeting was held to reconcile the views of the European Commission, European Parliament Environment Committee, and EU Council, and an agreement was reached at the 4th meeting held on December 16, 2013.

Table 1. Details of Tripartite Agreement Regarding F-Gas Regulation

		Current Regulations	Results of Tripartite Consultations
HFC Prohibition	Stationary air conditioners	None	Single split air-conditioning systems containing less than 3 kg of F-gas with a GWP of 750 or greater are to be prohibited from January 1, 2025.
	Refrigerators and freezers for commercial use (hermetically sealed systems)	None	Refrigerators and freezers for commercial use that contain F-gas with a GWP of 2,500 or more are to be prohibited from January 1, 2020. Hermetic-type refrigerators and freezers for commercial use that contain or rely upon F-gas with a GWP of 150 or more are to be prohibited from January 1, 2022.
	Stationary refrigeration systems	None	Multipack centralized refrigeration systems for commercial use with a capacity of 40 kW that contain or rely upon F-gas with a GWP of 150 or more (except in the primary refrigerant circuit of cascade systems where an F-gas with a GWP of less than 1,500 may be used) will be prohibited from January 1, 2022.
	※Each member state Consideration for building code	※Exemptions for HFC prohibitions are added: • Where technically feasible alternatives are not available or cannot be used for technical or safety reasons, the Commission may authorize a time-limited exemption of up to 4 years following a request of an EU Member State. • The Commission shall collect information on the national codes, standards, or legislation of Member States with respect to using alternative refrigerants in refrigeration and air conditioning equipment and shall publish a synthesis report by January 1, 2017.	
Pre-charge prohibition	None	Prohibition begins from January 1, 2017. However, equipment pre-charged with HFCs that are accounted for within the quota system may be placed on the market. A verifiable declaration of conformity is necessary.	
Cutback in amount of HFCs placed on the market	None	Cutback to 21% in 2030. (The Council proposal for a CO ₂ equivalent with the average total quantity for the years 2009–2012 was adopted for the base amount.)	
Quota system for refrigerant supply	None	Quota amount for the new market entry amount is 11%.	

After approval by the Committee of the European Parliament, this revised proposal will be submitted to a vote of the plenary session of the European Parliament (scheduled for March 11). Once approved by the EU Council, it will be promulgated and is expected to take effect

from January 1, 2015.

2.2.3 Trends in United States

As for the trends in the United States, there are the North American proposals to the Montreal Protocol conferences, CACC trends, ASHRAE standards trends, trends for revision of the UL standards, and SNAP trends. However, the AHRI refrigerant evaluation program “Low-GWP Alternative Refrigerant Evaluation Program” is primarily mentioned here. The AHRI started AREP in the spring of 2011. Candidate alternative refrigerants are being solicited, and tests and results by standardized methods are announced. The alternative refrigerant candidates are not prioritized, and policy is entrusted to market evaluation. In this program, a total of twenty-one companies participated as evaluators, and five companies participated as refrigerant suppliers. Low-GWP refrigerant candidates were announced at the end of October 2012. Later, refrigerant performance was evaluated by compressor calorimeter tests, system drop-in tests, and soft-optimized system tests, and the project’s primary period ended at the end of 2013. Because many reports have already been produced, we introduce the participating companies. The following URL can confirm the details.

http://www.ahrinet.org/App_Content/ahri/files/RESEARCH/AREP_Final_Reports/

Table 2.2.3.1 Companies Participating in AREP Project

US Equipment Manufacturers	Equipment Manufacturers Outside the US
Carrier Corporation	ARMINES-MINES Paris Tech (France)
Emerson Climate Technologies	Embraco Brazil (Brazil)
Goodman Manufacturing	Embraco Slovakia Sro (Slovakia)
Johnson Control Inc.	GD Midea Air-Conditioning Equip (China)
Oak Ridge National Lab.	Daikin Industries, Ltd (Japan)
Lennox Industries Inc.	Shanghai Hitachi Electrical Appliances Co., Ltd. (China)
Tecumseh Company Co.	Refrigerant manufacturers
McQuay International	Arkema Inc.
Trane/Ingersoll Rand	E.I. du Pont de Nemours and Co.
Hussmann Corp.	Honeywell International, Inc
Climate Master	Mexichem Fluor, Inc
Manitowoc Ice	Daikin Industries, Ltd
Follett Co.	
Thermo King/Ingersoll Rand	
University of Maryland	

Table 2.2.3.2 Summary of AHRI's Low-GWP AREP Drop-in Test Reports (No. 1– No. 14)

No	Report Themes (Test Refrigerant)	Evaluating Company	Test Refrigerant	GWP Value
1	System Drop-in Test in a 5-RT Air-Cooled Water Chiller (R410A)	Trane (US)	Arkema ARM32a (R1234yf/R32/R125/R134a) (20:25:30:25)	1,577
			Arkema ARM70a (R1234yf/R32/R134a) (40:50:10)	482
			DuPont DR5 (R1234yf/R32) (27.5:72.5)	490
			Mexichem HPR1D (R1234ze/R32/R744) (60:6:34)	407
			Honeywell L41a (R1234yf/R1234ze/R32) (15:12:73)	494
			Honeywell L41b (R1234ze/R32) (27:73)	494
2	System Drop-in Test in Ice Machines (R404A)	Manitowoc Ice (US)	Honeywell L40 (R1234yf/R1234ze/R32/R152a) (20:30:40:10)	285
			Honeywell L41a (R1234yf/R1234ze/R32) (15:12:73)	494
			Honeywell N40b (R1234yf/R134a/R32/R125) (30:20:25:25)	1,311
3	System Drop-in Test in Air Source HP (R410A)	Oak Ridge Lab	National Refrigerant (R32/R152a) (95:5)	647
4	System Drop-in Test in Split System HP (R410A)	Lennox	R32	675
5	Soft-optimized System Test in 3-ton Split System HP (R410A)	Goodman	R32	675
6	System Drop-in Test in 5-RT Air-Cooled Water Chiller (Cooling Mode) (R22)	Trane (US)	Arkema ARM32a (R1234yf/R32/R125/R134a) (20:25:30:25)	1,577
			DuPont DR7 (R1234yf/R32) (64:36)	246
			Honeywell L20 (R1234ze/R32/R152a) (35:45:20)	331
			Mexichem LTR4X (R1234ze/R134a/R32/R125) (31:16:28:25)	1,265
			Mexichem LTR6A (R1234ze/R32/R744) (63:7:30)	206
			Daikin D52Y (R1234yf/R32/R125) (60:15:25)	959
7	System Drop-in Test in 230-RT Water-Cooled Water Chiller (R134a)	Trane (US)	Arkema ARM42a (R1234yf/R134a/R152a) (82:7:11)	117
			Honeywell N13a (R1234yf/R1234ze/R134a) (18:40:42)	604
			Honeywell N13b (R1234ze/R134a) (58:42)	604
			R1234zeE	6
			DuPont OpteonXP10 (R1234yf/R134a) (56:44)	631
8	System Drop-in Test in Commercial Bottle Cooler/Freezer (R134a)	Hussmann (US)	R1234yf	4
			Honeywell N13a (R1234yf/R1234ze/R134a) (18:40:42)	604
			R1234zeE	6
			DuPont OpteonXP10 (R1234yf/R134a) (56:44)	631
9	System Drop-in Test in Trailer Refrigeration Unit Designed for R404A	Ingersoll- Rand & Thermo King	Arkema ARM30a (R1234yf/R32) (71:29)	199
			DuPont DR7 (R1234yf/R32) (64:36)	246
			Honeywell L40 (R1234yf/R1234ze/R32/R152a) (20:30:40:10)	285
10	System Soft-Optimized Test in Split System HP (R410A)	Lennox	HFO1234yf	4
11	Compressor Calorimeter Test of R-410A Alternatives (R410A)	Oak Ridge National Laboratory	R32	675
			DuPont DR5 (R1234yf/R32) (27.5:72.5)	490
			Honeywell L41a (R1234yf/R1234ze/R32) (15:12:73)	494
12	System Drop-in Test in Bus Air-Conditioning Unit Designed for R134a	Ingersoll- Rand & Thermo King	Mexichem AC5 (R1234ze/R32/R152a) (83:12:5)	92
			Honeywell N13a (R1234yf/R1234ze/R134a) (18:40:42)	604
13	System Drop-in Test in Bus Air-Conditioning Unit Designed for R407C	King	Honeywell L20 (R1234ze/R32/R152a) (35:45:20)	331
			Daikin D52Y (R1234yf/R32/R125) (60:15:25)	959
14	System Drop-in Test in Air-Cooled Screw Chiller (R134a)	Johnson Controls	Arkema ARM42a (R1234yf/R134a/R152a) (82:7:11)	117

Table 2.2.3.3 Summary of AHRI's Low-GWP AREP Drop-in Test Reports (No. 15–No. 32)

No	Report Subject (Test Refrigerant)	Evaluating Company	Test Refrigerant	GWP Value
15	System Drop-in Test in VRF Multi-Split HP (R410A)	Daikin	R32	675
16	System Drop-in Test in Water-To-Water HP (R410A)	Climate-Master (US)	R32	675
			National Refrigerant (UK) (R32/R152a) (95:5)	647
			DuPont DR5 (R1234yf/R32) (27.5:72.5)	490
17	Compressor Calorimeter Test (R22)	EMBRACO	R1270	1.8
18	Compressor Calorimeter Test (R134a)	EMBRACO	Honeywell N13a (R1234yf/R1234ze/R134a) (18:40:42)	604
			Arkema ARM42a (R1234yf/R134a/R152a) (82:7:11)	117
19	Compressor Calorimeter Test (R134a)	EMBRACO	Honeywell N13a (R1234yf/R1234ze/R134a) (18:40:42)	604
20	System Drop-in Test in Air Source HP (R410A)	Univ. of Maryland: Goodman-manufactured	R32	675
			Daikin D2Y-60 (R1234yf/R32) (60:40)	272
			Honeywell L41a (R1234yf/R1234ze/R32) (15:12:73)	494
21	Compressor Calorimeter Test (R404A)	Oak Ridge National Laboratory	Arkema ARM31a (R1234yf/R32/R134a) (51:28:21)	492
			Daikin D2Y65 (R1234yf/R32) (65:35)	239
			Honeywell L40 R1234yf/R1234ze/R32/R152a) (20:30:40:10)	285
			R32/R134a (50:50)	1,053
22	System Drop-in Test in Split System HP (R410A)	Carrier	Arkema ARM70a (R1234yf/R32/R134a) (40:50:10)	482
			DuPont DR5 (R1234yf/R32) (27.5:72.5)	491
			Honeywell L41a (R1234yf/R1234ze/R32) (15:12:73)	494
			Honeywell L41b (R1234ze/R32) (27:73)	494
			R32	675
23	System Soft-Optimized Test in Air Source HP (R410A)	Univ. of Maryland	Honeywell L41a (R1234yf/R1234ze/R32) (15:12:73)	494
24	Compressor Calorimeter Test in R-410A Scroll Type	Emerson	DuPont DR5 (R1234yf/R32) (27.5:72.5)	490
25	System Drop-in Test in a 200 RT Air-Cooled Screw Chiller (R134a)	Daikin-McQuay	R1234ze (E)	6
			Daikin D4Y (R1234yf/R134a) (60:40)	574
26	Compressor Calorimeter Test in a R410A Rotary	Shanghai Hitachi	R32	675
27	System Drop-in Test in An Air to Water HP (R410A)	CEP Mines PARISTECH	Arkema ARM70a (R1234yf/R32/R134a) (40:50:10)	482
			DuPont DR5 (R1234yf/R32) (27.5:72.5)	490
28	Compressor Calorimeter Test in Reciprocating Compressors (R404A)	Embraco SI	Honeywell L40 R1234yf/R1234ze/R32/R152a) (20:30:40:10)	285
29	Compressor Calorimeter Test in Reciprocating Compressors (R404A)	Embraco SI	DuPont DR7 (R1234yf/R32) (64:36)	246
30	Compressor Calorimeter Test in Reciprocating Compressors (R134a)	Embraco SI	R1234yf	4
31	System Drop-in Test in Split A/C System (R410A)	Shanghai Hitachi	R32	675
32	System Soft-Optimized Test in Air Source	Univ. of Maryland	Daikin D2Y-60 (R1234yf/R32) (60:40)	272

	HP(R410A)		
※	Testing method reference list	Johnson Controls	<ul style="list-style-type: none"> · System evaluation method, reference list for evaluation results for each type of alternative refrigerant, etc. · Twenty-eight page report

2.2.4 International Trends

Concerning HFC regulations, there are numerous global trends, and only a few of them are presented here.

- (1) The G20 Summit was held in St. Petersburg, Russia, on September 5–6, 2013. HFC countermeasures were included in an item related to climate change in the summit statement.

[Extract from G20 Summit Statement]

“We also support complementary initiatives, through multilateral approaches that include using the expertise and the institutions of the Montreal Protocol to phase down the production and consumption of hydrofluorocarbons (HFCs), based on the examination of economically viable and technically feasible alternatives. We will continue to include HFCs within the scope of UNFCCC and its Kyoto Protocol for accounting and reporting of emissions.”

- (2) On June 8, 2013, the United States and China agreed at a summit meeting to cooperate toward reductions in the manufacture and use of HFCs. A global phase-down of HFCs could reduce carbon emissions by 90 Gt (CO₂ conversion) by 2050, which would be equivalent to around two full years’ worth of the world’s greenhouse gas emissions. The United States clearly stated HFC emission reductions even in an action plan for countermeasures to global warming announced on June 25. President Obama emphasized in a speech on the same day that the HFC measures by the United States and China are “a significant step in the reduction of greenhouse gases.” In the past four years, the United States had, together with Canada and Mexico, jointly proposed HFC reductions under the Montreal Protocol, but countries like China had strongly opposed them. If only for this reason, it is said to be extremely significant to have an agreement by which the two largest countries emitting greenhouse gases express the importance of HFC measures to the world.
- (3) The Twenty-Fifth Meeting of the Parties to the Montreal Protocol (MOP 25) was held in Bangkok on October 21–25, 2013. Continuing the efforts of the previous meeting, a proposal was submitted related to regulations for HFC production and reduction. In addition to the discussions that were held related to such issues as handling this proposal and HFC alternative refrigerant technologies, the activities included discussions of indispensable use applications such as for methyl bromide, which is an ozone-depleting substance (ODS), and investigations such as for ODS alternatives. Amendment proposals were also submitted at this time in continuation of the previous year’s proposals, including an amendment proposal by the three North American countries (US, Canada, and Mexico) that seeks to amend the Montreal Protocol in order to regulate HFC production and consumption. Although there continued to be great anxiety and resistance from some developing countries concerning this proposal, which adds to the substances subject to regulation by the Montreal Protocol that are not ozone-depleting substances, an official discussion group was opened related to HFC control through the Montreal Protocol because many participating countries supported debate at the next assembly. In this discussion group, the views of each country were considered in relation to the Kyoto Treaty, which regulates the issues concerning the technological aspects for HFC alternatives and funds, legal issues for cases that regulate HFCs in the Montreal Protocol, and HFC emissions. It was decided to open a discussion group related to HFC management.
- (4) In international standards, the revised proposal for ISO5149, for which debate has continued for more than 15 years, was passed after being voted on by each country. The safety standards for equipment are structured in four parts: 1) the amount of refrigerant charge, 2) device structure, 3) installation, and 4) certification of qualified personnel. In the 1993 edition of the current ISO5149, there are three classifications for refrigerants—non-flammable, flammable, and flammable and toxic—and no exceptions for the use of flammable refrigerants are recognized. Concerning this revision, work has advanced for the introduction of new safety classifications that include mildly flammable refrigerants. Each country voted in the middle of October 2013, and, excluding Part 4, it was rejected. However, this rejection was mainly because of the procedure and syntax, as well as a written error in a table. There was no rejection in relation to the handling of mildly flammable refrigerants (2L). For this reason, a revote was performed in November 2013, and it passed in January

2014. There was a total of 27 votes for approval, with 4 votes (Part 2, 3) and 5 votes (Part 1) for disapproval. There was opposition from the US, Australia, New Zealand, Italy, and Finland relating to Part 2 and Part 3. In ISO5149, the refrigerant charge amount is regulated corresponding to flammability. In addition, explosion proof electrical equipment is required for a flammable refrigerant when used in such places as mechanical rooms, but mildly flammable 2L refrigerants have been excluded from this requirement.

3. Progress at the University of Tokyo

3.1 Introduction

According to the Kyoto Protocol, emissions of greenhouse gases, including hydrofluorocarbons (HFCs), should be reduced. Therefore, refrigerants with low global warming potential (GWP), such as R32 and R1234yf, are expected to be the next generation of refrigerants. However, these low-GWP refrigerants are often flammable. Table 3.1.1 lists the physical and flammability properties of the typical refrigerants (Takizawa, 2012; JFMA, 2012). Here, LFL is the lower flammability limit, UFL is the upper flammability limit, BV is the burning velocity, and MIE is the minimum ignition energy.

To obtain information needed to assess the risks of using these refrigerants, we performed studies in the following areas.

1. Simulation of leakage of mildly flammable refrigerants
2. Testing of thermal decomposition products of lower-GWP refrigerants
3. Risk of diesel combustion during pump-down of the heat pump

Table 3.1.1 Physical and flammability properties of low-GWP refrigerants (Takizawa, 2012; JFMA, 2012)

Refrigerant	GWP ^{*1}	LFL ^{*2}	UFL ^{*3}	BV ^{*4}	MIE ^{*5}
R290 (propane)	< 3	2.1 vol. %	9.5 vol. %	38.7 cm/s	0.246 mJ
R717 (ammonia)	< 1	15.5 vol. %	27 vol. %	7.2 cm/s	380–680 mJ
R32	675	13.3 vol. %	29.3 vol. %	6.7 cm/s	15 mJ
R1234yf	4	6.2 vol. %	12.3 vol. %	1.5 cm/s	200 mJ
R1234ze(E)	4	7.0 vol. %	9.5 vol. %	—	—

*1 GWP: Global warming potential

*2 LFL: Lower flammable limit

*3 UFL: Upper flammable limit

*4 BV: Burning velocity

*5 MIE: Minimum ignition energy

3.2 Simulation of leakage of mildly flammable refrigerants

3.2.1 Introduction

When refrigerants leak into a space, they tend to accumulate at the floor of the space when they are heavier than air (Kataoka *et al.*, 1996). As shown in Fig. 3.2.1, when the refrigerant concentration is greater than the LFL, when there is an ignition source, and when the air velocity is lower than the burning velocity, the refrigerant may ignite. When leakage occurs from a room air conditioner (RAC), there is always a region where the refrigerant concentration is higher than the LFL because the refrigerant concentration is 100% near the outlet of the leakage port. Thus, appropriate safety standards must be prepared for using air-conditioning equipment containing flammable refrigerants, because of the risk of explosion.

It is important to understand refrigerant diffusion phenomena when preparing safety standards. It is also necessary to clarify the effects of parameters on the diffusion phenomena of refrigerants that are heavier than air. Numerical analysis is an effective tool for this purpose because it is very difficult to measure the diffusion of a refrigerant in a large space. In this study, diffusion phenomena were numerically analyzed when a refrigerant leaked into a large space from a room air conditioner (RAC), a variable refrigerant flow (VRF), and a chiller. Based on the calculation results, the refrigerant concentration distributions, the volumes and positions of the flammable regions, and their changes over time were determined.

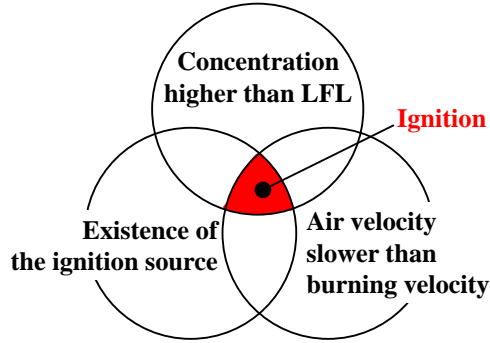


Fig. 3.2.1 Mechanism of ignition

3.2.2 Calculation Method

Table 3.2.1 lists the leakage scenarios considered in this study. The commercial computational fluid dynamics (CFD) program STAR-CD was used to simulate refrigerant diffusion phenomena. The problem of advection–diffusion of a mixture in a three-dimensional space is governed by the continuity, Navier–Stokes, energy conservation, and convective diffusion equations.

Both the air and the refrigerant were assumed to be ideal gases, and the density was calculated using the equation of state of an ideal gas. PISO or SIMPLE was used for the pressure–velocity coupling scheme, and UD and MARS were employed for the discretization scheme. Standard and realizable $k-\epsilon$ turbulence models were used in case Nos. 1–22 and Nos. 23–32, respectively. For the boundary conditions, constant flow at the inlet boundary was assumed, and a constant pressure corresponding to the atmospheric pressure or a free outflow condition at the outlet boundary was assumed. The law of the wall was assumed at the wall boundary.

Table 3.2.1 Leakage scenarios

case No.	Type	Refrigerant	Charged amount	Leakage velocity	Ventilation air flow	Air vent	case No.	Type	Refrigerant	Charged amount	Leakage velocity	Ventilation air flow	Air vent			
1	wall-mounted indoor unit of RAC	R32	1.0 kg	125 g/min	$0 \text{ m}^3/\text{h}$	exist	17	VRF	R32	26.3 kg	10→0 kg/h	$0 \text{ m}^3/\text{h}$	exist			
2				250 g/min	$0 \text{ m}^3/\text{h}$	exist	18				R1234yf	29.4 kg	10 kg/h	$0 \text{ m}^3/\text{h}$	none	
3				1000 g/min	$0 \text{ m}^3/\text{h}$	exist	19							$0 \text{ m}^3/\text{h}$	exist	
4		R1234yf	1.4 kg	175 g/min	$0 \text{ m}^3/\text{h}$	exist	20						$169 \text{ m}^3/\text{h}$	exist		
5				350 g/min	$0 \text{ m}^3/\text{h}$	exist	21						$0 \rightarrow 169 \text{ m}^3/\text{h}$	exist		
6				1400 g/min	$0 \text{ m}^3/\text{h}$	exist	22						$10 \rightarrow 0 \text{ kg/h}$	$0 \text{ m}^3/\text{h}$	exist	
7				R290	0.2 kg	50 g/min	$0 \text{ m}^3/\text{h}$		exist	23	water-cooled chiller	R32	23.4 kg	75 kg/h (burst leak)	$0 \text{ m}^3/\text{h}$	exist
8						125 g/min	$0 \text{ m}^3/\text{h}$		exist	24						
9	floor-mounted indoor unit of RAC	R32	1.0 kg	250 g/min	$0 \text{ m}^3/\text{h}$	exist	25					$545 \text{ m}^3/\text{h}$	exist			
10		R1234yf	1.4 kg	350 g/min	$0 \text{ m}^3/\text{h}$	exist	26		R1234yf	23.4 kg	70 kg/h (burst leak)	$0 \text{ m}^3/\text{h}$	exist			
11	outdoor unit of RAC	R32	1.0 kg	250 g/min	$0 \text{ m}^3/\text{h}$	(outdoor)	27				9 kg/h (rapid leak)	$0 \text{ m}^3/\text{h}$	exist			
12		R1234yf	1.4 kg	350 g/min	$0 \text{ m}^3/\text{h}$	(outdoor)	28					$545 \text{ m}^3/\text{h}$	exist			
13	VRF	R32	26.3 kg	10 kg/h	$0 \text{ m}^3/\text{h}$	none	29	R1234ze(E)	23.4 kg	54 kg/h (burst leak)	$0 \text{ m}^3/\text{h}$	exist				
14					$0 \text{ m}^3/\text{h}$	exist	30						$545 \text{ m}^3/\text{h}$	exist		
15					$169 \text{ m}^3/\text{h}$	exist	31						7 kg/h (rapid leak)	$0 \text{ m}^3/\text{h}$	exist	
16					$0 \rightarrow 169 \text{ m}^3/\text{h}$	exist	32							$545 \text{ m}^3/\text{h}$	exist	

3.2.3 Analytical Model

Fig. 3.2.2 shows the geometries analyzed. The details of these geometries are described below.

(a) Leakage from a Wall-mounted Indoor RAC Unit

Refrigerant was modeled as leaking from a wall-mounted indoor unit into a space $2.8 \text{ m} \times 2.5 \text{ m} \times 2.4 \text{ m}$ in size. The indoor unit was located 1.8 m above the floor at the center of one of the walls. The size of the indoor unit was $0.6 \text{ m} \times 0.24 \text{ m} \times 0.3 \text{ m}$, and the indoor unit had an air outlet with a size of $0.6 \text{ m} \times 0.06 \text{ m}$. The refrigerant leaked from this air outlet. Approximately 200,000 non-equidistant mesh points were used to discretize the governing equations. The refrigerants considered were R32, R1234yf, and R290 (propane).

(b) Leakage from a Floor-mounted Indoor RAC Unit

Refrigerant was modeled as leaking from a floor-mounted indoor unit into a space equal in size to that into which refrigerant was modeled as leaking from the wall-mounted indoor unit. The indoor unit was located on the floor at the center of one of the walls. The size of the indoor unit was $0.7 \text{ m} \times 0.21 \text{ m} \times 0.6 \text{ m}$, and the indoor unit had an air outlet with a size of $0.46 \text{ m} \times 0.045 \text{ m}$. The refrigerant leaked from this air outlet. Approximately 240,000 non-equidistant mesh points were used to discretize the governing equations. The refrigerants considered were R32 and R1234yf.

(c) Leakage from an Outdoor RAC Unit

Refrigerant was modeled as leaking from an outdoor unit placed on a balcony with a size of $5.0 \text{ m} \times 1.2 \text{ m} \times 1.1 \text{ m}$. The outdoor unit was located on the floor at the left side of the balcony. The size of the outdoor unit was $0.77 \text{ m} \times 0.29 \text{ m} \times 0.68 \text{ m}$, and the outdoor unit had a fan that was 0.4 m in diameter. The refrigerant leaked from the fan. In addition, wind with a velocity of 0.5 m/s was assumed to be blowing around the balcony. Approximately 350,000 non-equidistant mesh points were used to discretize the governing equations. The refrigerants considered were R32 and R1234yf.

(d) Leakage from a Variable Refrigerant Flow

Refrigerant was modeled as leaking from a VRF placed in an office with a size of $6.5 \text{ m} \times 6.5 \text{ m} \times 2.7 \text{ m}$. The indoor unit of the VRF was located on the ceiling at the center of the office. This indoor unit had an air outlet that was $0.45 \text{ m} \times 0.0645 \text{ m}$ in size and a suction that was 0.37 m in diameter. The refrigerant leaked from the air outlet and suction. The office also had an air supply $0.2 \text{ m} \times 0.2 \text{ m}$ in size and exhaust grills, and the gap under the door was $1.5 \text{ m} \times 0.01 \text{ m}$. Approximately 200,000 non-equidistant mesh points were used to discretize the governing equations. The refrigerants considered were R32 and R1234yf.

(e) Leakage from a Water-cooled Chiller

Refrigerant was modeled as leaking from a water-cooled chiller placed in a machine room with a size of $1.28 \text{ m} \times 1.28 \text{ m} \times 1.28 \text{ m}$. The chiller, located 1.01 m from the wall, was assumed to have a nozzle-shaped leakage port 100 mm in length, located 150 mm from the floor. The inner diameter of the nozzle depended on the type of leakage: $\varphi = 4.0 \text{ mm}$ for a rapid leakage and $\varphi = 8.0 \text{ mm}$ for a burst leakage.

The air inlet and exhaust duct inlet were located on the ceiling above the chiller and at the bottom of the machine room, respectively. The areas of the air inlet and exhaust duct inlet were calculated as described below.

The velocity and openness at the air inlet and exhaust port were as follows:

- (at the air inlet) velocity: $v_{in} = 2.0 \text{ m/s}$, aperture ratio: $\alpha_{in} = 0.7$
- (at the air exhaust duct) velocity: $v_{out} = 4.0 \text{ m/s}$, aperture ratio: $\alpha_{out} = 0.3$

The air ventilation volume per hour q was calculated from the following equation.

- Air ventilation volume: $q = XV \text{ [m}^3/\text{h]}$

where X and V are the number of air vents and the volume of the machine room (m^3), respectively.

The areas of the air inlet and exhaust duct inlet, A_{in} and A_{out} , respectively, were obtained from the following equation.

$$q = \alpha_{in} v_{in} A_{in} = \alpha_{out} v_{out} A_{out}$$

The refrigerants considered were R32, R1234yf, and R1234ze(E).

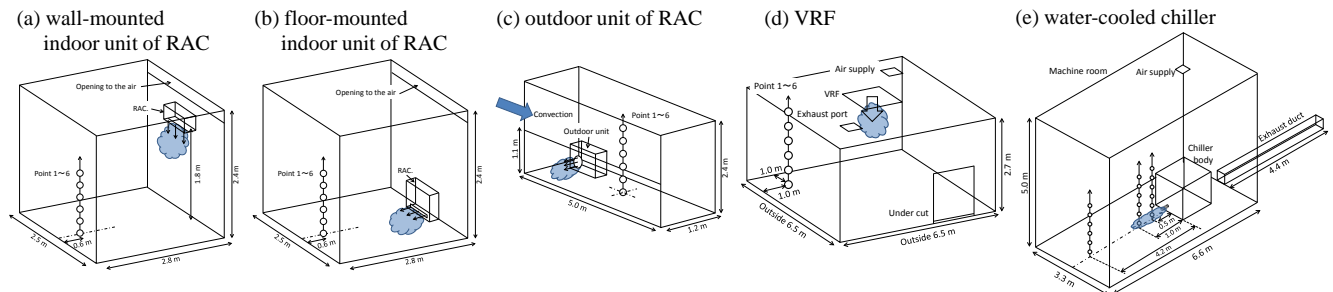


Fig. 3.2.2 Analytical geometries

3.2.4 Results and Discussion

Table 3.2.3 presents the calculation results. The term $\Sigma(V \cdot t)$ represents the product of the flammable gas volume and the presence time. This value is associated with the risk of combustion and is called the flammable volume time (FVT) below. The term V_{FL} represents the flammable gas volume, and the term V_{BVFL} represents the flammable gas volume with an air velocity lower than the burning velocity.

(a) Leakage from the Wall-mounted Indoor RAC Unit

The calculation results shown in Table 3.2.3 for case Nos. 1–8 represent the leakage from the wall-mounted indoor RAC unit. As these results show, the FVT is very small, even if a mildly flammable refrigerant leaks from the wall-mounted indoor unit. In addition, as the results for case Nos. 1–6 show, the FVT values determined with consideration of the burning velocity are equal to zero. These results suggest that ignition does not occur because of the convection caused by the refrigerant leakage, even if an ignition source exists. Therefore, no combustion occurs if no ignition source exists inside the indoor unit. For case No. 7, although the calculated value is higher than the maximum allowable fill ratio of propane, the refrigerant leakage represents a great hazard because the FVT value is very high compared to those for other cases. For case No. 8, the MIE of propane is lower than R32 and R1234yf, and the quenching distance of propane is very narrow. Therefore, leakage of propane is a hazard because a flame transmits easily.

(b) Leakage from the Floor-mounted Indoor RAC Unit

The calculation results shown in Table 3.2.3 for case Nos. 9 and 10 represent the leakage from the floor-mounted indoor RAC unit. According to Table 3.2.3, both the terms $\Sigma(V_{FL} \cdot t)$ and $\Sigma(V_{BVFL} \cdot t)$ are very similar. These results suggest that the air velocity is lower than the burning velocity in the combustion region. Therefore, if an ignition source exists in the combustion region, there is a risk of combustion throughout much of the combustion region. In addition, because the LFL of R1234yf is lower than that of R32, the presence time of R1234yf is longer than that of R32. Thus, the risk of combustion with R1234yf is higher than that with R32.

Therefore, safety regulations are required when flammable refrigerants are used in air conditioners because the risk of leakage from a floor-mounted indoor unit is higher than with a wall-mounted indoor unit.

(c) Leakage from the Outdoor RAC Unit

The calculation results shown in Table 3.2.3 for case Nos. 11 and 12 represent the leakage from the outdoor RAC unit. Table 3.2.3 shows that the flammable gas volume existed for a long time, for the same reason as that explained for the floor-mounted indoor unit. Therefore, the balcony with drains and undercuts are preferred for safety because an outdoor unit has a fan near the floor level, which may lead to spreading of the flammable region into entire balcony area.

(d) Leakage from the Variable Refrigerant Flow

The calculation results shown in Table 3.2.3 for case Nos. 13–22 represent the leakage from the VRF. According to Table 3.2.3, the existence of an air vent as an air supply source affects the FVT and presence time. In addition, the released period of the VRF is more than 150 min because of the large amount of refrigerant leaked. Therefore, although the flammable gas volume is small, the FVT ($\Sigma(V_{FL} \cdot t)$) is longer than that for leakage from a wall-mounted RAC unit. On the other hand, the FVT decreases significantly when the air velocity is considered. For R1234yf, the risk of ignition is very low because the burning velocity is low. For R32, safety regulations pertaining to, for example, a refrigerant leakage sensor, alarm, and ventilation are required when flammable refrigerants are used in air conditioners.

(e) Leakage from the Water-cooled Chiller

The calculation results shown in Table 3.2.3 for case Nos. 23–32 represent the leakage from the water-cooled chiller. Fig. 3.2.3 shows the LFL isosurface for the case in which V_{FL} reaches its maximum value, and Fig. 3.2.4 shows how $\Sigma(V_{FL} \cdot t)$ and V_{FL} change with time. In the cases of Nos. 26, 27, and 29, calculation stopped at 100 seconds after the refrigerant had leaked out completely, although there was a flammable region at that time. Therefore, the actual existence time and the FVT must be larger than the values listed in Table 3.2.3. In addition, although humidity was

not considered in this study, in the case of leakage of R1234ze(E), it is important to take humidity into account because this refrigerant is non-flammable when the humidity is zero.

These results indicate that the ventilation air flow has a large effect on the FVT, as do the VRF results. For example, comparing case Nos. 24 and 25 or case Nos. 27 and 28, the effects of five numbers of ventilation times in the case of rapid leakage of R32 and R1234yf, respectively, are evident. According to the results, in the case of rapid leakage of both R32 and R1234yf, $\Sigma(V_{FL} \cdot t)$ is very small and $\Sigma(V_{BVFL} \cdot t)$ equals zero, because the ventilation air makes the refrigerant flow through the exhaust duct to the outlet. This result might be attributed to the large number of ventilation times. On the other hand, for the non-ventilation case, the FVT of R1234yf is larger than that of R32, because the LFL of R1234yf is lower than that of R32 and the presence time of R1234yf is longer than that of R32, as described before.

Furthermore, the leakage velocity was assumed to be much higher than that in case of leakage from an RAC or VRF, which leads to a zero or very small $\Sigma(V_{BVFL} \cdot t)$, even if $\Sigma(V_{FL} \cdot t)$ increases. However, if there is no ventilation air flow and there is a high-concentration region after the refrigerant leaks out completely, as in case Nos. 26, 27, and 29, $\Sigma(V_{BVFL} \cdot t)$ might increase.

The results for the leakage from the water-cooled chiller indicate that sufficient ventilation air flow is needed to keep the room safe when flammable refrigerants are used in chillers. A leakage sensor is also required.

3.2.5 Results of the Simulation of Leakage of Mildly Flammable Refrigerants

The simulation and experiments conducted in this study to examine leakage of refrigerants into a space yielded the following findings.

1. In the case of leakage from a wall-mounted indoor unit, combustion does not occur if an ignition source does not exist inside the indoor unit.
2. In the case of leakage from a floor-mounted indoor unit, safety regulations are required when flammable refrigerants are used in air conditioners.
3. In the case of leakage from a floor-mounted indoor unit or outdoor unit, the risk of combustion is higher with R1234yf than with R32.
4. In the case of leakage from an outdoor unit, the balcony with drains and undercuts are preferred for safety because an outdoor unit has a fan near the floor level, which may lead to spreading of the flammable region into entire balcony area.
5. In the case of leakage from a VRF, when the burning velocity is considered, the FVT is much smaller.
6. In the case of leakage from a water-cooled chiller, the ventilation air flow has a large effect on the FVT. When there is no ventilation air flow and the velocity of the refrigerant leakage is high, the FVT might increase after the refrigerant leaks out completely.

Table 3.2.3 Predicted $\Sigma(V_{FL} \cdot t)$ and $\Sigma(V_{BVFL} \cdot t)$

case No.	Presence time, min	$\Sigma(V_{FL} \cdot t)$, m ³ min	$\Sigma(V_{BVFL} \cdot t)$, m ³ min	case No.	Presence time, min	$\Sigma(V_{FL} \cdot t)$, m ³ min	$\Sigma(V_{BVFL} \cdot t)$, m ³ min
1	4.01	1.18×10^{-2}	0	17	8.36	3.14×10^{-2}	0
2	4.01	1.23×10^{-2}	0	18	176.47	2.152	0
3	8.01	9.79×10^{-3}	0	19	176.42	0.661	0
4	8.01	1.07×10^{-2}	0	20	176.41	0.583	0
5	1.03	3.73×10^{-2}	0	21	176.41	0.592	0
6	1.05	4.34×10^{-2}	0	22	10.25	2.14×10^{-2}	0
7	1473.00	7689	7688	23	18.72	0.013	0
8	4.73	0.258	0.161	24	140.40	0.599	0.000022
9	111.00	136.83	136.81	25	140.40	0.002	0
10	309.00	507.82	507.50	26 ^{*1}	up to 22.62	up to 127.84	up to 3.449
11	45.00	43.01	42.50	27 ^{*1}	up to 157.67	up to 1108.44	up to 44.15
12	93.00	62.54	61.53	28	156.00	0.008	0
13	157.85	1.622	0.021	29 ^{*1}	up to 27.67	up to 361.62	0 ^{*2}
14	157.82	0.831	0.011	30	26.00	0.014	0 ^{*2}
15	157.82	0.702	0.014	31	200.58	16.352	0 ^{*2}
16	157.82	0.725	0.011	32	200.58	0.009	0 ^{*2}

*1 the condition that calculation stopped at 100 second after refrigerant completely leaked out

*2 R1234ze(E) is non-flammable on the condition whose relative humidity equals zero

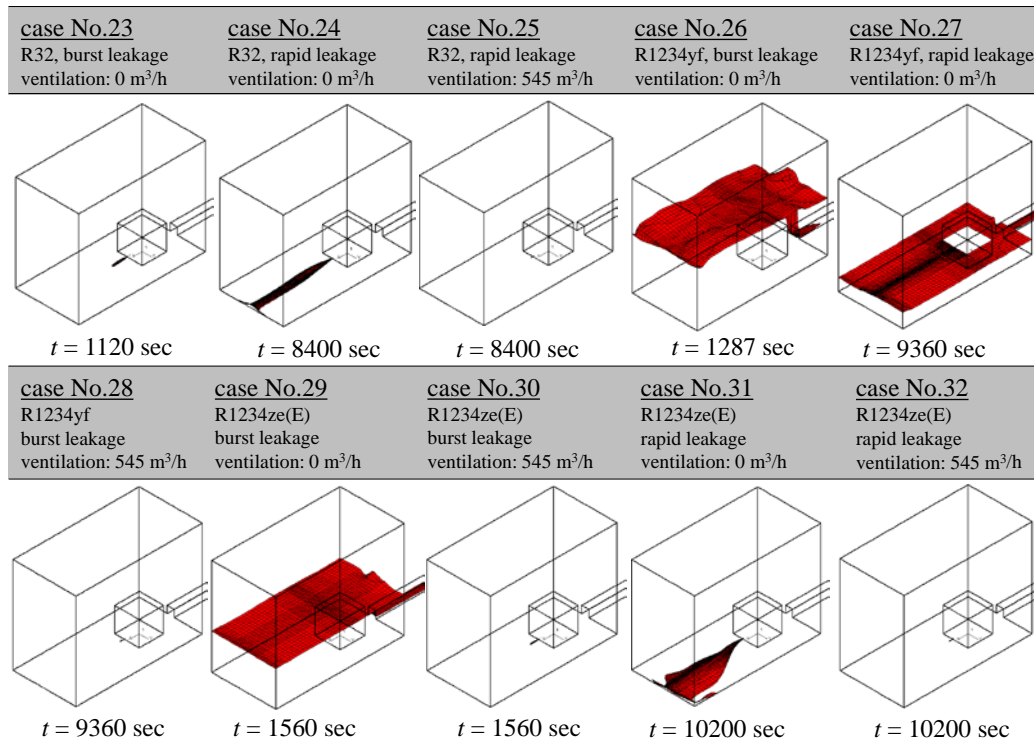


Fig. 3.2.3 LFL isosurface when V_{FL} reaches its maximum value

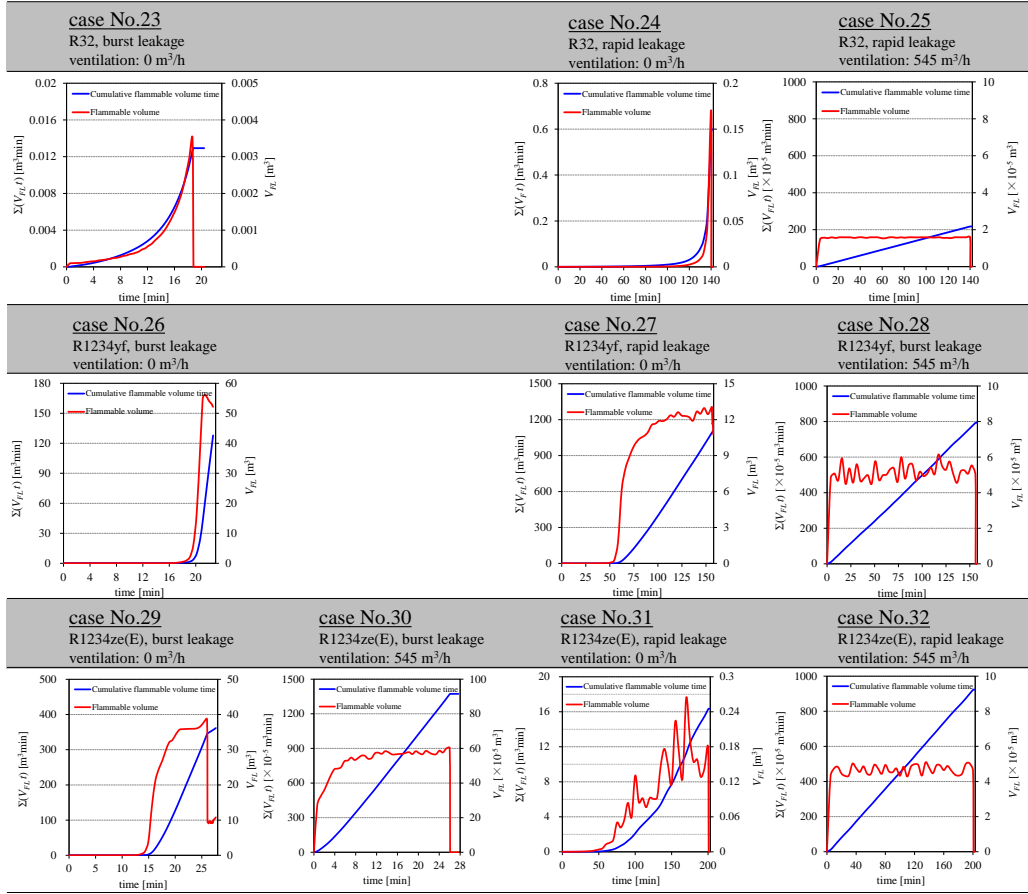


Fig. 3.2.4 $\Sigma(V_{FL} \cdot t)$ and V_{FL} changes with time

3.3 Thermal decomposition products of lower-GWP refrigerants

3.3.1 Introduction

To analyze the risks of using lower-GWP refrigerants, it is necessary to clarify their decomposability and products. However, the high reactivities of products such as hydrogen fluoride (HF) make this quantification difficult. Moreover, Takizawa et al. (2011) has suggested that the reactivity of a molecule with more fluorine atoms than hydrogen atoms, such as R1234yf, is affected by humidity. Thus, its flammability limits and product composition depend on the relative humidity of the surrounding air.

The experiment described in this section was carried out to quantify HF, the main toxic product, and to analyze other products in the thermal decomposition of refrigerants.

3.3.2 Experimental Apparatus and Methods

(a) Experimental Apparatus

There are two causes of HF generation from refrigerants: thermal decomposition by heating and combustion. In this research, only thermal decomposition was studied. A schematic diagram of the experimental apparatus fabricated to study thermal decomposition by heating is shown in Fig. 3.1.1. This experimental apparatus consisted of four parts: gas mixing, heating, measuring, and detoxification parts.

The gas mixing part was used to mix refrigerant and air at a specified concentration and humidity. The concentration was controlled by mass flow controllers, and the humidity was controlled by a dehumidifier and humidifier. The heating part was used to heat a gas sample and make it react in a straight Inconel 600 pipe (inner diameter 10.7 mm)

or mullite ($3\text{AlO}_3 \cdot 2\text{SiO}_2$) pipe (inner diameter 11 mm), and included a 550-mm-long electric furnace around the pipe. Three thermocouples were set on the outside wall, and for the mullite tube, three additional thermocouples were set on the inside wall of the pipe. To prevent these thermocouples from corroding, the inside ones were mounted in a mullite protection tube with an outer diameter of 6 mm. The gas sample flowed in the gap, 2.5 mm wide, with a cross-sectional area of 0.67 cm^2 , between the two tubes. The measuring part consisted of gas cells for Fourier transform infrared spectroscopy (FT-IR). To broaden the concentration measurement range, two cells with different path lengths were used. The detoxification part consisted of an absorbance tube that exhausted into a fume hood

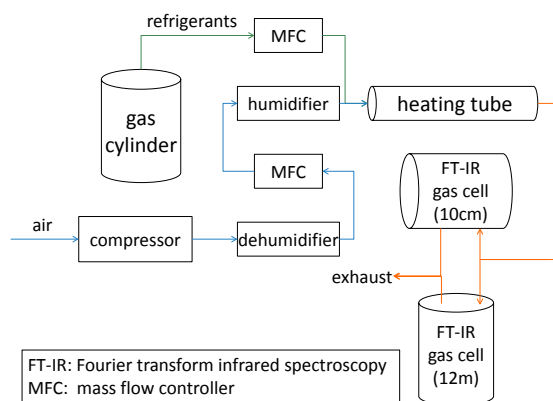


Fig. 3.3.1 Schematic diagram of the experimental apparatus

(b) Materials Tested

The materials tested were mixtures of refrigerants (R32, R1234yf, and R134a) and air.

(c) Measuring Instruments

An FT/IR-4200 (by JASCO), gas cell (temperature-controlled, 10-cm path length, by Harrick), and CaF_2 windows were used to measure the concentrations of the refrigerants and products.

To avoid instrument corrosion caused by the HF, FT-IR was conducted using a detector that was not exposed to the sample gas.

(d) Quantifying Method

Each molecule was quantified by absorption in particular wavenumbers. For refrigerants, criteria were established from measurements taken while the electric furnace was off and was at room temperature. For HF and COF_2 , data from Northwest-Infrared (PNNL, 2012) were used as criteria.

(e) Experimental Conditions

The following parameters were used as the experimental conditions.

- 1) Temperature of the heater: up to 700°C
- 2) Concentration of the refrigerant: four points under its LFL
- 3) Total flow rate: 100–200 ml/min
- 4) Humidity: up to 60% RH

3.3.3 Results and Discussion

(a) Results for the Inconel Tube

The concentrations of refrigerant, HF, and COF_2 after heating versus the heater temperature are shown below for each refrigerant. The variable parameter is absolute humidity [g/m^3], and the fixed parameters are the refrigerant concentration (2.5 vol. %) and the total flow rate (200 ml/min.).

• **R32**

The concentrations of R32 and HF in the case of R32 testing are shown in Figs. 3.3.2 and 3.3.3. A decrease in the R32 concentration and an increase in the HF concentration began when the heater temperature was in the range of 570–590°C. The amount of COF₂ generated was less than 0.01 vol. %. In addition, the decrease in the R32 concentration was not affected by the humidity.

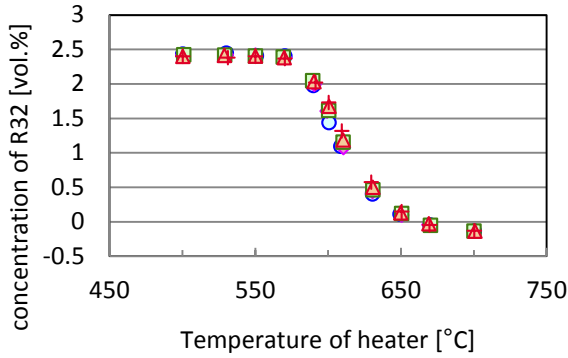


Fig. 3.3.2 Concentration of R32 versus heater temperature (total 200 ml/min, 2.5 vol.% with air)

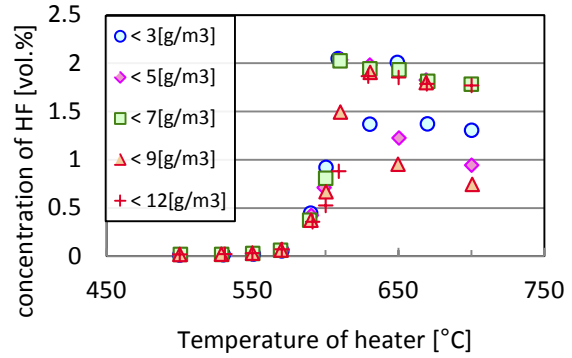


Fig. 3.3.3 Concentration of HF versus heater temperature (total 200 ml/min, 2.5 vol.% with air)

• **R1234yf**

The concentrations of R1234yf, HF, and COF₂ in the case of R1234yf testing are shown in Figs. 3.3.4, 3.3.5, and 3.3.6. In this experiment, the results gradually changed when the experiment was repeated using the same tube. Before the change, the decrease in the R1234yf concentration and the increase in the HF concentration began when the heater temperature was in the range of 500–550°C, and generation of COF₂ began at 600°C. In addition, the decrease in the R1234yf concentration was not affected by the humidity. After the change, the decrease in the R1234yf concentration started at a lower temperature, and at a given temperature, the concentration of R1234yf was lower and the concentration of one of the products was higher than before the change. Moreover, the decrease in the R1234yf concentration was affected by the humidity.

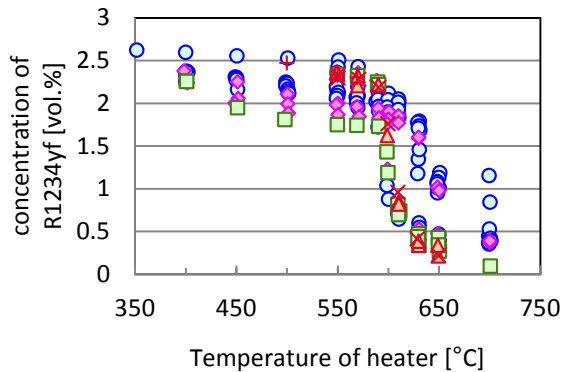


Fig. 3.3.4 Concentration of R1234yf versus heater temperature (total 200 ml/min, 2.5 vol.% with air)

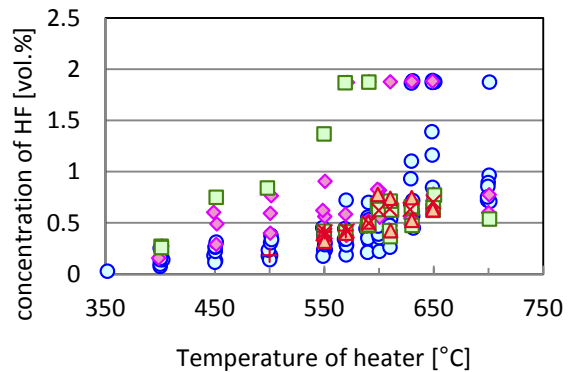


Fig. 3.3.5 Concentration of HF versus heater temperature (total 200 ml/min, 2.5 vol.% with air)

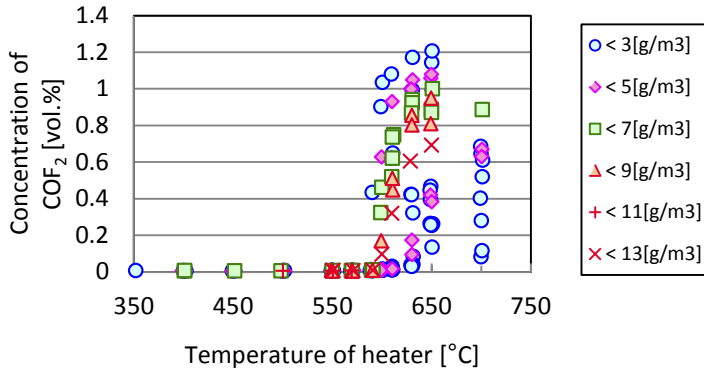


Fig. 3.3.6 Concentration of COF₂ versus heater temperature (total 200 ml/min, 2.5 vol.% with air)

• **R134a**

The concentrations of R134a, HF, and COF₂ in the case of R134a testing are shown in Figs. 3.3.7, 3.3.8, and 3.3.9. The decrease in the R134a concentration and the increase in the HF concentration began when the heater temperature was in the range of 500–550°C, and generation of COF₂ began when the temperature exceeded 650°C. The decrease in the R134a concentration was not affected by the humidity.

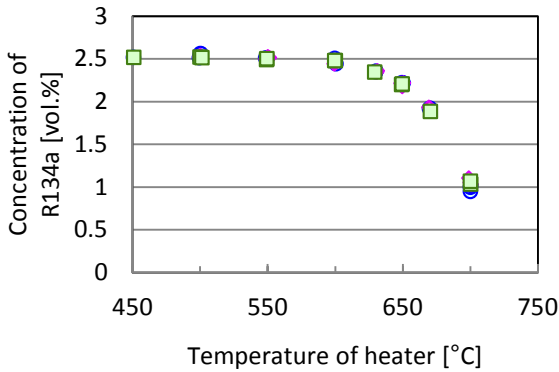


Fig. 3.3.7 Concentration of R134a versus heater temperature (total 200 ml/min, 2.5 vol.% with air)

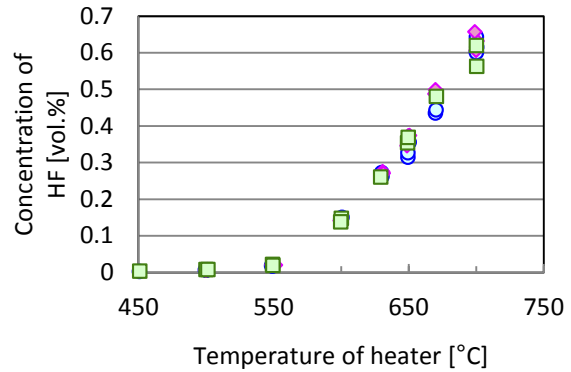


Fig. 3.3.8 Concentration of HF versus heater temperature (total 200 ml/min, 2.5 vol.% with air)

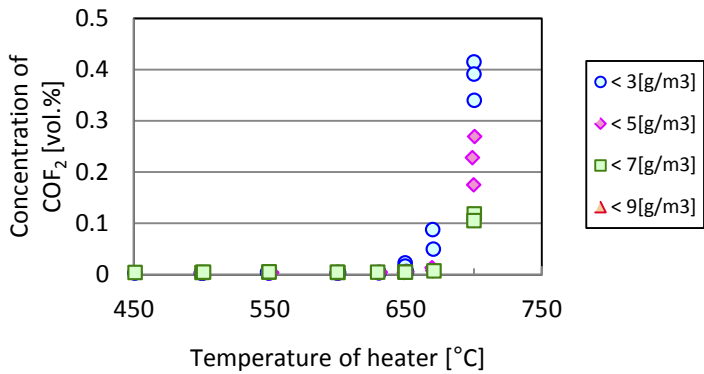


Fig. 3.3.9 Concentration of COF₂ versus heater temperature (total 200 ml/min, 2.5 vol.% with air)

(b) Discussion for the Inconel Tube

Even though an Inconel tube was used to avoid reducing the repeatability of the tests, changes occurred during the R1234yf testing. In addition, soot dust was found in the tube. Removal of such soot dust is expected to improve the repeatability of the tests.

(c) Results for the Mullite Tube

The remain rates of the refrigerants are plotted against the heater temperature without humidification in Figs. 3.3.10 and 3.3.11. The variable parameter is the refrigerant concentration (vol. %), and the flow rate shown is the total for the refrigerant and air. For both refrigerants, there was little decomposition when the heater temperature was 500°C or lower, but when the heater temperature was 550°C or higher, the remain rate decreased. The remain rates of R1234yf are plotted against the humidity before heating in Figs. 3.3.12 and 3.3.13. Takizawa et al. has suggested that the reactivity of R1234yf is affected by humidity, but these results do not show the reactivity of the refrigerant being affected by the humidity during testing. The amount of HF generated in the experiment illustrated in Fig. 3.3.10 is shown in Fig. 3.3.14. As the temperature and/or concentration increased, the generation of HF also increased. However, although it was expected that the HF concentration would be proportional to the R32 concentration, the effect of the concentration was much smaller, and the amount of HF generated was $1/10-1/30$ of the value estimated from the decomposition of R32.

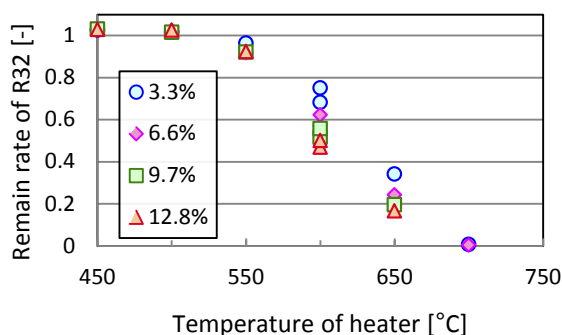


Fig. 3.3.10 Remain rate of R32 versus heater temperature (dry, total 100 ml/min with air)

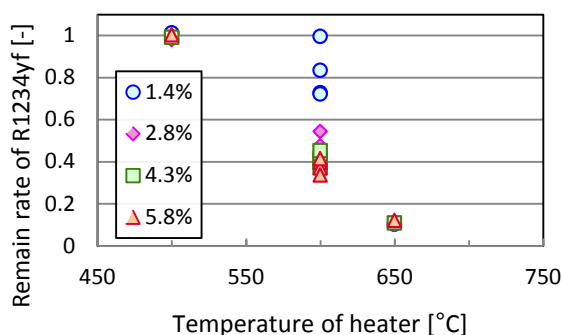


Fig. 3.3.11 Remain rate of R1234yf versus heater temperature (dry, total 100 ml/min with air)

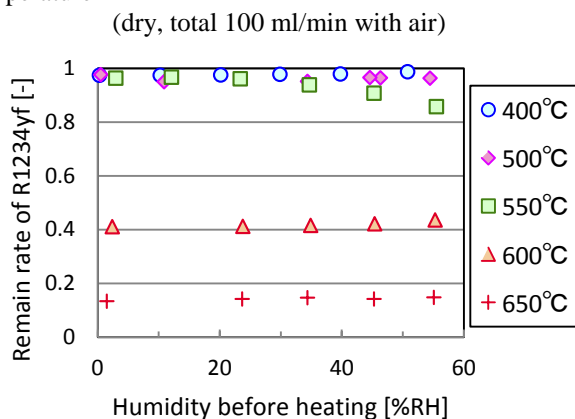


Fig. 3.3.12 Remain rate of R1234yf versus humidity (total 100 ml/min, 2.8 vol. % in air)

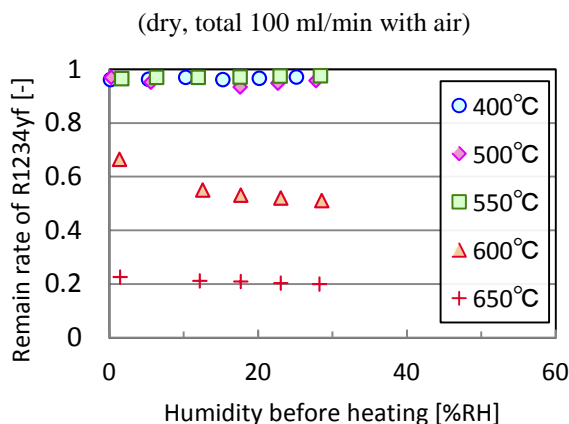


Fig. 3.3.13 Remain rate of R1234yf versus humidity (total 200 ml/min, 2.8 vol. % in air)

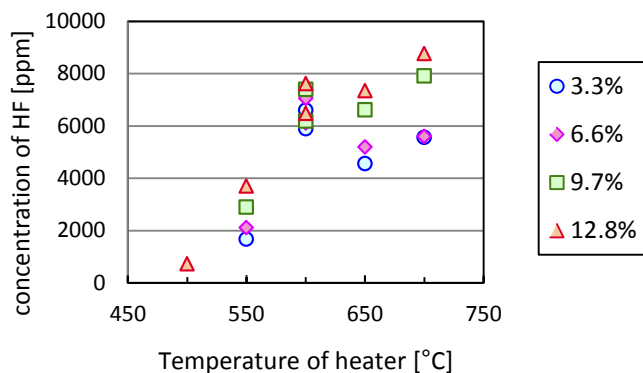
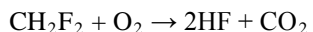


Fig. 3.3.14 Hydrogen fluoride versus heater temperature (R32, dry, total 100 ml/min with air)

(d) Discussion for the Mullite Tube

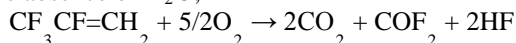
In the experiment conducted with R1234yf, the amount of HF generated was too small to detect. It is believed that this does not mean that no HF was generated but rather that the R1234yf or its decomposition products trapped the HF on the wall of the heating pipe. However, the mechanism for this trapping is not clear. The chemical reactions that occur in the thermal decomposition of the refrigerants considered are shown.

For R32:

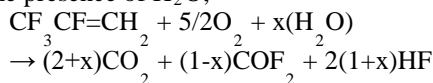


For R1234yf:

In the absence of H_2O ,



In the presence of H_2O ,



However, in the experiments conducted in this research, not only was the amount of HF generated lower than the estimated value, but the COF_2 peak at approximately $1,930\text{ cm}^{-1}$ was also not detected when the R1234yf concentration was sufficiently high to consume the humidity (H_2O) in the air. The reason for the absence of R1234yf was assumed to be a reaction between the wall and HF that can be expressed as $\text{AlO}_3 + 3\text{HF} \rightarrow \text{AlF}_3 + 3/2\text{H}_2\text{O} + 3/4\text{O}_2$. This reaction produced H_2O , which reacted with the COF_2 . It is not clear why no HF was detected in the experiment conducted with R1234yf. However, after this experiment, when only air flowed and the heater were set at 600°C , HF was detected after one or two hours. This suggests that the trapping of HF on the wall was facilitated more by R1234yf than by R32.

3.3.4 Conclusions Concerning Thermal Decomposition Products of Lower-GWP Refrigerants

For two lower-GWP refrigerants and a conventional refrigerant, the lower-limit temperatures of thermal decomposition and the amounts of decomposition products were measured in a way that was relatively unaffected by the wall material. In future experiments, we plan to reduce the effect of soot in the pipe used, employ common wall materials such as stainless steel, and examine reaction rates and mechanisms.

3.4. Risk of Diesel combustion during pump-down of the heat pump

3.4.1 Introduction

During the pumping down of refrigerants (refrigerant collection) in heat pump equipment, the lubricant oil and the refrigerant may reach the self-ignition combustion point as the temperature rises due to adiabatic compression of the gaseous mixture of a flammable refrigerant, lubricant oil, and air. This phenomenon has caused incidents of accidental destruction of outdoor air conditioning units (TRK, Tokyo Metropolitan Government, 2012). Because of the mild flammability of R1234yf and R32, which are considered low-GWP refrigerants, it is necessary to estimate their safety in comparison to R410A, which is a nonflammable refrigerant (JFMA, 2012). This section describes an examination of the differences in the combustion conditions for each refrigerant conducted using an experimental apparatus to reproduce diesel explosions. It must be kept in mind that the results shown here do not indicate that the refrigerants tested pose high combustion risks. It is the nature of the apparatus used and the conditions of the experiments that made it easy to induce diesel explosions.

3.4.2 Experimental Device and Method

Fig. 3.4.1 below shows a schematic diagram of the equipment used in the experiment. The equipment's main components are an air supply system, a refrigerant supply system, a temperature control system, a lubricant oil supply system, and a compressor (model engine) driven by a motor.

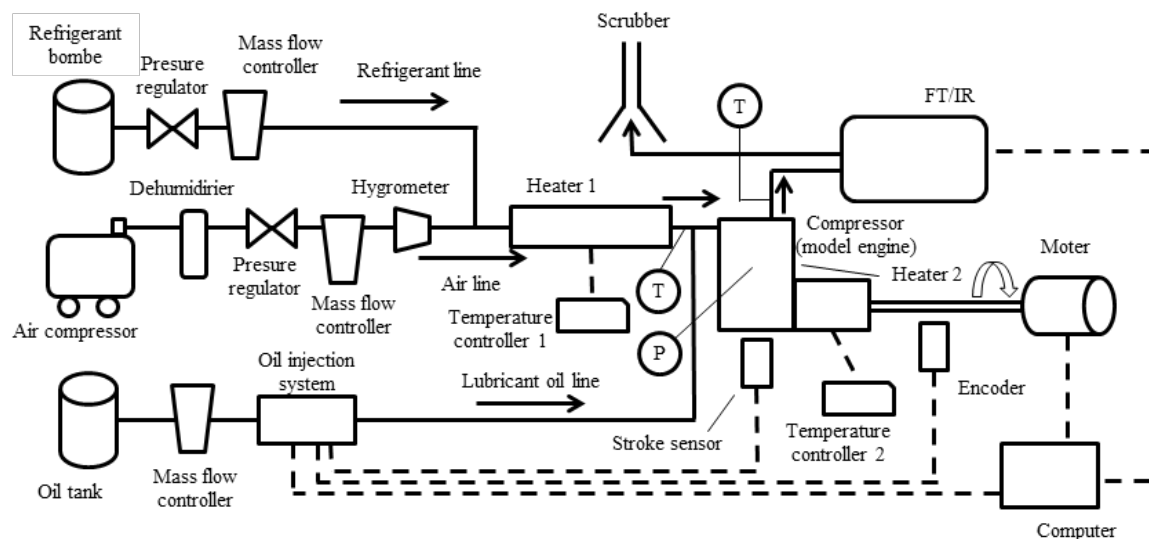


Fig. 3.4.1 Experimental apparatus

(a) Air Supply System

The air is compressed to 0.7 MPa by a compressor (oil-free air compressor 39L/ACP-160SL, made by EARTH MAN), passes through a dehumidifier (air dryer GK3103D-AC100V, made by CKD), and is reduced to a pressure of 0.3 MPa by a pressure regulator (AR20-02BE, made by SMC). The flow rate is controlled by the mass flow controller (MODEL8550MC-0-1-1, made by Kofloc).

(b) Refrigerant Supply System

The vapor refrigerant from the refrigerant bomb is reduced to a pressure of 0.3 MPa by a pressure regulator (SRSERIES, made by Yamato Sangyo). The flow rate is controlled by the mass flow controller (FCST1500FC-8J3-F400L-N2, made by Fujikin). The refrigerant mixes with the air.

(c) Temperature Control System

The temperature of the gaseous mixture of the air and the refrigerant is measured by a sheathed thermocouple and is controlled by heater 1 and the temperature controller (FHP-201, made by Tokyo Garasu Kiki, TC-1000, made by As one). Heater 2 controls the temperature of the model engine to equalize the temperature of the engine intake gas and that of the engine surface. These heaters are used to establish experimental conditions that make it easy to induce an explosion.

(d) Lubricant Oil Supply System

The lubricant oil exits the oil tank and passes through the flow meter (micro-flow meter MODEL213-311/295, made by TOYO CONTROL). The oil is then raised to a pressure of 150–180 MPa by the oil injection system (a common rail electric control fuel injection system, made by FC DESIGN) and is injected in the form of a spray. The timing of the injection is determined using an encoder and a stroke sensor fitted to the engine.

(e) Compressor

The model engine (R155-4C, made by ENYA, 4 cycle, 25.42-cc stroke volume, 16.0 compression ratio) is used as a compressor and is driven by a motor (MELSERVO-J3, made by Mitsubishi Electric) that is directly connected to its stroke shaft. A computer controls the number of revolutions per minute.

(f) Measuring System

The temperatures of the intake and exhaust gas of the engine are measured using sheathed thermocouples. The pressure in the engine is measured using a pressure gauge (6045A, made by KISTLER). The engine crank angle is measured using an encoder. These measurements, along with the flow rate of the oil and an injecting signal, are recorded by a computer using a data logger (data logger system NR-2000, made by KEYENCE). The exhaust gas is analyzed using an FT/IR (Fourier transform infrared spectrometer FT/IR-4700, made by Jasco).

(g) Experimental Method

Table 3.4.1 lists the refrigerants and the lubricant oil used in the experiment. In addition to R410A (the main existing refrigerant), R1234yf and R32 (new refrigerants), as well as R134a (a pure nonflammable refrigerant) and nitrogen gas (inert gas), were used for comparison. The flow rate of the oil was determined from the theoretical air/fuel ratio, which is calculated from the air flow ratio determined by the number of revolutions per minute and the stroke volume of the engine. The calculated theoretical air/fuel ratio was 9.5, according to the results of a CHO analysis of the oil conducted by SVC Tokyo. The experimental parameters were the number of revolutions per minute, the refrigerant, and the concentration of the refrigerant.

Table 3.4.1 Refrigerant and lubricant oil

Item	Test substance
Refrigerant	R1234yf, R32, R410A, R134a, N ₂
Lubricant oil	PAG (VG46)

We investigated the self-ignition combustion of a gaseous mixture of air and lubricant oil in experiment 1. Table 3.4.2 lists the conditions of the experiment. The flow rate of the oil was set to the theoretical air/fuel ratio. We measured the differences in the pressure in the engine caused by the injection of the air–oil mixture.

Table 3.4.2 Conditions of experiment 1

Air-oil mixing gas	
Number of revolutions, rpm	500-1500
Air flow rate, l/min	6.3-18.8
Inlet gas temperature, °C	250
Oil flow rate, l/min	$(0.765-2.295) \times 10^{-4}$

In experiment 2, we measured the self-ignition combustion of gaseous mixtures of air, refrigerant, and lubricant oil, for a range of refrigerant concentrations. Table 3.4.3 lists the conditions of the experiment. The flow rate of the oil was fixed for any given concentration of the refrigerant.

Air-refrigerant-oil mixing gas	
Number of revolutions, rpm	500-1500
Refrigerant concentration, vol%	0-100
Mixture flow rate, l/min	6.3-18.8
Inlet gas temperature, °C	260
Oil flow rate, l/min	$(0.765-2.295)\times 10^{-4}$

We measured the exhaust gas of the gaseous mixture of the air, refrigerant, and lubricant oil at self-ignition combustion by FT/IR. Table 3.4.4 lists the conditions of the experiment. Northwest-Infrared data were used for identification of the products (PNNL, 2012). We used a spectrum of $4,039\text{ cm}^{-1}$ for quantitative analysis of the HF to avoid noise caused by H_2O and CO_2 .

Air-refrigerant-oil mixing gas	
Number of revolutions, rpm	1500
Refrigerant concentration, vol%	20, 30(R32)
Mixture flow rate, l/min	18.8
Inlet gas temperature, °C	260
Oil flow rate, l/min	2.295×10^{-4}

3.4.3 Results

In experiment 1, we examined the change in the pressure in the engine due to the presence of the lubricant oil. In experiment 2, we reproduced the state of air mixing at pump-down by changing the concentration of the refrigerant and measured the pressure in the engine. We examined the effect of the refrigerant on the pressure rise in the engine by analyzing the exhaust gas.

(a) Results of Experiment 1

Fig. 3.4.2 shows the representative pressure changes in the engine when the gaseous mixture of air and lubricant oil was compressed. The number of revolutions per minute was 1,500 rpm, and the temperature of the intake gas was 25°C . The horizontal axis shows the crank angle, which reached the top dead center at 360° . The engine moved smoothly without the injection of the oil, which indicates that combustion did not occur. The pressure rose drastically with the injection of the oil. The exhaust gas changed to white and a loud noise and strong vibration were observed. It is possible that the lubricant oil self-ignited because of the temperature increased induced by adiabatic compression.

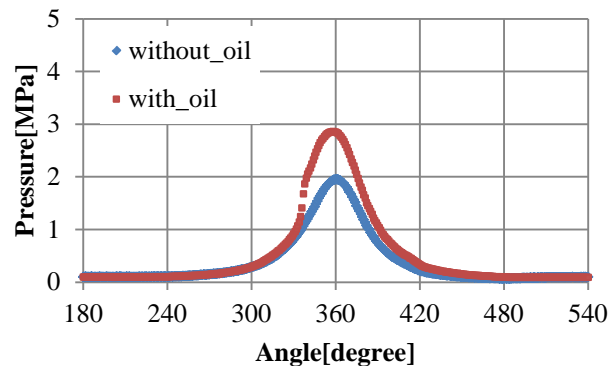


Fig. 3.4.2 Pressure in the engine

(b) Result of Experiment 2

Figs. 3.4.3 and Fig. 3.4.4 show the representative pressure change in the engine when the gaseous mixture of air, refrigerant, and lubricant oil was compressed, for refrigerants R1234yf and R134a, respectively. The number of revolutions was 1,500 rpm.

In the case of R1234yf, self-ignition combustion occurred and the pressure rose when the refrigerant concentration was 0%, which is similar to the results of experiment 1. The exhaust gas was white at this point. When the refrigerant concentration was more than 30–40%, no drastic rise in the pressure was observed and little white gas was observed. The maximum pressure decreased as the concentration of the refrigerant increased. At low refrigerant concentrations, the pressure increased more than the pressure at 0% concentration. The maximum pressure then rose to approximately 5 MPa. At this point, the color of the exhaust gas changed to black, and intense noise and vibration occurred. As the concentration of the refrigerant decreased, the maximum pressure decreased.

Combustion did not occur at any concentration of the refrigerant without the injection of oil. The exhaust gas was neither white nor black, and the engine moved smoothly. These results were similar to those for R1234yf, R32, and R410A.

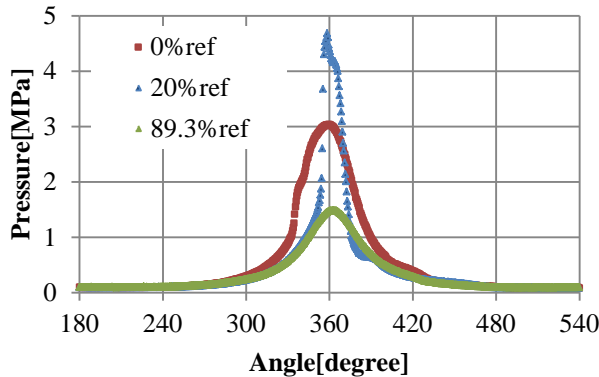


Fig. 3.4.3 Pressure in the engine with an R1234yf gas mixture

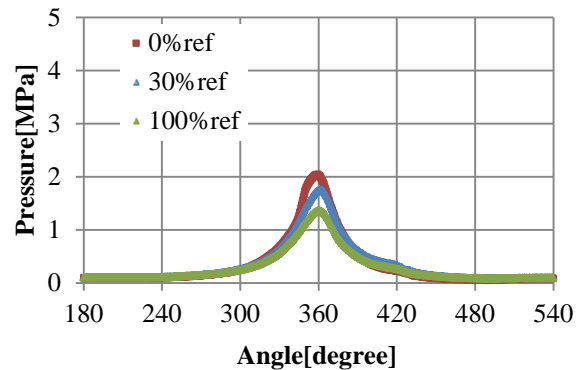


Fig. 3.4.4 Pressure in the engine with an R134a gas mixture

With R134a and N_2 , on the other hand, combustion did not occur at refrigerant concentrations of more than 70%, and the engine moved smoothly. Combustion occurred at refrigerant concentrations of less than 50%. The exhaust gas was white and there was a slight vibration. The emission of black exhaust gas and the intense vibration that occurred with the previous refrigerant did not occur in this case. The maximum pressure increased as the concentration of the refrigerant decreased and reached a maximum when the concentration of the refrigerant reached 0%.

Fig. 3.4.5 and Fig. 3.4.6 show the results of experiment 2. The horizontal axis shows the volume concentration of the refrigerant, and the vertical axis shows the maximum pressure normalized with respect to the pressure at a refrigerant concentration of 0%. The theoretical value was calculated by assuming adiabatic compression, based on the ratio of the specific heat of the air to that of the refrigerant.

In the case of R1234yf, when the refrigerant concentration was greater than 50%, self-ignition did not occur, and the maximum pressure was almost equal to the pressure without the oil. The maximum pressure increased as the concentration of the refrigerant decreased, presumably because of the change in the ratio of the specific heat of the air to that of the refrigerant. Self-ignition occurred when the concentration of the refrigerant decreased further. At that point, the maximum pressure was higher than that of the air only, which implies that the refrigerant itself caused the combustion reaction. These results were similar to those for R32 and R410A.

In the case of R134a, as in the case of R1234yf, self-ignition did not occur at the high end of the range of refrigerant concentrations. Self-ignition occurred when the concentration of the refrigerant decreased; however, the maximum pressure was lower than that of R1234yf and reached a maximum at a refrigerant concentration of 0%, which suggests that combustion of the refrigerant itself did not occur. These results were similar to those for N_2 .

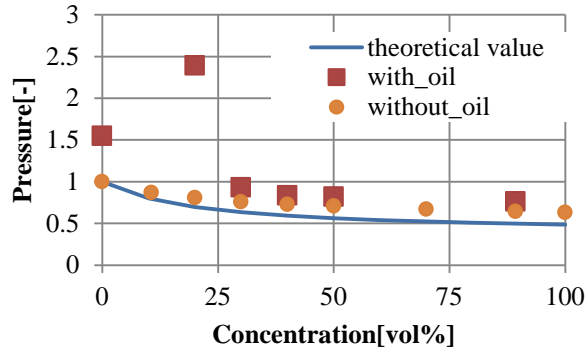


Fig. 3.4.5 Maximum pressure in the engine versus the concentration of R1234yf

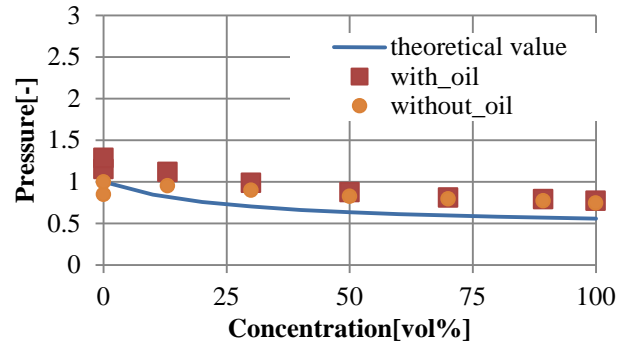


Fig. 3.4.6 Maximum pressure in the engine versus the concentration of R134a

(c) Results of Experiment 3

Fig. 3.4.7 shows the results of an analysis of exhaust gas by FT/IR when the gaseous mixture of the air, R1234yf, and lubricant oil was compressed and combustion occurred. When the combustion of the gaseous mixture occurred, production of HF and COF₂, which results from the decomposition and decreasing concentration of the refrigerant, was observed. The formula for the chemical reaction between oxygen and R1234yf is shown below (JSRAE, 2013). Production of HF and COF₂ was also observed with the other three refrigerants. In the case of R410A, the concentration of R32 decreased particularly notably, indicating that the R32 combusted.

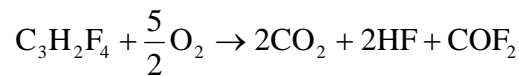


Table 3.4.5 shows the absorbance of HF. The cause of the differences of HF concentration for each refrigerant is not revealed.

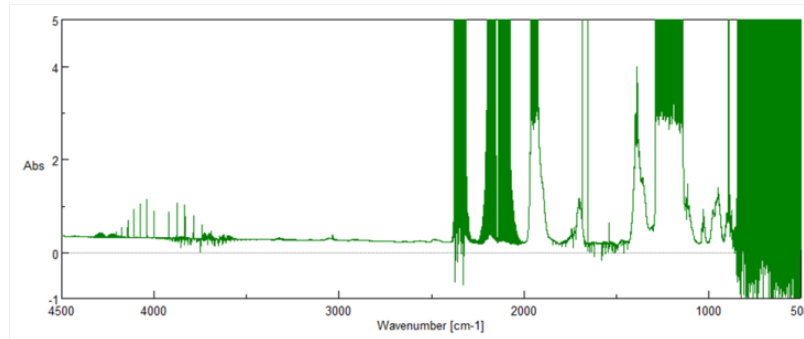


Fig. 3.4.7 Infrared absorption spectrum of exhaust for R1234yf gas mixture

Table 3.4.5 HF absorbance for each refrigerant

Refrigerant	HF concentration [vol. %]
R1234yf	0.361
R32	0.182
R410A	0.261
R134a	0.126

3.4.4 Conclusions Concerning the Risk of Diesel Combustion during Pump-Down of a Heat Pump

Fig. 3.4.8 shows a schematic diagram of the concentration of refrigerant and the maximum pressure due to compression of a gaseous mixture of air, refrigerant, and lubricant oil. The concentration of the refrigerant is plotted on the horizontal axis, and the maximum pressure is plotted on the vertical axis. In the range of high refrigerant concentrations, no combustion occurred with any of the refrigerants, and the maximum pressure increased as the

concentration of the refrigerant decreased. In the range of low refrigerant concentrations, self-ignition of the lubricant oil occurred first. With a refrigerant of high flammability, the maximum pressure is higher because of combustion of the refrigerant itself. With a refrigerant of low flammability, on the other hand, the refrigerant itself does not combust and the maximum pressure remains low.

The results for R1234yf, R32, and R410A were similar to those for the high-flammability refrigerant discussed above. The results for R134a were similar to those for the low-flammability refrigerant. Regardless of whether or not combustion occurred, HF and COF₂ were detected in the exhaust gas for all of the refrigerant, which indicates that the refrigerants reacted in some way.

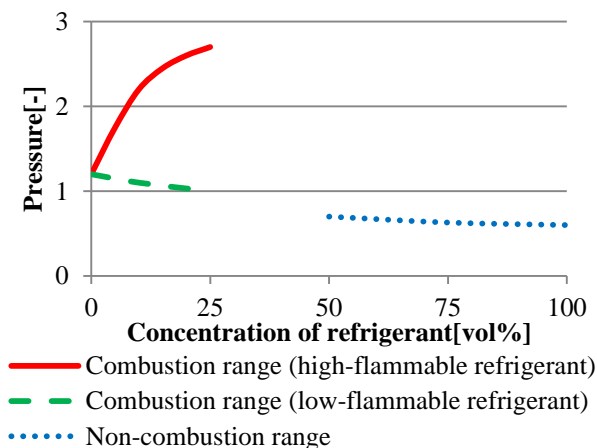


Fig. 3.4.8 Schematic diagram of the relationship between the maximum pressure and the concentration of refrigerant

References

- Japan Fluorocarbon Manufacturers Association (JFMA) ed., 2012, List of CFCs, HCFCs and fluorocarbons' environmental and safety data, JFMA, <http://www.jfma.org/atabase/table.html> (in Japanese)
- The Japan Society of Refrigerating and Air Conditioning Engineers (JSRAE), 2013, *Risk Assessment of Mildly Flammable Refrigerants 2012 Progress Report*, JSRAE, http://www.jsrae.or.jp/info/2012progress_report_e.pdf
- Kataoka, O., Yoshizawa, M., Ohnishi, H., and Ishida, S., 1996, Flammability evaluation of HFC-32 and HFC-32/134a under practical operating conditions, *Proceedings of the International Refrigeration Conference*, Purdue, USA, July 1996.
- National Institute of Standards and Technology (NIST), 2011, Chemistry WebBook, NIST, <http://webbook.nist.gov/chemistry/>
- Pacific Northwest National Laboratory (PNNL), 2012, Northwest-Infrared, <https://secure2.pnl.gov/nsd/nsd.nsf/Welcome>
- Takizawa, K., Tokuhashi, K., Kondo, S., and Nagai, H., 2011. Flammability evaluation of R-1234yf and R-1234ze(E), *Proceedings of the 49th Combustion Symposium*, 146-147, Yokohama, Japan (in Japanese).
- Takizawa, K., 2012. Flammability properties of 2L refrigerants, *Proceedings of the International Symposium on New Refrigerants and Environmental Technology 2012*, Kobe, Japan.
- Tokyo Metropolitan Association of Refrigerating Air Conditioning Equipment (TRK), *Technical Report* (in Japanese).
- Tokyo Metropolitan Government, 2012. The report on an accident caused by a technical error during removal operation of RAC, (in Japanese), <https://www.shouhiseikatu.metro.tokyo.jp/attention/aircon.html>

4. Progress at Kyushu University

4.1 Introduction

The research group is working on the following subjects under the NED project titles “Development of low-GWP refrigerants suitable for vapor compression heat pump systems.”

1. Focusing on a new refrigerant, HFO-1234ze(Z), for which data are not yet available in the public domain, in order to clarify its chemical characteristics including safety, thermodynamic, and transport properties; heat transfer characteristics; and performance of the basic heat pump cycle.
2. To explore and select a low-GWP refrigerant mixture, which is composed of HFO refrigerants including HFO-1234ze(Z), HFC refrigerants, and natural refrigerants, for use in commercial air conditioning systems. To clarify the thermodynamic and transport properties, heat transfer characteristics, and performance of the basic heat pump cycle for the low-GWP refrigerant mixture.
3. To build a fundamental technology for the practical use of the low-GWP refrigerant mixture.

The results of thermodynamic and transport property measurements, proposal of the equation of state (EOS), and heat transfer experiment on HFO-1234ze(Z) are mentioned in this report. Additionally, with the selected refrigerant mixture HFO-1234ze(E)/HFC-32/CO₂, validation of the mixture model, as well as the results of the experiment on heat transfer and performance of a basic heat pump cycle are presented.

4.2 Thermodynamic Properties and Heat Transfer Characteristics of HFO-1234ze(Z)

4.2.1 Thermophysical properties of HFO-1234ze(Z)

By an isochoric method, $P\rho T$ properties and saturated vapor pressure of HFO-1234ze(Z) were measured. Ten values for the density varying from 223.7 to 833.2 kg/m³ were obtained in the temperature range 403–423.3 K; while 19 values for vapor pressure were obtained in the temperature range 310–420 K and pressure range 263–3333 kPa. In addition, 263 values for the $P\rho T$ property along with 11 isochoric curves were obtained in the temperature range 310–440 K and pressure range 263 kPa–6 MPa.

By the visual observation of meniscus disappearance taking into consideration the intensity of critical opalescence, as well as from the break point of isochors, the vapor-liquid coexistence curve and critical parameters were determined as follows:

$$T_c = 423.27 \pm 0.03 \quad \text{K} \quad (4.1)$$

$$\rho_c = 470 \pm 5 \quad \text{kg/m}^3 \quad (4.2)$$

$$P_c = 3533 \pm 10 \quad \text{kPa} \quad (4.3)$$

A new equation of state was developed for HFO-1234ze(Z), which provides better representation of experimental data than the preliminary equation. Fig. 4.2 is the newly obtained P - h diagram. The new equation is valid for temperatures from 273 K to 430 K and for pressures up to 6 MPa with an uncertainty of 0.15% for vapor pressures, 0.4% for vapor densities, 0.2% for liquid densities, and 0.05% for the vapor-phase sound speeds. The equation exhibits reasonable extrapolation behavior in regions away from the valid range. Fig. 4.3 shows deviations in experimental vapor pressures from calculated values with the equation of state. In Fig. 4.2, the vapor-liquid coexisting curve obtained from the equation is plotted using experimental data for the saturated liquid and vapor densities. These figures suggest that the equation of state developed in this work has sufficient accuracy for most technical applications.

The FLD file for REFPROP based on the developed equation of state is available from the NIST website.

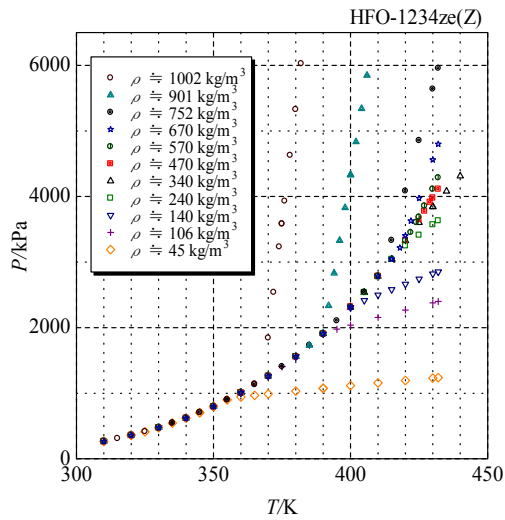


Fig. 4.1 $P\rho T$ properties of HFO-1234ze(Z)

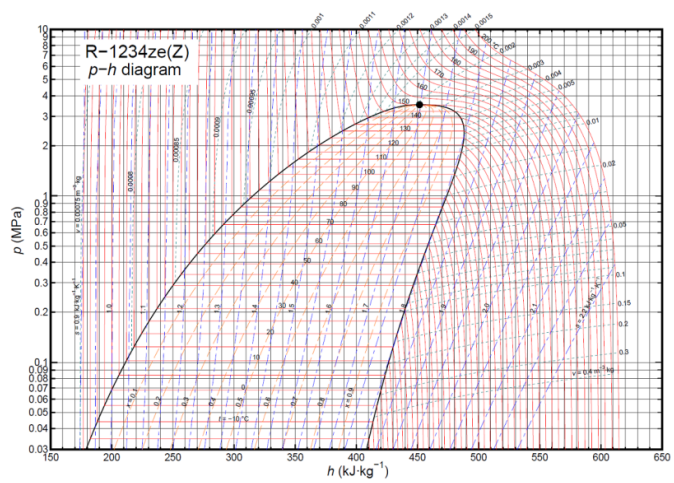


Fig. 4.2 $P-h$ diagram for HFO-1234ze(Z)

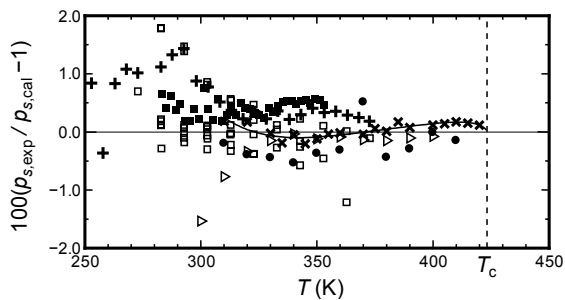


Fig. 4.3 Deviations in experimental vapor pressures from values calculated using the equation of state:
 (□●) Kayukawa *et al.* (2012)
 (×) Higashi *et al.* (2013)
 (▷) Tanaka *et al.* (2013)
 (■+) Fedele *et al.* (2013)
 (—) Vapor pressure correlation by Higashi *et al.* (2013)

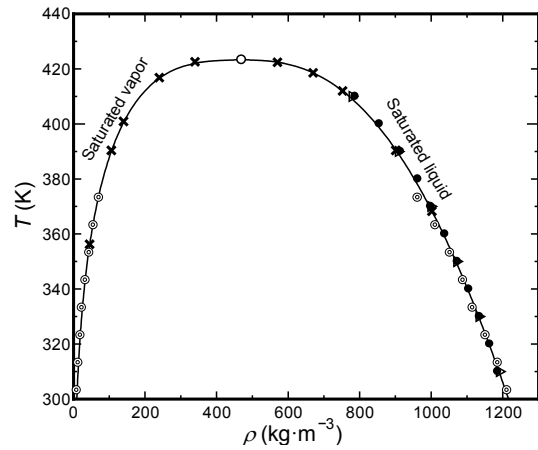


Fig. 4.4 Vapor-liquid coexistence curve for HFO-1234ze(Z):
 (●) Kayukawa *et al.* (2012)
 (×) Higashi *et al.* (2013)
 (⊙) Raabe (2012)
 (▷) Tanaka *et al.* (2013)
 (—) Equation of state
 (○) Critical parameters calculated from the equation of state (470.615 kg/m^3 , 423.27 K)

4.2.2 Transport properties of HFO-1234ze(Z)

This year, the thermal conductivity of HFO-1234ze(Z) vapors was measured, as was done for the saturated liquids of HFO-1234ze(Z), HFO-1234ze(E), and HFC-32 reported last year. Moreover, the liquid viscosity of HFO-1234ze(E) and HFO-1234ze(Z) was measured.

The thermal conductivity of HFO-1234ze(Z) was measured by a transient hot-wire method, in which two Pt wires (15 mm) of different lengths were used under isopycnic conditions. Figs. 4.5 (a) and (b) show the measurement conditions and measurement results, respectively. In Fig. 4.5, the lines for HFC-32 and HFO-1234ze(E) show values calculated using REFPROP9.1, and the line for HFO-1234ze(Z) denotes a correlation obtained from the extended corresponding states (ECS) model coupled with the equation of state developed by Akasaka *et al.* (2013). The calculated and measured values of vapor thermal conductivity show excellent agreement.

Figs. 4.6 (a) and (b) respectively show the measurement conditions and results for HFO-1234ze(E) liquid viscosity. Figs. 4.7 (a) and (b) show measurement conditions and results for HFO-1234ze(Z). The liquid viscosities were measured by the capillary method in which two capillary tubes of different lengths were used to cancel the end-effects, under isobaric conditions corresponding to the saturation temperatures of 99.5, 90, and 70 °C. The lines denote the values calculated using REFPROP9.1 and the ECS model of Akasaka *et al.* (2013). The liquid viscosities of both HFO-1234ze(E) and HFO-1234ze(Z) drastically decrease with increasing temperature. At a given temperature, the viscosity of HFO-1234ze(Z) is notably higher than that of HFO-1234ze(E). These tendencies are qualitatively identical to those of the predicted values; in particular, the predicted viscosity of HFO-1234ze(E) agrees well with the measured viscosity. On the basis of measured viscosity, the ECS model will be modified for HFO-1234ze(Z).

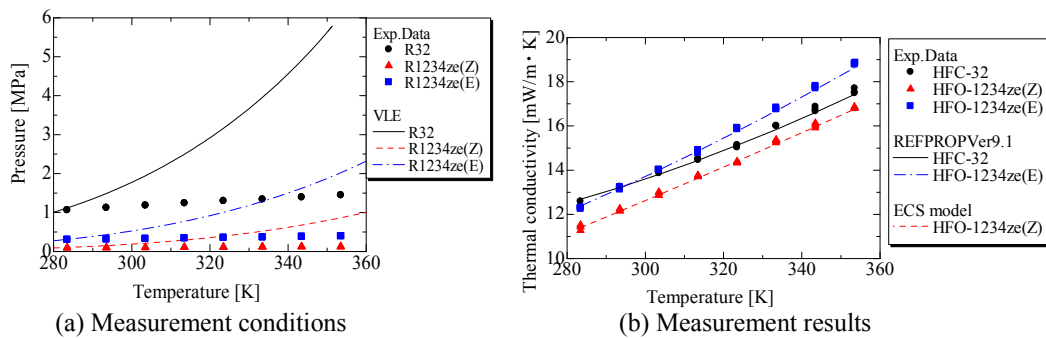


Fig. 4.5 Thermal conductivity of HFO-1234ze(Z) vapors

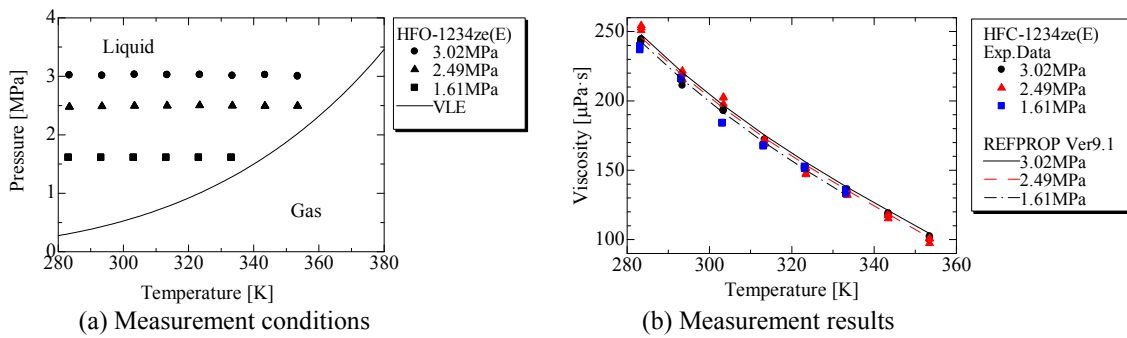


Fig. 4.6 Liquid viscosity of HFO-1234ze(E)

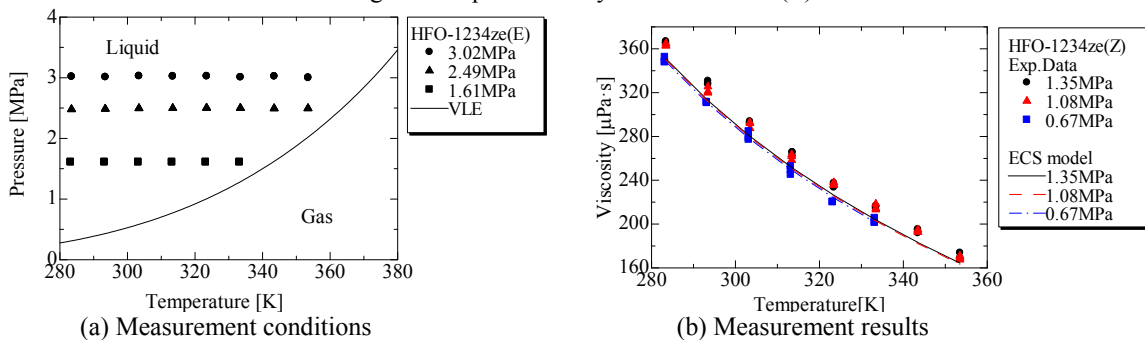


Fig. 4.7 Liquid viscosity of HFO-1234ze(Z)

4.2.3 Heat transfer characteristics of HFO-1234ze(Z)

(a) Heat transfer in horizontal microfin tubes

The evaporation and condensation heat transfer coefficients (HTCs) and pressure gradients of HFO-1234ze(Z) flowing in a microfin tube were measured using a vapor compression cycle. The test tube used was a copper tube with an outer diameter of 6.08 mm, a fin root diameter of 5.49 mm, and an equivalent inner diameter of 5.34 mm,

with 48 helical inner microfins. The fin height, lead angle, and surface enlargement were respectively 0.255 mm, 20.1°, and 2.24. The test section was divided into four subsections. The pressure gradients at intervals of 554 mm and HTC over the 414 mm active heat transfer length were measured.

Fig. 4.8 shows the HTCs during the evaporation and condensation of HFO-1234ze(Z). The experiments were carried out at a mass velocity of 200 kg/(m²s), a heat flux of 10 kW/m², and saturation temperatures of 30 and 65 °C for evaporation and condensation, respectively. The results for HFC-134a and HFO-1234ze(E) are plotted in Fig. 4.8. The lines show the HTCs predicted using the correlation of Mori *et al.* (2002) and Cavallini *et al.* (2009). For evaporation, the HTCs of HFO-1234ze(Z) are lower than those of HFC-134a and HFO-1234ze(E) at vapor qualities lower than 0.3. However, except that region, the HTCs of HFO-1234ze(Z) are somewhat higher than those of the other two refrigerants. These characteristics were well predicted using the FLD file provided by Akasaka *et al.* (2013) by the existing correlations.

Figure 4.9 shows the pressure gradients of HFC-134a, HFO-1234ze(E), and HFO-1234ze(Z) during evaporation and condensation under the same conditions as those indicated in Fig. 4.8. The lines show pressure gradients predicted using the correlation of Kubota *et al.* (2001) and Yonemoto-Koyama (2007). The pressure gradients of HFO-1234ze(Z) are larger than those of HFC-134a and HFO-1234ze(E). The main cause for this is the higher vapor velocity of HFO-1234ze(Z) due to the lower vapor density. From the same reason, the pressure gradients in condensation at the saturation temperature of 65 °C are approximately 1/3 of those at 30 °C. As reduced pressure/temperature increases, the vapor density increases; thus, the pressure gradients decreases as vapor velocity decreases. These characteristics are well predicted by the existing correlations.

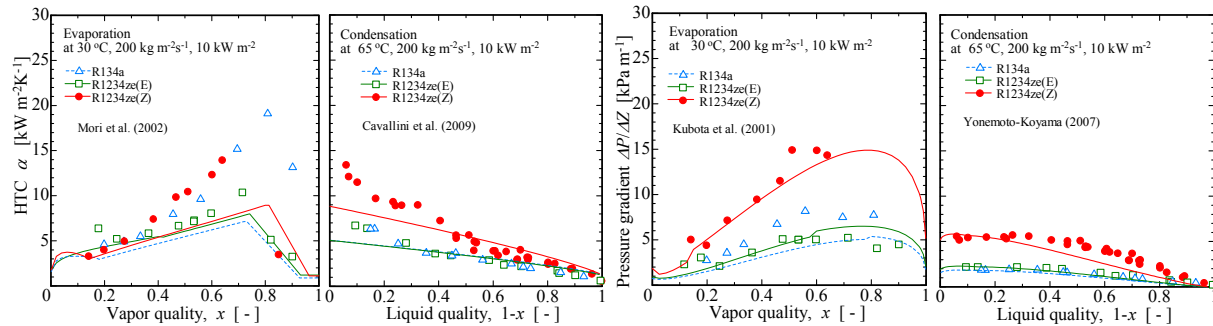


Fig. 4.8 HTC in horizontal microfin tube

Fig. 4.9 Pressure gradient in horizontal microfin tube

(b) Heat transfer on horizontal smooth tubes

The condensation and pool boiling HTCs on a horizontal plane tube were measured by a test loop with natural circulation. The outer diameter of the test tube and heat transfer length were 19.12 mm and 400 mm, respectively.

Fig. 4.10 shows variations in condensation HTCs against the degree of wall subcool for HFC-134a, HFO-1234ze(E), and HFO-1234ze(Z). The symbols denote experimental HTCs, with vertical and horizontal bars indicating the measurement uncertainty in HTC and degree of subcool. The solid and dashed lines denote theoretical HTCs predicted using the Nusselt theory (1916). The condensation HTC of HFC-134a, in which the thermodynamic properties are most authorized, agrees with the theoretical HTC within the measurement uncertainty. From this result, the validation of this experimental method is demonstrated.

The experimental values of HFO-1234ze(E) and HFO-1234ze(Z), as shown respectively in Figs. 4.10(b) and (c), agreed with the theoretical values calculated using the FLD file provided by Akasaka *et al.* (2013) within approximately 10%. Among the tested refrigerants, the condensation HTC of HFO-1234ze(Z) was the highest, followed by those of HFC-134a and HFO-1234ze(E). This order can be explained by the thermodynamic properties of the refrigerants. The liquid thermal conductivity and latent heat of HFC-134a and HFO-1234ze(Z) were 8–20% and 6–24% higher than those of HFO-1234ze(E), respectively. The above-mentioned tendency could be precisely predicted using the Nusselt theory (1916) by employing the provided FLD file.

Fig. 4.11 shows variations in pool boiling HTC against wall heat flux. The solid and dashed lines denote the values calculated using the correlation of Stephan-Abdelsalam (1978) proposed for the pool boiling of other refrigerants. The pool boiling HTC of HFO-1234ze(Z) is considerably lower than that of HFC-134a and HFO-1234ze(E). At the given saturation temperature, the reduced pressure of HFO-1234ze(Z) ranges from 0.02 to 0.15. This value is notably lower than those of the others, and thus, the surface tension of HFO-1234ze(Z) is larger. For balancing the surface tension, the bubble departure diameter becomes larger and more wall superheat is required for boiling.

Figs. 4.12(a)–(c) show the pictures of nucleate boiling on the wall surface of HFC-134a, HFO-1234ze(E), and HFO-

1234ze(Z) at a saturation temperature of 20 °C and a heat flux of 15 kW/m². Fig. 4.12(d) shows the picture of HFO-1234ze(Z) at a saturation temperature of 40 °C and a heat flux of 15 kW/m². The bubble diameter of HFO-1234ze(Z), as shown in Fig. 4.12(c), is clearly larger than that of other refrigerants (Figs. 4.12(a) and (b)). By contrast, the nucleation site density of HFO-1234ze(Z) is smaller than that of other refrigerants. Gaertner-Westwater (1960) remarked that the bubble departure diameter increases with decreasing nucleation site density. Therefore, the pool boiling HTC of HFO-1234ze(Z) is low mainly due to the smaller nucleation site density. This also decreases the pool boiling HTC.

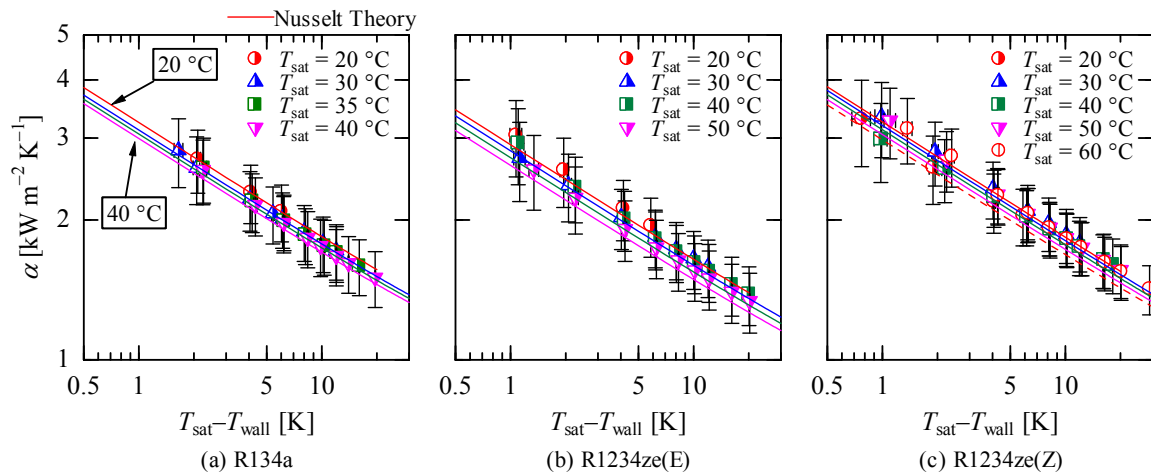


Fig. 4.10 Condensation HTC on horizontal smooth tube

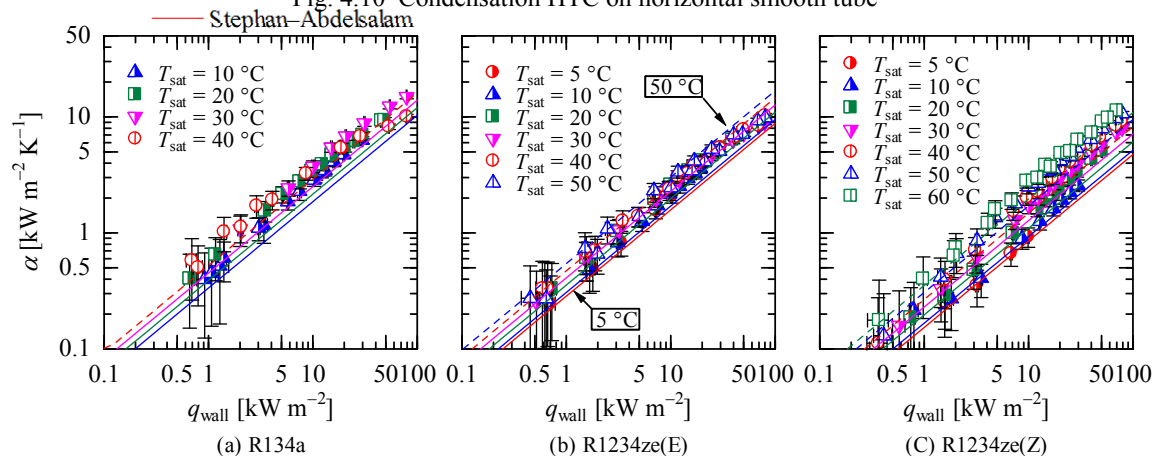


Fig. 4.11 Pool boiling HTC on horizontal smooth tube

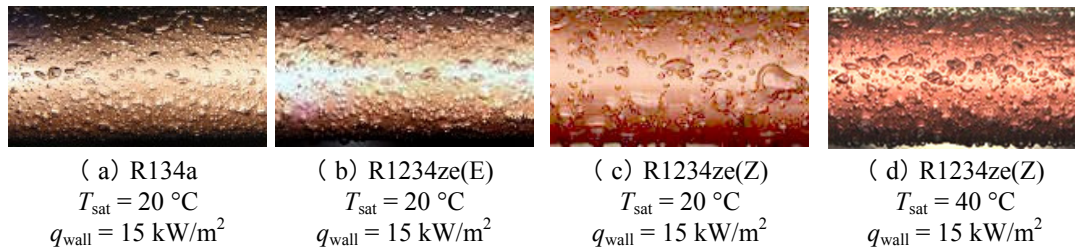


Fig. 4.12 Nucleate boiling sites of R134a, R1234ze(E), and HFO-1234ze(Z)

4.2.4 Cycle performance of HFO-1234ze(Z)

To find the optimum temperature range for the heat source, drop-in experiments and numerical analysis were carried out for high-temperature applications of HFO-1234ze(E) and HFO-1234ze(Z). A test loop made to measure the

cycle performance by the drop-in experiment mainly consisted of a hermetic compressor, a solenoid expansion valve, and two double-tube-type heat exchangers with counter-flow configurations. Table 4.1 lists the test conditions employed in the drop-in experiments for HFO-1234ze(E), HFO-1234ze(Z), and HFO- 1234ze(E)/HFC-32 (95/5 mass%).

Fig. 4.13 presents the experimental results for COP and heating load. Under the conditions listed in Table 4.1, the COP and heating load of HFO-1234ze(E) are clearly higher than those of HFO-1234ze(Z). Adding HFC-32 (5 mass%) to HFO-1234ze(E) somewhat improves the COP and heating capacity of both. Although the COP of HFO-1234ze(Z) is relatively high at a smaller heating load, this drastically decreases with increasing heating load. This suggests that HFO-1234ze(Z) is most likely suitable for a higher temperature range than the test condition.

Fig. 4.14 shows the breakdown of the irreversible losses and COP obtained by a numerical analysis at condensation temperatures of 75, 105, and 125 °C, and a heating load of 1.8 kW. The calculation method is validated from the fact that the calculated COPs of HFO-1234ze(E) and HFO-1234ze(Z) at condensation temperature of 75 °C are almost identical to the experimental results shown in Fig. 4.13. The irreversible loss in the compressor and the irreversible loss caused by a pressure drop for HFO-1234ze(Z) are remarkably higher than those for HFO-1234ze(E) at 75 °C because of an insufficient volumetric capacity of HFO-1234ze(Z). As condensation temperature increases from 75 to 105 °C and then to 125 °C, the irreversible losses in the compressor and pressure drop decrease and the COP of HFO-1234ze(Z) increases. This suggests that HFO-1234ze(Z) is beneficial for rather high-temperature applications than air conditioners.

Table 4.1 Conditions for drop-in experiment

Water Temp.	Cond.	[°C]	50→75
	Eva.		45→39
Degree of superheat		[K]	3
Heat transfer rate		[kW]	1.2–2.4

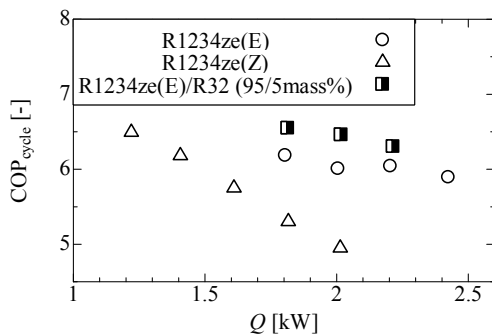


Fig. 4.13 Drop-in experiment results for COP

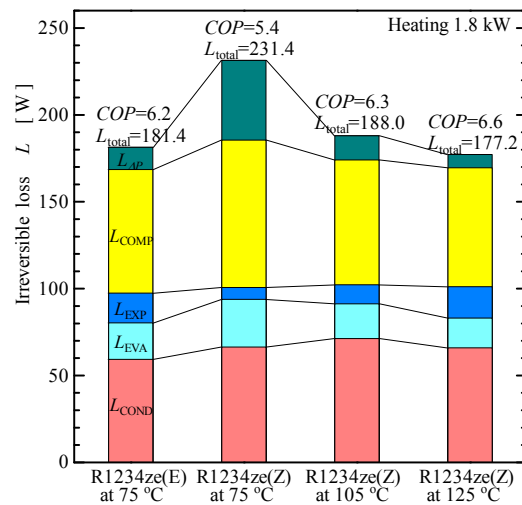


Fig. 4.14 Break down of irreversible loss of various condensing temperatures obtained by numerical calculations

4.3 Thermodynamic Properties and Heat Transfer Characteristics of Low-GWP Refrigerant Mixtures

To evaluate the thermodynamic performance of ternary HFO-1234ze(E)/HFC-32/CO₂ mixtures, measurement of the heat transfer coefficient and drop-in experiment were conducted this year. As the first step, last year, two mass fractions of HFO-1234ze(E)/HFC-32/CO₂ were selected from a brief assessment. Fig. 4.15 illustrates the assessment results for the thermodynamic characteristics. The lines in the ternary diagram represent the contours of GWP, temperature glide, the COP ratio, and volumetric capacity ratios relative to HFC-410A. On the basis of the criteria

listed in Table 4.2, two compositions were selected. The ternary blend “A” (HFO-1234ze(E)/HFC-32/CO₂, 53/43/4 mass%) was used to achieve a GWP just below 300. The ternary blend “B” (HFO-1234ze(E)/HFC-32/CO₂, 262/29/9 mass%) was used to achieve a GWP just below 200. In Fig. 4.15, the red and blue symbols indicate the selected ternary blend A and B, respectively.

Condition	A	B
GWP	<300	<200
Temperature glide	<10 K	<15 K
Volumetric capacity ratio	>0.8	
COP ratio	>1.0	

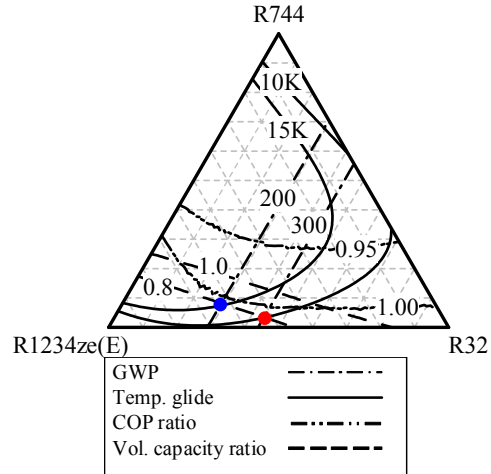


Fig. 4.15 Thermodynamic assessment results. (Calculation conditions: condensation temp. of 30 °C, subcool of 0 K, evaporation temp. of -3 °C, superheat of 3 K, and compressor efficiency of 0.85)

4.3.1 Thermophysical properties of low-GWP refrigerant mixture

As with HFO-1234ze(Z), the thermophysical properties were measured for the selected ternary mixture 54 mass% HFO-1234ze(E) + 43 mass% HFC-32 + 3 mass% CO₂.

By an isochoric method, $P\rho T$ properties and saturated vapor pressure of this mixture were measured. Thirteen values for the density varying from 240.6 to 807.5 kg/m³ were obtained in the temperature range 345.9–363.1 K. Further, 101 values for $P\rho T$ properties along the 6 isochoric curves were obtained in the temperature range 310–385 K, density range 181–666 kg/m³, and pressure range 1784 kPa–6.9 MPa.

From the visual observation of meniscus disappearance, the break point of isochors, the vapor-liquid coexistence curve, and the critical parameters were determined as follows:

$$T_c = 361.83 \pm 0.03 \quad \text{K} \quad (4.4)$$

$$\rho_c = 466 \pm 5 \quad \text{kg/m}^3 \quad (4.5)$$

$$P_c = 5394 \pm 10 \quad \text{kPa} \quad (4.6)$$

A mixture model was presented for the ternary HFO-1234ze(E)/HFC-32/CO₂ mixture. The multifluid approximation explicit in Helmholtz free energy forms the basis of the model presented in this work. The approximation represents total interaction between molecules in the ternary mixtures as the sum of each binary pair interaction. In this work, a new binary model for the binary pair of HFO-1234ze(E)/HFC-32 was combined with available models for the other two binary pairs.

Fig. 18 shows the vapor-liquid coexistence curve obtained from the new mixture model for HFO-1234ze(E)/HFC-32, as well as from the experimental data. Although a slightly different behavior was observed for the saturated vapor densities, the model showed good representation of the saturated liquid densities and critical parameters. Fig. 19 shows the vapor-liquid coexistence curve obtained using the ternary mixture model incorporating the new binary model for HFO-1234ze(E)/HFC-32. Since the ternary model did not use additional parameters for ternary mixtures, the curve was completely predictive. In spite of this, the experimental saturated liquid densities were well represented by the model, and the calculated critical parameters almost corresponded to experimental values.

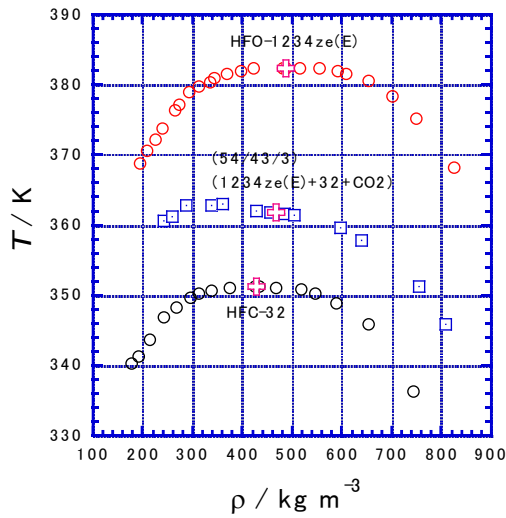


Fig. 4.16 T - ρ diagram for HFO-1234ze(E)/HFC-32/CO₂

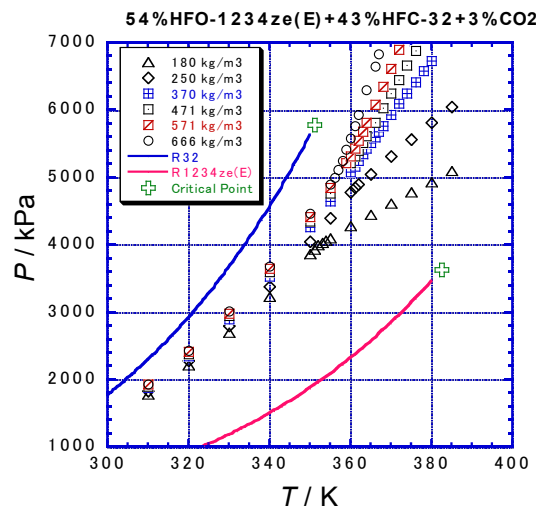


Fig. 4.17 P - T diagram for HFO-1234ze(E)/HFC-32/CO₂.

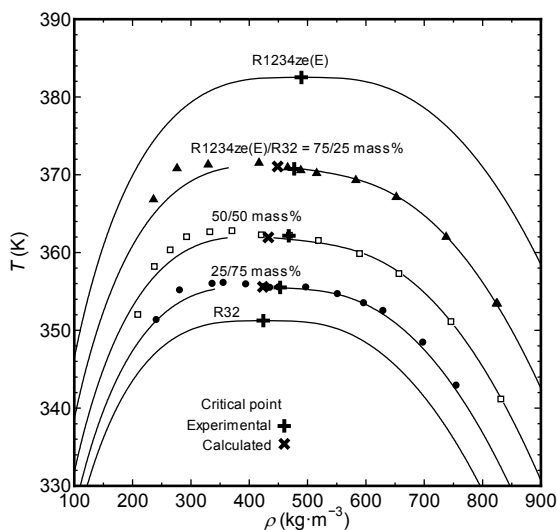


Fig. 4.18 Vapor-liquid coexistence curve for HFO-1234ze(Z)/HFC-32:
 (▲□●) Experimental data obtained in this project
 (—) Binary mixture model for HFO-1234ze(Z)/HFC-32.

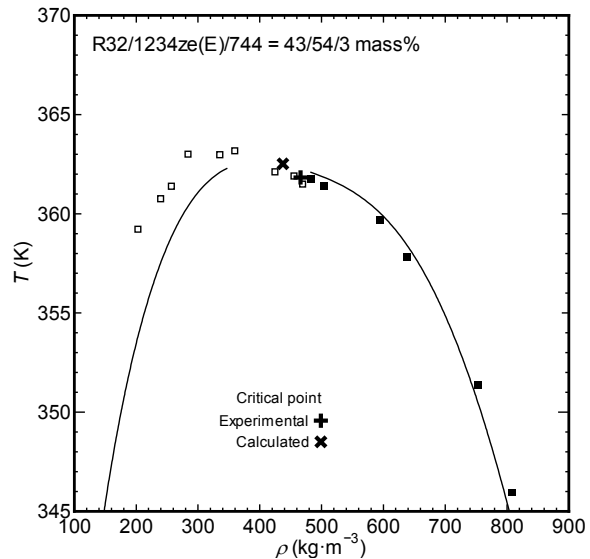


Fig. 4.19 Vapor-liquid coexistence curve for HFO-1234ze(Z)/HFC-32/CO₂:
 (□■) Experimental data obtained in this project
 (—) Ternary mixture model for HFO-1234ze(Z)/HFC-32/CO₂.

4.3.2 Heat transfer characteristics of low-GWP refrigerant mixtures

(a) Heat transfer in horizontal microfin tubes

HTCs and pressure gradients in a microfin tube were measured for a low-GWP refrigerant mixture as well as for HFO-1234ze(Z). The experiments were carried out at average saturation temperatures (the average of dew point and boiling point) of 10 and 40 °C for evaporation and condensation, respectively. These are typical operation conditions for air conditioners. The test refrigerants were: a binary mixture (HFO-1234ze(E)/HFC-32: 70/30 mass%) and a ternary mixture (HFO-1234ze(E)/HFC-32/CO₂: 62/39/9 mass%) with a GWP of 200, as well as a binary mixture (HFO-1234ze(E)/HFC-32: 60/40 mass%) and a ternary mixture (HFO-1234ze(E)/HFC-32/CO₂: 53/43/4 mass%) with a GWP of 300. The circulation composition was measured at the outlet of the sub-cooler. With the circulation

composition, the refrigerant temperature and vapor quality were calculated using mixing parameters (Akasaka, 2013), which were optimized on the basis of the measurement data of Higashi *et al.* (2013) and others.

Fig. 20 shows the measured evaporation and condensation HTC. The HTCs of refrigerant mixtures are significantly lower than those of single components. This is a typical behavior of mass transfer resistance caused by the volatility difference between the components.

As it has already been remarked in previous studies, the resistance decreases HTC more when the temperature glide is larger, the mole fraction difference between the liquid and vapor of each component is larger, and the vapor velocity is lower. The experimental condensation HTCs of the ternary mixture (HFO-1234ze(E)/HFC-32/CO₂: 62/39/9 mass%) that had the largest temperature glide was the lowest among the tested refrigerants. Thus, the tendency of condensation HTCs was qualitatively identical to those reported previously. On the other hand, in the case of evaporation, there was no significant difference between each refrigerant because the HTCs of all the tested refrigerants were significantly low. Nevertheless, the HTC of (HFO-1234ze(E)/HFC-32/CO₂: 62/39/9 mass%) having the highest mass fraction of CO₂ was the lowest because of the lower vapor velocity due to higher vapor density.

Fig. 20 shows the measured pressure gradients. In contrast to HTCs, these pressure gradients are comparable to those of single components. The evaporation pressure gradient of refrigerants contains more CO₂ and HFC-32 tends to be smaller, owing to their higher vapor density. In the case of condensation, pressure gradients are smaller than those of evaporation, and the difference between each refrigerant is relatively small.

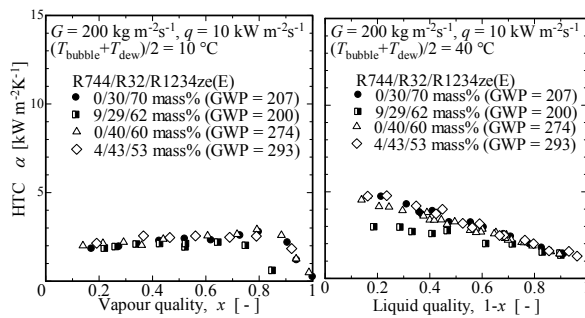


Fig. 4.20 HTC of low-GWP refrigerant mixtures

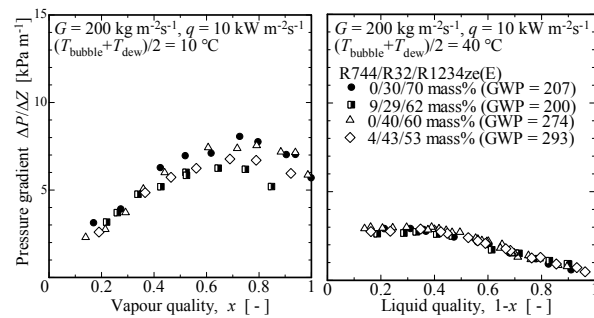


Fig. 4.21 Pressure gradient of low-GWP refrigerant mixtures

(b) Heat transfer in plate heat exchangers

The flow pattern of air-water flow was visualized; further, the void fraction was measured using a transparent acrylic plate having herringbone grooves. Then, the HTC of HFO-1234ze(E) in a stainless steel plate heat exchanger having herringbone grooves, which was placed in a pump loop, was measured. Of the stainless test plate with a thickness of 10 mm, on the side surfaces of both the heat source and refrigerant, 5 grooves were made for inserting thermocouples at 22.4 mm intervals. The local heat fluxes at the points, where surface temperatures of the heat source and refrigerant sides were measured, were determined by considering one-dimensional steady state heat conduction over the test plate. From the local heat fluxes and the measured surface temperatures, the HTCs were obtained at condensation temperatures from 35 to 40 °C, evaporation temperatures from 5 to 10 °C, and a mass velocity of 10 kg/(m²s).

Figs. 22 (a) and (b) plot the surface temperature distribution and local HTC during condensation. As condensation proceeds, the temperature difference between the right and left increases and the local HTC monotonically decreases. The local HTC on the left side, where refrigerant speed is most likely higher near the inlet/outlet, is slightly higher than that on the right side.

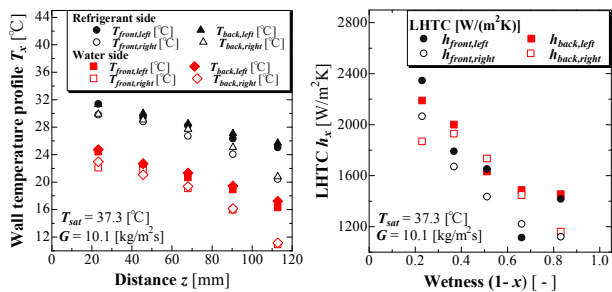
Figs. 23 (a) and (b) plot the surface temperature and local HTC during the evaporation process, similar to that for condensation. As the vapor quality increases, the right-side local HTC decreases. Probably, this is caused by the strong misdistribution of the refrigerant flow. The left-side HTC, which is close to the inlet/outlet and thin liquid film could be formed by the high-speed vapor flow, is relatively higher; moreover, the local HTC is decreased by the thicker liquid film because of the slow vapor flow.

4.3.3 Cycle performance of low-GWP refrigerant mixtures

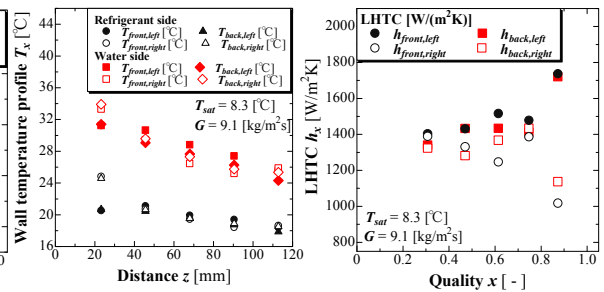
To evaluate the cycle performance of the ternary mixture HFO-1234ze(E)/HFC-32/ CO₂ and HFO-1234ze(Z), drop-

in experiment was conducted. The properties of refrigerant mixtures were evaluated at the circulation composition that was measured at the subcooler outlet. Table 4.3 lists the test conditions for heating and cooling modes. Table 4.4 lists the test refrigerants. Test refrigerants were ternary mixtures (HFO-1234ze(E)/HFC-32/ CO₂: 53/43/4 mass% and 62/29/9 mass%), binary mixtures (HFO-1234ze(E)/HFC-32: 57/43 mass% and 72/28 mass%), and HFC-410A as the conventional refrigerant. The compositions of the binary mixtures were determined from the criteria at a GWP of 300 and 200.

Fig. 24 presents the experimental results for COP and heating/cooling load. In general, the COP decreases with increasing heating/cooling load because the irreversible loss increases with increasing mass flow rate and compression ratio. The COPs of the binary and ternary mixtures with a GWP of 200 are equivalent to or lower than that of HFC-410A. In the case of the binary mixture with a GWP of 200, compared with HFC-410A, irreversible losses of compressor and pressure drop are supposed to be large because of the smaller volumetric capacity. In the case of the ternary mixture with a GWP of 200, irreversible loss in the evaporator is larger than that in the case of HFC-410A because of the very larger temperature glide that is unmatched to the distribution of water temperature. On other hand, the COPs of the binary and ternary mixtures with a GWP of 300 are equivalent to or higher than that of HFC-410A



(a) Wall temperature distribution (b) Local HTC
Fig. 4.22 Condensation HTC



(a) Wall temperature distribution (b) Local HTC
Fig. 4.23 Evaporation HTC

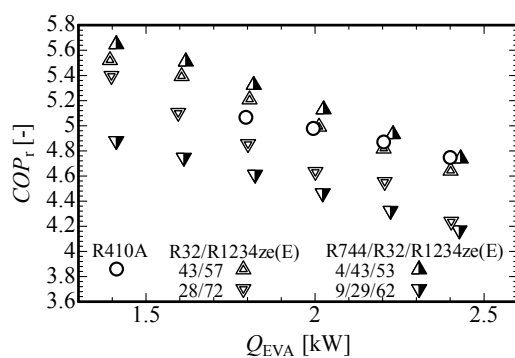
Table 4.3 Conditions for drop-in experiment

	Heating	Cooling
Heat source temp. [°C]	15 → 9	20 → 10
Heat sink temp. [°C]	20 → 45	30 → 45
Degree of superheat [K]	3	
Heat transfer rate [kW]	1.6 ~ 2.6	1.4 ~ 2.4

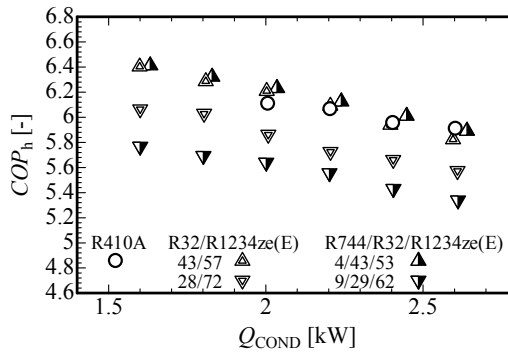
Table 4.4 Test refrigerants

Refrigerants	GWP	Temp. glide [K]
R-32/1234ze(E)	43/57	294
	28/72	194
R-744/32/1234ze(E)	4/43/53	294
	9/29/62	200
R-410A	2088	0.11

* At bulk temperature 10 °C



(a) Cooling mode



(b) Heating mode

Fig. 4.24 Results of drop-in experiments

4.4 Conclusions

In this paper, some of the NEDO-funded research carried out this year has been presented. From the research, thermodynamic and transport properties of HFO-1234ze(Z) have been clarified. On the basis of precise measurement results, an equation of state has been proposed. The FLD file built in the proposed equation of state has been distributed by NIST, so that the properties of HFO-1234ze(Z) can be calculated using REFPROP 9.1. Further, HFO-1234ze(Z) heat transfer characteristics for some configurations have been reported. Additionally, for the selected low-GWP refrigerant mixture, HFO-1234ze(E)/HFC-32/CO₂, the measurement results for thermodynamic properties and the validation of the mixing model have been reported. On the basis of these verification results, the heat transfer characteristics and cycle performance have also been clarified.

References

- Fedele, L., Di Nicola, G., Brown, J. S., Bobbo, S., Zilio, C., 2013. Measurements and Correlations of cis-1,3,3,3-Tetrafluoroprop-1-ene (R1234ze(Z)) Saturation Pressure. To be published in *Int. J. Thermophys.*
- Higashi, Y., Hayasaka, S., Ogiya, S., 2013. Measurements of PVT Properties, Vapor Pressures, and Critical Parameters for Low GWP Refrigerant R-1234ze(Z). In: *Proceedings of Fourth Conference on Thermophysical Properties and Transfer Processes of Refrigerants* (Paper No. TP-018), Delft, The Netherlands.
- Kayukawa, Y., Tanaka, K., Kano, Y., Fujita, Y., Akasaka, R., Higashi, Y., 2012. Experimental Evaluation of the Fundamental Properties of Low-GWP Refrigerant HFO-1234ze(Z). In: *Proceedings of the International Symposium on New Refrigerants and Environmental Technology 2012*, Kobe, Japan.
- Raabe, G., 2012. Molecular Modeling of Fluoropropene Refrigerants. *J. Phys. Chem. B*, 116(19), 5744-5751.
- Tanaka, K., Maruko, K., Fujimoto, Y., Tanaka, M., 2013. PVT Properties of R1234ze(Z). In: *Proceedings of Fourth Conference on Thermophysical Properties and Transfer Processes of Refrigerants* (Paper No. TP-072), Delft, The Netherlands.
- Akasaka, R., Higashi, Y., Koyama, S., 2013. A Fundamental Equation of State for Low GWP Refrigerant HFO-1234ze(Z). In: *Proceedings of Fourth Conference on Thermophysical Properties and Transfer Processes of Refrigerants* (Paper No. TP-052), Delft, The Netherlands.
- Mori, H., Yoshida, S., Koyama, S., Miyara, A., Momoki, S., 2002. Prediction of Heat Transfer Coefficients for Refrigerants Flowing in Horizontal Spirally Grooved Evaporator Tubes. In: *Proc. 14th JSRAE Annual Conf.*, 97-100 (in Japanese).
- Cavallini, A., Del Col, D., Mancin, S., Rossetto, L., 2009, Condensation of Pure and Near-Azeotropic Refrigerants in Microfin Tubes: A New Computational Procedure, *Int. J. Refrig.*, vol. 32: p. 162-174.
- Yonemoto R., Koyama S., 2007, Experimental Study on Condensation of Pure Refrigerants in Horizontal Micro-fin Tubes: Proposal of Correlations for Heat Transfer Coefficient and Frictional Pressure Drop, *Trans. JSRAE*, 24 (2), 139-148 (in Japanese).
- Kubota, A., Uchida, M., Shikazono, N., 2001. Predicting Equations for Evaporation Pressure Drop Inside Horizontal Smooth and Grooved Tubes, *Trans. JSRAE*, 18(4), 29-37 (in Japanese).
- Nusselt, W., 1916, Die Oberflächenkondensation des wasserdampfes., *Veeines Dtsch. Ingenieure*, vol. 60, no. 27, pp. 541-546.
- Stephan, K., Abdelsalam, M., 1978, Heat-Transfer Correlations for Natural Convection Boiling, *Int. J. Heat Mass Transfer.*, vol. 23, pp. 73-87.
- Gaertner, R. F., Westwater, J. W., 1960. Population of Active Sites in Nucleate Boiling Heat Transfer, *Chem. Eng. Prog.*, Symp. Ser., vol. 56, no. 30.

5. Physical Hazard Evaluation of A2L Refrigerants Based on Several Conceivable Accident Scenarios

5.1 Introduction

In Tokyo University of Science, Suwa, the project titled “Evaluation of Combustion and Explosion Hazards and Risk Assessment on A2L Refrigerants for the Air-conditioning Systems” has been performed in cooperation with the Research Institute for Safety and Sustainability (RISS), AIST. This project consists of two main subjects: (I) “Evaluation on fundamental properties of combustion and explosion on A2L refrigerants” (conducted by RISS, AIST) and (II) “Physical hazard evaluation on A2L refrigerants based on several conceivable accident scenarios” (conducted by Tokyo University of Science, Suwa). We aim to perform a more detailed evaluation of the physical hazard of A2L refrigerants on the basis of actual handling situations by collating the results obtained by each subject. In this report, we describe the outline of the subject (II) conducted in FY2011-FY2013.

5.2 Assumed Accident scenarios

We assumed three main accident scenarios as shown in Figure 1. In this report, the following scenario including sub-scenario are used.

- (1) **Scenario #1:** A room air conditioning system containing an A2L refrigerant is simultaneously used with a fossil-fuel heating system inside a general living space.
- (2) **Scenario #2:** An air conditioning system containing an A2L refrigerant is handled at the factory for the service and maintenance.

In this scenario, we focused on the following three sub-scenarios.

- (a) *Sub-scenario (a):* A serviceman uses a portable lighter to smoke in a space in which an A2L refrigerant has leaked and accumulated,
 - (b) *Sub-scenario (b):* An A2L refrigerant leaks from a fracture or pinhole in the pipes or hoses such as that used to connect a car air conditioning system and a collection device,
 - (c) *Sub-scenario (c):* An A2L refrigerant leaks inside a model device such as a collection device for the service and maintenance.
- (3) **Scenario #3:** An A2L refrigerant is used in the Variable Refrigerant Flow (VRF) system

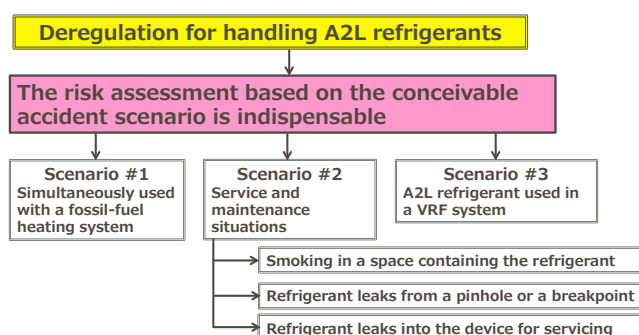


Figure 1 Outline of the Physical hazard evaluation on A2L refrigerants based on several conceivable accident scenarios conducted by Tokyo University of Science, Suwa.

5.3 Details of Physical Hazard Evaluation in Each Scenario

5.3.1 Scenario #1: Simultaneously used with a fossil-fuel heating system

5.3.1.1 Outline

In Scenario #1, we focused on two different utilization cases: an A2L refrigerant leaks from an air-conditioning system into a general living space in which a fossil-fuel heating system has already been operating (*Case (i)*), and a fossil-fuel heating system operating in the general living space in which the leaked A2L refrigerant has already leaked and accumulated (*Case (ii)*). Because the evaluation details of the physical hazards on this scenario was already described in the previous progress report (Imamura et al, 2013) and reference (Imamura et al, 2012), only a summary is provided in this report.

5.3.1.2 Experiment

A commercial room air conditioning system for an area of 6 Tatami mats (about 11 m²) was installed on the wall of an experimental facility (cube, 2800 mm each side) where the center of the ventilation outlet was located 700 mm below the ceiling and at the center in horizontal direction. Refrigerant was leaked in the downward vertical direction from the ventilation outlet. In *Case (i)*, a radiative oil stove (power: 2.4 kW, designed to heat 13 m²) and an oil fan heater (power: 3.2 kW, designed to heat 16 m²) were employed as the representative fossil-fuel heating system which had already operated inside the general living space. In *Case (ii)*, a ceramic heater (FPS1, Yarkar Ceramic Co., Ltd.) was employed as the heating source instead of the fossil-fuel heating system because the heating source had to be controlled remotely.

R1234yf, R32 and R410A were employed as the test refrigerants. The amount of leaked refrigerant was 800 g, which was based on the amount of refrigerant contained in most commercial air conditioning systems (NITE, 2010). In addition, two leak rates were used: 10 g/min and 60 g/min as the set value.

In this experiment, the concentrations of the refrigerant and hydrogen fluoride (HF) that was produced by combustion or thermal decomposition were measured using Fourier transform infrared spectroscopy (FT-IR, JASCO, FT-IR4200).

5.3.1.3 Summary

Major findings obtained by the experiments in this scenario are as follows:

- (1) Even if all of the A2L refrigerant installed inside a room air conditioning system leaked and remained inside the model general living space (about 7.8 m²), no flame propagation was observed across the entire room because the refrigerant concentration inside the room did not exceed the lower flammable limit (LFL).
- (2) If a refrigerant came into contact with the heated body of the radiative stove or open flame of the fan heater, HF concentration greater 3 ppm, which is the maximum limit of permissible concentration, was generated regardless of the variety of refrigerant including R410A, which is the representative refrigerant now in use.
- (3) For the case with the radiative stove, the HF concentration increased with the operation of the air conditioning system and an increase in the leak rate. However, for the case with the fan heater, this trend was not always confirmed.
- (4) HF concentration for the case with the fan heater was greater than that that with a radiative stove.

5.3.2 Scenario #2: Service and maintenance situations

5.3.2.1 Sub-scenario (a): Physical hazard evaluation by smoking inside the space in which an A2L refrigerant accumulated

Outline In this scenario, we evaluated the physical hazard for the case that a commercial portable gas lighter was used inside a space in which an A2L refrigerant leaked and accumulated at the service and maintenance factory. The possibility of ignition from the heat of the cigarette tip was ignored because this type of ignition rarely occurs even for methane gas which is well-known for being a highly flammable gas (Holleyhead, 1996).

Mixture composition of the lighter fuel/A2L refrigerant/air Because details of the method used for determining the mixture composition of the lighter fuel/A2L refrigerant/air was described in the previous progress report (Imamura et al, 2013) and reference (Imamura et al, 2013), only an outline is provided in this report.

We assumed n-butane was the fuel of gas lighter, and the mixture of n-butane and A2L refrigerant could be regarded as a single fuel gas. This mixture is called “*fuel mixture*” in this section. The flammable zone of this *fuel mixture* in air was estimated simply using the Le Chaterlier’s relation and assuming that the concentration of n-butane at the outlet of the lighter must exceed the LFL. As a result, the concentration of the *fuel mixture* was within the estimated flammable zone when the A2L refrigerant with concentration less than LFL was mixed with n-butane and air. We focused on the mixture having this composition.

Experiment The operation device for a portable gas lighter, which consisted of a pneumatic cylinder (SSD-X, CKD Corp.) and jig was located 300 mm above the bottom of the acrylic pool with dimensions of 1000 mm cube at the center of horizontal plane. Air for the operation was supplied remotely using a solenoid valve at a pressure of 0.15

MPa. A piezo gas lighter and commercial turbo gas lighter were employed as the ignition source. R1234yf, R1234ze(E), and R32 were employed in the evaluation. The A2L refrigerant was leaked in a downward direction from a height of 750 mm above the bottom of the pool. The target leakage rate was 10 g/min for all of refrigerants. The refrigerant concentrations at the 6 vertical positions (0, 100, 300, 500, 750, and 1000 mm in height from the bottom of the acrylic pool) were measured using FT-IR before pushing the button of the piezo gas lighter. The vertical distribution of the refrigerant concentration was constant for heights less than 500 mm. The operation to push the button of the lighter was maintained for 2 or 10 s per cycle. This operation was repeated for 5 or 9 cycles at intervals of 5 s per cycle. The situation at the lighter outlet was observed using a digital video camera (SANYO Xacti, 30 fps).

Summary

(1) Piezo gas lighter

For the case of the accumulated A2L refrigerant with a LFL concentration, a pale quick emission was observed near the outlet of the lighter, but the pale emission was quenched 1/30 s later. The flame propagation to the entire refrigerant in surroundings was not observed. For the case of the accumulated A2L refrigerant with a concentration of LFL/2, an open flame was generated at the gas lighter for several cases. However, the flame also failed to propagate to the entire refrigerant. These trends were also confirmed for the other refrigerants.

(2) Turbo gas lighter

For R1234yf and R32, the ignition property was nearly identical to the case using a piezo gas lighter. However, for R1234ze(E) with almost an LFL and 71% R.H., a small flame propagation to the refrigerant in surroundings was confirmed for several cases. Afterwards, the experiment was performed using identical conditions, but flame propagation was not confirmed. Although the apparent reason for this trend has not been verified, it was considered to be that the concentration of refrigerant at the outlet of a lighter may have decreased due to the repeated operation of pushing the button, so that the flame generated at the outlet of the lighter propagated to the refrigerant. However, the flame did not propagate to the entire refrigerant in surroundings, it was so quenched 1 - 2 s afterwards.

5.3.2.2 Sub-scenario (b): Physical hazard evaluation when an A2L refrigerant leaks from a pinhole or fracture in a pipe or hose

Outline In this scenario, we assumed the situation that an A2L refrigerant leaked from a fracture or pinhole formed in pipes or hoses during the factory service and maintenance. We evaluated whether some ignition possibilities for the entire refrigerant jet leaked from a fracture or pinhole when there is an ignition source such as an electric spark near the refrigerant jet. We also evaluated the severity of the refrigerant jet igniting. The results of this scenario are reported in the references (Imamura et al, 2013, 2014).

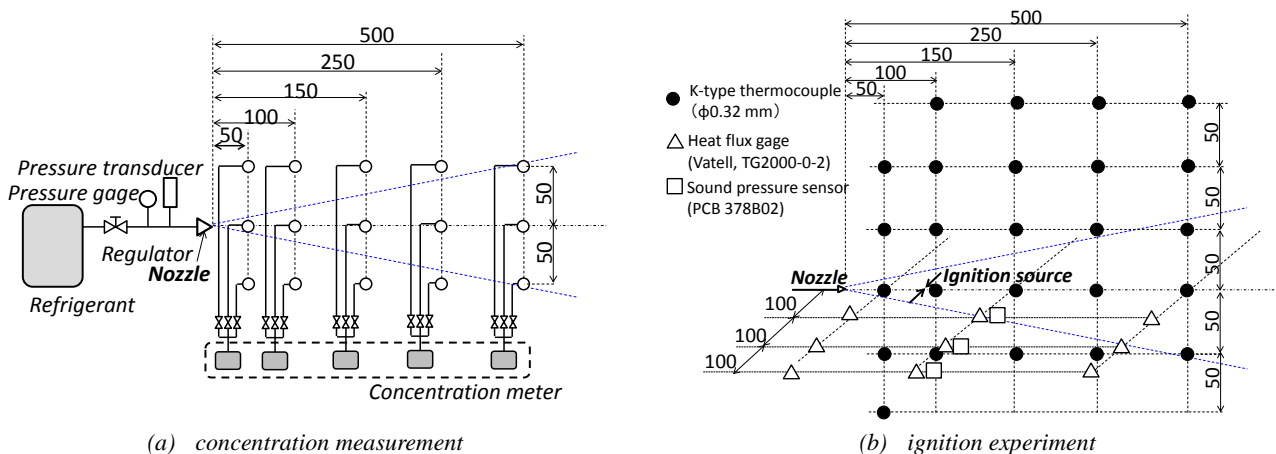


Figure 2 Schematic diagram of measuring positions. (Scenario #2, sub-scenario (b))

Experiment

(1) Refrigerant leakage system

The model leakage system consisted of a refrigerant cylinder, balance, regulator, pressure gage, and pinhole unit. These components were connected by copper and stainless tubes. The outside diameter of these tubes was 6.35 mm ϕ (1/4"). The leak pressure was monitored by a pressure gage (Swagelok, PGI63B-MG2.5-LAQX) and strain gage type pressure transmitter (PGS-20KA, Kyowa Electric Instruments, Co., Ltd.). The pinhole was modelled using a cap type coupling (1/4", Swagelok SS-400-C) with a hole in the center. Two patterns were used for the hole shape: a circular pinhole and rectangular slit. The pinhole diameter was 0.2, 1.0, 3.0, and 4.0 mm ϕ , and the dimension of the rectangular slit was 1.0 mm x 4.0 mm. The 4.0 mm ϕ pinhole diameter is assumed to be the very severe accident case, i.e., the pipe or hose is broken. Two patterns were set for the direction of the rectangular slit: the longer side was oriented either vertically or horizontally.

(2) Concentration measuring system

Before conducting the ignition experiment, concentrations of the leaked refrigerant jet were measured using five ultrasonic gas analyzers (US-II-T-S, Daiichi Nekken Co., Ltd.). The measured positions of concentration were at 50, 100, 150, 250, and 500 mm in the downstream direction and -50, 0, 50 mm in vertical direction from the center of a pinhole, i.e., the concentrations of refrigerant were measured at 15 positions, as shown in Figure 2(a). The positive value of the height indicates an upward vertical direction from the same center height of a pinhole. Refrigerant concentrations were measured for 30 s at each position because the refrigerant concentration approximately attained a uniform value within a period of less than 30 s after opening the valve.

(3) Ignition experiment

In the ignition experiment, a single spark (DC), a continuous spark (AC) and an open flame were employed as the ignition source. A single spark was generated using a high-voltage system (MEL1140B, Genesis Co., Ltd.): the energy of the spark was approximately 10 J. A continuous spark was generated using a neon transformer (CR-N16, Kodera Electronics, Co., Ltd.). The open flame length was about 50 mm. These ignition sources were located 90 mm downstream from the center of a pinhole with the same height as the center of the pinhole. Temperatures (25 points, by K-type thermocouples with 0.32 mm ϕ), heat fluxes (9 pieces of thermogage, TG2000-2, Vatell Co., Ltd.) and sound pressures (3 pieces of microphone, PCB, 378B02) were measured. The measured positions of these parameters are shown in Figure 2(b).

(4) Experimental conditions

R1234yf, R1234ze(E), and R32 were used as the test refrigerant. The leak pressure and amount rapidly decrease with time because the temperature of the leaked refrigerant decreases owing to adiabatic expansion. Therefore, the repeatability of the mass flow rate and amount was not always well. However, for the actual accident situation of a pipe breaking, it is considered to be that the leak pressure and amount will decrease similar to this experiment. In the actual situation for the service and maintenance, it is considered to be that the pipe of 1/4" ϕ of outside diameter is generally used, so the leakage from hole of 4 mm ϕ diameter is corresponds to very severe accident case. In addition, though the leakage of refrigerant with vapor pressure is comparatively smaller than the maximum pressure of refrigerant in the air conditioning system in operation, the operation of the air conditioning system will be suspended in the service and maintenance. Therefore it is considered to be that the cases that refrigerant leaked from 4 mm ϕ diameter of pinhole with the vapor pressure are assumed very severe accident cases.

Summary

(1) Formation of flammable zone

Figure 3 shows the iso-concentration maps of the refrigerant concentration. The iso-concentration curve is drawn for every 2.5 vol% except for Figure 3(d), which is drawn for every 1.0 vol%. The iso-concentration curve of 12.5 vol% for Figures 3(a), (b), (e), and (f) and 5.0 vol% for Figures 3(c) and (d) which correspond to a concentration slightly lower than LFL (R32: 13.5 vol%, R1234yf: 6.8 vol% (Takizawa et al, 2009)) are shown as bold curves.

Figures 3(a) and (c) show the iso-concentration maps for the 4 mm ϕ pinhole without a pressure regulator and assuming that the refrigerant directly leaked from a pipe fracture as the conceivable very severe accident case. The tip of the bold curve only reached the 100 mm downstream position from a fracture, and the end of the

bold curve in vertical direction only reached less than ± 50 mm. In short, the flammable zone was only formed locally even for the conceivable very severe accident case.

Figures 3(b) and (d) show the iso-concentration maps for the 0.2 mm ϕ pinhole without a pressure regulator and assuming that the refrigerant leaked from a pinhole or crack formed in the pipes or hoses. A flammable zone was no longer formed. According to Figures 3(e) and (f), influences of the direction of the rectangular slit on the forming of a flammable zone were hardly confirmed.

(2) Ignition and flame propagation

Figure 4 shows the photos when the leaked refrigerant jet came into contact with the AC continuous discharge, i.e., the ignition source. When the refrigerant leak began, a pale emission near the electrode was observed (Figure 4(a)). Then, the pale emission became larger with time as it traveled downstream away from the ignition source, as shown by the open circles in Figures 4(b) and (c). However, because the temperature of the leaked refrigerant decreased with time and the leaked refrigerant was fogged, the pale emission vanished with time (Figure 4(d), (e)). When the time increased further and the leaked refrigerant jet was steady, a pale emission became visible again. However, the flammable zone was only formed around the electrode, and the flame propagation to entire the refrigerant jet was not observed (Figure 4(f)). In the actual situation for the service and maintenance, the energy by electrostatic discharge and friction spark discharge can be considered as the representative ignition source. However, the maximum energy by these ignition sources is less than 1 J. Even if the A2L refrigerant leaked from the fracture of pipe assuming the very severe accident case, the possibilities of ignition and flame propagation of A2L refrigerant by the conceivable ignition source in the actual situation is extremely low. Because the ignition and flame propagation were not confirmed in the present experiment, an energy of 10 J, which is higher than that in the actual situation was provided to the A2L refrigerant.

5.3.2.3 Sub-scenario (c): Physical hazard evaluation when an A2L refrigerant leaks inside a device for the service and maintenance

Outline In this scenario, we assumed that the A2L refrigerant leaked in a device for the service and maintenance such as the collection device. We experimentally evaluated whether the A2L refrigerant is ignited by spark discharge from the electric relay inside the device. The results of this scenario are reported in the references (Imamura et al, 2013, 2014).

Experiment The model collection device, i.e., an acrylic pool of 1000 mm cube was produced assuming that the A2L refrigerant leaked in the device for the service and maintenance. The results obtained in the present experiment will provide more dangerous results than the actual situation because the model collection device will be larger than that in the actual situation. The model collection device consisted of five pieces of acrylic board (thickness: 2 mm) and a sheet of vinyl to relieve the pressure rise in the model collection device due to the combustion of the refrigerant. In the actual situation, a slit is fixed to the collection device to prevent the accumulation of refrigerant in the device if the refrigerant leaks. Therefore, in the present experiment, a pair of slits on the facing planes of the model collection device was fixed.

The refrigerant concentration in the model collection device was measured using the ultrasonic gas analyzers (US-II-T-S, Daiichi Nekken Co., Ltd.) before ignition. The measuring positions were at the center in the horizontal and at 0, 100, 250, 500, and 750 mm in height. The refrigerant leaked in the upward vertical direction from the 4 mm ϕ outlet without the pressure regulator assuming the very severe accident case. The leak rate was approximately 400 g/min, and the leak period was 1 min. The width of the facing slit was varied 0, 1, 5, 10, and 20 mm.

In the ignition experiment, a DC spark (Yokogawa Denshikiki Co., Ltd., 16J) was used as the ignition source. The ignition source was located at the center of the model collection device. The DC spark was generated 30 s after the refrigerant leakage stopped. This DC spark was generated six times per second.

Summary

(1) Concentration distribution in the model collection device

For $w_s = 0$ mm (w_s : slit width), the refrigerant concentration immediately increased after leakage began and

continued to increase. After the refrigerant leakage ceased 60 s later, the refrigerant concentration slightly decreased and then it maintained a uniform value. After that the time variation of the refrigerant concentration was barely observed. It was considered to be that the leaked refrigerant accumulated and remained in the model collection device.

For $w_s = 1$ mm, after the refrigerant leakage ceased, the refrigerant concentration maintained a uniform value,

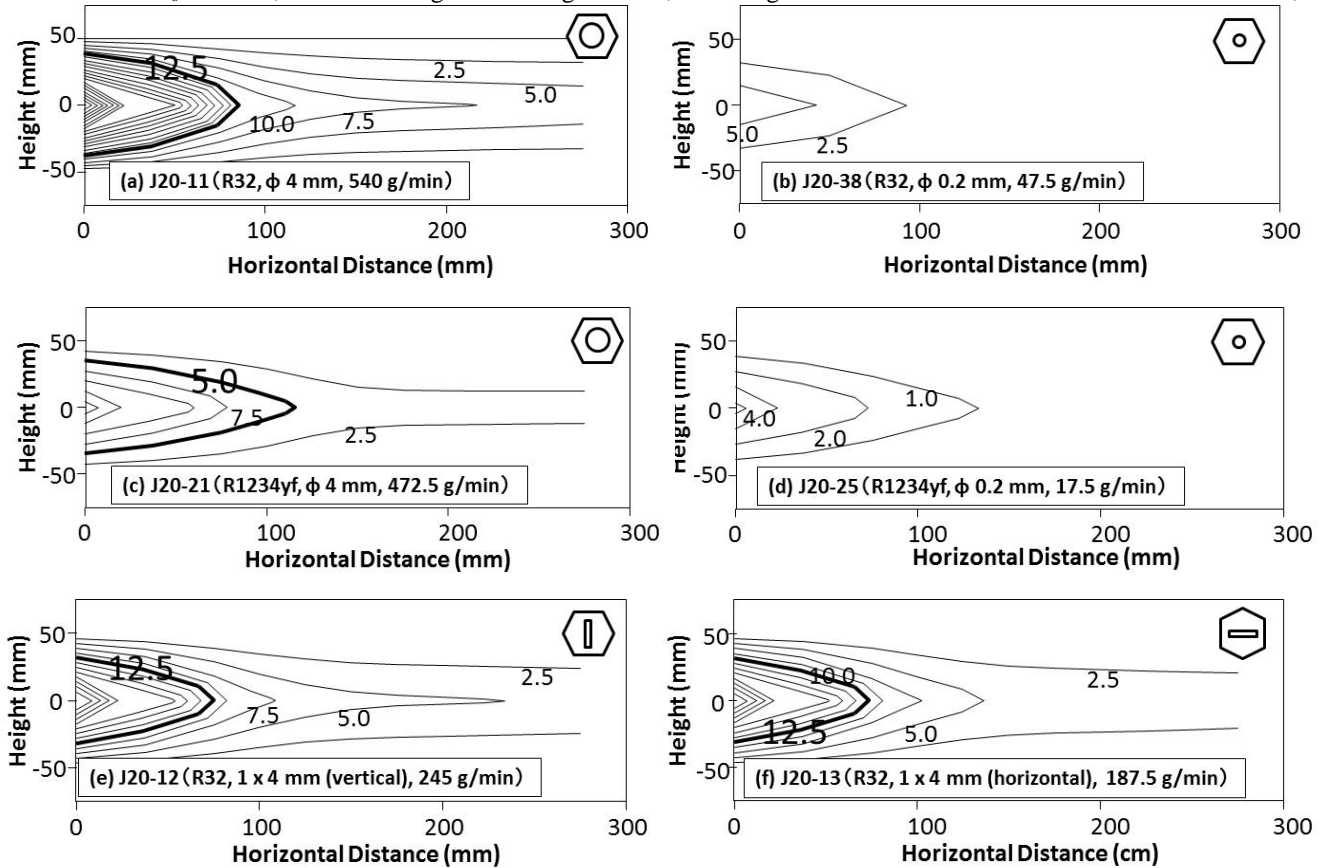


Figure 3 Iso-concentration maps near the leaked refrigerant jet. The number in these maps indicates the concentration of refrigerant (vol%)

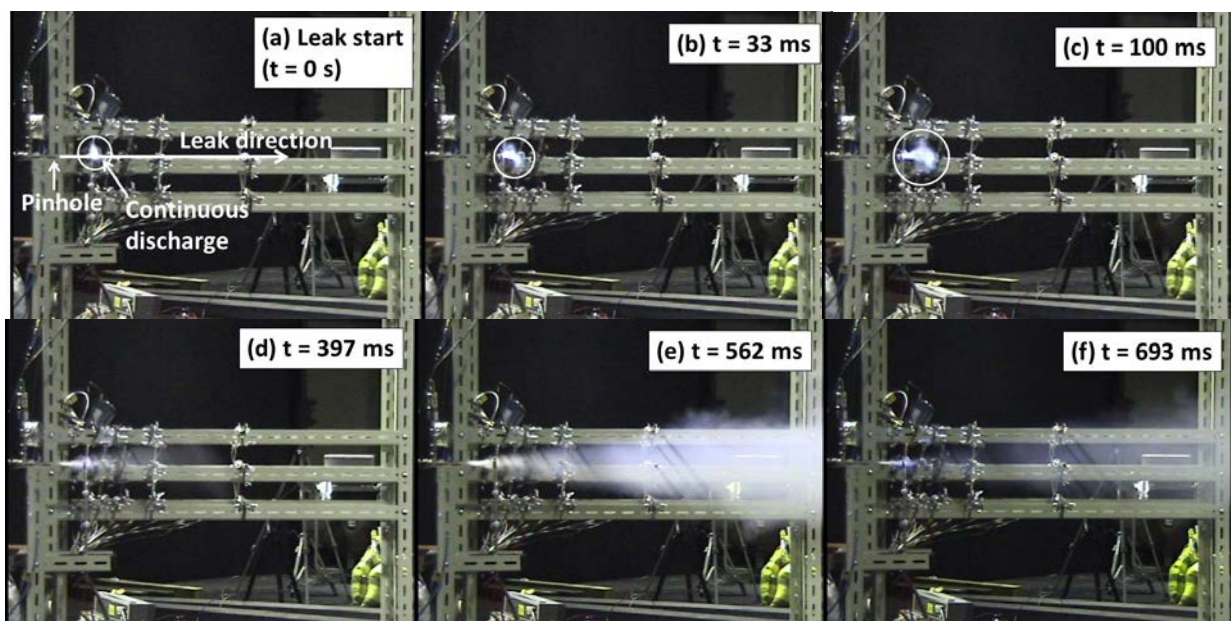


Figure 4 Photographs of the leaked refrigerant jet coming into contact with the AC spark discharge. Refrigerant: R32, Pinhole diameter: 4 mm ϕ , Leak rate: 413 g/min

and then the concentration slowly decreased. The concentration at the comparatively higher position ($z = 750$ mm and 500 mm) decreased with time because the refrigerant diffused to the outside through the facing slit. However, the decrease in concentration with time near the bottom ($z = 0$ mm and 100 mm) was slower than that at the higher positions ($z = 750$ mm and 500 mm). The period when the refrigerant concentration at $z = 500$ mm, which is the ignition source was located exceeded the LFL was about 480s.

For $w_s = 20$ mm, after the refrigerant leakage ceased, the concentration of refrigerant immediately decreased monotonously with time. The trend that the concentration was easy to decrease with time at higher positions was confirmed. The period when the refrigerant concentration at $z = 500$ mm exceeded the LFL was about 60 s.

(2) Ignition and flame propagation

Figure 5 shows photos of the model collection device with no slit ($w_s = 0$ mm). R1234yf around the ignition source ignited and a pale flame propagated in upper vertical direction with buoyancy generated by the flame of the R1234yf. The R1234yf flame approached at the ceiling of the model collection device, and then propagated downward. However, flame did not immediately propagate towards the unburned R1234yf because the burning velocity of R1234yf is very small and oxygen, which is needed to burn, was in short supply. Thus, the pale flame and unburned R1234yf balanced at a certain height. After that a sheet of vinyl that covered a side plane burned and fresh air flowed into the model collection device. Then, the flame propagated through the entire model collection device.

For the actual situation, the conceivable ignition source is the spark discharge at the electrical device inside the collection device. The maximum energy contained in this spark discharge is a few mJ. The ignition and flame propagation as shown in Figure 5, are confirmed with 16 J of energy, which is too stronger than the above spark discharge in the actual situation. In other words, the energy of the spark generated in this experiment is much larger than that in the actual situation. Therefore, the ignition and flame propagation, as seen in Figure 5, for the actual situation is extremely low even if the refrigerant leaked and accumulated inside the collection device.

On the other hand, for $w_s = 20$ mm, ignition and flame propagation were not observed although the ignition spark was generated in the period when the refrigerant concentration exceeded the LFL. This was because the refrigerant in the model collection device flowed with a particular velocity in the model collection device. It was considered to be that the burning velocity of R1234yf is very small (1.2 cm/s (Takizawa, et al, 2009)): therefore, the flame cannot propagate to the entire R1234yf in the model collection device.

5.3.3 Scenario #3: A2L refrigerant was installed in a VRF system

5.3.3.1 Outline

In Scenario #3, we evaluated the physical hazard when A2L refrigerant installed in a VRF system leaked. In this fiscal year, we focused on clarifying the properties of the flame behavior, blast wave pressure, temperature, and heat flux

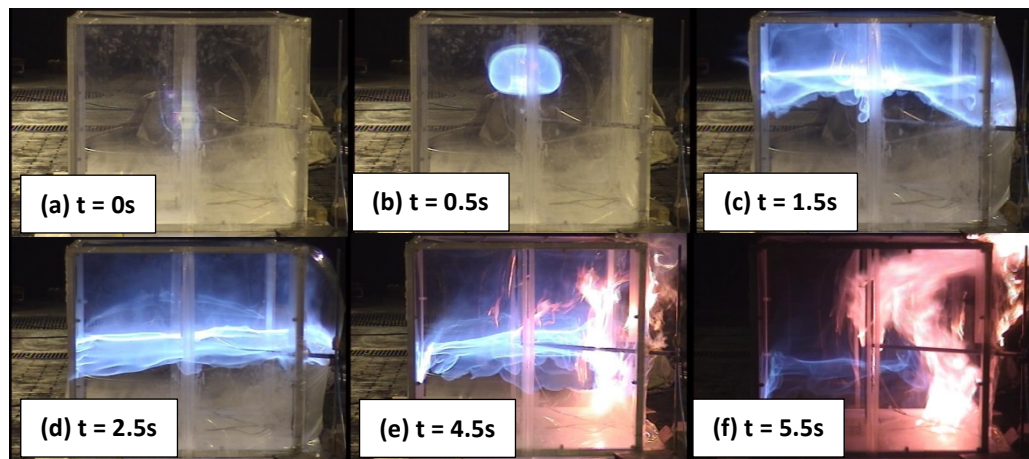


Figure 5 Photographs of the accumulated refrigerant inside the model collection device. Slit width: $w_s = 0$ mm, Refrigerant: R1234yf, Leak rate: 380 g/min, Leak amount: 380 g

originating from the combustion of the A2L refrigerant as well as clarifying the scale effect of these properties by a series of laboratory-scale experiments. We focused on two accident cases: (a) the A2L refrigerant leaked into the space where the ignition source already existed (called “*Case (i)*”), and (b) the ignition source was generated inside the space where the A2L refrigerant has already accumulated (called “*Case (ii)*”).

5.3.3.2 Experiment

Experimental equipment

An acrylic pool, i.e., 1000 mm cube (with 10 mm thickness board), was developed for the model space. Each face of this pool was covered by the acrylic boards, but there was an opening of 300 mm x 600 mm in the ceiling. This opening was covered with a ceramic flange in which a thermogage (TG-2000, Vatel Corp.) and K-type thermocouple (0.32 mm ϕ) were installed. The face of the flange, thermogage, and tip of thermocouple were located at the same level. A microphone (378B02, PCB, Inc.) was set at 500 mm near the wall of the pool to measure the pressure of the blast wave generated by the combustion.

Methods of refrigerant leakage

The refrigerant was leaked in the vertical downward direction through the copper tube with 1/4” outside diameter. The leak height was varied 0, 500, 750, 1000 mm high above the bottom of the pool. The leak rate was set to approximately 10 and 60 g/min for *Case (i)* and 10 g/min for *Case (ii)*. The concentrations of the refrigerant at 6 vertical positions (0, 100, 300, 500, 750, and 1000 mm in height) were measured by FT-IR before conducting the ignition experiment. R1234yf and R32 were used as the test refrigerant. The amount of leak refrigerant was set so that the concentration at the position of ignition source (300 mm in height) achieves LFL, C_{st} , a little higher than C_{st} . The variable of C_{st} indicates the stoichiometric concentration.

Ignition source

For *Case (i)*, a commercial candle with a flame length of approximately 20 mm was used as the ignition source. In *Case (ii)*, a commercial match was employed. The tip of the match was put on the Ni-Cr hot wire coil. An AC10V voltage was supplied to this Ni-Cr hot wire coil through an AC transformer. Then, the match was ignited by the energy from the Ni-Cr hot wire coil. After a match was ignited, the power supply to the Ni-Cr hot wire coil was immediately cutoff. In addition, the Ni-Cr hot wire coil without a match was also used as the ignition source to simulate the more severe scenario.

5.3.3.3 Summary

Distribution of the refrigerant concentration

For the refrigerant leaked near the bottom of the pool, the refrigerant concentration exhibited a comparatively high concentration at $z = 0$ m (near the bottom), and the concentration decreased with height. In short, there was the slope of concentration in vertical direction. This slope of concentration became easy as the leak height rose. The concentration slope under 750 mm in height was almost uniform regardless of height in the case of 1000 mm of leak height (leakage from ceiling).

Combustion behavior

(1) *Case (i)*

For the 10 g/min for leak rate, ignition and flame propagation to the entire accumulated refrigerant were not confirmed, and the candle flame went out automatically. For this case, significant increases in the pressure of the blast wave, heat flux, and temperature were not observed. However, for 60 g/min, a small flame propagation to the accumulated refrigerant was confirmed.

(2) *Case (ii)*

For a match flame as the R1234yf ignition source, the accumulated refrigerant ignited for all leak heights. The humidity was around 50 % R.H. for all cases. The handstand cone shape flame formed, and this flame moved and propagated in an upward vertical direction owing to the buoyancy originating from the flame itself. The flame was maintained for some time after coming into contact with the pool ceiling. A significant increase in the pressure of the blast wave was observed. The maximum temperature increase was about 900 °C. The flame

propagation to the accumulated refrigerant under the ignition source was not observed.

For a Ni-Cr hot wire coil as the R1234yf ignition source, ignition and flame propagation were not confirmed for all cases. For these cases, the humidity was about 20 - 30 %R.H. This indicates: such that the ignition and flame propagation greatly depended on the humidity not the ignition source.

For R32, it was ignited using both a match flame and Ni-Cr hot wire coil. The humidity of these cases was 30 - 60 % R.H., and the influence of humidity on the combustion behavior of R32 was hardly confirmed. A flattened fireball shape flame formed near the ignition source. Afterwards, the flattened fireball flame rose with the buoyancy, which originated from flame itself, and collided with the ceiling. The flame remained at the ceiling for some time, after that it automatically quenched. The significant increases in the blast wave, temperature, and heat flux were observed. These parameters were greatly affected by the leak height. The pressure of blast wave obtained for 500 and 750 mm height exhibited comparatively higher values. Because there were large amounts of refrigerant that exceeded the LFL located at the space above the ignition source.

However, at most, pressure of the blast wave only corresponds to the phenomena that the 10 mm thick acrylic board was slightly lifted. The pressure of the blast wave that breaks the acrylic pool (1m³ cube) was not generated.

5.4 Conclusions

5.4.1 Scenario #1: Simultaneously used with a fossil-fuel heating system

In this scenario, no flame propagation to the entire refrigerant was observed and HF generation as much as R410A, i.e., the present representative refrigerant was confirmed. More HF was generated when there were some flows inside the room.

5.4.2 Scenario #2: Service and maintenance situation

- (1) We conducted the physical hazard evaluation assuming that a serviceman used a portable gas lighter to smoke where the A2L refrigerant accumulated. It was verified that there are several possibilities that the mixture composition of a lighter fuel/A2L refrigerant/air exceeds the LFL. However, although the ignition experiment using a commercial piezo gas lighter was conducted above the estimated mixture composition, no ignition and flame propagation were observed in any of the tested refrigerants (R1234yf, R1234ze(E), R32). For a commercial turbo gas lighter, ignition and flame propagation near the outlet of the lighter was observed for some R1234ze(E) cases. The relative humidity in this case was 71 % R.H. and room temperature was 19 °C. However, the flame quickly went out, and a blast wave pressure capable of breaking an acrylic pool was not confirmed.
- (2) We conducted the physical hazard evaluation assuming that the A2L refrigerant leaked from a fracture or pinhole in the pipes or hoses. Even if the refrigerant leaked from a 4 mm ϕ pinhole, which is the conceivable very severe accident case, a flammable zone was only formed locally around the pinhole for all test refrigerants. Even if the energy is much larger than that of an electrostatic and spark discharge which are possible in actual situations, the flame propagation to the entire refrigerant jet was not observed, and significant increases in blast wave pressure, heat flux, temperature, and HF concentration were not confirmed. Therefore, even if the A2L refrigerant leaked from the pipe fracture, the possibility of ignition and flame propagation of the A2L refrigerant by the conceivable ignition source in the actual situation is extremely low.
- (3) We conducted the physical hazard evaluation assuming that the A2L refrigerant leaked into the device for the service and maintenance. If there was no structure to diffuse the leaked and accumulated refrigerant, the leaked refrigerant in the device accumulated and remained long time. It could be ignited, and the flame could propagate the entire device by a strong spark of 16 J. However, the possibilities of ignition and flame propagation of the accumulated refrigerant are extremely low because the generation of that much energy is hardly in actual situations. In addition, the minimum ignition energy of the A2L refrigerant is much larger than the spark discharge energy generated from the electrical device in the collection device. If there was a slit with a width greater than 20 mm, the accumulation of the refrigerant inside the device could be immediately

prevented, and most of the ignition and flame propagation could be prevented.

5.4.3 Scenario #3: A2L refrigerant was installed in a VRF system

We conducted the physical hazard evaluation assuming that the A2L refrigerant leaked from a VRF system in the laboratory-scale experiment. The distribution of refrigerant concentration in a pool greatly depended on the leak height. The trend that large slope of concentration in vertical direction was confirmed so that the leak height was lower. In the ignition experiment, the flame propagated upward in the vertical direction, and significant increases of the blast wave pressure, temperature, heat flux, and HF concentration were confirmed. It was found that the scale of the flame propagation and increases of these parameters depend on the amount of refrigerant that exceeded LFL located above an ignition source. However, the pressure of blast wave slightly lifted the 1000 mm x 1000 mm x 10 mm (12 kg weight) acrylic board. The pressure of the blast wave that breaks the acrylic pool (1m³ cube) was not generated.

Acknowledgements

This study has been conducted as a part of the “Technology Development of High-Efficiency Non-fluorinated Air Conditioning Systems” research project and performed by the New Energy and Industrial Technology Development Organization (NEDO). The authors would like to sincerely thank Dr. Tatsuya Miyashita a former graduate student of Tokyo University of Science, Mr. Hiroyuki Mitsuishi, Dr. Yohsuke Tamura and Mr. Masayuki Takeuchi of Japan Automobile Research Institute (JARI), Mr. Takanori Morimoto, Dr. Kyoko Kamiya and Mr. Yuta Yamazaki of Japan Specialist in Law Engineering Corporation, and Mr. Shunta Nakamura and Mr. Shunsuke Mashimo undergraduate students at the Tokyo University of Science, Suwa for their kind supports with the experiments.

References

- Holleyhead, R.: “Ignition of Flammable Gases and Liquids by Cigarettes: a Review”, *Science and Justice*, 36(4), (1996), pp.257-266.
- Imamura, T. and Sugawa, O.: Physical hazard evaluation of A2L-Class Refrigerants using Several Types of Conceivable Accident Scenarios, Risk assessment of mildly flammable refrigerants 2012 Progress Report (2013), pp.35-42.
- Imamura, T., Miyashita, T., Kamiya, K., Morimoto, T. and Sugawa, O.: Physical hazard evaluation for using air conditioning systems having low-flammable refrigerants with the fossil-fuel heating system at the same time, *Transactions of the Japan Society of Refrigerating and Air Conditioning Engineers*, Vol.29, No.4 (2012), pp.401-411 (in Japanese).
- Incorporated Administrative Agency National Institute of Technology and Evaluation (NITE): <http://www.prtr.nite.go.jp/prtr/pdf/estimation23/syosai/syosai23t.pdf>, (2010), (in Japanese).
- Imamura, T., Miyashita, T., Kamiya, K. and Sugawa, O.: Ignition hazard evaluation on leaked A2L refrigerants by commercial-use electronic piezo lighter, *Journal of Japan Society for Safety Engineering*, Vol.52, No.2 (2013), pp.91-98 (in Japanese).
- Imamura, T., Morimoto, T., Yamazaki, Y., Kamiya, K., Mitsuishi, H. and Sugawa, O.: Experimental study on ignition hazards of leaked A2L refrigerant from a pinhole, *Proceedings of Asia Pacific Symposium on Safety 2013*, Singapore (2013), Paper No.C3-03.
- Imamura, T., Kamiya, K. and Sugawa, O.: Ignition hazard evaluation on A2L refrigerants in situations of service and maintenance, 10th International Symposium on Hazards, Prevention, and Mitigation of Industrial Explosions, Bergen (2014), submitted.
- Takizawa, K., Tokuhashi, K. and Kondo, S.: Flammability assessment of CH₂=CFCF₃: Comparison with fluoroalkenes and fluoroalkanes, *Journal of Hazardous Materials*, Vol.172 (2009), pp.1329-1338.

6. Progress Report of Research Institute for Innovation in Sustainable Chemistry, AIST

6.1 Introduction

This research involved evaluating the flammability of low-GWP refrigerants under practical conditions and the development of an ignition energy evaluation method for them. The flammability properties of these refrigerants were evaluated under various temperature and humidity conditions considering their practical applications, and their safety in terms of flammability was compared with that of nonflammable refrigerants currently in use. The ignition energy evaluation method was developed to improve the current situation, where there is a wide variation in published ignition energy values for mildly flammable compounds, in order to provide a reliable index on fire risk. In this report, we describe our progress on these three subjects.

6.2 Evaluation of flammability under practical conditions

6.2.1 Temperature and humidity dependence of flammability properties

(a) Temperature and humidity effects on flammability limits of several 2L refrigerants: The effects of temperature and humidity on the flammability limits of refrigerants are important because the refrigerants are used under various conditions. Typical 2L compounds were measured following the ASHRAE method. Table 6.1 lists the observed temperature coefficients of the flammability limits. In general, the temperature dependence of the flammability limits can be explained by White's rule. According to this rule, the lower and upper flammability limits are expressed by the following equations:

$$L = L_{25} \left\{ 1 - \frac{100C_{p,L}}{L_{25} \cdot Q} (t-25) \right\} \quad \text{and} \quad U = U_{25} \left\{ 1 + \frac{100C_{p,L}}{L_{25} \cdot Q} (t-25) \right\} \quad (6.1)$$

where L_{25} and U_{25} are the lower and upper flammability limits (vol%) at 25 °C, respectively; $C_{p,L}$ is the heat capacity of unburned gas at the lower flammability limit; and Q is the molar heat of combustion of the fuel gas.

Table 6.1: Temperature dependence of flammability limits of several 2L refrigerants

Refrigerant	LFL		UFL	
	Obs.	Pred.	Obs.	Pred.
R717	-0.0086	-0.0095	0.0208	0.0189
R32	-0.0070	-0.0064	0.0091	0.0133
R143a	-0.0051	-0.0038	0.0080	0.0093
R1234yf (dry)	-0.0133	-0.0029	0.0102	0.0052
R1234yf (wet)	-0.0045	-0.0028	0.0098	0.0071
R1234ze(E) (wet)	-0.0104	-0.0029	0.0174	0.0061

As presented in the above table, the temperature dependences of the flammability limits for ammonia, R32, and R143a basically agree with the values predicted by the above equations. However, the temperature dependences of the

flammability limits of R1234yf and R1234ze(E) were considerably larger than those predicted by the equations. With regard to the humidity effect on the flammability limits, measurements were performed over a humidity range of 0%–90% corrected for a temperature of 23 °C. The flammability limits of ammonia, R32, and R143a were found to not be greatly affected by the humidity of air. On the other hand, the flammable ranges of R1234yf and R1234ze(E), whose molecules contain more F-atoms than H-atoms, were found to be markedly dependent on the humidity. Figure 6.1 shows the humidity effect on the flammability limits of R1234yf and R1234ze(E).

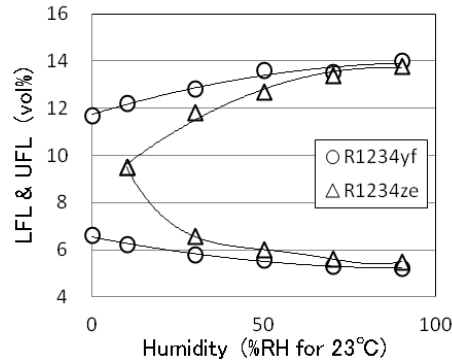


Figure 6.1: Humidity effect on flammability limits of R1234yf and R1234ze(E)

All the measurements were performed at 35 °C.

(b) Flammability property of non-flammable refrigerants under high humidity conditions: The effect of relatively high humidity (i.e., up to 50% at 60 °C) on the flammability property in air was measured for R410A, R410B, R134a, and R125. The measurements were performed following the ASHRAE method. Under this humidity condition, R410A, R410B, and R134a became flammable, whereas R125 did not. For the first three samples, the limiting humidity condition to make the gas flammable was determined. In addition, the effect of temperature up to 100 °C was examined for these materials at a relative humidity of 50% corrected for a temperature of 23 °C. The results showed that all four samples remained non-flammable under this condition. Table 6.2 lists the observed flammability limits of R410A, R410B, and R134a at a relative humidity of 50% and temperature of 60 °C.

Table 6.2: Flammability properties of R134a, R410A, and R410B at a relative humidity of 50% and temperature of 60 °C

Refrigerant	LFL		UFL	
	vol%	±	vol%	±
R134a	11.5	0.3	15.9	0.4
R410A	15.6	0.2	21.8	0.4
R410B	16.3	0.3	20.9	0.4

(c) Flammability limits for binary mixtures of ammonia with multi-fluorinated compounds: Flammability limits for binary mixtures of ammonia with R1234yf, R1234ze(E), R134a, and R125 were measured in dry air. The measurements were made using the ASHRAE method. The flammability limits of ammonia and R1234yf mixtures were found to be very different from the values predicted by Le Chatelier’s equation. Le Chatelier’s equation was modified by introducing an ellipse function to analytically express the flammability limits of the mixtures of arbitrary concentrations as follows:

$$1/L = (c_{am}/L_{am}) \left(1 + p_1 c_{yf} + p_2 \sqrt{c_{yf} - c_{yf}^2} \right) + (c_{yf}/L_{yf}) \left(1 + p_3 c_{am} + p_4 \sqrt{c_{am} - c_{am}^2} \right) \quad (6.2)$$

where L , L_{am} , and L_{yf} are the flammability limits of the mixture, ammonia, and R1234yf, respectively. c_{am} and

c_{yf} are the fractions of ammonia and R1234yf, respectively, in the mixture, and $c_{am} + c_{yf} = 1$. p_1-p_4 are parameters that are adjusted to appropriately explain the observed values. Figure 6.2 compares the observed and calculated values for ammonia/1234yf mixtures; the open circles represent the observed values, the solid lines show the calculated values, and the dotted lines show the values predicted by Le Chatelier's equation.

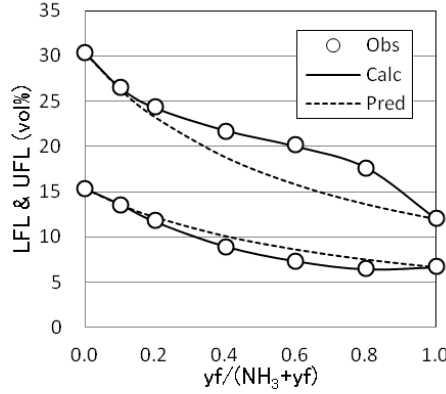


Figure 6.2: Flammability limits for R717/R1234yf mixtures
All the measurements were performed at 35 °C.

R1234ze(E) was found to be non-flammable in dry air but flammable if more than 4% ammonia was added. If the ammonia content exceeded 20%, the flammability limits became very close to the corresponding ones for R1234yf and ammonia. In contrast, the flammable regions of ammonia mixed with those of R134a and R125 were much narrower than the mixtures of R1234ze(E). The ellipse-modified Le Chatelier's equation was extended to successfully explain the flammability limits of these mixtures as follows:

$$1/L = (x_{am}/L_{am}) \left(1 + q_1 x_{ze} + q_2 \sqrt{x_{ze} - x_{ze}^2} \right) + (x_{ze}/L_{FIP}) \left(1 + q_3 x_{am} + q_4 \sqrt{x_{am} - x_{am}^2} \right) \quad (6.3)$$

where L and L_{am} are the flammability limits of the mixture and ammonia, respectively, and L_{FIP} is the limiting mixture concentration at FIP. $x_{ze} = c_{ze} f$ and $x_{am} = 1 - x_{ze}$, where f is the extension factor and c_{ze} is the fraction of R1234ze(E) in the mixture. q_1-q_4 are parameters that are fitted to the observed values. Note that Equation (6.3) coincides with Equation (6.2) when f is equal to unity. Figure 6.3 compares the observed and calculated flammability limits of the ammonia/1234ze(E) mixtures. In this case, FIP was located at c_{ze} 0.96; therefore, the extension factor became 1.04. The flammability limits of ammonia/134a and ammonia/125 mixtures can also be explained by using the above equation.

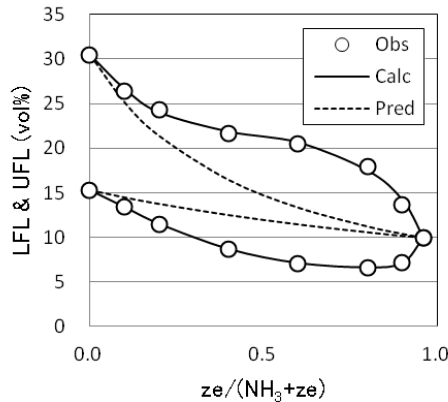
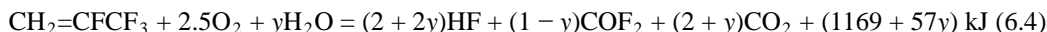


Figure 6.3: Flammability limits for R717/1234ze(E) mixtures
All the measurements were performed at 35 °C.

(d) Humidity effects on burning velocity of several 2L refrigerants: The combustion reaction of R1234yf with the surrounding air is expressed by the following equation:



where y denotes the moles of water vapor in the gas mixture.

Since the fluorine-to-hydrogen ratio of R1234yf molecules is higher than unity, excess fluorine produces COF_2 without proceeding to HF formation when in dry air. With the addition of a hydrogen-supplying compound such as water vapor into the reaction system, fluorine can produce HF, which increases the heat of combustion. When the F/H ratio becomes unity, the heat of combustion becomes maximum. Similar behavior was expected for R1234ze(E) in moist air, but the heat of combustion was slightly lower than in the case with R1234yf.

Figure 6.4 shows the dependence of S_u on the refrigerant concentration at the absolute humidity of 0.03 g-water/g-dry air. For both R1234yf and R1234ze(E), S_u showed similar tendencies as the refrigerant concentration and reached its maximum at slightly refrigerant-lean conditions. $S_{u,\text{max}}$ was ca. 6 cm s^{-1} for 1234yf and 5 cm s^{-1} for 1234ze(E). S_u may continue to increase with the absolute humidity until 0.052 g-water/g-dry air, as suggested by the increased heat of combustion in Equation (6.4). For comparison, a similar flammability test was done for R32 in moist air. The heat of combustion was unchanged by humidity because R32 has an F/H ratio of unity. The stoichiometric S_u in moist air at an absolute humidity of 0.022 g-water/g-dry air was 6.7 cm s^{-1} , which is almost the same as $S_{u,\text{st}}$ of 6.6 cm s^{-1} in dry air. Thus, humidity does not affect the flammability of R32.

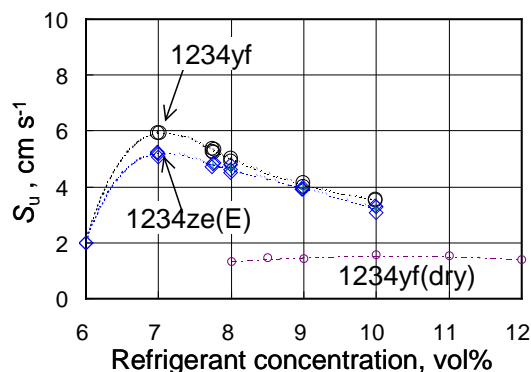


Figure 6.4: Concentration dependence of S_u at 25°C for R1234yf and R1234ze(E) in moist air at absolute humidity of 0.03

The flammability of R1234yf may increase with the humidity until the overall $F/(H + F)$ in the gas mixture reaches 0.5. However, it was difficult to obtain the worst case at the ambient temperature because of the difficulty with controlling the high humidity. Instead of water vapor, we used ammonia as the hydrogen-supplying compound. Figure 6.5 shows the $S_{u,\text{st}}$ vs. mixing ratio of the hydrogen-supplying compound for the R1234yf- NH_3 system. Similar to the R1234yf- H_2O system, $S_{u,\text{st}}$ of R1234yf+ NH_3 increased with the added NH_3 and became maximum at R1234yf: $\text{NH}_3 = 1:1$. The corresponding $S_{u,\text{st}}$ was 8.6 cm s^{-1} , which is even higher than the $S_{u,\text{max}}$ of pure NH_3 .

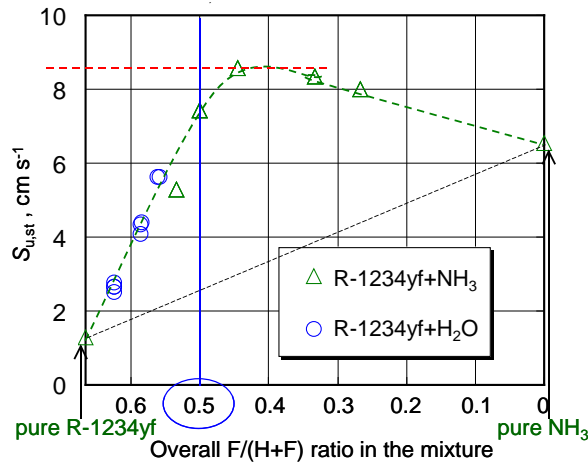


Figure 6.5: $S_{u,st}$ vs. mixing ratio of hydrogen-supplying compound: R1234yf–H₂O and R1234yf–NH₃.

(e) Humidity effect on quenching distance of R1234yf: Details on the quenching distance measurement are described in section 6.3. In this section, we discuss the humidity effect on the quenching distance of R1234yf. Experiments were conducted at 25 °C in dry air and 60 °C in moist air. First, we determined the concentration that provides the optimum $d_{q,h}$ to be 8.8 vol% at 50% RH. Second, we fixed the R1234yf concentration at 9 vol% and measured $d_{q,h}$ over a wide range of humidity. Figure 6.6 shows the humidity effect on $d_{q,h}$ for R1234yf. When moisture was added to the gas mixture, $d_{q,h}$ decreased dramatically. $d_{q,h}$ became less than 5 mm at ca. 40% RH, which corresponded to an overall F/H ratio of ca 1.0.

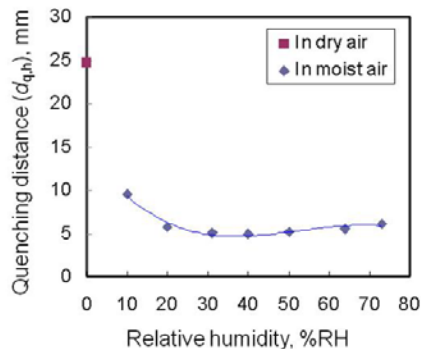


Figure 6.6: Humidity effect on quenching distance of R1234yf. Dry conditions: 25 °C and 10 vol% in microgravity. Wet conditions: 60 °C and 9 vol% in Earth gravity.

As discussed above, the flammability limits, burning velocity, and quenching distance of R1234s became worse as the humidity of air increased. This is because these compounds have a much higher F/H ratio than unity and H₂O molecules supply H atoms to the reaction system. If these compounds are used at the optimum humidity, their flammability will exceed that of ammonia. Thus, care should be taken when R1234yf and R1234ze(E) are mixed with a compound having an F/H ratio of less than 1.0, such as ammonia. Such a mixture will show higher flammability than expected from the individual components.

6.2.2 Flammability evaluation in comparison with nonflammable refrigerants in use

(a) Toward establishment of index on degree of non-flammability: Many refrigerants are mixtures of a few different compounds. They usually contain non-flammable components. At present, however, there is no way of estimating the degree of non-flammability. Thus, we recently introduced the concept of limiting methane

concentration (LMC): the minimum methane concentration to be added to non-flammable gas to make the mixture flammable. On the other hand, to establish an index to measure the degree of non-flammability, an indicator is needed that varies linearly with the mixing ratio of the added non-flammable component to a selected standard flammable gas. The F-number is known to greatly deviate from linearity with decreasing flammability when mixed with a non-flammable component. Instead, we introduce the new F2-number, which is defined by the following equation:

$$F2 = (U - L)^2 / UL \quad (6.5)$$

This value is the square of the normalized flammable range and approximates the strength of the combustion power.

The next question is how to select a standard flammable gas. For the above LMC, methane was selected as the standard gas. However, as was apparent for ammonia, which was considered in the preceding section, methane is not necessarily a good standard gas. This is because methane as ammonia has excess hydrogen atoms in the molecule, so interactions occur between combustion reactions if they are mixed with molecules having excess fluorine atoms. Therefore, we adopted R32 as a standard gas as it has equal numbers of hydrogen and fluorine atoms in the molecule. Figure 6.7 plots the F2-number against the mixing ratio of various gases to R32. The top one is for nitrogen and carbon dioxide; the middle one is for methane, R152a, and R1234yf; and the bottom one is for R1234ze(E), R134a, and R125. The linearity was good for nitrogen and carbon dioxide; fair for methane, R152a, R125, and R134a; and poor for R1234yf and R1234ze(E).

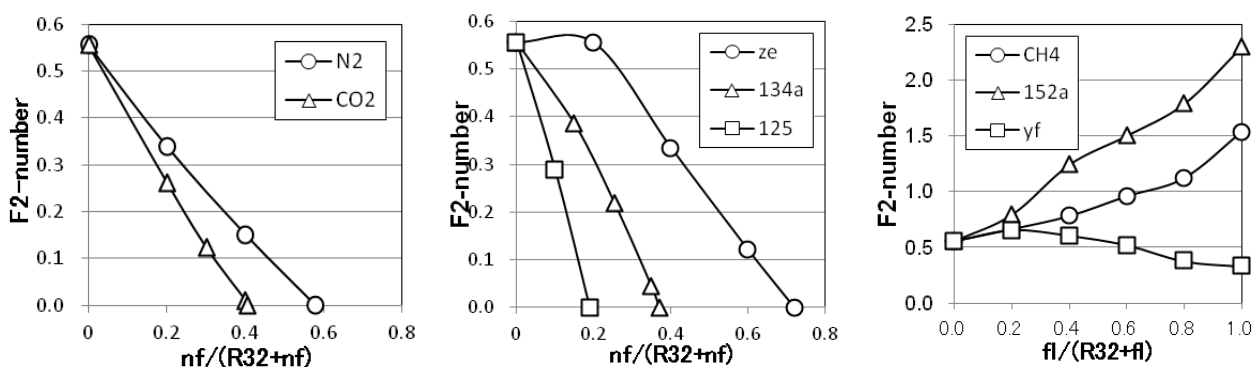


Figure 6.7: F2-number versus mixing ratio of various gases to R32

(b) Thermal decomposition of refrigerants: The effects of the R1234yf concentration and total flow rate on the thermal decomposition of R1234yf were investigated by using a flow reactor. The thermal decomposition of R1234ze(E) and R22 was studied at $\phi = 1$ and a total flow rate of $100 \text{ cm}^3/\text{min}$. Figure 6.8 shows a schematic diagram of the experimental apparatus. The flow rates of the refrigerant and air were measured and controlled by calibrated mass flow controllers, and the refrigerant/air mixture was continuously supplied to a heated tube reactor (Inconel, 12.7 mm outer diameter, 10.2 mm inner diameter, 44 cm length). The reaction temperature was measured by thermocouples (1 mm outer diameter, Type K) that were inserted in the tube (Inconel, 3.175 mm outer diameter, 1.4 mm inner diameter, 62 cm length) at the center of the reactor tube. The concentrations of the refrigerant and decomposition products such as HF were measured by using FT-IR (cell length was 10 cm, ZnSe windows). The O_2 concentration was measured by GC (TCD detector, Ar carrier, 3 mm diameter \times 3 m length SUS column packed with Molecular Sieve 13X-S, column temperature of $30 \text{ }^\circ\text{C}$). To adjust the IR intensity, N_2 was added to the reaction gas immediately behind the reactor. The gas was treated with soda lime before being introduced to GC. The exhaust gas was also treated with soda lime. The experiment was started at room temperature, and the temperature was increased in a stepwise fashion. The refrigerant, O_2 , and products were measured under steady-state conditions.

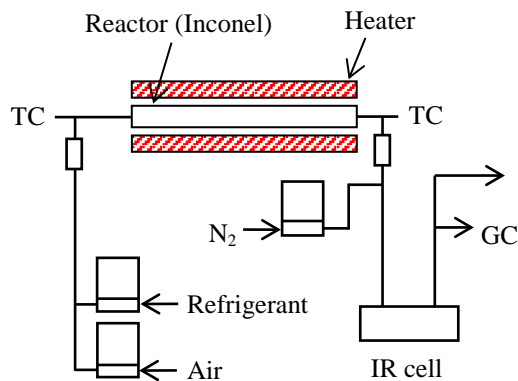


Figure 6.8: Schematic diagram of experimental apparatus

The dependency of the thermal decomposition on the R1234yf concentration was studied at concentrations of 1.0 vol% ($\phi = 0.12$) to 15.0 vol% ($\phi = 2.10$) at a constant total flow rate (100 cm³/min). Figures 6.9 and 6.10 show the thermal decomposition results of R1234yf for R1234yf = 1.0 and 15.0 vol%, respectively. Here, O₂ consumption and products such as HF were based on the supplied mole of R1234yf. R1234yf was observed to decompose at a certain temperature depending on the concentration and total flow rate, and the decomposition considerably increased at this temperature. For R1234yf = 7.8 vol% ($\phi = 1.0$), decomposition of R1234yf was observed at around 600 °C or higher, and the decomposition temperature increased with decreasing R1234yf concentration (decomposition temperature for R1234yf = 5.0, 3.0, 2.0, and 1.0 vol% were around 620–630, 630–640, 660–720, and 670–770 °C, respectively). On the other hand, the decomposition temperature did not change if $\phi > 1$, as shown in Figure 6.10. The major products were HF, COF₂, CO₂, and CO; O₂ consumption and products such as HF increased with the decomposition rate of R1234yf. No detectable differences were observed between the clean reactor and reactors that had been used in previous experiments. The dependency of the thermal decomposition on the total flow rate was studied between 20 and 200 cm³/min at a constant R1234yf concentration of 7.8 vol%. When the total flow rate was increased, the decomposition temperature was also found to increase (decomposition temperatures for total flow rates of 20, 50, 100, and 200 cm³/min were around 570–580, 600 or slightly lower, 600, and 630 °C, respectively).

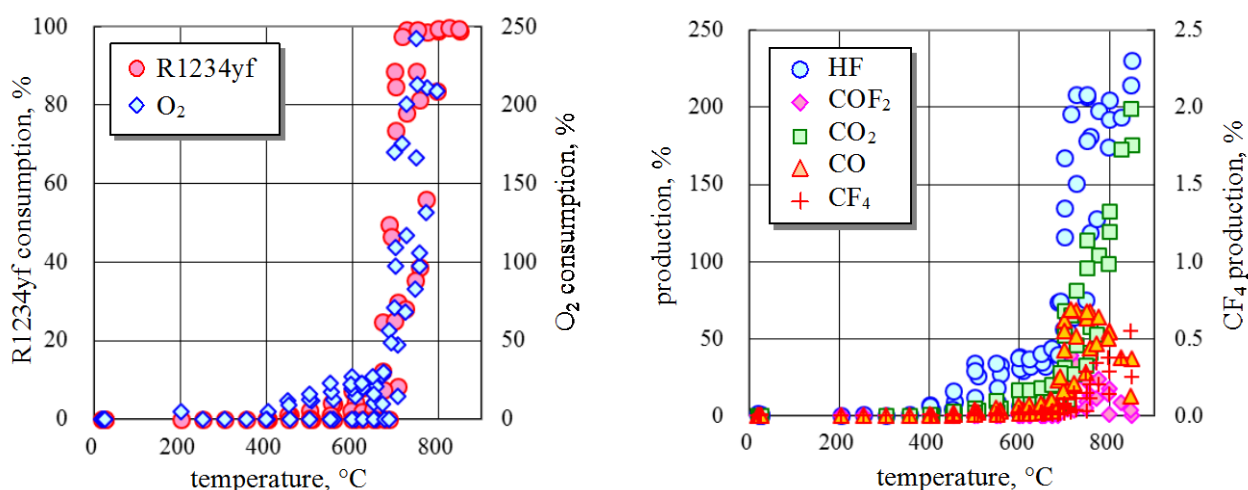


Figure 6.9: Results for thermal decomposition of R1234yf: R1234yf = 1.0 vol% ($\phi = 0.12$), total flow rate = 100 cm³/min

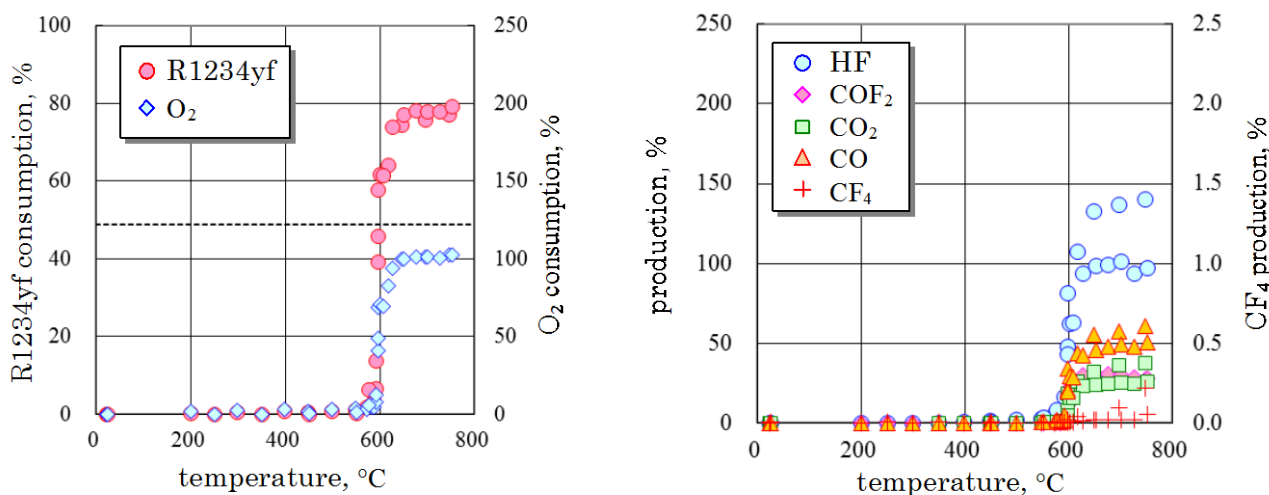


Figure 6.10: Results for thermal decomposition of R1234yf: R1234yf = 15.0 vol% ($\phi = 2.10$), total flow rate = 100 cm^3/min

Figure 6.11 shows the thermal decomposition results of R1234ze(E). R1234ze(E) was observed to decompose at 550 °C or higher, and consumption of O₂ and products such as HF were observed at 600 °C or higher when the clean reactor was used in the experiment. When a contaminated reactor was used in the experiment, however, R1234ze(E) was observed to decompose at 350 °C or higher, whereas consumption of O₂ and products such as HF were not observed up to around 550 °C. The reproducibility of the consumption rate for R1234ze(E) at 350–550 °C was good; however, the open small symbols in Figure 6.11 represent the results of three experiment runs, and the amounts of decomposition products in the reactor may have differed. Note that, at 550–600 °C, R1234ze(E) consumption was observed; in contrast, O₂ consumption and products were not observed in this temperature range if a clean reactor was used. Therefore, in this temperature range, the consumption of R1234ze(E) may be affected by trace amounts of decomposition products. When the reactor tube was contaminated by more than the threshold value of decomposition products, the temperature for decomposition initiation of R1234ze(E) decreased by approximately 200 °C; the decomposition of R1234ze(E) did not depend on the amount of decomposition products that was attached to the reactor tube.

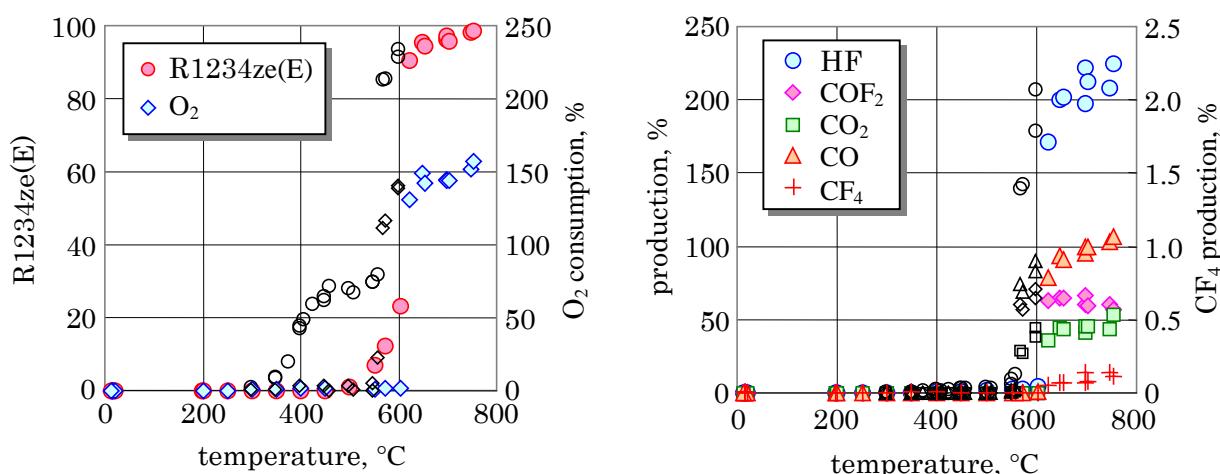


Figure 6.11: Results for thermal decomposition of R1234ze(E): R1234ze(E) = 7.8 vol% ($\phi = 1$), total flow rate = 100 cm^3/min . Open small symbols represent measurements taken when decomposition products contaminated the reactor

Figure 6.12 shows the thermal decomposition results of R22. The consumption of R22 and O₂ and products such as HF were observed at 450 °C or higher when a clean reactor was used for the experiment. At 450–650 °C, the consumption

and production gradually increased with increasing temperature. When a contaminated reactor was used for the experiments, R22 consumption was observed at 300 °C or higher, whereas O₂ consumption and products such as HF were not observed up to around 450 °C. At 450 °C or higher, no differences between clean and contaminated reactors were observed for O₂ consumption and production such as HF. When a contaminated reactor was used, a large scatter was observed for R22 consumption at 300–600 °C. Thus, R22 consumption may depend on the amount of decomposition products.

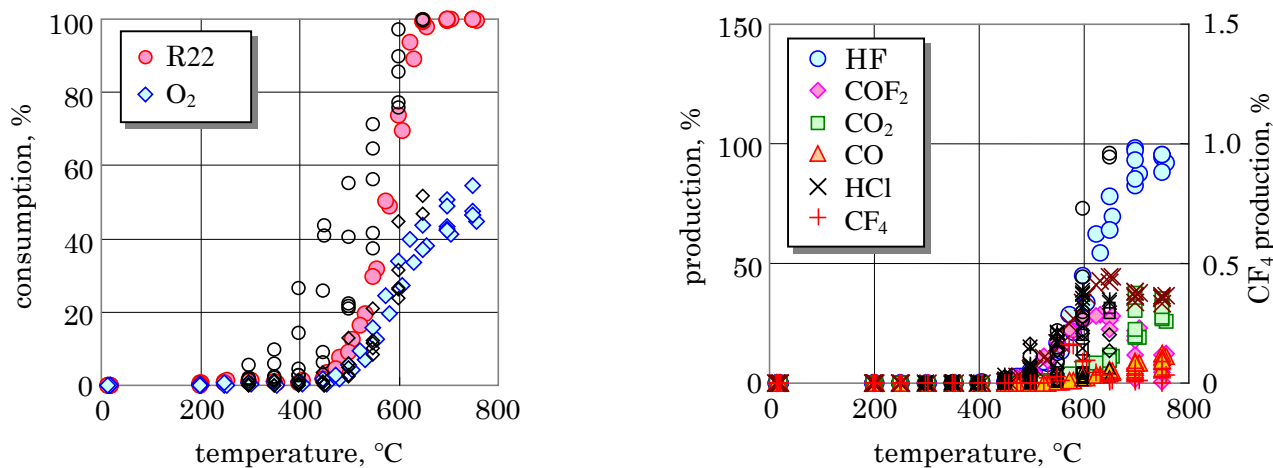


Figure 6.12: Results for thermal decomposition of R22: R22 = 21.9 vol% ($\phi = 1.0$), total flow rate = 100 cm³/min. Open small symbols represent measurements taken when decomposition products contaminated the reactor

6.3 Development of ignition energy estimation method

6.3.1 Estimation of minimum ignition energy

For 2L compounds with a maximum burning velocity ($S_{u,max}$) of less than 10 cm s⁻¹, the reported E_{min} varies widely from below 10 mJ to over 10 J. This makes assessing the fire risk based on E_{min} very difficult. The difficulty in determining a reliable E_{min} lies in the fact that E_{min} is very dependent on the electrode size, the gap between the electrodes, and the ignition spark density and duration. Compared to E_{min} measurement, d_q measurement seems to be much easier and provide more reliable data for mildly flammable compounds. Therefore, we first carry out comprehensive measurement of d_q for compounds having a wide variety of flammability intensities and then attempt to estimate E_{min} by using the experimental burning velocity (S_u) and d_q . To obtain a test method appropriate for determining d_q of various compounds under equivalent test conditions, we tested various conditions such as the geometry and size of the electrodes.

(a) Quenching distance measurement: The experimental setup and procedure were similar to ASTM-E582. The target compounds were the highly to only mildly flammable 11 compounds listed in Table 6.3. For the combustion vessel, the cylinder (inner diameter; 160 mm, length; 150 mm) was made of acrylic plastic. The cathode electrode was fixed, whereas the anode electrode could be moved with a micrometer to provide an adjustable gap within 0.001 mm. The parallel plates were made of machinable glass ceramic (Macor) instead of the borosilicate glass specified in ASTM-E582. The plates could be removed from the electrodes; we tested plates with diameters of 5, 25, 50, 75, and 100 mm to examine the effect of the plate size on d_q . We judged whether ignition could be achieved between the parallel plane plates. We obtained d_q by changing the gap between the plates with a micrometer. d_q was determined as the average value between the maximum gap width at which flame propagation could not be observed in ten successive

experiments and the minimum gap width at which flame propagation could be observed within ten successive experiments.

Because the slowly propagating flame was significantly affected by the buoyancy, we measured d_q both in the vertical position (i.e., same position as the ASTM-E582 apparatus) $d_{q,v}$ and in the horizontal position $d_{q,h}$ of the parallel plates. For R1234yf, a reliable $d_{q,h}$ has not yet been obtained. $d_{q,v}$ increased almost monotonically with increasing plate size, and we may not have determined the converged values. We performed a microgravity experiment at the AIST Hokkaido center to remove the buoyancy effects and obtain more reliable d_q for R1234yf.

Table 6.3: Measured quenching distance and estimated E_{\min} for 11 compounds

Name	Formula	$S_{u,\max}$, cm s ⁻¹	$d_{q,h}$, mm	$d_{q,v}$, mm	ϕ_{\min}	Estimated $E_{\min}^{b)}$, mJ	Calibrated $E_{\min}^{b)}$, mJ
Propane	C ₃ H ₈	38.7	1.70	1.70	1.13	0.35 (0.35)	0.247
Isobutane	(CH ₃) ₂ CHCH ₃	34.2	2.00		1.16	0.62	0.44
R152a	CH ₃ CHF ₂	23.6	2.33		1.17	0.90	0.63
1243zf	CH ₂ =CHCF ₃	14.1	3.33		1.24	2.2	1.5
HFC-143	CH ₂ FCHF ₂	13.1	3.58	3.48	1.30	2.9 (2.6)	2.0 (1.8)
R152a/134a (50/50vol%)	CH ₃ CHF ₂ /CH ₂ FCF ₃	11.7	4.08	3.88	1.29	3.8 (3.0)	2.7 (2.1)
HFC-254fb	CH ₂ FCH ₂ CF ₃	9.5	5.23	4.35	1.35	12 (5.3)	8.4 (3.7)
R143a	CH ₃ CF ₃	7.2	7.03	6.00	1.36	27 (13)	19 (9.4)
Ammonia	NH ₃	7.1	8.95	7.45	0.99	45 (19)	32 (14)
R32	CH ₂ F ₂	6.7	7.55	6.45	1.19	29 (14)	20 (9.8)
R1234yf	CH ₂ =CFCF ₃	1.5	24.75 ^{a)}	16.75	1.23	770 ^{a)} (80)	540 ^{a)} (56)

a) d_q measured in microgravity. b) number in parentheses is E_{\min} estimated from $d_{q,v}$. Others estimated from $d_{q,h}$. c) 11% reduction of adiabatic flame zone diameter $d_q - \delta$ to make the E_{\min} of propane equal to 0.247 mJ, which is the most cited value reported by Lewis and Von Elbe (1987).

First, we examined the effect of the size of the parallel plane plates on d_q . Figure 6.13 shows the results for seven compounds at the concentrations of the lowest $d_{q,h}$. For propane, the converged $d_{q,h}$ value was obtained by using plates with diameters of 25 mm or larger. For R32 and ammonia, however, the 25-mm diameter plates were not sufficiently large to obtain the converged $d_{q,h}$ values. The $d_{q,h}$ of R32 and ammonia were 5.95 and 6.85 mm, respectively, with 25-mm plates and 6.45 and 7.45 mm, respectively, with 100-mm plates in the vertical position. ASTM-E582 specifies that the plate diameter be 5–10 times the electrode gap, as indicated by the chain line in Figure 6.13; this appears to be reasonable based on the observations in the present study.

Table 6.3 lists the converged $d_{q,v}$ and $d_{q,h}$ for all of the compounds except R1234yf. For R1234yf, the $d_{q,v}$ and d_q in microgravity with 100-mm plates are listed, although the 100-mm diameter plates did not seem to be sufficiently large to obtain the converged d_q for R1234yf.

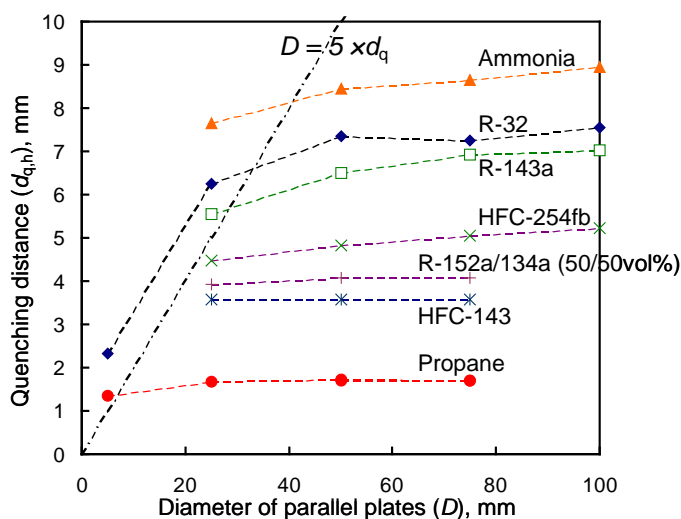


Figure 6.13: $d_{q,h}$ versus diameter of parallel plates

(b) Estimation of minimum ignition energy: The minimum ignition energy is the energy that is just necessary to establish the minimal flame sphere with the minimum radius necessary for self-sustained propagation. According to the simple heat loss theory proposed by Lewis and Von Elbe (1987), E_{\min} is written by

$$E_{\min} = (1/6)\pi d_{\min}^3 \rho_b c_p (T_b - T_u) \quad (6.6)$$

Here, d_{\min} is the diameter of the minimal flame in free space; ρ_b is the burned gas density; c_p is the average isobaric heat capacity; and T_b and T_u are the burned and unburned gas temperatures, respectively.

Solving Equation (6.6) requires T_b and the size of the minimal flame to be determined. Lewis and von Elbe (1987) postulated that the minimal flame has a diameter that is equal to the parallel plate quenching distance d_q and the same temperature as the adiabatic flame temperature T_{ad} . Their calculated E_{\min} qualitatively agreed with the experimental values for various compounds but was quantitatively several times greater than the experimental E_{\min} on average.

We examined the relationship between d_{\min} in Equation (6.6) and the parallel plate quenching distance d_q by measuring the minimum flame radius of the self-sustained propagating flame $r_{f,\min}$ for the R32/air mixture at 21 vol% ($\phi = 1.27$). Note that since the Schlieren technique visualizes the change in density, the r_f obtained from the Schlieren image includes the flame kernel radius and most of the flame thickness.

By comparing the measured quenching distance and minimum flame diameter for R32, the parallel plate quenching distance $d_{q,h}$ was found to be substantially equal to the minimum flame diameter $2r_{f,\min}$. Thus, the two different test results were confirmed to substantially represent the same quenching processes.

Based on the previous discussion, Equation (6.6) is rewritten as

$$E_{\min} = (1/6)\pi (d_q - 2\delta)^3 \rho_b c_p (T_b - T_u) \quad (6.7)$$

$$\delta = 2\lambda_{av} / (c_p \rho_u S_{u,\max}) \quad (6.8)$$

Here, we considered d_{\min} in Equation (6.6) to be the diameter of the flame kernel. Assuming that $T_b = T_{ad}$, E_{\min} was obtained from the experimental d_q and $S_{u,\max}$. The results are listed in the seventh column of Table 6.3. Overall, E_{\min} as estimated by Equation (6.7) was slightly higher than the lowest experimental E_{\min} values reported in the literature. However, the agreement between the calculated and experimental E_{\min} was considered to be better than that in the literatures. For propane, the estimated E_{\min} of 0.35 mJ was approximately 40% higher than the lowest experimental value of 0.247 mJ reported by Lewis and Von Elbe (1987) but well within the range of reported E_{\min} values. We calibrated the calculated E_{\min} by decreasing the flame kernel diameter ($d_q - 2\delta$) in Equation (6.7) by 11% so that the E_{\min} of propane would become the most cited value of 0.247 mJ; these values are listed in the eighth column of Table 6.3. Such calibration is justified considering the similarity in the minimal flame structures for all of the compounds.

For 2L refrigerants, the estimated E_{\min} was considerably lower than the values in the literature that were measured by the ASTM E582 method.

6.3.2 Flame extinction diameter

When an electrical component with openings, such as a circuit breaker or magnetic contactor, operates in a flammable gas atmosphere, the electric spark generated by the component can be an ignition source. Even though ignition occurs at the electrode gaps inside the enclosure, combustion will not be transmitted to the flammable gas atmosphere outside the enclosure unless the diameter of the opening of the enclosure exceeds the critical value d^* . In this report, we call d^* the “extinction diameter.” Figure 6.14 shows a schematic drawing of the apparatus for measuring the extinction diameter. Experiments were carried out in the same vessel used for the quenching distance measurement. A thin square PTFE plate with a circular opening was set at a distance h from the ignition point. The plate had a thickness of 1 mm. We observed whether the flame sphere could go through the opening.

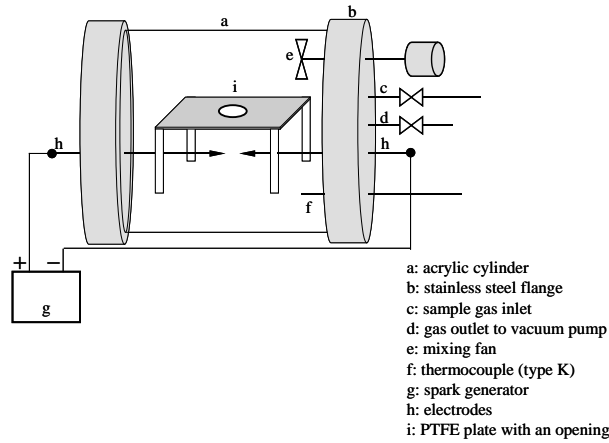


Figure 6.14: Apparatus for extinction diameter measurement

Figure 6.15 shows the measured d^* as a function of h for three 2L compounds: R32, R717, and HFC-254fb. In the small h region, d^* decreased rapidly with increasing h . As h increased further, d^* decreased gradually and finally reached an almost constant value. This tendency may reflect the formation process of stable flames.

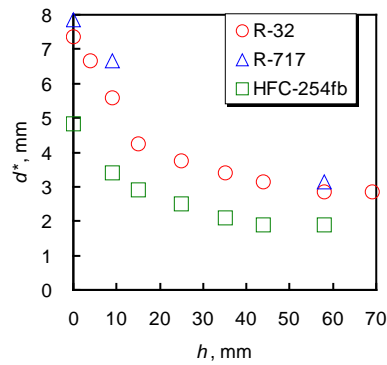


Figure 6.15: d^* vs. h for R32, R717, and HFC-254fb

Considering the application of d^* to practical risk assessment, the effect of the shape of openings on d^* is also of interest. We measured the flame extinction size of rectangular openings with aspect ratios (b/a) of 3 and 5 and generalized the extinction size by introducing the effective diameter (d_{eff}), which may be taken as the hydraulic diameter:

$$d_{eff} \equiv 4A/P, \quad (6.9)$$

where A is the cross-sectional area of the opening and P is the perimeter of the opening. For a circle, $d_{eff} = d$.

Figure 6.16 shows the results of 21 vol% R32/air using rectangular openings and circular openings as a function of h . The results of the rectangular openings agreed with those of the circular openings, which validated the introduction of the hydraulic diameter. Thus, we can generalize the extinction diameter of openings.

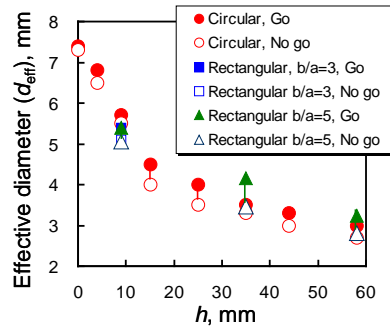


Figure 6.16: d_{eff} versus h for R32/air measured with various openings. Circle: circular opening. Square: rectangular opening with $b/a = 3$. Triangle: rectangular opening with $b/a = 5$. Filled symbols represent “go,” and open symbols represent “no go.”

Consider the application of d^* . Figure 6.17 compares the extinction diameters of several refrigerants with the openings of the electrical components. At $h = 9$ mm, the flame of propane could go through the opening with $d = 1.25$ mm. On the other hand, the flame of R32 could not go through the opening with $d = 5.5$ mm. This indicates that, if ignition occurs inside an electrical component, the propane flame will easily go through the small opening of the equipment and propagate outside the component, whereas the R32 flame will not go through the opening and will be extinguished within the component enclosure. If we measure h and d_{eff} of an electrical component and the combination of h and d_{eff} lies below the d^* curve of the refrigerants, as shown in Figure 6.15, the flame will not go through the opening. Otherwise, it will be necessary to change h and/or d_{eff} of the component for safety reasons until the combination falls below the d^* curve in Figure 6.15.

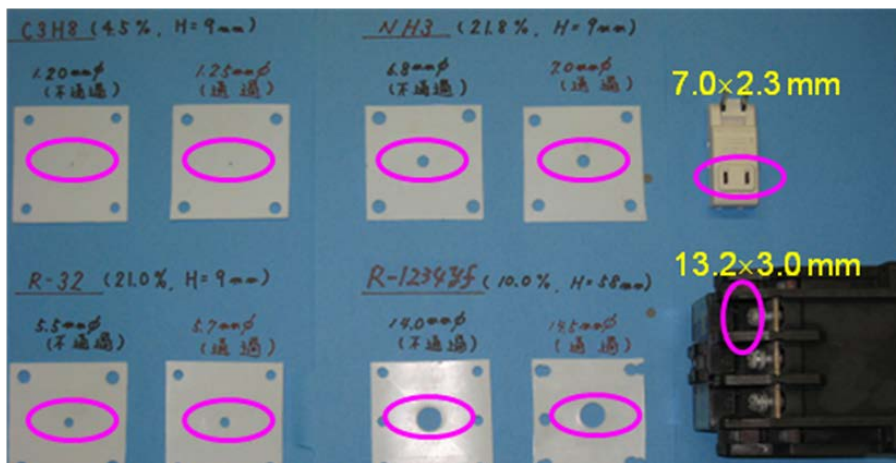


Figure 6.17: Comparison of extinction diameters (at $h = 9$ mm) with openings of electrical components.

6.3.3 Incendivity test using practical electrical components

An incendivity test was carried out by using a magnetic contactor (MC) connected with a high power load. The target refrigerants were R32 and R1234yf. Figure 6.18 shows the experimental apparatus and the MC inside the combustion vessel, which was connected with the motor. First, we removed the lid of the MC (blue part of Figure 6.18 (7)) and observed whether ignition occurred with the spark generated by disconnecting the MC. The spark energy was

approximately 4 J or lower, which is usually higher than the E_{\min} of the refrigerants listed in Table 6.3. In more than 300 trials, we observed only a single ignition for R-32. For R1234yf, we did not observe any ignition. With the lid, no flame propagation was observed for R32 and R1234yf. This result may be rationally explained by the larger extinction diameter of these refrigerants than the size of the opening of the MC.

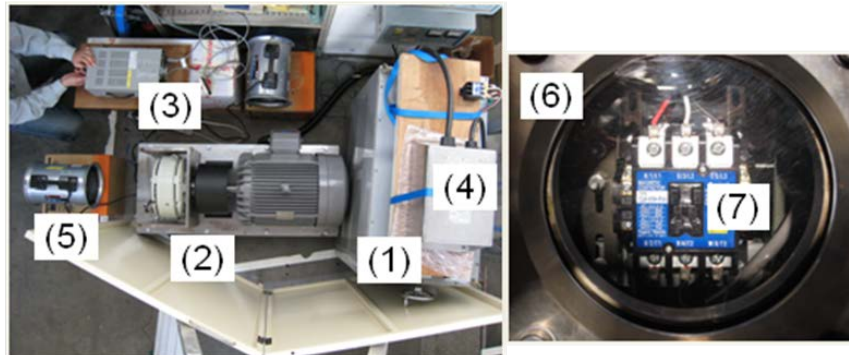


Figure 6.18: Experimental apparatus of incendiability test using magnetic contactor.

(1) Motor, (2) Loader using powder brake, (3) Load controller (power supply), (4) Slidac (voltage transformer, 200 and 220 V), (5) Cooling blower, (6) Cylindrical vessel (I.D. = 310 mm, L = 310 mm, V = 24.3 L) (7) Magnetic contactor (65 A rating)

6.3.4 Summary of ignition energy evaluation

Based on the above experimental results, we found the following:

- 2L refrigerant compounds with $S_{u0,max}$ below 10 cm s^{-1} have E_{\min} that is greater than that of propane by more than an order of magnitude. E_{\min} is greater than the spark energy from the human body.
- 2L refrigerants have a quenching distance that is more than three times that of propane. Thus, electrical components will frequently generate sparks for gaps narrower than d_q of 2L refrigerants. In such cases, the conductive heat loss to the electrodes will significantly increase the energy necessary for ignition of the 2L refrigerant. This may be one of the main reasons why R32 ignition occurred very rarely with a magnetic contactor that had a spark energy that was much greater than the E_{\min} of R32.
- 2L refrigerants have a flame extinction diameter several times larger than that of propane. Even though there are small openings on the enclosures of potential igniters such as magnetic contactors and sockets, the flame of 2L refrigerants cannot go through the openings, and such igniters will not become an ignition source of the refrigerant.

References

Lewis, B., Von Elbe, G., 1987, "Combustion, Flames and Explosions of Gases", Third ed., Academic Press, New York, p. 333-361.

7. Physical Hazard Assessment on Explosion and Combustion of A2L Class Refrigerants

Difluoromethane (R32, CH₂F₂) and 2,3,3,3-tetrafluoropropene (R1234yf, CH₂=CF₂CF₃) have zero ozone depletion potential (ODP) and low global-warming potential (GWP). In particular, R1234yf has a low GWP of less than 150, as established by EC (2012); thus, these two compounds are expected to be the next generation of refrigerants. Although these refrigerants perform better than existing refrigerants in terms of lower ODP and GWP, they exhibit a mild flammability. Thus, evaluating the combustion safety of A2L refrigerants in the event of leakage into the atmosphere due to an accident is necessary. To address the issue of global warming due to conventional refrigerants, ASHRAE (2010) defined the optional Class 2L to classify refrigerants with lower flammability and is preparing to promote the conversion of air-conditioning equipment from conventional refrigerants to the next generation of refrigerants. In this study, the experimental flammability of gases such as R32 and R1234yf was analyzed by using a large spherical combustion vessel to evaluate their fundamental flammability characteristics and assess their safety. Flammability properties such as the flame velocity, burning velocity, and deflagration index were evaluated. The effects of flame lifting due to buoyancy and humidity on the flammability characteristics were considered. A numerical simulation and combustion model were developed to estimate the potential risk of combustion and explosion in actual situations, and the autoignition temperature of A2L/2L refrigerants was determined.

Symbols

dP/dt	rate of pressure rise (100 kPa/s)
K_G	deflagration index for gases (100 kPa m/s ²)
P	pressure (100 kPa)
P_{red}	reduced maximum pressure (as a result of venting)
V_{vessel}	volume of the vessel (m ³)
T	temperature (K)
S_f	flame speed (cm/s)
S_u	burning velocity (cm/s)
t	time (s)

Greek

ϕ	equivalent ratio
ρ	density (kg/m ³)

Subscripts

u	unburned gas
b	burned gas
0	at standard temperature and pressure/at initial condition
max	maximum value
μg	under micro gravity

7.1 Combustion and explosion assessment for A2L/2L

To utilize these mildly flammable gases safely, ASHRAE (2010) added the optional 2L subclass to the existing Class 2 (lower flammability) to classify the safety of refrigerants. R32 and R1234yf are classified as A2L refrigerants, which are defined as having low toxicity and low flammability with a maximum burning velocity of ≤ 10 cm/s. A2L refrigerants have such a low burning velocity that a lifted flame front due to buoyancy significantly affects their combustion behavior. In terms of safety, investigating the fundamental flammable properties of these alternative refrigerants is important. In this study, a large-volume spherical vessel was prepared to observe and evaluate the effect of buoyancy on the flammable properties of R32 and R1234yf; the flame propagation behaviors of these two refrigerants were observed using a high-speed video camera. The flame propagation velocity was estimated by image

analysis of the high-speed video images. The burning velocity was estimated from the flame speed and the pressure profile; the latter was measured using the spherical vessel method under the assumption of a spherical flame front expansion (Takizawa *et al.*, 2009). The maximum peak pressure (i.e., maximum overpressure relative to the pressure in the vessel during combustion) and deflagration index (i.e., constant that defines the maximum rate of pressure increase with time of combustion as defined by ISO 6184-2 (1985) and NFPA68 (2007)) were evaluated according to the pressure profile. Ignition tests using mixture gases with an electric discharge were conducted for a varying equivalent ratio ϕ , which is the ratio of the fuel–oxygen ratio to the stoichiometric fuel–oxygen ratio: $\phi 0.8$ – $\phi 1.2$ for R32 and $\phi 1.2$ – $\phi 1.4$ for R1234yf. In the current fiscal year, the flammability in the presence of moisture and elevated temperatures was investigated based on concern over the summer season, and the burning behavior at ignition was investigated. An evaluation scheme for the potential risk of combustion and explosion in actual situations was developed from the experimentally obtained K_G values.

7.1.1 Experiment

Figure 7-1 shows the experimental apparatus with the spherical vessel. The spherical vessel had a diameter of 1 m and volume of 0.524 m³. A pressure transducer was placed on top of the vessel. The pressure profile formed during combustion was recorded by a data logger. The burning behavior was observed with a high-speed video camera through a PMMA viewing port. The R32 burning behavior was investigated at equivalent ratios of $\phi 0.8$ – $\phi 1.2$. The R1234yf burning behavior was evaluated at equivalent ratios of $\phi 1.2$ – $\phi 1.4$ against a reference ratio of $\phi 1.325$ (mixing ratio of 10 vol%, which Takizawa *et al.* (2009) reported as giving the maximum burning velocity for R1234yf when using the spherical vessel method (Metghalchi and Kech, 1980 and Hill and Hung, 1988)). Pressure transducers were used to introduce fuel gas into the vessel up to a certain partial pressure (BGs in Figure 7.1). Air was then introduced into the vessel until the total pressure in the vessel was conditioned at an atmospheric pressure of 101,325 Pa. For the gas introduction and mixing procedure, gas circulation was maintained by a diaphragm pump (DP in Figure 7.1) during the fuel introduction into the vessel. The electrode for the electric spark was a set of horizontally opposed tungsten wires that were 1 mm in diameter; the gap length between wires was 7 mm. The vessel was equipped with a jacketed mantle heater that covered the entire area of the vessel to maintain the operating temperature of the vessel (Figure 7-1, right picture). The electrode wire was changed to 0.3 mm in diameter to avoid heat loss and structural disturbance. The electrode provided a spark upon the application of a high-voltage power supply to ignite the mixture gas. The discharge voltage and current were recorded by an oscilloscope, and the discharge energy was estimated. The flame front expansion behavior was recorded by the high-speed camera, and the recorded video image sequences were visually analyzed; the flame velocities in the side and upper directions were evaluated.

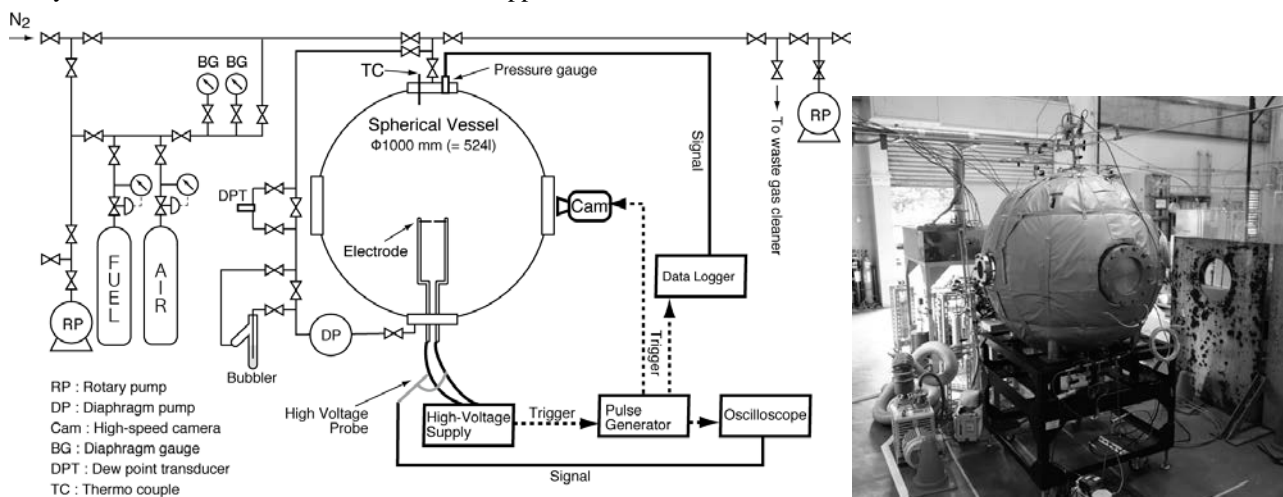


Figure 7-1: Schematic drawing and picture of experimental apparatus.

7.1.2 Flame velocity and burning velocity

Image observation

Figure 7-2 shows example high-speed video images for the flame front propagation behaviors of R32 $\phi 0.9$ and $\phi 1.2$. The flame expanded while slowly climbing upward. The shape of the flame front, which is the interface between the unburned and burned gas, was distorted under the influence of buoyancy and viscosity. The expansion behaviors between $\phi 0.9$ and $\phi 1.2$ were almost the same other than their temporal response. The left picture in Figure 7-3 shows high-speed video images for the flame front propagation behavior of R1234yf $\phi 1.35$. No clear and smooth flame front was observed; the flame front was convoluted without symmetry and floated upward. Furthermore, the ignition characteristics of R1234yf were unstable and depended on not only its flammability but also experimental conditions such as the discharge energy, duration of discharge, and electrode geometry. Because it was difficult to examine the possibility of these effects, alternatives such as a small spherical vessel (30 L) and compact elongated cylindrical vessel (10 cm in inner diameter and 20 cm in length) were prepared to investigate the flammable behavior at ignition. The right picture in Figure 7-3 shows the test results for the compact elongated vessel. A smooth and clear flame front was observed that could not be seen in the large and small spherical vessels. The relation between the fluid dynamics from the high temperature produced by the burned gas and buoyancy and the slow burning velocity at the bottom of the flame resulted in the squeezed flame front shape. The flammability of the mixture gas in the closed vessel was affected by not only the fuel/air mixture ratio, initial pressure, and initial temperature but also the vessel size and shape, ignition source, and other factors. These results suggest the influence of the small vessel volume and shape; thus, the effect of fluid dynamic behavior on flammability must be considered in scaled-up situations.

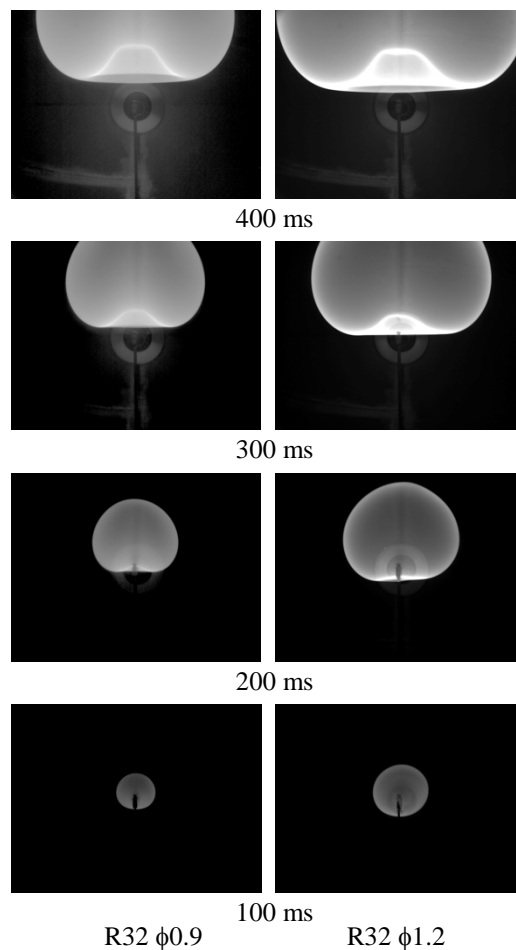


Figure 7-2: Images of flame front propagation for R32 ($\phi 0.9$ for left, $\phi 1.2$ for right).

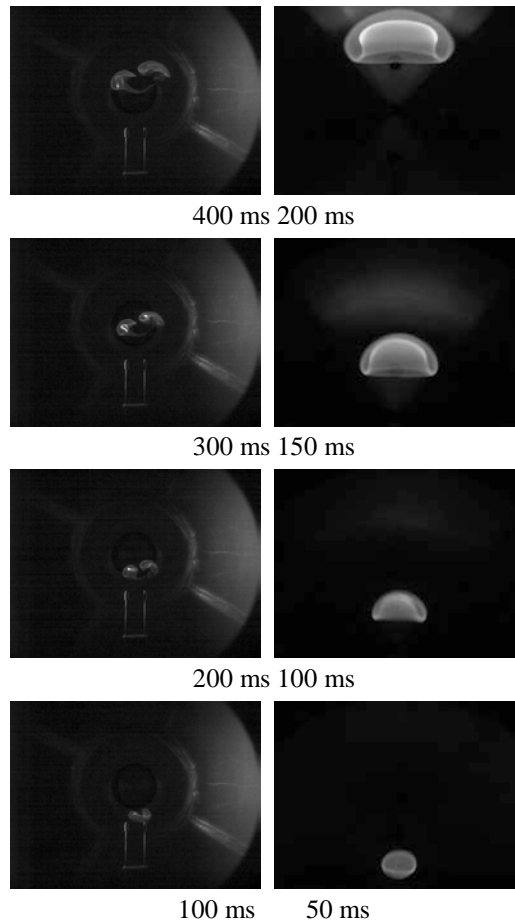


Figure 7-3: Images of flame propagation for R1234yf (ϕ 1.35, left: large spherical vessel; right: compact elongated vessel).

Figure 7-4 shows pressure profiles for R32 ϕ 0.8–1.2 as measured by a pressure transducer. The profiles all seemed to show that the pressure increased in stages. A possible cause may be the influence of the reflected flame front from the top wall. The arrival time of the upper direction flame front to the top of the vessel could be predicted from image analysis: about 0.5 s for ϕ 0.9 and 0.46–0.47 s for ϕ 1.0–1.2. Thus, the pressure reached a peak maximum far behind the arrival time of the flame front. The flame front rose in the upper direction owing to buoyancy, whereas the unburned gas remained in the lower half of the vessel. The underside of the flame front was accompanied by a complicated flow of unburned gas.

Pressure profiles for R1234yf were also measured; these are shown in Figure 7-5. The profile trends associated with the equivalent ratio were not simple. This seems to be due to the influence of the unstable ignition characteristics. The pressure increased to the peak maximum very gradually compared with R32 and took more than 6 s. The profile for the pressure increase at ϕ 1.35 was small, and no increase in pressure was observed at ϕ 1.4; therefore, most fuels seemed to remain without burning.

Flame speed and burning velocity

The maximum flame width and flame top position from the ignition point were visualized for R32, and the flame speed S_f was estimated based on the temporal differentiation of the flame width and height of the flame top profile. The flame speeds in the upper direction increased 1.2–2.0 times more than those in the side direction as time progressed, owing to buoyancy associated with the increase in volume of the burned side. For R1234yf, proper evaluation of the maximum flame width and flame top position was difficult because a clear and smooth flame front was not observed.

The burning velocity S_u was evaluated from the flame speed S_f (Pfahl *et al.*, 2000) as follows:

$$S_u = \left(\frac{\rho_b}{\rho_u} \right) \cdot S_f \quad (7-1)$$

where ρ is the density (m^{-3}) and subscripts u and b of ρ denote unburned and burned gas, respectively. ρ_u is the density at the initial condition, and the unknown ρ_u density was estimated using the chemical equilibrium calculation developed by Gordon and McBride (1994) under the assumption of a constant pressure during combustion. S_f is the flame speed ($\text{cm} \cdot \text{s}^{-1}$). In this study, the upward flame speed S_f was estimated from the rate of change in the flame top position (cm) with time along with the sideward flame speed S_f , which was estimated from the rate of broadening of the half-flame width r_f (cm) (Pfahl *et al.*, 2000). The sideward S_f minimizes the influence of buoyancy, whereas the upward S_f involves the apparent speed due to buoyancy. The burning velocity S_u was also calculated by the spherical vessel method (Metghalchi and Keck, 1980, and Hill and Hung, 1988) under the assumption of a spherical flame front expansion as follows:

$$S_u = \frac{R}{3} \left[1 - (1-x) \left(\frac{P_0}{P} \right)^{\frac{1}{\gamma_u}} \right]^{-2/3} \cdot \left(\frac{P_0}{P} \right)^{\frac{1}{\gamma_u}} \frac{dx}{dt} \quad (7-2)$$

where R is the inner radius of the chamber (m), x is the mass fraction of burned gas, P_0 is the initial pressure in the chamber (Pa), P is the instantaneous pressure during burning in the chamber (Pa), and γ_u is the specific heat ratio. The values of x and γ_u for each instantaneous pressure were estimated using the equilibrium code (Gordon and McBride, 1994).

As shown in Figure 7-6, the burning velocity S_u was estimated by using the sideward flame speed S_f for R32. The burning velocity according to the spherical-vessel (SV) method was also estimated from the obtained pressure profiles and numerical computation under the assumption of spherical flame propagation for R32, as shown in Figure 7-6. Although the flame did not propagate with a spherical shape, as shown by the high-speed video images presented in Figure 7-2, S_{u0} was estimated and used to investigate the deviation due to distortion from buoyancy. During analysis, the pressure increase profile did not depart from the scope of the spherical flame front expansion in the early stages. S_{u0} was compared with the reference S_{u0} values for R32 (Takizawa *et al.*, 2005). The burning velocities based on the flame speed and SV method showed similar equivalent ratio dependencies, but the SV method slightly underestimated S_{u0} . As shown in Figures 7-3 and 7-5, the flame front expansion was convoluted except for $\phi 1.325$, and applying the SV method was difficult. Therefore, the burning velocity S_{u0} was estimated for R1234yf $\phi 1.325$ only; this is shown in Figure 7-7. For R1234yf, the buoyancy had a particular influence on the flame expansion behavior. Takizawa *et al.* (2010) estimated S_{u0-ug} for R1234yf under a microgravity environment, and it is shown as a reference in Figure 7-7.

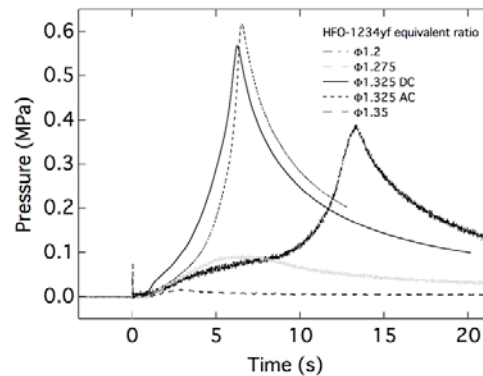
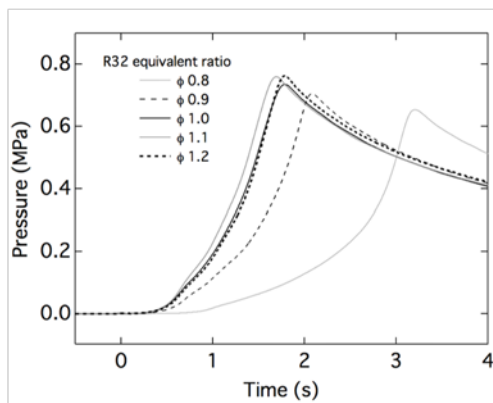


Figure 7-4: Pressure profile for R-32 (ϕ 0.8–1.2). Figure 7-5: Pressure profile for R-1234yf (ϕ 1.2–1.35).

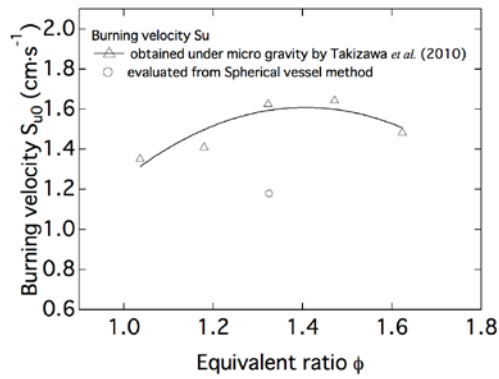
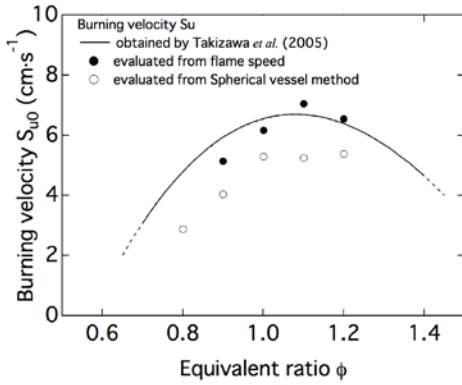


Figure 7-6: Estimated burning velocity for R-32. Figure 7-7: Estimated burning velocity for R-1234yf.

7.1.3 Effect of moisture

Kondo *et al.* (2012) have reported the effects of temperature and humidity on the flammability limits of some A2L/2L refrigerants; this is an important issue, especially with the hot and humid climate of Japan. Temperatures of over 30 °C and 80% humidity are often recorded in the summer. To control the humidity in the mixture gas, the dew-point transmitter MICHELL SF72 was used to measure the dew point in the chamber and set in the circulation loop, as shown in Figure 7-1. The moisture was added to the mixture gas on the circulation loop by a bubbler. The humidity of the mixture gas was evaluated according to the dew point (dp) and temperature. In the experiment, about 56% RH was attained at the given temperature of 30 °C.

Flammability tests were conducted under dry (10–30 °C) and wet (60% RH at 30–35 °C) conditions for R32 at ϕ 1.1 and for R1234yf at ϕ 1.325 (Saburi *et al.*, forthcoming). With the addition of the moisture and elevated temperature, R32 exhibited a flammable process with almost the same flame front shape as under the dry condition, and R1234yf showed a relatively clear flame front shape compared with the dry condition. A blue flame was observed for R1234yf under the dry condition, but a luminous flame was observed under the wet and elevated temperature conditions. These results are being prepared for publication, and the effects of moisture and temperature on the flammable behavior of R1234ze are also under investigation.

Research on the effect of buoyancy on the flammability behavior that considers humidity will continue to be conducted.

7.1.4 Deflagration index, K_G value

The deflagration index K_G was estimated to analyze the recorded pressure profiles. K_G is commonly used to estimate and design the explosion venting area of enclosures; it is defined by ISO6184-2 (1985) and NFPA68 (2007) and is described in the following equation

$$K_G = \left(\frac{dP}{dt} \right)_{\max} \cdot V_{\text{vessel}}^{\frac{1}{3}} \quad (7-3)$$

where P is the pressure (100 kPa), t is the time (s), and V_{vessel} is the volume of the vessel (m^3). A larger K_G requires a larger venting area to prevent the enclosure from bursting. Table 7-1 summarizes the deflagration indices for gases K_G of each refrigerant along with other properties such as P_{\max} , S_f , and S_u . The physical interpretation that K_G is determined after the reflection of the flame front at the top wall must be considered, but the evaluated values may be useful for designing the venting area.

Table 7-2 lists P_{\max} and K_G with other major gases in descending order of K_G . The table indicates that K_G values for R32 and R1234yf were considerably small and the same as or less than that for ammonia (i.e., 10) given in NFPA68

(2007). The results of the evaluated fundamental flammability characteristics will be expanded in scale for application to flammable behavior at actual scales, and an evaluation scheme for the potential risk of combustion and explosion in actual situations will be considered.

Table 7-1: Summary of evaluated properties for refrigerants.

Refrigerant	Equivalent Ratio ϕ	P_{\max} (100kPa)	K_G (100kPa m s ⁻¹)	Flame speed S_f		Burning velocity S_u		
				$S_{f,t=0.1s}$ (cm s ⁻¹)	S_f (cm s ⁻¹)	S_u (cm s ⁻¹)	S_{u0} (cm s ⁻¹)	S_{u0} (cm s ⁻¹)
R32	0.8	6.5	9.4	–	–	–	2.87	4.80 ^a
	0.9	7	9.2	41.4	39.8–53.3	5.13	4.03	5.93 ^a
	1	7.4	8.1	52.4	51.6–63.1	6.15	5.29	6.55 ^a
	1.1	7.6	8.7	58.6	56.4–63.3	6.76	5.24	6.69 ^a
	1.2	7.6	8.9	56.0	54.4–58.6	6.5	5.38	6.39 ^a
R1234yf	1.2	3.9	1.5	–	–	–	–	–
	1.275	1	0.6	–	–	–	–	–
	1.325	6.2	5.6	–	–	–	1.18	1.625 ^b
	1.35	0.2	0.2	–	–	–	–	–

a Ref. (Takizawa *et al.*, 2005)

b Ref. (Takizawa *et al.*, 2010), Obtained data under micro-gravity (S_{u0-ug}).

7.2 Numerical simulation for combustion of A2L/2L

To apply refrigerants safely to air-conditioning equipment, the potential risk of combustion and explosion in actual situations should be evaluated by using the results of the laboratory-level fundamental evaluation. The relationship between the deflagration index and the influence on human and structures was considered with the help of the concept of vent design using K_G values. For example, the reduced effect of the pressure due to an aperture in the room can be evaluated based on vent design. It is difficult to address a variety of evaluation endpoints, such as the installation configuration of air-conditioners, accident conditions, and the scale of leakage, by means of experimental measures, but a numerical simulation is an effective method. First, a non-reactive numerical simulation can be performed to reproduce the experimental results in the large spherical vessel and evaluate the effect of the reduced pressure rise (P_{red}) if an aperture exists in the vessel. Then, the capability of evaluating the reduced effect due to an aperture in the actual room can be reviewed according to the design scheme described in NFPA68 (2007). A numerical combustion model for A2L/2L–air premixed gases should be constructed, and the development of a computational fluid dynamics (CFD) code incorporated with the combustion model will enable the combustion behavior of refrigerants under various conditions to be simulated to help estimate the flame propagation distance and blast pressure. The combustion model can be validated by simulating and reproducing the combustion behavior in experiments. The basic concept of the combustion model is based on Zimont (2000); it is the solution to a transport equation for the variable c with regard to the degree of reaction progress using a function for the burning velocity S_u . The burning velocity is obtained as a time-dependent variable by analyzing experimental data obtained during the project and is believed to be a laminar flame based on the current results. On a practical scale, there is concern over some deviations from the experimental results due to various instabilities, especially those resulting from the effect of buoyancy. Development of a model that considers these factors is in progress.

7.3 Combustion and explosion of A2L/2L by excess energy

7.3.1 Estimation of potential risk of explosion

To achieve practical application of A2L/2L refrigerants and enhance safety, the potential risk of explosion, including detonation, should be considered. At present, there have been few reports on this matter. As an implicit but useful reference, a comparison of explosion characteristics such as the minimum ignition energy (MIE), detonation limit, and K_G with other flammable gases should be very informative. Table 7-2 lists flammable parameters such as P_{max} , K_G , burning velocity, and flammability and detonation limits for mixtures with air that were taken from Mannan (2005). P_{max} and the burning velocity appear to have the same tendency as K_G . Further comparison for the combustion and explosion risks of A2L/2L refrigerants with other flammable gases should be considered.

Table 7.2: Comparison of P_{max} , K_G and other parameters with other gases.

Flammable Material	P_{max} (100 kPa)	K_G (100 kPa·m·s ⁻¹)	Burning velocity (cm·s ⁻¹)	Flammability limits (%)	Detonation limits (%) ^{*3}		Autoignition Temperature (°C) ^{*7}
					Confined tube	Unconfined	
Acetylene	10.6 ^{*1}	1415 ^{*1}	166 ^{*2}	2.5—80.0 ^{*3}	4.2—50.0		305
Hydrogen	6.8 ^{*1}	550 ^{*1}	312 ^{*2}	4.2—75.0 ^{*3}	18.3—58.9		400
Ethylene			80 ^{*2}	2.70—36.0 ^{*3}	3.32—14.70		490
Diethyl ether	8.1 ^{*1}	115 ^{*1}	47 ^{*2}				
Benzene			48 ^{*2}	1.3—7.9 ^{*3}	1.6-5.55		562
Ethane	7.8 ^{*1}	106 ^{*1}	47 ^{*2}	3.0—12.4 ^{*3}	2.87—12.20	4.0-9.2	515
Propane	7.9 ^{*1}	100 ^{*1}	46 ^{*2}	2.1—9.5 ^{*3}	2.57—7.37	3.0-7.0	450
Butane	8.0 ^{*1}	92 ^{*1}	45 ^{*2}	1.8—8.4 ^{*3}	1.98—6.18	2.5-5.2	405
Ethyl alcohol	7.0 ^{*1}	78 ^{*1}		3.3—19.0 ^{*3}	5.1—9.8		
Methanol	7.5 ^{*1}	75 ^{*1}	56 ^{*2}				
Methane	7.1 ^{*1}	55 ^{*1}	40 ^{*2}				
Ammonia	5.4 ^{*1}	10 ^{*1}	7.2 ^{*4}	15—28 ^{*5}			651
R32	7.6 [†]	9 [†]	5 [†]	13.3—29.3 ^{*6}			
R1234yf	6.2 [†]	6 [†]	1 [†]	6.2—12.3 ^{*6}			

*1 Ref. (NFPA68, 2007), Table E.1 (0.005 ft³ sphere; E = 10 J, normal condition). *2 Ref. (NFPA68, 2007), Table D.1.

*3 Ref. (Mannan, 2005), Detonation limits obtained for confined tube. *4 Ref. (ISO/DIS 817, 2010)

*5 Ref. (NFPA325, 1994) *6 Ref. (JFMA, 2013)

*7 Ref. (Mannan, 2005), Table 16.4 † This work.

7.3.2 Autoignition temperature

The autoignition temperature (AIT) is the lowest temperature at which a flammable substance will ignite in air at normal atmospheric pressure without an external energy supply such as a spark or flame. To estimate the autoignition characteristics of A2L/2L refrigerants, a test will be conducted according to the ASTM E 659 standard test method (ASTM, 2005). This method determines the autoignition temperature of liquid chemicals in air or solid chemicals that readily melt and vaporize at temperatures below the test temperature in a uniformly heated vessel at atmospheric pressure. We will employ this method for flammable gases in the presence of moisture; some metals will be used as catalysts.

The test equipment, which has an operating temperature range of up to 1000 °C, is shown in Figure 7-8; it will be operated in open air, so an abatement system for toxic product gas is under construction. The test of refrigerants using this system will be performed soon. The autoignition characteristics of A2L/2L refrigerants and other flammable gases such as propane and ammonia will be compared.

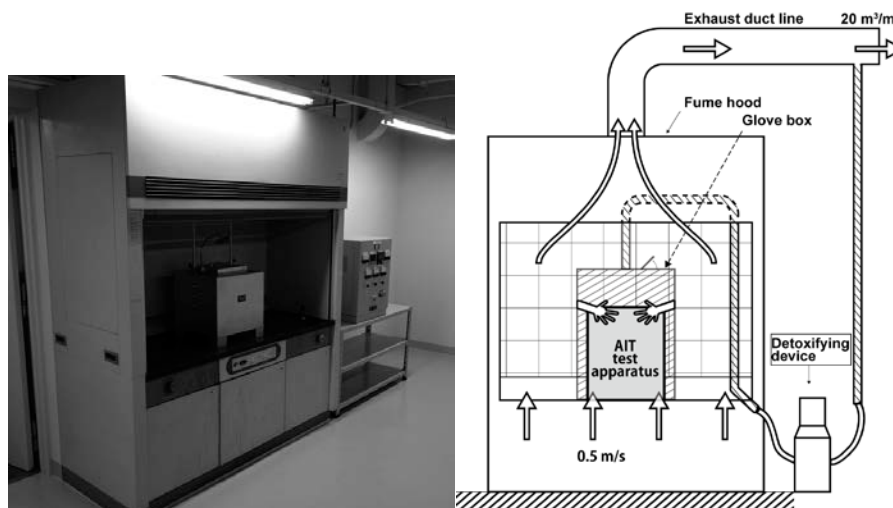


Figure 7-8: ASTM E659 autoignition test equipment.

7.4 Conclusion

To evaluate the fundamental flammability characteristics of A2L refrigerants and assess the safety of their use, flammability properties such as the flame velocity, burning velocity, and deflagration index were evaluated. The effects of flame lifting due to buoyancy and humidity on the flammability characteristics were considered. A numerical simulation and combustion model were developed to estimate the potential risk of combustion and explosion in actual situations and determine the autoignition temperature of A2L/2L refrigerants. Physical hazards with regard to the explosion and combustion of A2L class refrigerants were evaluated. Flammability characteristics such as the flame speed, burn velocity, K_G value, and peak pressure were evaluated in a premixed gas combustion test; the effects of buoyancy and moisture were considered through numerical simulation. To assess the explosion risk of A2L/2L refrigerants, the burning velocity and detonation limits were compared with those of other flammable gases.

References

- American Society for Testing and Materials, 2005, Standard Test Method for Autoignition Temperature of Liquid Chemicals, ASTM E 659–78.
- ASHRAE, 2010, Designation and Safety Classification of Refrigerants, ANSI/ASHRAE Standard 34-2007 Addendum ak.
- European Commission, 2012, Proposal for a Regulation of the European Parliament and of the Council on Certain Fluorinated Greenhouse Gases, COM (2012) 643 final.
- Gordon, S., and McBride, B. J., 1994, Computer Program for Calculation of Complex Chemical Equilibrium Compositions and Applications, I. Analysis, NASA RP-1311.
- Hill, P. G., and Hung, J., 1988, Laminar Burning Velocities of Stoichiometric Mixtures of Methane with Propane and Ethane Additives, *Combustion Science and Technology*, **60**, pp.7–30.
- ISO 6184-2, 1985, Explosion Protection Systems– Part 2: Determination of Explosion Indices of Combustible Gases in Air, (1985).
- ISO/DIS 817, 2010, Refrigerants: Designation and Safety Classification, International Organization for Standardization, Geneva, Switzerland, (current DRAFT DFS/ISO/FDIS 817:2012).

- Japan Fluorocarbon Manufacturers Association, 2013, Environmental and Safety Data List of Specified Fluorocarbons (CFC/HCFC) and Other Fluorocarbons (in Japanese), URL: <http://www.jfma.org/database/table.pdf> (2013), 31 Feb. 2014 .
- Kondo, S., Takizawa, K. and Tokuhashi, K., 2012, Effects of Temperature and Humidity on the Flammability Limits of Several 2L Refrigerants, *Journal of Fluorine Chemistry*, **144**, pp. 130–136.
- Mannan, S., 2005, *Lee's Loss Prevention in the Process Industries*, 3rd ed., Elsevier, **2**, p.1383.
- Metghalchi, M., and Keck, J. C., 1980, *Combustion and Flame*, **38**, pp. 143–154.
- NFPA, 1994, NFPA 325 Guide to Fire Hazard Properties of Flammable Liquids Gases, and Volatile Solids, NFPA.
- NFPA, 2007, Guide for Venting of Deflagrations 2007 Edition, NFPA **68**, (2007).
- Pfahl, U. J., Ross, M. C., and Shepherd, J. E., 2000, Flammability Limits, Ignition Energy, and Flame Speeds in H₂-CH₄-NH₃-N₂O-O₂-N₂ Mixtures, *Combustion and Flame*, **123**, pp. 140–158.
- Saburi, T., *et al.*, forthcoming, Flammable behaviour of A2L refrigerants in the presence of moisture, *10th ISHPMIE*, Bergen, #**110**.
- Takizawa, K., *et al.*, 2009, Flammability Assessment of CH₂=CFCF₃: Comparison with Fluoroalkenes and Fluoroalkanes, *Journal of Hazardous Materials*, **172**, pp. 1329–1338.
- Takizawa, K., Takahashi, A., Tokuhashi, K. Kondo, S., and Sekiya, A., 2005, Burning Velocity Measurement of Fluorinated Compounds by the Spherical-Vessel Method, *Combustion and Flame*, **141**, pp. 298–307.
- Takizawa, K., Tokuhashi, K., Kondo, S., Mamiya, M., and Nagai, H., 2010, Flammability Assessment of CH₂=CFCF₃ (R-1234yf) and its Mixtures with CH₂F₂ (R-32), *2010 International Symposium on Next-generation Air Conditioning and Refrigeration Technology*, Tokyo, P 08.
- Zimont, V., 2000, Gas Premixed Combustion at High Turbulence: Turbulent Flame Closure Combustion Model, *Experimental Thermal and Fluid Science*, **21**, pp. 179–186.

8. Efforts of the Japan Refrigeration and Air Conditioning Industry Association

8.1 Progress by Mini-Split Risk Assessment SWG

8.1.1 Outline of Mini-Split Risk Assessment SWG

The mini-split risk assessment SWG considered a 2.2–8 kW small business–use air conditioner mounted on a wall. Small business–use air conditioners are equivalent to residential air conditioners. A risk assessment of residential-use multi-split type air conditioners, where two or more indoor units are installed for one outdoor unit, was also started last year. The SWG worked on the risk assessment of floor-standing type small air conditioners of 8 kW or less for households. Figure 8.1.1 shows the installation of wall-mounted and floor-standing residential air conditioners.

In order to carry out the risk assessment of one-to-one air conditioners in stores (3.6–25 kW), a mini-split risk assessment SWG (II) was formed. The SWG (II) promoted risk assessment by collecting experts on various components.

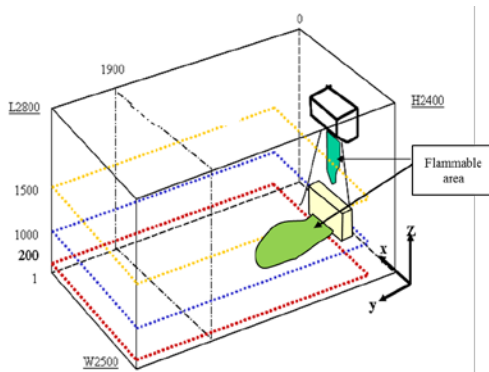


Fig 8.1.1 Indoor space

Strategy of Risk Evaluation		Risk					
Likelihood →	Frequently	10^{-2}					
	Some time	10^{-3}					Not acceptable
	Rare	10^{-4}					Acceptable with condition
	Usually not	10^{-5}					Acceptable
	Very difficult	10^{-6}					
	Extremely difficult	10^{-7}					
	Near zero	10^{-8}					
Possibility of incident:			0	I	II	III	IV
			No damage	Minor damage (smoke from product)	Light damage (fire from product, light injury)	Major damage (fire, human injury)	Lethal damage (permanent injury, death, burn down house)
			→Severity				

Fig 8.1.2 Risk map

This interim report describes the risk assessment results for the following.

- (1) Wall-mounted type 2.2 kW mini-split air conditioner using R32 and R1234yf (residential and small business–use air conditioners).
- (2) Floor-standing type 2.8 kW air conditioner using R32.
- (3) One-to-one 7.1 kW ceiling installation air conditioners for stores using R32.

A risk assessment was carried out on multi-unit air conditioners for home use; there were no practical problems, but there were regulatory problems.

8.1.2 Risk assessment procedure

Alternative refrigerants for use in mini-split air conditioners, such as R32 alone or R32 refrigerant mixed with R1234yf and R134a, have been proposed to prevent global warming. Naturally, these proposed refrigerants do not destroy the ozone layer. The mini-split risk assessment SWG flagged safety as a potential problem with using these refrigerants, and studies were performed to plan countermeasures. A risk assessment was performed to compare R290, as a representative natural refrigerant, with R32 and R1234yf. The risk assessment then evaluated the presence of ignition sources and flammable regions. Yao and Kataoka (2000) performed a risk assessment of a room air conditioner using propane to calculate the probability of ignition sources and flammable regions materializing simultaneously by fault tree analysis (FTA).

The flammability hazard of changing from a conventional air conditioner to one using a mildly flammable refrigerant was evaluated. Risk assessment techniques have changed since 2000; the handbook from the Ministry of Economy, Trade and Industry (2011) was referred to as much as possible. In order to judge the safety, we referred to the risk map presented in Figure 8.1.2 in

particular.

8.1.3 Ignition sources

If the R32 refrigerant used in a mini-split air conditioner leaks to the environment, a flammable atmosphere can form in rare cases. In that case, sparks from electrical equipment, metal collision, and static electricity or the open flame of combustion equipment such as oil stoves are assumed to be ignition sources. In addition, smoking objects can ignite oil and gas by a spark to produce an open flame. These ignition sources were examined in detail in the 2011 and 2012 progress reports of the Japan Society of Refrigerating and Air Conditioning Engineers. The SWG referenced the reports by Imamura et al. (2012), Takizawa (2011), and Goetzler et al. (1998) to describe the following items assumed to be ignition sources:

- (1) An electromagnetic contactor with no cover ignites at 7.2 kVA or more. However, if a contact is covered with a clearance of 3 mm or less, it does not ignite until 12 kVA or more. Low-voltage electrical equipment in Japanese homes almost never ignites.
- (2) R32 is not ignited by burning tobacco that does not emit a flame.
- (3) Static electricity caused by humans in a living space almost never cause ignition.

Based on the above considerations, the ignition sources of outdoor and indoor mini-split air conditioner units using R32 or R1234yf were assumed to be open flame in the risk assessment. Note that the ignition sources of store air conditioners, which have a different environment, are described separately.

8.1.4 Results for Flammable Region

8.1.4.1 Flammable Space

The flammable space assumed in this risk assessment was the same as the space described by Yao et al. (2000). As an indoor space with an air conditioner was the most important consideration in the risk assessment, a small room with a floor area of 7 m² and height of 2.4 m was used for the leakage space. The installation position of the indoor wall-mounted type unit was set at a height of 1.8 m from the floor, and the floor-standing type unit was set on the floor. Figure 8.1.1 shows a schematic diagram of the installation conditions of the air conditioner.

A semi-fireproof warehouse was constructed as per the Building Standard Law. In order for the warehouse to be considered narrow and high-risk, the capacity was set to 1000 m³, and it was assumed to store 10,000 air conditioners.

8.1.4.2 Generation of Flammable Region

Generating the flammable region is important to the risk assessment of mildly flammable refrigerants. Values for R32 and R1234yf were obtained using the same technique developed by Yao et al. (2000), and the simulation was performed at the University of Tokyo.

Table 8.1.1 presents the flammable time volumes used in this risk assessment.

Table 8.1.1 Flammable time volumes in leakage situations

	R290	R32	R1234yf
1.1 Logistics	5.50×10^1	2.00×10^{-4}	2.20×10^{-4}
2.2 Installation	7.16×10^2	2.40×10^{-3}	2.50×10^{-4}
2.5 Mistakes	7.75×10^{-2}	9.00×10^{-3}	1.30×10^{-2}
2.10 refrigerant charge	8.51×10^3	9.97×10^1	3.70×10^2
3.1 Indoor unit operation	1.41×10^1	5.00×10^{-4}	5.50×10^{-4}
3.5 Indoor unit stop	7.16×10^3	2.40×10^{-2}	2.50×10^{-2}
4.1 Outdoor unit	7.76×10^{-1}	9.00×10^{-2}	1.30×10^{-1}
5.1 Connecting pipe	8.51×10^3	9.97×10^2	3.70×10^3
7.8 Service/relief	7.75×10^{-2}	9.07×10^{-3}	1.30×10^{-2}
8 Disposal	Using similar situations and values		

(m³·min)

8.1.5 Questionnaire of Installation and Service

A questionnaire on refrigerant leakage and the use of fire during installation and service was sent by the JRAIA to construction vendors and service shops, and nearly 600 replies were received. The incidence of refrigerant leakage or fire use is as follows.

The incidence of refrigerant leakage at installations was 0.74%, which is comparable with the incidence of 0.77% during service. However, refrigerant leakage increased during charging and recovery. Small amounts of leakage may occur when a worker detaches and attaches a charge hose and connection joint. The reported refrigerant leakage may be 1/100 of the actual value. With respect to fire use, the amount of smoking during service was 1.3%, and other types of fire use were 4.2%. During service, pipes may sometimes need to be welded, so the use of fire sources such as burners or ignition lighters for a burner was assumed, which should increase the rate of fire usage.

Smoking is discussed later.

8.1.6 Results of Risk Assessment

8.1.6.1 Major Accident Probability

According to NITE, a home appliance has a major accident probability of 10^{-8} sets/year (base of 1 million sets). In other words, a product with one million units distributed a year is considered safe if a fatal accident occurs once in 100 years. The total number of mini-split air conditioners and residential air conditioners in Japan is about 100 million sets, so the target value in the FTA calculation was set to $\leq 10^{-10}$ sets/year.

8.1.6.2 Outline of Risk Assessment Results

Table 8.1.2 presents the current risk assessment results for the strongly flammable R290 refrigerant and mildly flammable R32 and R1234yf. The risk was estimated for each step of the refrigerants' life cycles: logistics, installation, use, service, and disposal. We decided that each company managed the production step individually.

The ignition probabilities of R32, R1234yf, and R290 were 2.1×10^{-12} , 2.2×10^{-12} , and 5.9×10^{-9} – 1.1×10^{-4} , respectively. The probabilities for R32 and R1234yf were generally smaller than the target value, and so they were considered to be safe. However, the ignition probabilities for R32 and R1234yf were 1.2×10^{-6} and 2.5×10^{-6} , respectively, during the logistics and service steps. These values are larger than the target value, so we considered the need for countermeasures. The target value is the value required by users when all of the hazards in the risk map of Figure 8.1.1 are assumed to lead to a fatal fire accident.

Table 8.1.2 Current risk assessment results

Risk: Ignition Probability			
	R290	R32	R1234yf
Logistics	1.9×10^{-8} – 4.9×10^{-6}	1.7×10^{-10}	1.9×10^{-10}
Installation	1.5×10^{-6} – 1.7×10^{-5}	1.2×10^{-6}	2.5×10^{-6}
Use (Indoor)	5.9×10^{-9} – 1.1×10^{-4}	2.1×10^{-12}	2.2×10^{-12}
(Outdoor)	9.7×10^{-13} – 1.9×10^{-8}	8.4×10^{-10}	1.2×10^{-9}
Service	9.3×10^{-6} – 1.7×10^{-5}	2.6×10^{-9}	2.8×10^{-9}
disposal	1.8×10^{-5} – 1.3×10^{-4}	5.3×10^{-11}	7.8×10^{-11}

The mini-split risk assessment SWG referred to target values from reports published in 2011 and 2012, so the values were slightly different. This can be a factor because the latest fire statistics should be considered when reviewing ignition sources. Outdoor use involves the installation of a fence (i.e., decorated enclosure for outdoor unit) and the installation of multiple air conditioners on an apartment veranda.

8.1.6.3 Reexamination of Risk Assessment Result

The risk assessment was reviewed to reflect on recent findings. In particular, an FTA of smoking as the dominant ignition source was

reviewed. According to a study by the Tokyo University of Science (Suwa), mildly flammable refrigerants such as R32 do not ignite from the fire from tobacco and piezoelectric lighters.

In addition, lighters are used for shorter durations of time than the time taken to smoke tobacco. The FTA was revised to consider time: e.g., percentage of lighter operation time relative to smoking time and percentage of smoking time. In addition, the ignition source percentage of the flammable region was added. This was confined to ignition by a match or oil lighter.

The FTA was reviewed for each step of the life cycle (i.e., logistics, installation, use, service, and disposal), and the new findings were as described above. Table 8.1.3 presents the results of the risk assessment review.

Table 8.1.3 Results of risk assessment review

Risk: Ignition Probability			
	R290	R32	R1234yf
Logistic	9.2×10^{-11} – 1.4×10^{-7}	4.1×10^{-12}	4.5×10^{-12}
Installation	3.7×10^{-9} – 2.2×10^{-8}	2.7×10^{-10}	3.1×10^{-10}
Use (Indoor)	5.0×10^{-13} – 9.5×10^{-9}	3.9×10^{-15}	4.3×10^{-15}
(Outdoor)	4.9×10^{-13} – 9.3×10^{-9}	1.5×10^{-10}	2.1×10^{-10}
Service	2.8×10^{-7} – 8.1×10^{-7}	3.2×10^{-10}	3.6×10^{-10}
disposal	4.1×10^{-7} – 5.1×10^{-7}	3.6×10^{-11}	5.3×10^{-11}

The ignition probability of indoor units was considerably less than the target value of 10^{-10} units/year derived from domestic air conditioners using R32 and R1234yf. These values were not considered to pose any problems. However, the ignition probabilities of outdoor units using these two refrigerants were 1.5×10^{-10} and 2.1×10^{-10} , respectively, which are slightly larger than 10^{-10} units/year. These FTA values assumed the hazard degree of severity to lead to a fatality (IV) according to the matrix of the risk map. However, a (IV) degree of severity for ignition in an open space such as outdoors needed to be verified.

The highest ignition probabilities were during service at 3.2×10^{-10} and 3.6×10^{-10} , respectively. The installation step also showed similar values. The probabilities during service and installation were higher than the target value of 10^{-10} units/year. However, the service and installation steps are performed by trained professionals who follow instructions or manuals with care and responsibility. We believe that the target values can be increased to 10 times from 1000 times to ensure safe use by professionals. Thus, the ignition probabilities during the service and installation steps are not a problem in practice.

8.1.7 Risk assessment of Floor-Standing Type Air Conditioners

8.1.7.1 Installation Patterns and Issues with Floor-Standing Type Air Conditioners

There are several indoor unit types of mini-split air conditioners other than the wall-mounted type; each requires a specific risk assessment based on the connection specifications and installation method. Figure 8.1.3 compares the installation patterns of ordinary air conditioners and multi-connection type mini-split air conditioners for residential use. Other types of residential air conditioners include floor-standing, ceiling-mounted cassette, wall-embedded, and built-in. In the current evaluation, the flammable refrigerant was fluorocarbon-based; it tends to accumulate near the floor because it is denser than air. Therefore, we assumed that floor-standing type units have the highest risk among indoor units in the case of a refrigerant leakage. This risk becomes even higher for multi-connection type residences that require more refrigerant charge than ordinary air conditioners. To avoid confusion, we first explain the risk evaluation of ordinary floor-standing type air conditioners before moving on to air conditioners for residences.

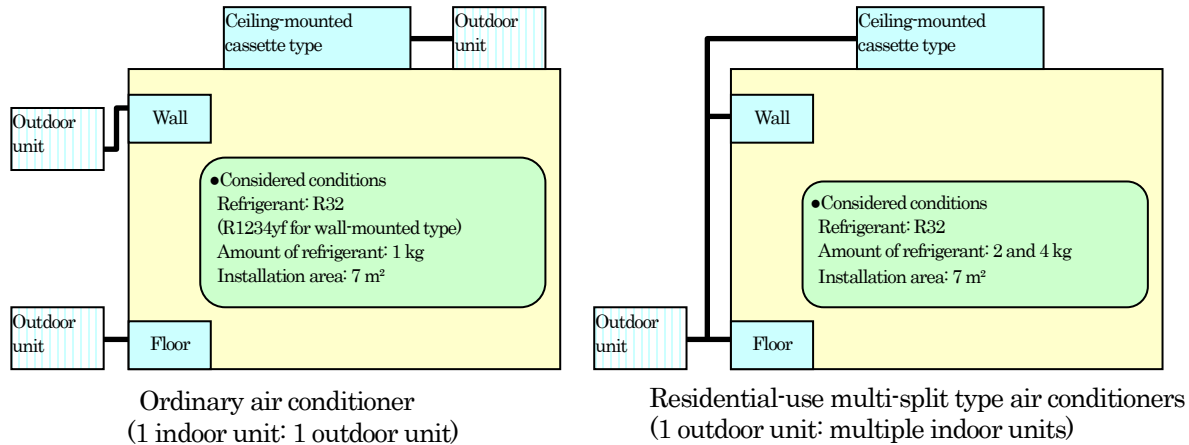


Fig 8.1.3 Installation pattern and considered conditions for residential-use multi-split type air conditioners

8.1.7.2 Ignition Sources and Combustible Space for Floor-Standing Type Air Conditioners

The ignition sources for floor-standing type air conditioners were assumed to be the same as those for wall-mounted type air conditioners. The residential space conditions were also taken to be the same as for the wall-mounted type: a small residential room with a floor area of 7 m² and height of 2.4m. The indoor unit was floor-standing. The volume of combustible air space was defined by a simple calculation to adjust the leakage height based on the values in Table 8.1.1.

8.1.7.3 Target Accident Probability for This Risk Assessment

The target accident probability in this risk assessment followed the same idea of NITE for wall-mounted type air conditioners. In some cases, floor-standing type air conditioners are installed by the same contractors who install residential-use air conditioners, but in most cases the installation is performed by well-trained professionals. The number of floor-standing type air conditioners in the market is as little as 1% of wall-mounted type air conditioners. Their specifications and usage are similar to those of package air conditioners and multi-type air conditioners for buildings; thus, we set the target accident probability during operation (hereafter: target value) to be less than 10⁻⁹. However, since the risk level can be lowered by an order of magnitude because of the better awareness of workers who perform the installation and service work, the target probability was set to less than 10⁻⁸. Table 8.1.4 compares the risk assessments of wall-mounted type mini-split air conditioners and ceiling-mounted cassette type air conditioners to floor-standing type air conditioners for the various stages of their life cycles.

Table 8.1.4 Life cycle stages and allowable values (accident probability)

Life stage	RAC (wall-mounted)	RAC (floor standing)	PAC (cassette-type)
Refrigerant	R32, R1234yf	R32	R32
Representative model	Wall-mounted Amount of refrigerant: 1.0 kg / 7 m ²	Floor standing Amount of refrigerant: 1.0 kg / 7 m ² In actual use (indoor): 10 m ²	Indoor unit: cassette, ceiling suspended Amount of refrigerant: 3 kg / 11 m ² Outdoor unit: Amount of refrigerant: 6 kg / 42 m ²
Transport, storage	10,000 units / 1,000 m ² (outdoor unit)	10,000 units / 1,000 m ² (outdoor unit)	2,300 units / 1,000 m ² (actual DAIKIN storehouse record)
Use	Indoor	· Probability of a quick leak 1.5E-5 · Ventilation condition: no ventilation, no opening · Ignition source: common + set for every presumable room · Calculation method of the probability of a fire accident: → Subject: instantaneous ON operation	· Probability of a quick leak (VRV × safety rate 3) 5.0E-6 × 3 · Ventilation condition: 3 mm × 900 mm opening · Ignition source: common + set for each industry · Calculation method of the probability of a fire accident: → Instantaneous ON operation according to the ignition source Judge if the operation is continuous
	Outdoor	· Probability of a quick leak 2.2E-7 ~ 2.8E-4 · Wind velocity: 1.0 m/s	· Probability of a quick leak (equivalent of VRV) Quick: 1.34E-3 Jet: 1.37E-4 Wind velocity: 0.0, 0.5 m/s
Service & repairing	Probability of a human error occurring: 1.0E-3	Probability of a human error occurring: 1.0E-3	Probability of a human error occurring: 1.0E-3
Disposal (Recycling method)	Removed by volume seller (pump-down) Collect refrigerant from unit → recycle center (according to the Home Appliance Recycling Act)	Removed by volume seller (pump-down) Collect refrigerant from unit → recycle center (according to the Home Appliance Recycling Act)	Collect refrigerant from outdoor unit · Place of installation · Other than place of installation
Setting risk tolerance level	Product diffusion: 100,000,000 units / 10 years. 1 accident in 100 years. Lower than 1E-10	Product diffusion: 200,000 units. 1 accident in 100 years. In use: Lower than 1E-08 During work: Lower than 1E-07 Equivalent risk tolerance level as for SWGII and VRV SWG types which are being discussed at the same time. In use: Lower than 1E-09 During work: 1E-08	Product diffusion: 6,000,000 units. 1 accident in 100 years. In use: Lower than 1E-09 During work: 1E-08 *1 *1 If the worker is working continuously, risk tolerance level will be considered 1 rank lower due to self-defense.

8.1.7.4 Considerations When Reassessing Risks for Floor-Standing Type Air Conditioners

Based on the results of the risk assessment using an FTA of floor-standing type air conditioners, as described above, we found that the allowable ignition probability with no countermeasures was 9.8×10^{-8} , which did not meet the target value.

As the refrigerant R32 is generally heavier than air, it tends to accumulate more easily at lower heights. Since the specific height of ignition sources from the floor can be defined, we considered reassessing risks by dividing the air space by the height. Specifically, we considered the height of each ignition source from the floor in the case of a refrigerant leak inside the residential space. Table 8.1.5 lists the specific height of each ignition source to demonstrate the particular heights of various human activities from the floor. Although the most dangerous status is when a person is lying down, we found that other ignition sources are relatively high above the floor.

Table 8.1.5 Specific heights of various indoor ignition sources

	Ignition source	Estimated height [cm]
	Gas oven	30 ~
	Gas stove	85 ~
	Gas rice cooker	85 ~
	Instantaneous water heater	150 ~
	Cigarette lighter	70 ~
	Cigarette lighter	20 ~
	Candle	45 ~
	Gas stove	39 ~

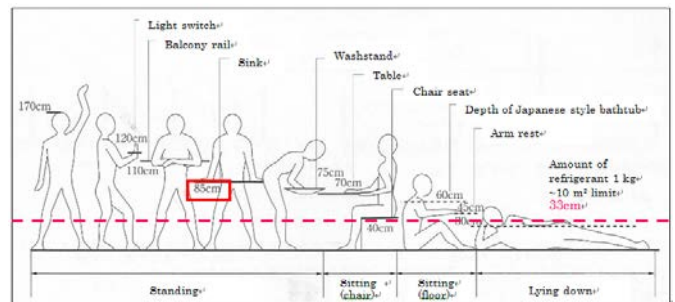


Fig 8.1.4 Heights of various life time

As presented in Table 8.1.5, we also examined the heights of ignition sources for the kitchen and the Japanese-style room to evaluate particular scenarios of air conditioner use inside a room, since these two spaces generally have many ignition sources. Table 8.1.5 presents various ignition sources and their heights in a kitchen and Japanese-style room. Based on the height from the floor, the highest risks in a kitchen and Japanese-style room are gas stoves and cigarette lighters, respectively. We reassessed floor-standing type air conditioners and calculated the height reached by the volume of combustible air space above the floor with a focus on the floor space. The strictest condition considered was that the entire amount of R32 refrigerant should leak and create an air space with the lowest possible LFL of the flammable concentration.

8.1.7.5 Risk assessment Results of Floor-Standing Type Air Conditioners

Table 8.1.6 presents the risk assessment results for floor-standing type residential air conditioners.

Table 8.1.6 Results of floor-standing residential air conditioner risk assessment

Risk: Ignition Probability		
Type	Representative model	R32
Logistics (for every storehouse)	Middle-size storehouse	3.6×10^{-11}
Installation	3.24 m ² veranda	4.0×10^{-11}
Use (indoor)	9.9 m ² room	9.9×10^{-10}
(outdoor)	3.24 m ² veranda	8.6×10^{-11}
Service	3.24 m ² veranda	2.6×10^{-10}
Disposal	3.24 m ² veranda	2.5×10^{-11}

In particular, Figure 8.1.5 shows the relationship between the floor space (room size) and the ignition probability in the case of a refrigerant leak from a small-size 2.8 kW class floor-standing type air conditioner. We also considered the height of the combustible space reached above the floor level in the case of an indoor refrigerant leak. Table 8.1.7 describes how the amount of refrigerant charge and the floor space affect the height that the combustible space reaches above the floor. As presented in Tables 8.1.6 and 8.1.7 and Figure 8.1.5 and considering the relationship between the amount of refrigerant charge and the floor area, we confirmed that the allowable probabilities were lower than 1.6×10^{-9} ; thus, no countermeasures are needed.

We then considered room sizes of 13–19 m², which are larger than the initial 7 m² assumed for floor-standing type air conditioners. We found that, by limiting air conditioner installation to rooms of more than 10 m² floor space, the allowable ignition probability during usage can be met.

For floor-standing type residential air conditioners, we found that the allowable ignition probability in the case of a 4 kg refrigerant leakage from an air conditioner installed in a room with a floor space of up to 13 m² can be met by using a fan or other method to disperse the refrigerant inside the air. However, according to the current international specifications for air conditioners (IEC60335-2-40), the upper limit of refrigerant charge for a floor-standing type air conditioner installed in a 13 m² room is 3 kg; therefore, further examination to ensure safety is necessary.

However, the above installation limitation does not obstruct most installation conditions for general floor-standing type air conditioners.

Table 8.1.7 Influence of refrigerant amount and floor space on height above floor level

<Heights reached above floor level per floor space in case of R32 refrigerant leakage at LFL concentration >

	Floor Space (m ²)		
	7m ²	9.9m ²	13.2m ²
Refrigerant 1kg	0.48m	0.33m	0.25m
Refrigerant 2kg	0.93m	0.66m	0.50m
Refrigerant 4kg	1.87m	1.32m	0.99m

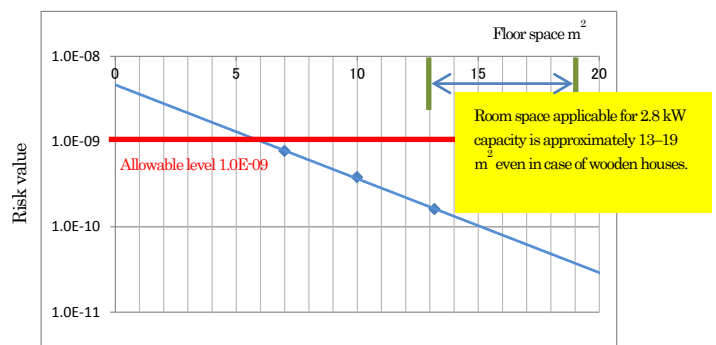


Fig 8.1.5 Allowable risk and floor space

8.1.7.6 Summary of Floor-Standing Type Air Conditioners and Future Development

So far, the mini-split risk assessment SWG had focused on wall-mounted type air conditioners, but the SWG then expanded the assessment target to residential air conditioners in order to accelerate measures to prevent global warming.

All types of residential air conditioners with refrigerant charges of about 1 kg were confirmed to have an ignition probability of 10^{-9} or less (less than 10^{-8} for workers/during the work step), which was the target value based on the risk assessment with the FTA. As an example of specific countermeasures, when the air conditioner units were used indoors in limited installation spaces, the ignition probability of 9.9×10^{-10} was met. For floor-standing type air conditioners (indoor), the installation height was found to have a large effect on the ignition probability as a risk factor.

Multi-split air conditioners with larger refrigerant charges and severe risk are being compared to one-to-one type residential air conditioners to evaluate the flammable region and installation space. In order to improve the accuracy of the FTA with regard to the ignition probability, the SWG is reviewing the height concept with regard to ignition sources and is continuing to study practical applications. The SWG will evaluate and confirm the degree of severity of risk with regard to outdoor use in collaboration with universities and research institutes.

8.1.8 Examination of Unexpected Risk

In the FTA described so far, risks were considered based on common conditions expected at each life cycle step (i.e., logistics, installation, use, service, and disposal). However, FTA was then performed again for unexpected conditions. We re-extracted events for conditions that are difficult to forecast. The risk assessment and consideration of these conditions are described in detail in the 2011 and 2012 progress reports of the Japan Society of Refrigerating and Air Conditioning Engineers. We listed the major points of these reports below:

- (1) Conditions outside the expected range that do not happen easily and require very small spaces, a large amount of leakage, and a strong ignition source.
- (2) Conditions where expansion damage is produced with a mildly flammable refrigerant beyond the damage from a natural disaster such as an earthquake, large fire, or tsunami.
- (3) Conditions where damage is not prevented and human error makes the situation worse.

The SWG members extracted the unexpected risks of 34 events at each life cycle step, and we evaluated each event. Only one of the 34 events was found to influence the FTA: "A home appliance retail store transfers an air conditioner for installation by a minivan, leakage occurs, the driver lights the cigarette, and the refrigerant is ignited and causes an explosion." This event was used as the unexpected risk. We studied this risk to improve the FTA and risk is below permissible level.

The FTA outlined in section 8.1.6 provided the correct static values in general for the logistics, installation, use, service, and disposal steps of the life cycle. Under the assumption of an unsteady risk, the calculated values of the FTA provided a suitable range under ordinary conditions. No conditions changed this significantly at each life step.

8.1.9 Physical hazard Evaluation of Generated Chemical Substance

Above, we described the fire hazard from the ignition combustion of a mildly flammable refrigerant. However, even nonflammable refrigerants such as conventional R410A and R22 can come in contact with burning appliances or high-temperature surfaces and generate harmful chemical substances.

According to Imamura et al. (2012), the exposure of refrigerant from a wall-mounted air conditioner to the heating apparatus of a reflective-type oil stove or kerosene fan heater by contact with a heating apparatus can cause an HF concentration exceeding the 3 ppm level permitted for workers.

There were no differences among R1234yf, R32, or R410A (the present refrigerant).

However, the following conditions are required to create a situation that is harmful to people regardless of the kind of refrigerant that reacts to generate HF.

- (1) HF should be generated.
- (2) HF should reach inhabited areas.
- (3) Evasive action is not taken despite the presence of HF.

HF can appear at dangerous concentrations that are tens of times greater than the 3 ppm.

Interviews by the mini-split risk assessment SWG indicated that an old air conditioner can smell foul. However, although the use of R410A and R22 in contact with burning appliances or high-temperature surfaces can generate harmful HF and phosgene and produce a foul odor, this does not lead to a serious hazard severity (III); the combustion products have not caused serious illness or hospital treatment for more than 20 years.

Generally speaking, small children and bedridden elderly people cannot take action to avoid exposure to HF. However, because there are very few situations in which such individuals live independently in areas where an air conditioner and heating appliance are used concurrently, it is unknown whether such a situation will lead to a serious hazard severity (III).

Even if the rapid burning of R1234yf and R32 by heating apparatus does not occur, the use of mildly flammable refrigerants may produce this phenomenon and create a physical hazard through the generation of HF and other chemical substances same as conventional refrigerant like R410A. We should be alert the warning in the same way as R410A.

8.1.10 Progress in Store Package Air Conditioner (Mini-Split Risk Assessment SWG (II))

8.1.10.1 Features of Store Package Air Conditioner

Store package air conditioners have a large amount of refrigerant compared to residential air conditioners and are installed in slightly wider spaces such as schools, offices, and small- and medium-sized stores. In the risk assessment of store package air conditioners, the refrigerant is considered to be combustible; the basic techniques used by the mini-split risk assessment SWG for residential air conditioners otherwise usage and installation conditions used by multi-unit air conditioners applied to the evaluation of store package air conditioners. Table 8.1.8 summarizes the main features of residential, store package, and VRV air conditioners. Figure 8.1.6 presents the risk assessment schedule for a store package air conditioner.

Table 8.1.8 Comparison of features of different air conditioners

Product	Residential air conditioner	Store package air conditioner	VRV
Horsepower (Outdoor standard)	0.8–3 HP	1.5–10 HP	5–60 HP
Cooling capacity	2.2–8.0kW	3.6–25kW	14.0–168kW
Refrigerant charge	1–2kg	2–10kg	5–50kg
Installation (Outdoor:indoor)	1:1	1:1–4	1–3:1–64
Type of indoor unit	Wall-mount Floor-standing Ceiling-cassette	Wall-mount Floor-standing Ceiling-cassette Ceiling-suspended Built-in duct	Wall-mount Floor-standing Ceiling-cassette Ceiling-suspended Built-in duct
Type of outdoor unit	Air-cooling	Air-cooling Ice-storage	Air-cooling Ice-storage Water-cooling
Indoor unit install location	Residence	Office Kitchen/Dining room Factory Karaoke room (Tightness)	Office Kitchen/Dining room Factory Karaoke room (Tightness)
Outdoor unit install location	Ground Veranda	Ground Each floor Semi-underground Narrow space	Ground Each floor Narrow space Machine room

Storage	Semi-fire protect warehouse Narrow warehouse	Semi-fire protect warehouse Narrow warehouse	Semi-fire protect warehouse
Logistics	Truck Mini-van	Truck Mini-van	Truck

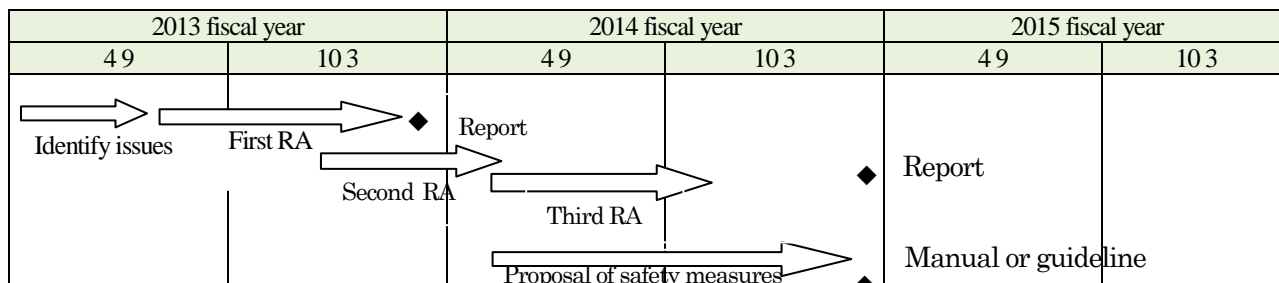


Fig 8.1.6 Risk assessment schedule of store package air conditioner

8.1.10.2 Risk assessment of Store Package Air Conditioner

Similar to the risk assessments performed for the VRV air conditioning and mini-split air conditioning, the risk of store package air conditioners were assessed as follows.

(1) Assumption of acceptable risk

For the 7.8 million units of store package air conditioners on the market, the allowable level of risk was a serious accident once every 100 years. In practice, the hazard of an ignition accident should be assessed, but this has not yet been completed. Thus, all accidents were treated as serious. In each stage of the life cycle excluding usage, workers handle the equipment. The workers are trained to control the risk and reduce the severity even in the event of an accident. Thus the allowable ignition probability was increased by an order of magnitude for these stages.

- Usage stage: 1.3×10^{-9}
- Excluding usage stage: 1.3×10^{-8}

(2) Assumption of refrigerant leakage probability

Since the design specifications of a store package air conditioner were found to be similar to those of a multi-unit building air conditioner, the refrigerant leakage probability based JARAIA questionnaire was set as follows:

- Indoor unit: 1.50×10^{-5} for rapid leakage; 1.03×10^{-3} for slow leakage
- Outdoor unit: 1.48×10^{-3} for rapid leakage; slow leakage was not considered because it does not produce a flammable region.

(3) Assumption of volume-time

In the model case for each life cycle stage, the amount of refrigerant leakage, installation volume, and airflow conditions were used to calculate the flammable volume-time.

(4) Probability of presence of ignition source

Ignition sources of mildly flammable refrigerants during each life cycle stage can include the open flame of combustion equipment, a brazing burner, and open flame from smoking, fire appliances, and electric sparks; the probability of the presence of these ignition sources was calculated.

In the FTA, we calculated the probability of the above points (2)–(4) to occur. For the risk assessment, the ignition accident probability needed to be calculated to determine if it satisfied the limit of point (1).

8.1.10.3 First Risk Assessment Results for Store Package Air Conditioner and Future Challenges

In the first risk assessment of store package air conditioners, the ignition probabilities of the model cases in Table 8.1.9 were calculated for each life stage.

The installation conditions for indoor use were the same as the first risk assessment of multi-unit building air conditioners. The

four-way ceiling cassette-type 7.1 kW air conditioner (refrigerant amount: 3 kg) is installed in general offices (floor area: 42 m², height: 2.7 m). Table 8.1.9 presents the risk assessment results.

Table 8.1.9 First risk assessment results of store package air conditioner

Risk: Ignition probability		
	Model	R32
Logistics	Semi-fireproof warehouse	1.6×10^{-12}
Installation	3.6–14.0kW	2.3×10^{-9}
Use (Indoor)	R32: maximum charge of 4 kg	5.0×10^{-11}
(Outdoor)	Indoor: Office ceiling cassette	6.7×10^{-10}
Service	Outdoor: On the ground	3.0×10^{-9}
disposal		2.5×10^{-9}

As shown in the table, the first risk assessment found that the ignition probabilities met the allowable value in all life stages. This model case considered common usage conditions and is believed to be applicable to a large percentage of the market. We then performed a second risk assessment for cases where the expected risk is large but the probability of occurrence is low. Table 8.1.10 summarizes the model cases.

Table 8.1.10 Each step of risk assessment for store package air conditioners

Step	System (Refrigerant charge)	Indoor unit	Indoor place	Outdoor Place	Storage	Transport
First	No additional charge Maximum: 4 kg	Ceiling cassette	Office	Ground	Middle warehouse	Truck
Second	Additional charge Maximum:8kg	•Ceiling cassette •Floor standing	•Office •Kitchen •Tight space	•Ground •Each floor •Semi-underground •Narrow space	•Truck •Small warehouse	•Truck •Minivan
Third	25kW, Ice thermal storage Maximum:19 kg	↑	↑	↑	↑	↑

A store package air conditioner can have a maximum amount of piping of 30 m for indoor and outdoor units without requiring additional refrigerant charge. We added local filling depending on the pipe length, which increased the amount of refrigerant held in the system as well as the risk of refrigerant leakage. Refrigerant that leaks from floor-standing type air conditioners tends to stay on the floor, so a flammable volume is easily generated.

Commercial kitchens, which have many ignition sources, and closed karaoke rooms with little natural ventilation required attention. Sometimes, the outdoor units of store package air conditioners are installed in narrow spaces. Store package air conditioners can be placed in relatively small spaces like a station wagon during transportation and small warehouses by a retailer. As noted above, the second risk assessment evaluated cases where the risk of ignition probability was expected to be higher. A risk assessment was also performed for 25kW ice thermal storage systems with refrigerant amounts in excess of 8 kg to consider the most severe cases. We plan to continue to develop safety measures as necessary.

8.1.11 Conclusion and Future Subject

The mini-split risk assessment SWG studied wall-mounted type mini-split air conditioners using R1234yf and R32. No issues with the refrigerants were confirmed by the results. For R1234yf, the flammable concentration varies with the humidity. The objective of the risk assessment was to determine if the mildly flammable refrigerant R410A can be applied to conventional mini-split air

conditioners using R32 without significant design changes. In order to match the conventional efficiency and performance from using R1234yf, the heat exchanger needed to be increased approximately 1.4 times in size, and a large compressor needed to be developed to ensure long-term reliability.

A risk assessment was also performed on floor-standing type air conditioners using R32. The results confirmed that this refrigerant can be used in limited installation space. The risk assessment for multi-unit residential air conditioners with multiple indoor units to one outdoor unit found that the relationship between the installation space and amount of refrigerant charge is one of the most important issues. Consistency with international standards on this matter is another issue and will continue to be the subject of further study by another working group of the Japan Refrigeration and Air Conditioning Industry Association.

A risk assessment was performed for one-to-one store air conditioners using R32. The primary risk assessment found that ceiling installations of store air conditioners were below the risk tolerance for ignition in all life cycle stages. Based on the results, safety measures are unnecessary.

To reduce the risk, the SWG revised the manual for service and installation. Similar to the manual issued by the Japan Refrigeration and Air Conditioning Industry Association, the SWG proposed countermeasures for R32 in particular.

The Tokyo University of Science (Suwa), University of Tokyo, and National Institute of Advanced Industrial Science and Technology participated in the mildly flammable refrigerant risk assessment study group to improve the accuracy of the FTA results. We also revealed the extent of the hazard severity. We describe the developments above to promote the risk assessment of mini-split air conditioners with higher accuracy.

Acknowledgments

Shigeharu Taira, Takeshi Watanabe, and Kenji Takaichi summarized the surveillance study for the JRAIA mini-split air conditioner risk assessment SWGs I and II. We thank the 11 committee members: Mr. Madoka Ueno of Sharp Co.; Mr. Tsuyoshi Yamada of Daikin Co.; Mr. Koichi Yamaguchi and Mr. Yasuhiro Suzuki of Toshiba Carrier Co.; Mr. Ryoichi Takafuji and Mr. Kazuhiro Dobashi of Hitachi Appliance Co.; Mr. Toshiyuki Fuji of Fujitsu General Co.; Mr. Tetsuji Fujino of Mitsubishi Heavy Industry; and Mr. Takao Hirahara, Mr. Hiroaki Makino, and Mr. Yasuomi Suzuki of Mitsubishi Electric Co.

We also thank Manager Matsuda and Section Chief Hasegawa of JRAIA for their secretarial work.

References

- Risk Assessment of Propane Room Air-conditioner, The International Symposium on New Refrigerants and Environmental Technology, Yao et al. (2000.9)
- Practical Business Method for Risk Assessment Handbook, MITI, (2011.6)
- Risk Assessment of HFC-32 and HFC-32/134a (30/7 wt%) in Split System Residential Heat Pumps: DOE/CE/23810-92
- Study on Minimum Ignition Energy of Mildly Flammable Refrigerant, Kenji Takizawa, AIST (2011)
- Flammability Characteristics of HFO-1234yf, Minor, AIChE Process Safety Progress (Vol. 29, No. 2)
- Determining Minimum Ignition Energies and Quenching Distances of Difficult to Ignite Components, Dean Smith, Journal of Testing and Evaluation, Vol. 31, No. 3
- Research on the Ascending Current of the Pan Installed in the Residential Gas Range, Honda, Osaka University Graduation paper
- Evaluation of Fire Hazards of A2L Class Refrigerant, The International Symposium on New Refrigerants and Environmental Technology, Imamura et al. (2012.11)
- Next Generation Low GWP Refrigerant HFO-1234yf Part 2, Minor et al., ASHRAE meeting N.Y. Jan (2008)
- Compact Handbook of Static Electricity, Static Electricity Society
- Evaluation of Refrigerant Leakage, The International Symposium on New Refrigerants and Environmental Technology, Hattori et al.

(2012.11)

- Physical Hazard Evaluation for using Air-Conditioning Systems Having Low-Flammable Refrigerants with the Fossil-fuel Heating System at the Same Time, Academic Journal Reito of JSRAE, Vol. 29 No. 4, pp. 401-411, Imamura et al. (2012)
- Progress Report of 2011, Japan Society of Refrigerating and Air Conditioning Engineers.
- Progress Report of 2012, Japan Society of Refrigerating and Air Conditioning Engineers.

8.2 Progress of SWG for VRF System Risk Assessment

8.2.1 Introduction

The risk assessment of VRF systems using mildly flammable low-GWP refrigerants was divided into first and second assessments. Fig. 8.2.1.1 shows an outline of the schedule. A risk assessment was conducted for each life stage, as shown in Fig. 8.2.1.2. In the first risk assessment, we examined the basic data and methodology necessary for fault tree analysis (FTA), including an estimate of the probability of refrigerant leaks occurring in the market, evaluation of the various causes of ignition, and examination of the calculation method to determine the probability of fire. Furthermore, we created fire accident scenarios and an FTA for typical installation cases in the market and estimated the probability of a fire accident occurrence. The second risk assessment examined installation cases considered rare in the market but possessing high risk, and safety measures were proposed to reduce such risks. The GL-13¹ safety guidelines for the safe use of mildly flammable refrigerants in VRF systems are slated for enactment in the autumn of fiscal 2014.

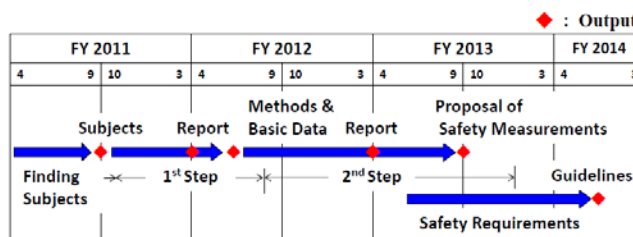


Fig. 8.2.1.1 Schedule of Risk Assessment for VRF with A2L



Fig. 8.2.1.2 Life Stage of Risk Assessment

8.2.2 Issues for VRF Systems Using Mildly Flammable

Table 8.2.2.1 presents the features of VRF systems. The most distinctive feature is the large amount of refrigerant charge in the refrigerant circuit that can be completely discharged from one indoor unit in the case of an indoor refrigerant leak. As there are many connections in the refrigerant piping, rigorous refrigerant leak checks are conducted in a two-layer check system after the piping is installed: once in the form of a tightness leak test at positive pressure and once to check for vacuum leaks at negative pressure. Additionally, specialist technicians and highly skilled service providers normally conduct mounting installation, repairs, and maintenance; this lowers the occurrence of operational errors.

Mildly flammable A2L refrigerants feature an especially high lower flammable limit (LFL) and minimum ignition energy (MIE) compared with other flammable refrigerants. The LFL is high, and it takes a large amount of refrigerant to generate flammable space. Moreover, even ignition sources that can ignite highly flammable propane gas cannot ignite an A2L refrigerant with a large MIE.

When calculating the probability of fire, ascertaining how flammable space occurs at the time of refrigerant leaks and which ignition sources are present that are capable of igniting refrigerant is necessary.

8.2.3 Identification of Risks

The second risk assessment investigated the likelihood of refrigerant accumulation according to the indoor unit

Table 8.2.2.1 Features of VRF system and A2L refrigerants

Features of VRF system (compared with pair system)	Risk
➢ Large amount of refrigerant charge that can all leak into just one room.	up
➢ Many joints connecting refrigerant circuit or parts of valves, vessels, and sensors.	
➢ Sealing of refrigerant is checked thoroughly for leakage.	down
➢ Highly skilled personnel for installation, repair, and maintenance.	
➢ A variety of system configuration : mode-free type, water-cooled or ice storage types, etc.	to be specified
➢ Wide range of capacities for outdoor and indoor units.	
Features of A2L refrigerants (compared with propane)	Risk
➢ Large amount of refrigerant to causes flammable cloud.	down
➢ Types of ignition sources are limited.	

¹ GL-13: Guideline of design construction for ensuring safety against refrigerant leakage from multi-split system air conditioners, published by The Japan Refrigeration and Air Conditioning Industry Association

configuration and installation site, the ignition source type according to the type of business installation, and ventilation conditions. Installation cases thought to have high risks were selected. Among indoor units, cases were selected for instances where floor-standing units were installed in restaurants having small rooms prone to refrigerant accumulation and open flames and for instances where ceiling cassette air conditioners were installed in *karaoke* shops that eliminated gaps under doors to prevent sound leakage, which would severely limit natural ventilation. Ceiling spaces are also usually assumed to have limited ventilation capabilities. Risks were extracted for outdoor units in areas prone to refrigerant accumulation as well as for units installed on each floor, semi-underground, or in machinery rooms. The risks when a slightly flammable refrigerant is improperly charged to an existing R410A unit were also investigated.

8.2.4 Preparations for Risk Assessment

8.2.4.1 Setting allowable levels

The probability of fire from an allowable risk is typically different depending on the degree of severity; however, as the assessment of the degree of danger was incomplete, we set allowable levels under the assumption that all fire accidents are serious and fatal. As there are approximately 10 million indoor units in use in the VRF system market, if the allowable level of a serious accident occurring were once every 100 years, the allowable level for time of use (indoors) would be 10^{-9} or less. The number of units was increased four times for time of use (outdoors), and we multiplied 10^{-9} by 4. Apart from the time of system operation, the people who normally handle equipment are service providers, not consumers, and it is likely that the degree of danger can be reduced through self-protection even if an accident occurs. Therefore, the allowable probability of an accident was increased by one order of magnitude and assumed to be 10^{-8} or less. This point incorporates the approach of Professor Mukaidono of Meiji University.

8.2.4.2 Probability of number of leaks occurring for different refrigerant leak velocities

The international standard (ISO 5149 Part 1 Ch A5) on the amount of refrigerant charge for VRF systems has adopted an indoor refrigerant leak velocity of 10 kg/h under the condition of no vibration from compressors. To understand the actual conditions, we recovered parts that caused refrigerant leaks in the market and determined the bore diameters by using a leak velocity test conducted with nitrogen. The refrigerant leak velocity was obtained from the bore diameters and refrigerant pressure.

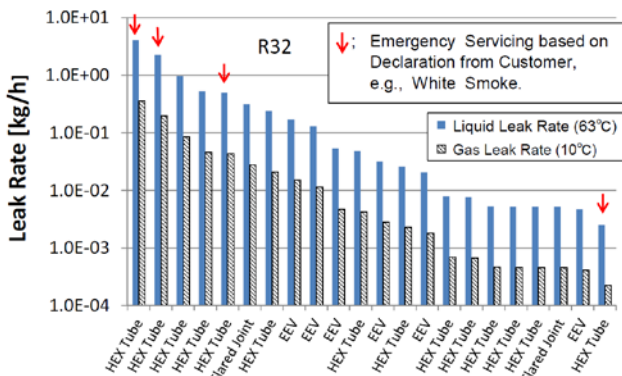


Fig. 8.2.4.1 Leak rate of indoor field samples

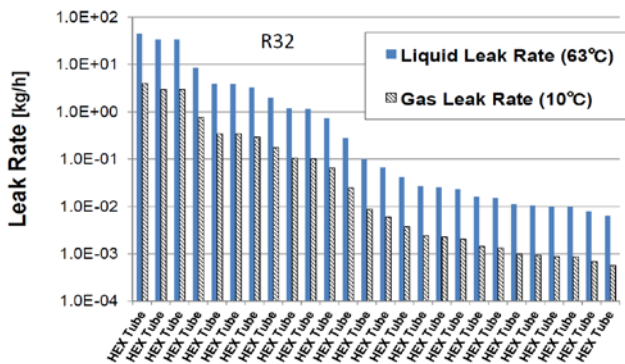


Fig. 8.2.4.2 Leak rate of outdoor field samples

Fig. 8.2.4.1 shows the results of the 22 indoor unit parts with leaks that were recovered from the market. The bars with arrows above them indicate emergency calls by service providers based on reports from customers of white smoke coming out of the indoor units. Of the four instances, the leak velocity of the liquid was relatively high for three of them (1–10 kg/h). The leak velocity was 0.01 kg or less in only one case. This one case was assumed to have no high-speed refrigerant leak; the customer reported the incident after seeing steam produced during operation after the equipment had run out of gas. As the other cases with white smoke indicated

Table 8.2.4.1 Probability of leak classified by leak rate

Number of leaks reports indicating rapid leaks, 2010, Manufacturer B				
	White Smoke	Smelled Burning	Holes in Pipe	Nrp
Indoor Unit	0	1	0	1
Outdoor Unit	1	3	3	7

Probability of leak classified in leak rate

		Total	Slow Leak ~1 [kg/h]	Rapid Leak ~10 [kg/h]	Burst Leak ~75 [kg/h]
Indoor Unit	Distribution Ratio [-]	1	0.986	0.014	0
	Probability of Leak [ppm]	350	345	5	0
Outdoor Unit	Distribution Ratio [-]	1	0.806	0.176	0.018
	Probability of Leak [ppm]	7800	6126	1338	137

[Method]

Leak Probability : Weighted mean value of probability for each JRAIA manufacturer

Number of rapid leaks = Nrp × 10 (indoor) or 100 (outdoor)

Number of burst leaks = Number of rapid leak × 0.1 (outdoor) , 0 (indoor)

Number of slow leaks = Total - (rapid + burst)

Nrp : Number of leaks as reported by customer or service technician indicating rapid leak, white smoke, smell (customer comment), or breakage or hole in pipe (service technician comment).

a refrigerant leak velocity of close to 10 kg/h, we can infer that, if a high-speed leak occurs, in many cases the customer would see white smoke and realize that there was an abnormality.

Table 8.2.4.2 Ignition Sources Y: Ignited N: not ignited

		Ignition Source	R32	R290 (ref.)	
Spark (in flammable cloud)	Electric Parts	Appliance (cause of fire)	Y	Y	
		Parts in Unit	N	Y	
		Power Outlet, 100V Light Switch	N	Y	
	Smoking Equipment	Match Oil Lighter Electric Gas Lighter	Y being evaluated N	Y Y Y	
Work Tool	Metal Spark (forklift) Electric Tool Recovery Machine	Y N N	Y Y Y		
	Body	Static Electricity	N	Y	
Open Flame (contact with flammable cloud)	Smoking Equipment	Match Oil or Gas Lighter	Y Y	Y Y	
		Combustion Equipment	Heater Water Heater Boiler Cooker	Y Y Y Y	Y Y Y Y
	Work Tool		Gas Burner	Y	Y

Table 8.2.4.3 Probability of human error

Phase	Mode of consciousness	Physiological state	Probability
0	Unconscious, Syncope	Sleeping	1
I	Blurring	Weary, Snoozing	> 1E-1
II	Normal, Relaxed	at rest, Usual working	1E-2 to 1E-4
III	Normal, Clear	Active state	< 1E-5
IV	Excited	in a hurry, panic	> 1E-1

Using a similar method, we also measured 26 leak samples from outdoor units. Fig. 8.2.4.2 shows the results. Compared with the indoor units, the outdoor units had higher leak velocities; in three cases, the

Table 8.2.4.4 Calculation of probability of fire

Trigger of Fire	PF	PT	PS
Ignition of Device	$PF_i = N/V_i \times M \times PL$ $= N/V_i \times V_f \times T_f \times PL$	$PT_i = N \times T_f$	$PS = V_r/V_f$
Generation of Flammable Space	$PF_g = N \times T_b \times V_f/V_r \times PL$	$PT_g = N \times T_b$	
Total	$PF = PF_i + PF_g$ $= N \times V_f/V_r \times (T_f + T_b) \times PL$ $= PT \times PS \times PL$	$PT = PT_i + PT_g$ $= N \times (T_f + T_b)$	$PS = V_r/V_f$

PF : Probability of Fire [time/(year × unit)]
 PL : Probability of Leak [time/(year × unit)]
 PT : Probability of Encounter in time between Ignition Source and Flammable Gas [-]
 PS : Probability of Encounter in space between Ignition Source and Flammable Gas [-]
 N : Number of Operations of Ignition Source [time/min]
 V : Volume [m³]
 T : Duration [min/time]
 M : Time Multiplied by Volume of Flammable Region [min × m³/time]

$$M = \int (V_f \times T_f) dt$$

suffix

- i : Trigger is Operation of Ignition Source
- g : Trigger is Generation of Flammable Space
- r : Room
- f : Flammable Region
- b : Ignition Source

become ignition sources for mildly flammable refrigerants, which have a high MIE value.

8.2.4.4 Probability of human error

Refrigerant leaks during work stages, which include installation, repair, and disposal, occur as a result of human error, such as incorrect valve operation by the service technician. Table 8.2.4.3 presents the error rates corresponding to worker conditions according to Hashimoto. The range between 10⁻² and 10⁻⁵ is set for normal, relaxed conditions; however, as service providers handling VRF systems are highly trained, we selected 10⁻⁴ within the FTA to represent the probability of human error.

8.2.4.3 Assessment of ignition sources

Table 8.2.4.2 presents the assessment of each type of ignition source. Although sparks from electrical parts and smoking devices are major ignition sources for highly flammable gases such as propene, they do not

8.2.4.5 Calculation method for probability of fire

A fire occurs when a refrigerant leak causes the formation of a flammable space and an ignition source that can ignite the A2L refrigerant encounters the flammable space in both space and time. Here, fire is defined as all ignition events if the flammable space of a refrigerant happens to contact ignition sources, regardless of the order of magnitude of the ignition. Table 8.2.4.4 presents this probability calculation.

The fire trigger is the operation of the ignition source (e.g., electric spark). In the case of flammable gas coming into contact with a burning candle and igniting, the trigger is the formation of a flammable space. If the formation of a flammable space happens first in time, the trigger is the operation of the ignition source; if the cause of ignition first exists in a continuous state, the trigger is the flammable gas. The probability of fire occurring from one ignition source is the sum of these two triggers. In order to calculate the risk of each life stage, the probability of fire is calculated after determining which trigger is dominant.

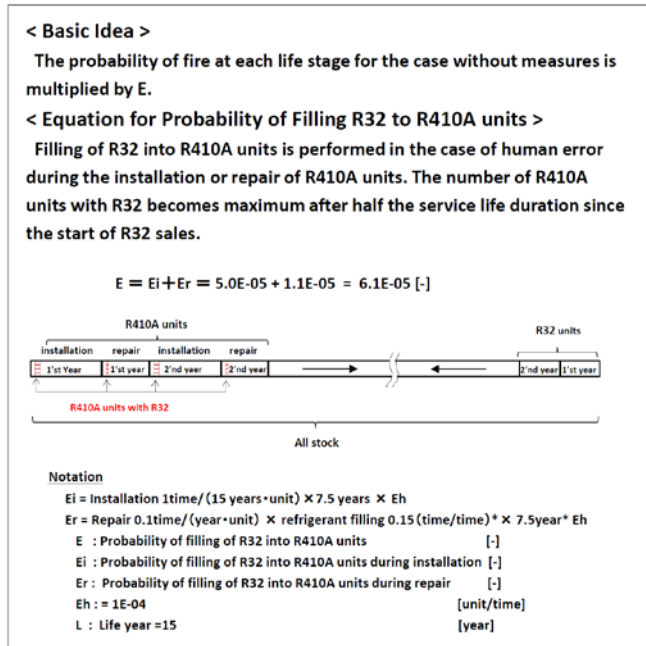


Fig. 8.2.4.3 Calculation of probability of fire caused by filling of R32 into R410A units

8.2.4.6 Method to predict accident probability from improper charge

In order to determine whether the service port specifications for equipment using a mildly flammable refrigerant should be changed from the specifications of conventional refrigerant equipment, we calculated the probability of an ignition accident occurring from R32 refrigerant being improperly charged to R410A equipment when the specifications are the same. Fig. 8.2.4.3 presents the calculation method.

8.2.4.7 Setting of indoor model

(1) Small conference room of office

The 56 kW model (20 hp) was selected to represent the outdoor unit capacity based on the survey results for the capacity distribution of a number of units shipped for office rooms. For the indoor unit capacity, the 7.1 kW model (2.8 hp) was selected in a configuration of eight indoor units connected per outdoor unit. Here, the air conditioning load was assumed to be 170 W/m² for the floor area. This is expressed in Fig. 8.2.4.4. The risk assessment was performed by targeting office room 1 (6.5 m × 6.5 m), which was assumed to be the size of a small conference room in an office.

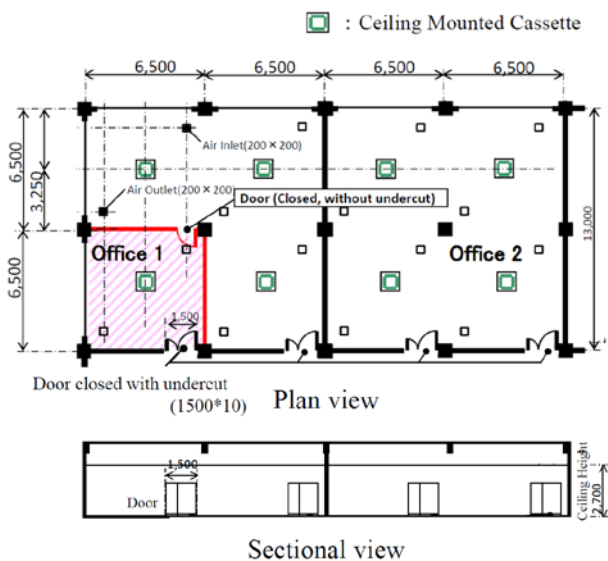


Fig. 8.2.4.4 Model of offices

Ventilation was provided by one air inlet and one air outlet in the ceiling and one gap under the door (undercut part). The ventilation flow from the air inlet and air outlet was 169 m³/h based on the registered number of people according to Article 28 of the Building Standard Act. Because the wind velocity was established to be 2.0 m/s as specified by the Public Buildings Association, the air inlet and air outlet were given dimensions of 0.2 m × 0.2 m. For

Table 8.2.4.5 Typical refrigerant charge amount

		Charge amount [kg]		
		R410A	R32	R1234yf
Outdoor Unit	56kW	19.0	16.1	18.1
Indoor Unit	7.1kW * 8units	-	-	-
Connecting Pipe	Liquid φ15.9 40m	7.6	6.5	7.2
	Liquid φ9.5 72m	4.3	3.7	4.1
Total		30.9	26.3	29.4

Table 8.2.4.6 Maximum refrigerant charge amount

	Charge amount [kg]		
	R410A	R32	R1234yf
Outdoor Unit (Shipment)	40.6	-	-
Additional amount (Installation)	63	-	-
Total	103.6	88.1	98.4

Table 8.2.4.7 Conditions and results of CFD simulations for office 1

No.	Refrigerant	Charge Amount M [kg]	Leak Velocity [kg/h]	Ventilation Amount [m ³ /h]	Undercut	Vent	Condition	Space-Time Product of Flammable region	
								M = 26.3 ⁽²⁾	M = 88.1
1	R32	26.3	10	0	N	Open	Most severe condition. Widest flammable space	1.70*10 ⁰	3.66*10 ⁴
2		88.1	10	0	Y	Open	Natural Ventilation through undercut	8.30*10 ⁻¹	2.80*10 ⁰
2'		10	0	Y	Closed	Natural Ventilation through undercut, Vent closed	1.62*10 ⁰	-	
4		1	0	Y	Open	Natural Ventilation through undercut	0.00*10 ⁰	-	
5		10	169	Y	Open	Mechanical ventilation, ACH=1.5 [h]	7.00*10 ⁻¹	-	
6		10	0 to 169 ⁽¹⁾	Y	Open	Vent. starts after leak detection	7.30*10 ⁻¹	-	
8		10 to 1 ⁽¹⁾	0	N	Open	Shut-off valve operates after leak detection	3.10*10 ⁻²	-	
9'		R1234yf	29.4	10	0	Y	Open	Effect of refrigerant in No.2	6.30*10 ⁻¹

*1) Operation after activation of leak detector

*2) Charge amount of R32, M = 29.4 [kg] in case of R1234yf

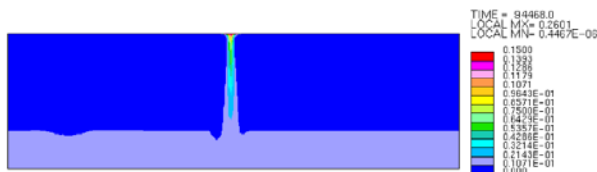


Fig. 8.2.4.5 Concentration Distribution in No. 4

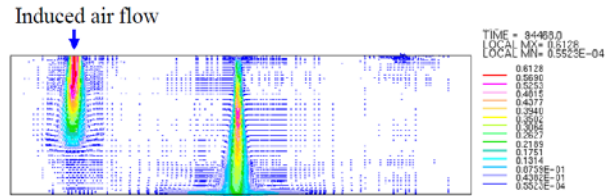


Fig. 8.2.4.6 Velocity Distribution in No. 4

the door configuration, the width was 1500 mm, and the dimensions of the door undercut was set to 10 mm. The amount of R410A was set as the standard refrigerant amount, and the calculation was performed by multiplying this value by a coefficient of 0.85 for R32 and 0.95 for R1234yf. Although the refrigerant amount (Table 8.2.4.5) was determined under the assumption of a typical installation, the case of the maximum refrigerant amount was also evaluated (Table 8.2.4.6).

Table 8.2.4.7 presents the simulation conditions and results for office room 1. Here, the slow and fast leak velocities for the refrigerant were 1 and 10 kg/h, respectively. Tokyo University and JRAIA collaborated on this research.

The average possible volume of flammable space decreased with operation of mechanical ventilation equipment (model no. 6) and an isolation valve that was installed for the refrigerant piping (model no. 8); the safety measures were also effective.

When natural ventilation was available from the door undercut, no flammable space was generated throughout the entire space (model no. 4) based on the refrigerant concentration distribution, expressed in Fig. 8.2.4.5, for the refrigerant leak velocity E = 1 kg/h. Fig. 8.2.4.6 presents the velocity distribution. The R32 concentration in space was not increased by the air flow from the air inlet and outlet in the ceiling. To lower the volume, the mechanical ventilation opening must be open, and an undercut must be established underneath the door. Namely, the existence of an air inflow and outflow is a necessary condition.

Incidentally, the results of a simple simulation where the concentration changes with the location were consistent with the refrigerant concentration by the ceiling installation type (Fig. 8.2.4.7). Thus, we decided to execute a simple simulation using models where the ventilation flow is regulated by the ceiling installation type.

(2) Small Rooms of Restaurants

Fig. 8.2.4.8 shows the models. Floor models were installed in the individual rooms of Japanese-style restaurants. The refrigerant amounts were set to 52.8 kg for R32 and 58.5 kg for R1234yf. Table 8.2.4.8 presents the analysis conditions and results. For the case without measures, ventilation openings for the air inlets and outlets were established in the ceiling, and the ventilation flow was set to 112 m³/h. When a gas cooking stove is being operated (calorie control amount of 3

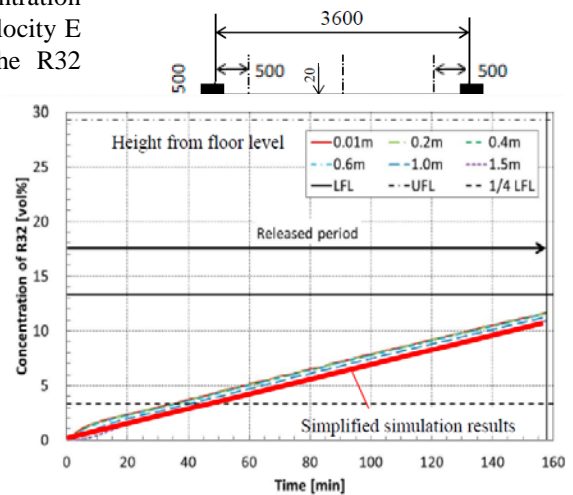


Fig. 8.2.4.7 Mean Concentration in No.1

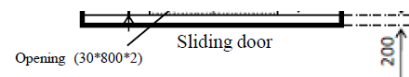


Fig. 8.2.4.8 Model of restaurant

Table. 8.2.4.8 Conditions and Results of CFD simulations for floor-standing unit in Japanese restaurant

	Analysis Condition					Flammable Region				
	Refrigerant	Charge [kg]	Leak Rate [kg/h]	Mixing in Unit	Ventilation Amount [m ³ /h]	Ventilation Condition		Mean Volume [m ³]	Time [min]	Space-Time Product [m ³ min]
						Inlet	Outlet			
Without Measures	R32	52.8	10	No Yes	112	Ceiling	Ceiling	1.17 1.28	910 900	1070 1150
With Measures	R32	52.8	10	Yes	164	Ceiling	300mm above floor level	0.01	320	416
							200mm above floor level	0.10	317	30.7
							30mm above floor level	1.30	317	2.40

kW), a ventilation flow of 500 m³/h is necessary to maintain an indoor CO₂ concentration of 1000 ppm; however, the threshold value was set to 1/5 of this value to ensure safety. When leaks occurred in the floor models, the refrigerant remained in the vicinity of the floor. However, when there was mechanical ventilation with air inlets and outlets installed in the ceiling, the flammable space became large without enabling dilution of the refrigerant. For cases where the measures are determined by GL-13, it is necessary to construct air outlets that are in the vicinity of the floor. The ventilation flow was set to 164 m³/h (= 10/0.061) to ensure that the concentration would not exceed RCL0.061 kg/m³ at a leak velocity of 10 kg/h. The results showed that changing the height (underside) of air outlets to 30–300 mm had a significant impact on the flammable space volume.

(3) Karaoke

Fig. 8.2.4.9 presents the models. We referred to an actual survey for the Nomura and Kitajima *karaoke* boxes. In order to prevent sound leakage, a ventilation system was employed without natural ventilation. The maximum refrigerant amount was set to 88.1 kg, the volume of the *karaoke* box was set to 9.5 m³, and customers changed once every 3 h. However, once the refrigerant concentration lowered after the customers changed, we made the entire room a flammable space for a short time. We assumed candles, combustion-type heaters, gas stoves, and electrical equipment, as shown in the figure, beginning with the *karaoke* equipment. The concentration was determined by the simplified simulation.

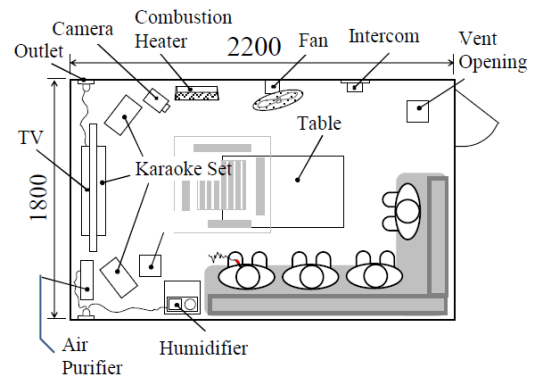


Fig. 8.2.4.9 Model of *karaoke*

(4) Ceiling Space

The compartment for the ceiling space of office room 1 in Fig. 8.2.4.10 was completely separated from the other spaces, and we hypothesized a worst-case scenario at the time of system operation in the FTA: the entire area becoming a flammable region after a refrigerant leak and having this last for ten years. As the ignition source, we considered the ignition of an indoor unit and short-circuit accidents. For servicing, we set the flammable region as continuing for 4 h; this was shorter than in the case of system operation because dilution can be expected through opening for inspection. The volume was determined by assuming a ceiling space for room 2.

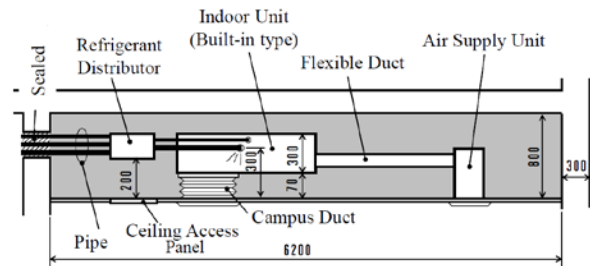


Fig. 8.2.4.10 Model of ceiling space

8.2.4.8 Setting of Outdoor Model

We selected an upper air outlet, three-sided-heat exchange type model with 56 kW (28 kW × 2 units), which is the most common among market installations. Fig. 8.2.4.11 presents the installation patterns. We assumed four installation patterns: a typical installation pattern with no obstructions in the vicinity, the installation pattern of each floor, the installation pattern in a machinery room, and the installation pattern of the semi-underground. The refrigerant amount was set as 85% (26.3 kg) of the regulation amount of R410A, and the conditions were set as a uniform leak from one heat exchanger in a connected installation.

Figs. 8.2.4.12–14 show the outdoor unit models. The

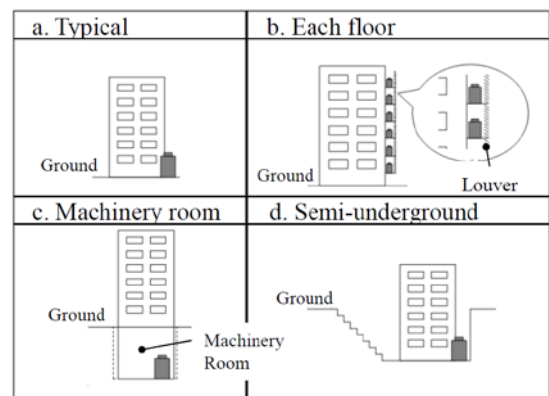


Fig. 8.2.4.11 Models of outdoor installation

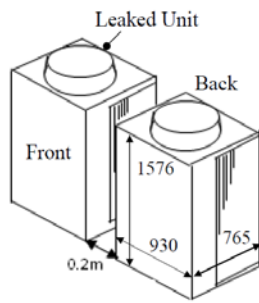


Fig.8.2.4.12 Usual

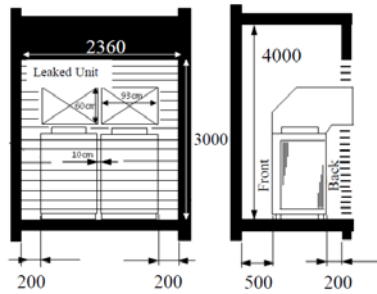


Fig.8.2.4.13 Each floor

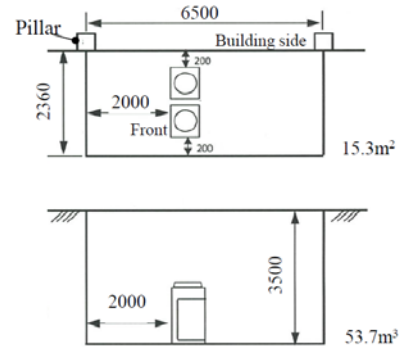


Fig.8.2.4.14 Semi-underground

Table 8.2.4.9 Conditions and results of CFD simulations for outdoor models

Condition				Results		
Case	Leak rate [kg/h]	Air velocity [m/s]	Leak time [min]	Mean volume [m ³]	Time [min]	Space-Time Product [m ³ × min]
Usual	10	0	158	0.0E+00	0	0.0E+00
Each floor				1.0E-06	4	4.3E-06
Usual	75		21	8.3E-02	21	1.8E+00
Each floor				1.9E-01	21	4.0E+00
Semi-underground	1.6E+01		3852	6.3E+04		
Usual	10		0.5	158	0.0E+00	0
Each floor		0.0E+00			0	0.0E+00
Usual	75	21		9.4E-03	21	2.0E-01
Each floor				1.8E-01	22	3.8E+00
Semi-underground	3.1E+00	280		8.8E+02		

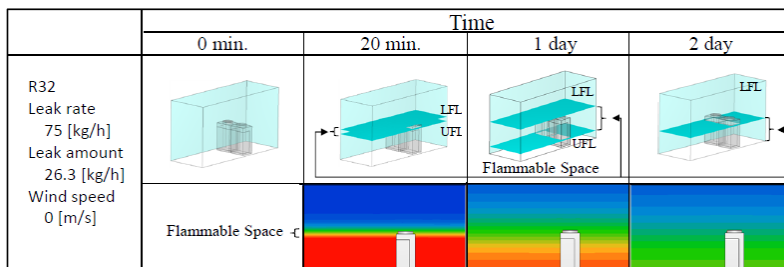


Fig. 8.2.4.15 Leak simulation results for semi-underground model

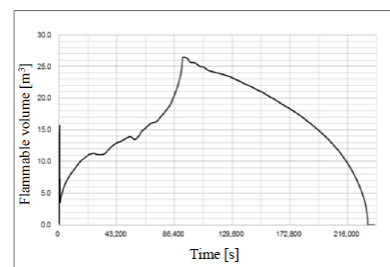


Fig. 8.2.4.16 Time-Flammable Volume

machinery room had dimensions of 6.6 m × 3.3 m × 5 m (height) and was equipped with a mechanical ventilation device.

Table 8.2.4.9 presents the conditions and results for a concentration distribution analysis of the outdoor models.

Fig. 8.2.4.15 shows the results for a concentration distribution analysis of semi-underground installations. The leak velocity was set to 75 kg/h. For the 20-min period until the leak was complete, a flammable region layer rose from the floor space, where the top concentration was LFL and the bottom concentration was URL. When the leak was complete, the thickness of the flammable region layer increased by diffusion.

For the installation patterns other than the semi-underground installations, the flammable region dissipated in tens of seconds after a refrigeration leak. In the case of semi-underground installations, refrigerant accumulated in the flammable region, which did not dissipate for 64 h. Fig. 8.2.4.16 indicates the time transition for the flammable regions of semi-underground installations.

8.2.5 Results of Risk Assessment and Safety Measures

In the first risk assessment (progress report presented in fiscal 2012), we created an FTA by following the risk

assessment of the R290 mini split. Here, because the ignition source evaluation and concentration analysis of the mildly flammable refrigerants were incomplete and the actual conditions in each work stage were not fully identified, the results overestimated the accident probability for each stage. These overestimations were caused by factors such as employing accident scenarios that estimated flammable spaces as being larger than in actual cases, including cigarette lighters, electrical outlets, and light switches as ignition sources, and by employing accident scenarios that estimated a burst leak after refrigerant recovery and ignition by a brazing burner. In the second assessment, we considered the ignition evaluation results of the Tokyo University of Science, Suwa, and the National Institute of Advanced Industrial Science and Technology, the concentration analysis results of Tokyo University and each company, and the workplace surveys to create an FTA that better reflected the actual conditions. The risk assessment results for each life stage are presented below.

8.2.5.1 During transportation storage (manufactured product)

Transportation storage was divided into warehouse storage and transportation, and various risk investigations were performed.

For the investigation, 1000 units were stored in a medium-sized warehouse with an area of less than 1000 m² and a standard fireproofing structure following the Building Standards Act. The value of space-time product is 8.4×10^{-3} [m³min] for storage. Cigarette lighters owned by workers and spark ignition at the time of freight handling of the forklift were assumed to be ignition sources, and the frequency of refrigerant leaks was set to be the same as during use. The storage frequency of air conditioners was set to 1/15 based on a service life of 15 years, and an FTA was created. This resulted in an ignition probability of 7.8×10^{-17} – 1.2×10^{-16} (ignition/unit for 1 year), which is below the allowance of 10^{-9} .

However, ignition sources are not believed to exist inside freight rooms, so there is no ignition combustion even if the refrigerant leaks. Because the leaked refrigerant simply diffuses from freight rooms, in which open fires are prohibited, at the time of loading and unloading, and there are no flammable regions, the necessity for an FTA investigation is extremely low. Thus, we determined that there is no risk at the time of transportation storage.

8.2.5.2 During installation

The risk assessment was performed as follows.

(a) The risk of brazing work for connecting pipes was estimated in detail. Usually, connection pipes are brazed when the pipe is not connected to the outdoor unit; consequently, there is little possibility that refrigerant will leak during brazing. However, because the possibility is not zero, we assumed that piping connections were brazed under actual conditions where the risk of outdoor units was 10% and calculated the fire probability for the ignition source (gas burner) based on the following assumptions.

(b) Using the survey analysis results for electric shock/secondary accidents, we calculated the probability for the presence of electrical sparks in a ceiling space.

(c) We considered the following causes of refrigerant leaks for outdoor units: (1) a faulty valve, (2) a charging mistake of R32 at the N2 permutation, (3) the reuse of existing piping, and (4) connecting a pipe to the outdoor unit prior to piping work. We assumed the following ignition sources for outdoor units: (5) preloading unconnected outdoor units in the work vicinity of brazing and (6) boilers.

We created an FTA that reflected the above factors and found the fire probability to be 94% for outdoor units in typical installations with no obstacles around them and 99% for indoor units with ceiling installations. The results were 1.9×10^{-9} , which is within the allowable level of fire probability.

For semi-underground outdoor units and machinery room installation cases, we exceeded our target values. For indoor units, all were within the allowable level. The major causes of ignition sources were brazing work for connection piping (prior to charging the refrigerant) and a boiler. Because the values were an order of magnitude higher than the target values for accident rates of these cases, we decided that carrying refrigerant leak detection devices during the performing of brazing work would be an effective countermeasure. As a result, all conditions fell to within the allowable level.

8.2.5.3 During system operation (indoors)

We investigated examples of typical installations and worst-case scenarios. For typical installations, we assumed offices (office 1: small rooms) and decided to investigate cases in which mechanical ventilation was implemented (model no. 5). First, in worst-case scenarios, we simply calculated the ignition probabilities for 28 types of building uses that differed in terms of the presence of ventilation, type of ignition source, and room size. Based on the results, we selected two installation cases where the fire probability was pre-estimated to be high for further investigation. The first case comprised a ceiling installation type with the possibility of open flame as ignition sources, a small room size, and a lack of door undercuts (e.g., *karaoke* rooms). The second case comprised a floor standing type with the possibility of open flame as an ignition source (e.g., small restaurant rooms for customers). We also decided to investigate the ceiling

space for office 1.

We assumed usage rates for equipment that accompany an open flame and calculated the ignition probability for the number of operation times of the ignition source and calculated the probability for other equipment (primarily electrical products) from NITE accident information on ignition probability rates.

In the results, we were not able to satisfy the allowable safety level of under 10^{-9} that was set in this risk assessment for the two worst-case scenarios. Thus, safety measures are necessary, and we confirmed that an allowable safety level of under 10^{-9} can be set by operating ventilation after detection of the refrigerant leak by equipment.

8.2.5.4 During system operation (outdoors)

For outdoor unit equipment, we established the four patterns shown in Fig. 8.2.4.11. We selected three items as ignition sources: smoking (match, lighter), electrical sparks of the outdoor unit, and a boiler. We calculated the fire probability from the space-time product value (estimated for machinery rooms from the space-time value calculated for semi-underground) based on the concentration analysis results and the number of times that the ignition source is operated; these are presented in Table 8.2.5.1. Those numbers were calculated based on the following: a smoking rate of 33.6% for Japanese men, at an average of 16 cigarettes a day (JT statistics); occurrence of 5.6 accidents every year on account of smoke and ignition from electric sparks (NITE statistics); and 0.1% market penetration rate of boilers.

Table 8.2.5.1 Number of operation times of ignition sources per volume and minute [times/(m³×min)]

	Smoking tool	Electric spark from its fire accident	Boiler
Usual	7.97E-08	9.43E-15	1.78E-08
Each floor	2.82E-06	6.68E-13	2.87E-06
Machinery room	1.87E-06	8.83E-14	
Semi-underground	1.03E-06	1.79E-13	6.69E-05

An FTA was created based on the above preconditions, and the fire probability for each pattern was calculated. It is shown that a fire probability is less than the criterion of 4.0×10^{-9} for typical and each floor installations; consequently, safety measures were unnecessary. The refrigerant diffusion velocity for leaks in semi-underground was extremely slow, the ignition probability was 1.1×10^{-7} , and the allowance level was not satisfactory. Incidentally, ventilation equipment is present in machinery rooms. Furthermore, because the boiler intake and exhaust also control the specialized duct, safety measures based on fixed conditions are unnecessary as refrigerant leaks do not come in contact with the burner.

For machinery room installations and semi-underground equipment, the fire probability changes according to the amount and spatial volume of the refrigerant or the height of the semi-underground. The maximum refrigerant amount needs to be regulated to correspond to standards that determine the necessity of safety measures and spatial volume for the installation of outdoor units and the amount of necessary ventilation. An investigation of the constraining conditions is planned for the future.

8.2.5.5 During repair

Having a burner for the primary ignition source significantly affects the fire probability within the FTA, and refrigerant leakage accompanying burner operation is one of the main factors for the formation of flammable regions. In the second risk assessment, the probability of fire accidents was within 10^{-8} for indoor ceiling installation, outdoor aboveground installation, outdoor installation to each floor, and ceiling space. However, because the values were exceeded for indoor floor-standing installation, outdoor semi-underground, and machinery room installation, safety measures were necessary. For indoor floor-standing installations, countermeasures include natural ventilation (according to ISO5149), installing the lower part of the door position 30 mm from the floor surface, training service providers (e.g., when a refrigerant leak is noticed during burner work, immediately extinguish the burner), and having workers carry refrigerant leak detection devices to check for refrigerant leaks during work. For outdoor installations, we controlled risks to within the allowance values by measures including installing ventilation devices together with semi-underground and machinery room installations, training service providers in the same way as for indoor installations (e.g., when a refrigerant leak is noticed during burner work, immediately extinguish the burner), and having workers carry refrigerant leak detection devices.

8.2.5.6 During disposal

We examined the risks during work to dismantle the units and pipes at an installation site. Ignition sources were assumed to be burners, electrical short-circuits accompanying wiring work, and smoking tools.

Regarding fire ignition scenarios from burners, we considered situations where fires are ignited from refrigerant leaking from units for replacement by burners being used in the piping work of new units. In this scenario, the refrigerant leak from removed old units was assumed to happen simultaneously while the burner was being used continuously for the working pipe of the new unit. We made the replacements comprise 50% of the total. Furthermore, we made 10% of the units operate with the simultaneous installation of new units during replacement. Consequently, this scenario established that 5% of the units operate during the dismantling.

In the results, the detected risks exceeded allowable values when outdoor units were installed semi-underground or in

machinery rooms. We assumed the following measures to lower fire probability:

Measure (1) Provide risk education and warning notices for smoking and using combustion equipment, and train workers to immediately extinguish the fire of burners during a refrigerant leak.

Measure (2) Require workers to carry a refrigerant leak detection device when working in small narrow places (e.g., semi-underground, machinery rooms).

Under these circumstances, we also considered the probability of forgetting to carry detection devices (10%).

For outdoor units installed semi-underground and in machinery rooms, the fire probability fell within the allowable risk range (under 10^{-8}) when both measures (1) and (2) were executed. Even for the other installation cases, measure (1) should be performed. For cases of replacement and simultaneous operation, measure (1) causes the fire probability to fall within the allowable risk range in all installation cases.

8.2.6 Summary of Results

Table 8.2.6.1 summarizes the results of the second risk assessment for R32. When the risk exceeded allowable levels, we executed safety measures to decrease the risk. In ceiling installation units/offices, the risk fell below the allowable level through the use of mechanical ventilation. VRF systems are most often applied in offices, and ceiling installation

Table 8.2.6.1 Summary of 2nd risk assessment for VRF with R32

Installation Case (charge kg) <floor area m ² *ceiling height m>		Life stage	Transport/Storage		Installation		Using (indoor) Using (outdoor)		Repairing		Disposal (removal)		
			Allowable		< 1E-08		< 1E-10 (indoor) < 4E-09 (outdoor)		< 1E-08				
			N	Y	N	Y	N	Y	N	Y	N	Y	
Indoor unit	Ceiling (26.3)	Office <40.6*2.7>	1.1E-15 ~ 2.7E-15	-	1.9E-09	-	3.5E-12 ^{*)}	-	8.7E-11	8.8E-12	2.9E-14	2.9E-15	
	Floored (52.8)	Restaurant <9.7*2.5>			1.9E-09	-	3.8E-07	8.4E-11	1.2E-08	3.9E-11	3.4E-12	3.4E-13	
	Ceiling (88.1)	Karaoke <4*2.4>			-	-	1.2E-06	0.0	-	-	-		
Outdoor unit	Typical (26.3)	-			1.9E-09	-	1.9E-11	-	1.4E-09	1.4E-10	2.4E-10	3.2E-11	
	Each floor (26.3)	- <3.4*4.0>			1.9E-09	-	3.0E-09	-	3.1E-09	3.4E-10	1.0E-09	1.4E-10	
	Semi-underground (26.3)	- <15.3*3.5>			1.1E-08	1.9E-09	1.1E-07	2.5E-13	3.6E-07	2.1E-09	3.3E-08	4.8E-10	
	Machinery room (26.3)	- <21.8*5>			1.1E-08	2.1E-09	3.2E-09 ^{*)}	-	8.6E-07	5.4E-09	2.2E-08	3.3E-10	
Ceiling space (26.3)	- <38.4*0.8>	-			-	-	-	3.0E-10	3.0E-11	3.0E-09	3.0E-10	7.2E-11	1.1E-11
False charge	Allowable	-			-	-	Included in indoor unit	< 1E-11 (indoor) < 4E-10 (outdoor)		< 1E-09			
	-	-			-	-	-	8.7E-11 (Karaoke) 1.2E-14 (Outdoor)	-	6.0E-13	3.0E-14		

*1) With mechanical ventilation

units make up more than 95% of the indoor units. Because the risk may be higher than the allowable values for ventilation and refrigerant conditions that differ from conditions established during this assessment, appropriate safety measures are needed that comply with ISO5149. In floor-standing installations/restaurants, the risk exceeded allowable values during the system operation and maintenance of indoor units for ceiling installation/karaoke. The risk also exceeded allowance levels except

Table 8.2.6.2 Indoor safety measures

Installation case		Using	Repairing
Floored	Restaurant	Mechanical Ventilation	Carrying leak detector +Education
Ceiling	Karaoke	Leak detection → Mechanical Ventilation	-

Table 8.2.6.3 Outdoor safety measures

Installation case	Installation	Using	Repairing	Disposal (Removal)
Semi-underground	Carrying leak detector	Mechanical Ventilation	Ventilation + Carrying leak detector +Education	Carrying leak detector +Education
Machinery room		Existing Mechanical Ventilation		

during transport/storage in semi-underground installations. All risks were lower than the allowable level with regard to improper charging in the life stages of system operation, repair, and disposal. Tables 8.2.6.2 and 8.2.6.3 present safety measures.

With regard to the life stage of repairs and disposal, which is when a burner is often used, service providers need to be trained, and the habit of carrying refrigerant leak detection devices during installation, repair, and disposal at sites prone to refrigerant accumulation needs to be cultivated.

Tables 8.2.6.4 and 8.2.6.5 indicate the ignition sources and refrigerant leaks that have the largest impact on the probability of accidental fires in risk scenarios. Open flames such as combustion-type heaters and gas stoves are the most common ignition sources during use, and welding burners are the most common sources during installation, repair, and disposal. To reduce risk, measures concerning open flames indoors and the handling of burners during work are necessary. Ignition by oil lighters is most common in offices, machinery rooms, and transportation storage facilities. Tokyo University of Science, Suwa, is currently evaluating how oil lighters can become ignition sources in a flammable space, and the risk values may change according to their results.

Table 8.2.6.4 Main ignition sources in risk scenario

Installation case	Life stage	Transport /Storage	Installation	Using (indoor) Using (outdoor)	Repairing	Disposal (removal)
Indoor unit	Ceiling	Office		Smoking tool Water heater	Braze burner	Braze burner
	Floored	Restaurant		Combustion heater Gas cooker		
	Ceiling	Karaoke				
Outdoor unit	Usual	-	Smoking tool	Braze burner	Braze burner	Braze burner
	Each floor	-				
	Semi-underground	-		Braze burner + Boiler		
	Machinery room	-		Smoking tool		
Ceiling space	-			Fire of A/C Power failure	Braze burner	Braze burner

Table 8.2.6.5 Main leak factor in risk scenario

Installation case	Life stage	Transport /Storage	Installation	Using (indoor) Using (outdoor)	Repairing	Disposal (removal)
Indoor unit	Ceiling	Office		Leak in stopping	Leak in pipe opening	Leak in recovery
	Floored	Restaurant				
	Ceiling	Karaoke				
Outdoor unit	Usual	-	Leak from outdoor unit	Valve operation + Transport damage	Leak in pipe opening	Leak in recovery
	Each floor	-		Above + valve operation		
	Semi-underground	-				
	Machinery room	-		Leak in closed space		
Ceiling space	-		Included in indoor unit	Leak from indoor unit	Leak in pipe opening	Leak in recovery

8.2.7 Future Development

8.2.7.1 Concerning safety measure for floor-standing units

In ceiling installation units, dilution occurs when the refrigerant mixes with the surrounding air according to the acceleration effect; the leaked refrigerant falls from the ceiling toward the floor (Fig. 8.2.4.6), and the indoor concentration becomes a near uniform distribution. However, this dilution effect cannot be anticipated for floor-standing units, and the floor level concentration becomes high; this makes it easy for flammable space to form.

Future investigation is necessary on safety measures for mildly flammable refrigerants, the natural ventilation effect of temperature deviation between indoors and outdoors, and the location of mechanical ventilation openings in floor-standing units to prevent suffocation accidents as per GL-13. However, GL-13 does not anticipate whether or not refrigerant accumulation in the vicinity of the floor will be diluted by low-to-high mechanical ventilation.

In the concentration distribution analysis, the formation of flammable space greatly changes according to the concentration boundary conditions for the leaked refrigerant emitted from the floor-standing unit. Three companies that use the low boy-type floor-standing unit performed experiments; a comparison with the analysis results (even of the mix inside the unit) showed that the experimental results could be reproduced. Currently, we can use this analysis method to effectively evaluate both mechanical ventilation and natural ventilation.

8.2.7.2 Handling of R1234yf and R1234ze

Because the work from risk assessment to safety measure proposal has been completed once, priority was given to R32 as the target refrigerant. Based on these results, there is a plan to evaluate the special characteristics and issues of R1234yf and R1234ze that differ from those of R32. Because their molecular weights are more than twice that of R32, the evaluation is proceeding with regard to the impact on refrigerant accumulation from a refrigerant leak when the gas density is high and whether this affects the flammable limit range spread when the air is humid.

8.2.7.3 Ideal for safety and market regulation

Because large amounts of refrigerant are used, executing necessary safety measures is important for the safe use of

mildly flammable refrigerants in VRF air conditioning systems that have higher risk than pair-type air conditioners. The JRAIA safety guidelines for GL-13 are to be revised in the future based on this risk assessment, which we feel should be disseminated.

The penetration of VRF systems with a mildly flammable refrigerant into the market is impossible if excessive safety measures are enacted when the necessity is low, which means that they will not help reduce global warming. Conversely, effective penetration reduces safety when safety measures are neglected for cases where the necessity is high.

Consequently, rules need to be imposed based on a risk assessment that reflects the current situation to enact safety measures that are logical and not excessive or insufficient. Although combustion heating devices at the time of use and brazing burner at the time of work (Table 8.2.6.4) were found to be the primary ignition sources in this risk assessment, ignition sources must be properly evaluated for safety measures to be effective. As a primary factor is the generation of flammable space, engineering measures should be investigated in order to further reduce the probability of a rapid refrigerant leak producing a flammable space.

Acknowledgments

This report was created through the joint cooperation of Yukio Kiguchi (Toshiba Carrier), Katsuyuki Tsuno (Panasonic), Hiroaki Tsuboe (Hitachi Appliances), Shuntaro Ito (Fujitsu General), Koji Yamashita (Mitsubishi Electric), Tatsumi Kannon (Mitsubishi Heavy Industries) and Chief Investigator Ryuzaburo Yajima (Daikin Industries). In addition, Hiroichi Yamaguchi (Toshiba Carrier), Eiji Sato (Hitachi Appliances), Takuho Hirahara (Mitsubishi Electric), Kenji Takaichi (Panasonic), Shinya Matsuoka (Daikin Industries), and Shigeharu Taira (Daikin Industries) lent their cooperation as observers. We express our deep appreciation to Kazuhiro Hasegawa (JRAIA Secretariat) for his valuable advice and for the time and support received from the Secretariat office.

References

Hashimoto, 1984, Japan Ergonomics , Japan Industrial Safety & Health Association
ISO5149-1, 2, 3, 4/FDIS, ISO Website,

2014, http://www.iso.org/iso/home/store/catalogue_tc/catalogue_tc_browse.htm?commid=50362

JRAIA, 2012, Guideline of Design Construction for Ensuring Safety against Refrigerant Leakage from Multi-split System Air Conditioners, JRA GL-13

Kataoka et al., 1999, Experimental and Numerical Analyses of Refrigerant Leaks in a Closed Room, ASHRAE Transact., Vol 105, Pt 2

Kitajima, 2010, Actual Survey on the Air Environment at Various Number of People in Karaoke Rooms, Shibaura Institute of Technology,

Mukaidono, 2009, Concept of Safety, Trends in Academic, Sep., P14

Nomura, 2010, Actual Survey of the Air Environment of 20 Karaoke Box Stores in Tokyo, Shibaura Institute of Technology

Public Buildings Association, 2006, Design Criteria for Building Facility Compiled by MLIT

Simplified Simulation Model, 2011, Progress Report by VRF SWG

The Building Standard Act, Article 28

The Building Standards Act, Order for Enforcement, Article 20, 2

Yao et al., 2000, Risk Assessment of Room Air Conditioner using R290, International Symposium on Environment and Alternative Refrigerants 2000, Kobe

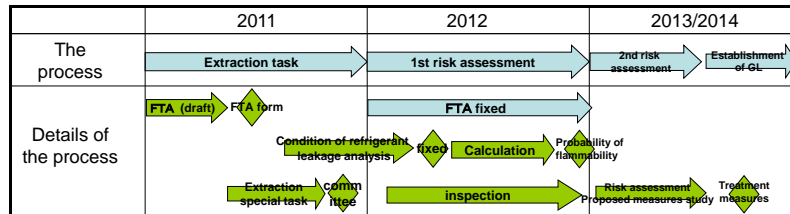
8.3 Chiller SWG: Chiller Risk Assessment and Guideline Establishment

8.3.1 Introduction

The heat-source system supplying hot or cold water to an air-conditioning system uses the hydrofluorocarbon (HFC) refrigerants R410A or R134a. Both refrigerants have a significant impact on global warming with a GWP exceeding 1000. Therefore, it is necessary to ultimately replace them with low GWP alternatives. Some refrigerants with a low GWP, such as R1234yf, R1234ze (E), and mixed refrigerants, have been evaluated in retrofit and performance tests. All of these low GWP refrigerants are mildly flammable. Risk assessments (RAs) of chillers, in which these two refrigerants and R32 were added, have focused on the ignition and burning characteristics of the refrigerants, and have been performed to evaluate security against fire accidents and burns.

The WG (chiller SWG), which consists of professional chiller engineers, was established by the Japan Refrigeration and Air Conditioning Industry Association (JRAIA) to perform RAs. Requirements for the chiller design and the condition of facilities that incorporate the measures and the actions defined by the RAs will be established as a JRAIA guideline (GL) in 2014. Progress toward this end is summarized in this report.

Table 8.3.1 Risk assessment process chart of chiller SWG



8.3.2 Scope

The scope of these requirements mainly includes air-cooled heat pumps installed outdoors and water-cooled chillers installed in a machine room as a central air-conditioning heat source, with the exception of mobile facilities and those with a cooling capacity ranging from 7.5 to 17,500 kW.

8.3.3 Prerequisite for performing risk assessments

Because the equipment has the same structure and potential applications as conventional equipment, the RAs^{1,2)} that have been performed are generally effective. The RAs have been performed in a manner that has improved their consistency and has focused on the differences in the flammability characteristics of refrigerants. In addition, we have referenced studies of the mini-split air conditioner and the multiple packaged air-conditioning unit system, for which RAs have been performed.

8.3.3.1 Risk map

Risks were clarified using the FTA method and a numerical evaluation was performed by plotting a risk map (R-map) (Fig.8.3.1) based on the probability of occurrence and severity of harm of each probable ignition source and case of refrigerant leakage. If a risk level was in the A or B region, measures and actions to reduce the probability of occurrence and the severity of harm were suggested to shift the risk level to the C region.

(1) Probability of occurrence

The stock of water-cooled chillers and air-cooled heat pumps in the Japanese market is estimated to be 134,000 units according to JRAIA shipment statistics. This represents less than one-thousandth of the stock of mini-split air conditioners. The probability of the occurrence of harm, based on the handbook³⁾ (HB), is described in Table 8.3.2.

(2) Severity of harm

The severity of harm is based on the definition of fire in the HB³⁾ (Table 8.3.3).

Table 8.3.2 Probability of occurrence of harm

Probability of occurrence of harm		Industrial-level product (adoption)
5	Frequent consumer goods: 10^{-3} industrial-level product: 10^{-1} (cases/units per year)	Number of accidents : once a year (per 10 units)
	Probable consumer goods: 10^{-4} industrial-level product: 10^{-2} (cases/units per year)	Number of accidents : once a year (per 100 units)
3	Occasional consumer goods: 10^{-5} industrial-level product: 10^{-3} (cases/units per year)	Number of accidents : 134 times a year
	Remote consumer goods: 10^{-6} industrial-level product: 10^{-4} (cases/units per year)	Number of accidents : 14 times a year
1	Improbable consumer goods: 10^{-7} industrial-level product: 10^{-5} (cases/units per year)	Number of accidents : once or twice a year
	Incredible consumer goods: 10^{-8} industrial-level product: 10^{-6} (cases/units per year)	Number of accidents : once or twice every ten years

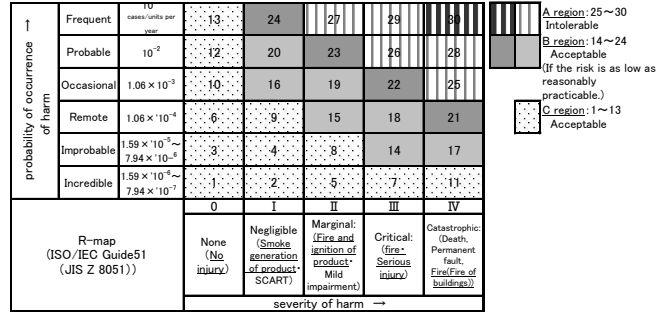


Fig.8.3.1 Risk assessment map

Table 8.3.3 Severity of harm

	Qualitative representation	Severity of harm
IV	Catastrophic	Building fires
III	Critical	Fire
II	Marginal	Fire and ignition of product
I	Negligible	Smoke generation of product
0	None	No injury

8.3.3.2 Definition of life stages

The term “Overhaul” has been added to the life stages in the existing reports^{1,2)}, with six life stages defined: “Logistics,” “Installation,” “Usage,” “Repair,” “Overhaul,” and “Disposal.” Each life stage is distinguishable for a water-cooled chiller or air-cooled heat pump, based on the installation conditions.

8.3.3.3 Evaluation according to the risk-assessment list

In the study, risks were quantified using the risk-assessment list. Combinations of extracted ignition sources and causes of leakage were listed for each life stage of the equipment. A risk evaluation using the R-map and the evaluation of the hazard level of different areas using JISC60079-10 was conducted simultaneously. The treatment of the extracted risk was expanded to the GL. Then, combinations with a sufficiently low risk of ignition and leakage were eliminated, allowing combinations with a greater risk to be fully evaluated.

The intrinsically safe design and requirements to be fulfilled where a risk was identified, as well as the facility requirements in KHK0302-2⁵⁾, JISC60079s⁴⁾, and ISO5149-3⁶⁾, were specified to determine the actions to be taken in the GL.

8.3.4 Settings used in the flammable space analysis model in the event of a refrigerant leak

For safety assessments, the time that flammability persisted for and the volume of the flammable space were calculated when a refrigerant leaked.

8.3.4.1 Analysis model of a machine room

(1) Definition of a machine room

A water-cooled chiller is normally installed in a machine room. Even if an inert gas is charged in the units, the ventilation system is installed in accordance with the technical standards^{5,6,8)} to avoid the danger of suffocation. The restriction of the ventilation volume and the installation of ignition sources as in the standards were applied to the analysis model.

(2) Area of the machine room

The mean, minimum, and maximum values of the machine room area for a specific chiller volume are summarized in the List of Completed Facility Research of the Journal of Heating and Air-Conditioning Sanitary Engineering (2007 - 2010) (Fig.8.3.2). In the analysis model, the area of the machine room is defined as the average value and the height of the machine room is defined as 5 m.

(3) The position of installed equipment

The shape of the machine room floor was a 1:2 rectangle. The chiller was assumed to be installed on one half of the floor and auxiliaries were installed on the other half. The maintenance space was 1.2 m or more on the front of the control panel and 1.0 m or more on the other sides (Fig.8.3.3).

(4) Assumption of ventilation volume, air supply, and exhaust louver area

The air was ventilated five times or more per hour by mechanical forced ventilation.⁹⁾ The air supply and exhaust louver area were determined by reference to the “Mechanical Equipment Construction Edition” of the Kagoshima Prefecture Building Standards. An air-supply port was installed immediately above the body of the equipment and an exhaust port was located on the wall behind the equipment (Fig.8.3.3).

(5) Refrigerant leakage point

It was presupposed that a refrigerant leakage point was located 0.15 m from the floor, which is the center of the front face of the machine. Refrigerant leakage occurred through a 0.1-m cylindrical nozzle at sonic speed.

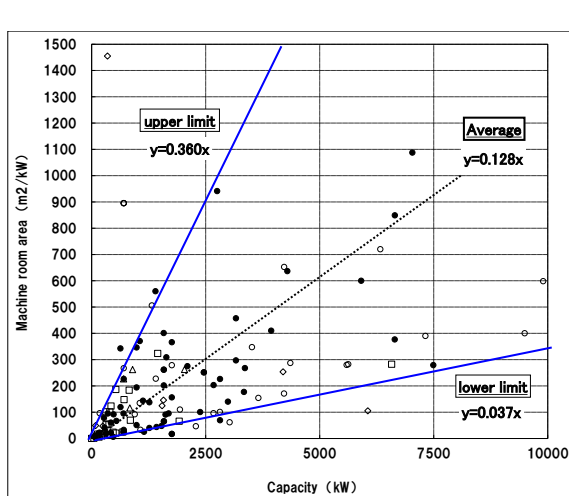


Fig.8.3.2 Relationship between machine room area and chiller capacity

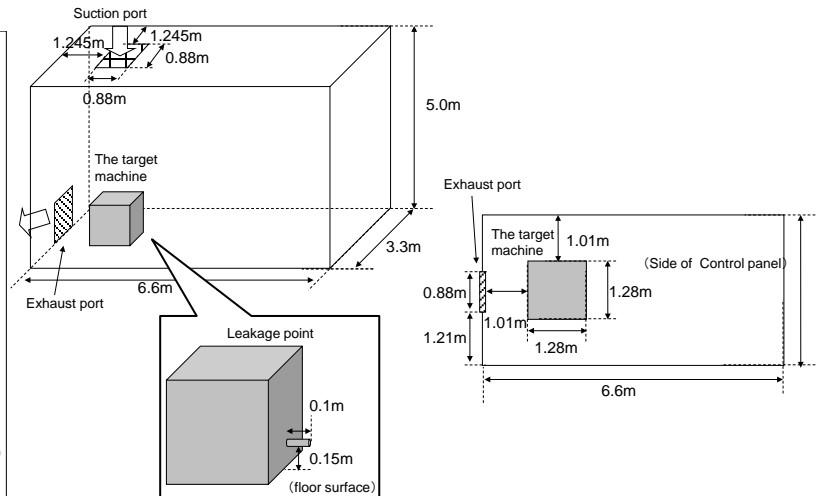


Fig.8.3.3 Outline of the machine room

8.3.4.2 Analysis model of equipment installed outdoors

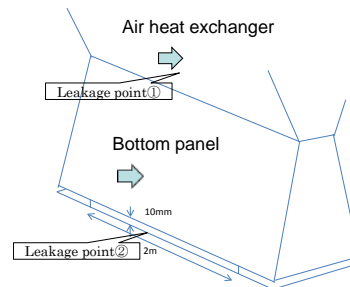
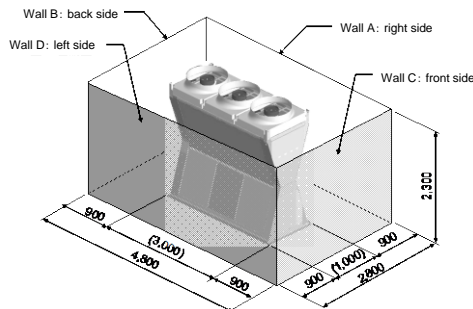


Fig.8.3.4 Air-cooled chiller analysis model

Compared to a water-cooled chiller installed inside the machine room, an air-cooled heat pump installed outdoors, without walls on all four sides, has less chance of forming a flammable space. Therefore, based on the soundproofing installation procedure described by the manufacturer, the analysis model included two walls (Wall A and B) and two walls (Wall C and D) with a 25% aperture ratio, thus creating an environment in which a flammable space is most readily formed (Fig.8.3.4).

The refrigerant leakage areas were:

- (1) Air-heat exchanger
- (2) Inside the decorative panel of the unit

With regard to (2), after a refrigerant is placed inside the panels, it could leak into the area outside the unit. The parts inside the heat pump were also considered to be an ignition source.

8.3.4.3 Definition of the flammable region and the amount of leaked refrigerant

The representative physical properties of the three target refrigerants are shown in Table 8.3.4. The leakage areas of a chiller are the same structure and size as in a multiple packaged air-conditioning unit system. Therefore, the leakage rate was determined in accordance with JRA GL-13⁸⁾ (Table 8.3.5).

Table 8.3.4 Flammability of refrigerants¹⁰⁾

		Stoichiometric concentration	Limit of flammability		Maximum burning rate	Combustion heat	Diffusion coefficient
		vol%	LFL vol%	UFL vol%	cm/s	10 ³ J/kg	cm ² /s
R32		17.36	13.5	27.5	6.5 ^{※4}	9.3	0.135
R1234yf	dry air	7.75	6.7	11.7	1.6	10.3	0.075
	wet air	7.41	5.15 ^{※1}	13.6 ^{※1}	5.9 ^{※2}	10.8 ^{※3}	
R1234ze(E)	dry air				10.2		0.074
	wet air		5.9 ^{※1}	12.6 ^{※1}	5.2 ^{※2}	10.7 ^{※3}	

※1 absolute humidity:0.016, ※2 absolute humidity:0.03, ※3 absolute humidity:0.052
※4 microgravity

Table 8.3.5 Type of leakage flow

		Type of refrigerant leak		
		Slow leak	Rapid leak	Rapid leak
Leak Rate	R32	1kg/h or less	10kg/h	75 or 200kg/h
	R1234yf	0.9kg/h or less	8.9kg/h	67 or 178kg/h
	R1234ze(E)	0.7kg/h or less	7.3kg/h	54 or 145kg/h
Probability of occurrence		It is unknown whether it is capable of detecting	Occasional	Remote
Position of occurrence		Pinhole, Welded part, Brazing part, cauterization part	Cracking flare, Flare welding part, Cauterization part	Slipping-out accident from flare fitting joint, Pipe fitting

8.3.4.4 Analysis of the flammable space for a refrigerant leak

(1) Analysis for a machine room

An evaluation was performed for the cases shown in Table 8.3.6.

- Case 1: To calculate the time period from the start of a refrigerant leak until it is ventilated, a non-stationary analysis was performed for a burst leak. In addition, the difference between the R32 and R1234ze(E) refrigerants was also evaluated.
- Case 2: The same leakage was considered, but by changing the level of ventilation, the formation of a flammable space was calculated (stationary analysis). Here, regardless of the refrigerant charge, the relationship between the flammable space and the level of ventilation was evaluated by infinitizing the refrigerant leakage time.

(2) Analysis for outdoor equipment

To calculate the probability of the presence of a flammable space, a non-stationary analysis was performed. The analysis conditions are described in Table 8.3.7.

Table 8.3.6 Analysis conditions (Machine room)

No	Machine room area [m ²]		Refrigerant	Type of leak	Ventilation rate [1/h]	Airflow rate [m ³ /h]
	A	B				
Case1	Non-stationary analysis	A	R1234ze(E)	Burst leak	54	1
		B				109
		C				218
		D				545
Case2	Stationary analysis	A	R32	Burst leak	54	1
		B				218
		C				218
		D				218

Table 8.3.7 Analysis conditions (Air-cooled chiller)

No	Leakage point	Refrigerant	Capacity [Hp]	Type of leak		Refrigerant charge [kg]	Wind velocity [m/s]
				[kg/h]	[kg/h]		
1	Point①	R32	30	slow leak	1	11.7	0
2				rapid leak	10		
3				burst leak	75		
1	Point②	R32	30	slow leak	1	11.7	0
2				rapid leak	10		
3				burst leak	75		
4				R1234yf	rapid leak		

8.3.4.5 Refrigerant leak analysis results

(1) Analysis of the machine room

a) Case 1

The variation of the refrigerant concentration at each evaluation point over time (ventilation rates of once/h and twice/h) is shown in Fig.8.3.5. The refrigerant concentration increased over time from the start of the leak and reached a maximum at the cessation of the leak at all evaluation points. At the cessation of the refrigerant leak, the area from the floor to the height of the machine was a flammable region with a volume of 27 m³ at a ventilation rate of once/h. However, at a ventilation rate of twice/h, a flammable space formed only in the area adjacent to the leakage point and the refrigerant concentration in this space only reached the LFL or lower. The time that flammability persisted for and the volume of the flammable space is shown in Table 8.3.8. In the flammable space, the refrigerant concentration extended between the LFL and the UFL and burning velocity constraints were not taken into account. From Table 8.3.8, if the air exchange rate was twice/h, the time that flammability persisted for and the volume of the flammable space was very low. Therefore, considering the velocity of the refrigerant, the possibility of ignition was small. A similar analysis with the refrigerant, R32 was performed at a ventilation rate of twice / h. The time that flammability persisted for and the volume of the flammable space is shown in Table 8.3.8. From a comparison of the results for R32 and R1234ze(E), it can be seen that R32 was present at a higher density in

the flammable space and was easily diffused, but because the concentration required to meet the LFL was high, the flammable space was reduced.

The alteration in volume of the flammable region at a ventilation rate of once/h to form a flammable space with/without consideration of the burning velocity is shown in Fig.5.4.6. An R1234yf flow rate of 1.5 cm/s was used as the burning velocity of R1234ze. The flammable space during the leak formed by centering around the area where the air velocity was faster than the burning velocity in the neighborhood of the leakage point. Therefore, the flammable space with consideration of burning velocity was very small compared to the situation where the burning velocity was not considered.

However, the flammable spaces have approximately the same volume regardless of the burning velocity because the air velocity throughout the machine room was low after the leak stopped. Therefore, the evaluation was performed in the flammable space without considering the burning velocity.

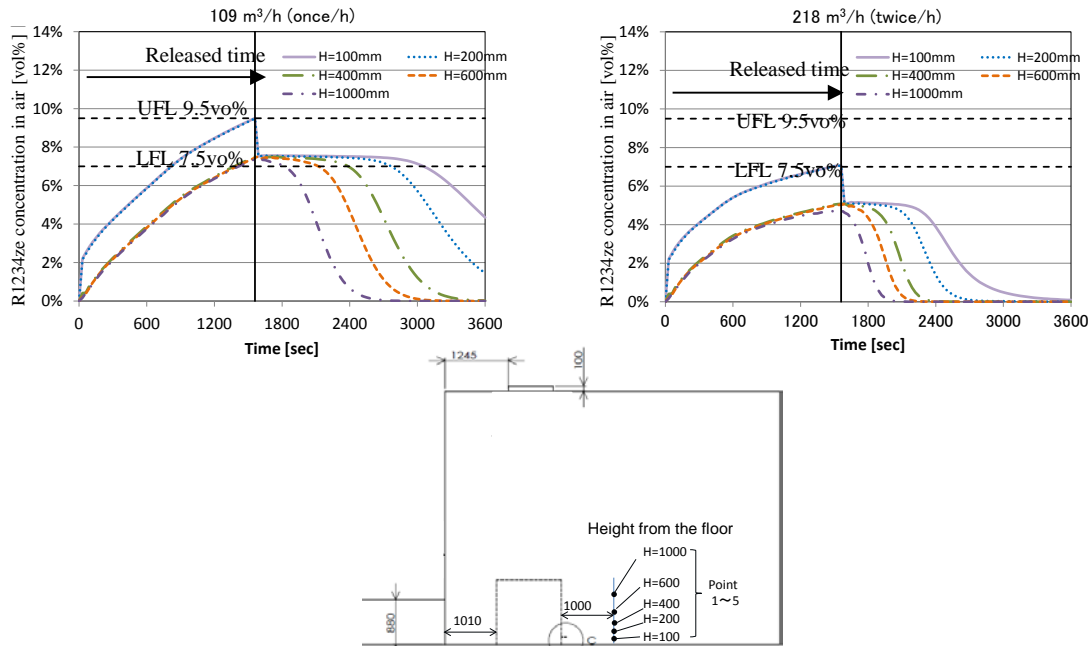


Fig.8.3.5 The results of non-stationary analysis (variation of concentration over time)

Table 8.3.8 The results of the non-stationary analysis

No	Air changes per hour (Ventilation air volume)	Time	Volume of flammable area		Time × Volume
			Maximum	Average	
	(m ³ /h)	min	m ³	m ³	m ³ ·min
Case1	A 1 (109)	56	27	6.4	36
	B 2 (218)	26	8.90E-04	2.70E-03	7.10E-02
	C 5 (545)	25	3.30E-04	2.70E-03	7.90E-04
	D 2 (218)	26	2.80E-05	1.70E-05	4.50E-04

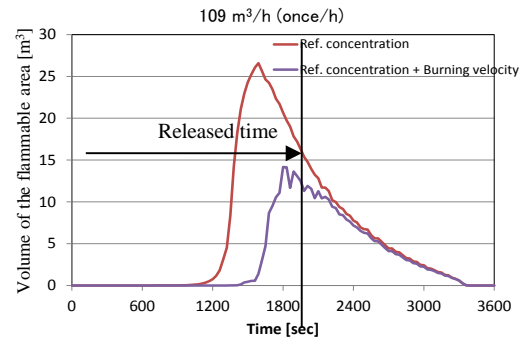


Fig.8.3.6 The results of non-stationary analysis (variation of concentration over time)

b) Case 2

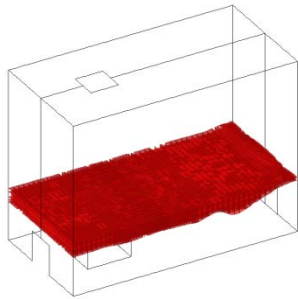
The results of the stationary analysis are shown in Fig.8.3.7. The red sections in Fig.8.3.7 indicate the LFL. At a ventilation rate of once/h, the LFL extended to the height of the machine and the space from the floor to the height of machine was above the LFL. At a ventilation rate of twice/h, the flammable space was only adjacent to the leakage point. As a result, this case, which infinitizes the amount of refrigerant required to fill the space, had the same tendency as case 1. The flammable space formed only in the area adjacent to the leakage point at a ventilation

rate of twice/h, and the refrigerant concentration of the other spaces was below the LFL. Therefore, the possibility of ignition was small.

As a result of the analyses of a) and b), and in consideration that an ignition source was not present at the leakage point, the possibility of ignition was very low for an average machine room designed to the ISO5149⁷⁾ standard, which specifies a mechanical forced ventilation of at least four/h. From the results of the steady-state analysis, regardless of the refrigerant charge, there is no possibility for a flammable space to form. Therefore, it is considered that there should be no restrictions on refrigerant charge in the chiller GL.

However, a narrow machine room that is smaller than the average value of the machine room area (Fig.8.3.3) must also be considered. Because the level of ventilation is reduced and the amount of leakage over time is relatively large even if ventilation was provided at the same level as in an average machine room, there was a possibility that a flammable space could form. Therefore, it is necessary to add a consideration for a narrow machine room in the GL by assuming that the minimum floor area would be 1/3 of the floor area of the average machine room. To consider the risk when ventilation was stopped due to equipment failure or other factors, the risk of ignition was evaluated in consideration of the presence or absence of interlock action due to the formation of a flammable space and a sufficient refrigerant concentration.

Case 2-A) One air change per hour
Flammable region volume 9.0 m³



Case 2-B) Two air changes per hour
Flammable region volume 1.6×10⁻² m³

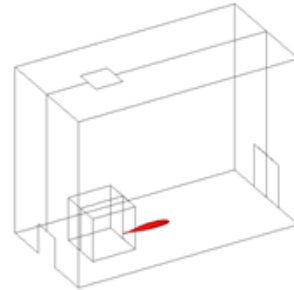


Fig.8.3.7 The results of non-stationary analysis

(2) Analysis of the outdoor equipment

a) Leakage from the air-heat exchanger

The results of the analysis are shown in Fig.8.3.8. Because diffusion was fast, a small flammable space was formed near to the refrigerant leakage point at a height of 1.13 m. Because the velocity of the refrigerant was small and the ignition source was not in the immediate vicinity of the air heat exchanger, the possibility of ignition was very small.

<Leakage point ①>

Burst leak 75 kg/h, Leakage time 9 min 21 s

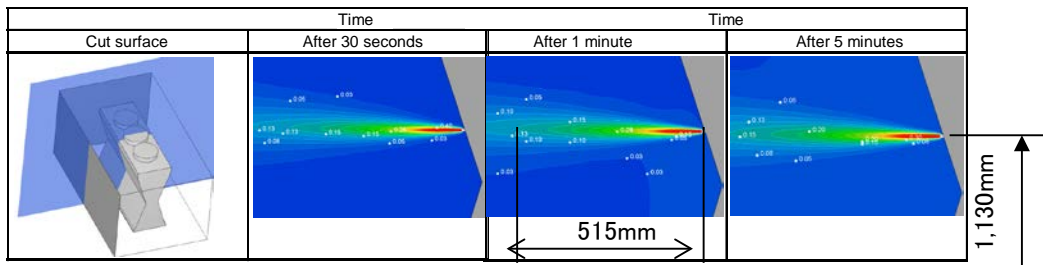


Fig.8.3.8 The results of non-stationary analysis

b) Leakage from the inside of the decorative panel of unit

The results of the analysis are shown in Fig.8.3.9. If the refrigerant leaks from a decorative panel on the outdoor equipment, it will accumulate at the bottom of the leakage point because the refrigerant is likely to have leaked from a slit in the bottom of the unit. The flammable space formed for about 1 minute. This space disappeared within one minute once the refrigerant leak stopped. Unlike leakage from the air heat exchanger, a flammable space was formed.

Therefore, to assess the ignition risk, it is necessary to consider the probable existence of an ignition source. It is not likely that ignition sources will be present in the region 50 mm above the floor surface.

With regard to the difference in refrigerants, the flammable space that formed with R32 was about two and a half times larger than that which formed with R1234yf. From the analysis of the outdoor unit, the use of R32 can be considered to be dangerous.

The results calculated for the space-time product of the flammable spaces of a) and b) are shown in Table 8.3.9. Because this analysis was very rough, it is necessary to review the results and perform additional analysis.

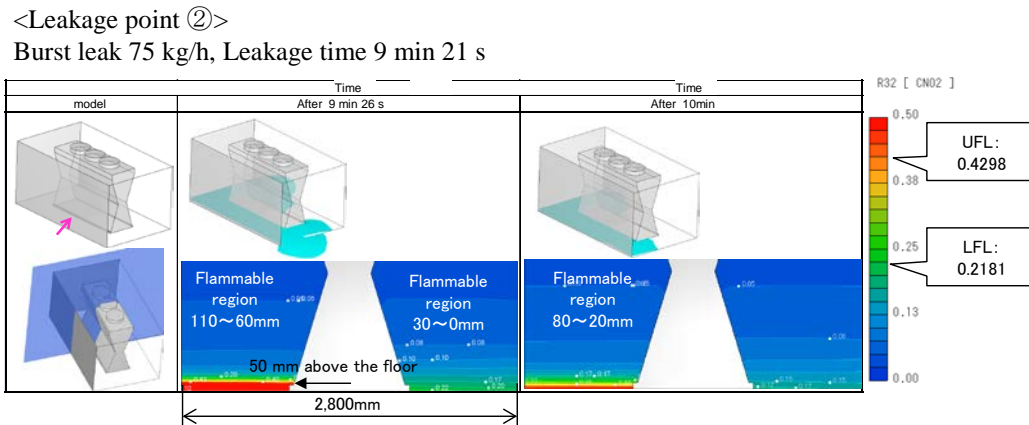


Fig.8.3.9 The results of non-stationary analysis

Table 8.3.9 The results of stationary analysis

No	Leakage point	Refrigerant	Type of leak	[kg/h]	Volume of flammable area [m ³]	Time [min]	Time × Volume [m ³ ·min]
1	Point①	R32	slow leak	1	1.60.E-07	702	1.12.E-04
2			rapid leak	10	1.16.E-05	70	8.11.E-04
3			burst leak	75	1.40.E-04	9	1.31.E-03
1	Point②	R32	slow leak	1	3.48.E-03	702	2
2			rapid leak	10	1.54.E-01	71	11
3			burst leak	75	4.02.E-01	11	452
4		R1234yf	rapid leak	8.9	5.66.E-02	79	448

8.3.5 Basic configuration of FTA

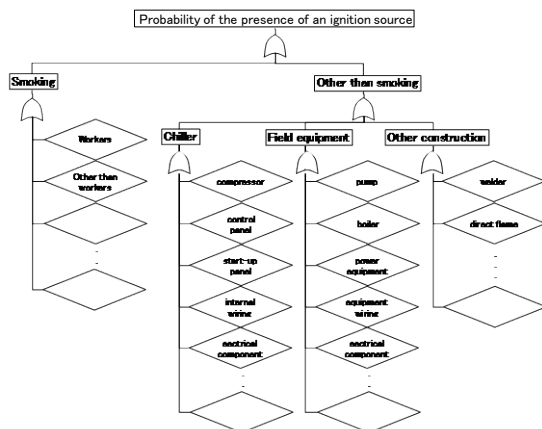


Fig.8.3.10-a Basic FTA for each life stage

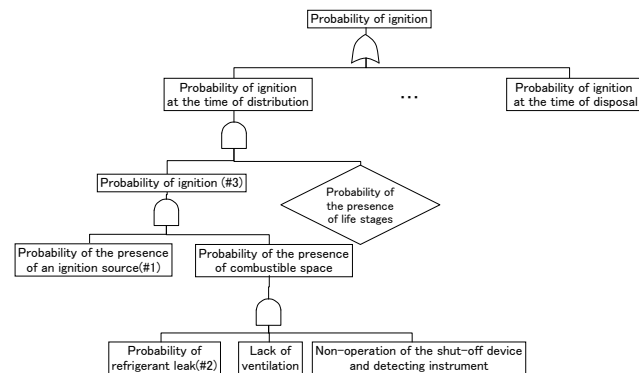


Fig.8.3.10-b Probability of ignition

There are a small number of operators and servicemen who can access the machine room. The room also includes other electrical equipment with a relatively large capacity (> 5 kVA), and the installation of equipment in addition to

combustion equipment, such as a boiler, is necessary. However, unlike the situation with a mini-split air conditioner or a multiple packaged air-conditioning unit system, a machine room and its installations can be safely controlled.

The basic FTA was configured to ensure a consistent probability of encountering refrigerant leaks and an ignition source throughout the six life stages (Fig.8.3.10-a). In addition, a common FTA was used to assess the probable existence of an ignition source so that it would not be overlooked in each life stage (Fig.8.3.10-b). The probability of a leak also was studied (not shown in a figure).

8.3.6 Machine-room requirements in KHKS0302-3 and ISO5149

KHKS0302-3⁵) is written in accordance with related standards such as the Refrigeration Safety Regulations, which are based on the High Pressure Gas Safety Act. To maintain the safety of the machine room, standards are applied concerning (1) ventilation through an opening or the installation of mechanical ventilation, (2) the additional installation of safety valves and gas-release tubes, (3) explosion-proof lighting to ensure adequate performance, and (4) fire prevention/extinguishing systems.

The most important difference between KHKS and ISO5149-3 (2014 version) is the ventilation volume prescribed. Whereas KHKS calculates the volume using the legal term “ton of refrigeration,” ISO5149-3 uses the refrigerant filling volume. Section 3.2.3 (Prevention of Stagnant Refrigerants) of KHKS states that “The machine room must be maintained in a way such that the concentration of refrigerant does not exceed its limit concentration even in the event of a leak of its entire amount.” If the subsequent formula used to calculate the amount of refrigerant used is based on the ton of refrigeration, the difference in the compression method causes the ventilation volume of a machine with the same amount of refrigerant to be different. Therefore, ventilation standards that are independent of the refrigerant charge of the instrument will be used in the GL, but the refrigerant charge will be used as required.

Another significant difference between KHKS and ISO5149-3 regards the standards adopted for the installation of ignition sources in a machine room. ISO5149-3 specifically prohibits the presence of open flames but has no surface-temperature standard for the equipment inside a machine room. For the GL, a surface-temperature standard based on the RAs will be necessary.

The GL will set a new standard regarding mildly flammable refrigerants (using KHK facility criteria, if possible) based on basic property data and leakage simulation.

8.3.7 Estimation of the probability of a refrigerant leakage accident

To estimate the probability of a refrigerant leakage accident, the following were investigated:

(a) Accidents occurring in 2010 that were listed in the High Pressure Gas Safety Act.

Types of target equipment and refrigerant leakages (burst/rapid/slow) were extracted.

(b) The number of refrigerant leak accidents investigated by each committee participating in the chiller SWG.

The number of refrigerant leakage accidents that occurred at each company participating in the SWG was investigated. In addition, by taking into consideration the number of chillers in stock as a proportion of the volume of shipments made by each company, the ratio of the number of chillers experiencing an accident to the number of in-stock chillers in the market was calculated.

The ratios obtained from the two investigation results generally matched. Therefore, the probability of an accident was calculated based on the result of (b). The result calculated was as follows:

Burst leak: 1.0×10^{-5} /chiller per year [Improbable]

Rapid leak: 1.6×10^{-4} /chiller per year [Remote]

8.3. 8 Legal handling of ammonia

Ammonia is a gas typically used in mildly flammable refrigerants. Its upper explosive limit is 28 vol% and its lower explosive limit is 15 vol%. As with the refrigerants subject to the RAs, it has mild flammability. This chapter summarizes the handling of ammonia according to the Refrigeration Safety Regulations.

8.3.8.1 Refrigeration Safety Regulations

Ammonia is listed as a flammable gas and as a toxic gas in Article 2 of the Refrigeration Safety Regulations. Based on these characteristics, a technical standard to determine its handling has been specified. The handling of flammable gases can be summarized as follows:

- (1) The structure of the machine room shall be such that it is free of any stagnant gas in the event of a refrigerant-gas leak (Article 7, item 3).
- (2) The location of the opening of the release tube for safety valves and similar equipment shall be appropriate to the properties of the refrigerant gas (Article 7, item 9).
- (3) The liquid level measurement instrument shall not be a round glass level instrument. For a glass tube instrument, breakage prevention measures and leak prevention measures in the event of breakage shall be taken (Article 7, items 10 and 11).
- (4) In accordance with its scale, appropriate fire extinguishing equipment shall be installed in appropriate locations (Article 7, item 12).
- (5) The electrical equipment within refrigerant equipment shall be structured such that it has an explosion-proof capacity appropriate to the installation location and type of refrigerant gas (flammable gases excluding ammonia) (Article 7, item 14).
- (6) Leak-detection equipment shall be installed in any location where stagnant gas may occur (Article 7, item 15).
- (7) Measures shall be taken to remove refrigerant gases in a safe and quick manner (Article 7, item 16).
- (8) Measures shall be taken to prevent any danger at the time of maintenance (Article 9, item 3 (b)).

8.3.8.2 Exclusion from the application of Article 7, item 14

Ammonia is excluded from the application of item (5) (Article 7, item 14). This exclusion is in accordance with the technical reference¹¹⁾. An experiment was conducted to determine: 1) the concentrations that define the explosive limits in which a gas easily ignites, 2) the amount of ignition energy generated if it ignites, 3) the spatial distribution of explosive concentrations, and 4) the connection between the ignition frequency and time. The reference states that the validity of the Refrigeration Safety Regulations was reconfirmed based on factors 1) to 4).

Accordingly, in this SWG, the validity of the explosion-proof capacity was also evaluated by focusing on factors 1) to 4) as a guideline.

8.3.9 Derivation of ignition probability

The probability of ignition was derived by the following procedure.

8.3.9.1 Surface temperature of equipment in the machine room

Among the machines and instruments installed in the same area as the target equipment, those listed below, which have relatively high surface temperatures, were investigated.

- 1) Heat source unit (e.g., boiler)
- 2) Electric motor drive (e.g., pump motor)
- 3) Ventilation (e.g., ventilation fan)
- 4) Lighting apparatus (e.g., fluorescent light, incandescent lamp)
- 5) Heating appliance (e.g., electric heater)

The results of ignition tests using mildly flammable refrigerants¹²⁻¹⁴⁾ performed at locations such as Tokyo University of Science, Suwa, and the National Institute of Advanced Industrial Science and Technology will be compared to the surface temperatures of equipment inside the machine room to specify the surface-temperature limits inside a machine room.

8.3.9.2 Smoking rate

Burning cigarette ends and lighter/match flames can be considered to be ignition sources. Therefore, the smoking behavior of servicemen was investigated.

- Fifty-three percent of the servicemen smoked and 28% had smoked on-site. During the past year, 7% of all servicemen sampled had smoked on site.
- A lighter is used as the ignition source by 99.6% of smokers while 0.4% use a match.

Assuming that the proportion of servicemen that smoke on site is 7%, the number of cigarettes smoked per person per day is 19.1¹⁵⁾, the working hours per day are 8, the ignition source is only a match, and the time when an open flame exists per smoking event is 2 s, the probability (ignition frequency) of an ignition source existing because of smoking is estimated to be of the order of 10^{-8} to 10^{-9} .

8.3.9.3 Electrical components

Among the electrical components (e.g., electric motor drive, electromagnetic switch, electromagnetic contactor, printed-wiring board, and transformers) to be mounted on a chiller unit, an electromagnetic contactor, in which an arc is generated, has the greatest possibility of providing an ignition source. The rating capacity of each type of electromagnetic contactor and the capacity (horsepower) of the chiller have been summarized.

There is a wide range of chiller capacities among the target equipment and the electromagnetic contactors used also have a wide range of capacities. For a product with 20 horsepower or less, the capacity is generally less than 5 kVA. Electrical components with capacities less than 5 kVA are not considered to be ignition sources, as agreed by other SWGs. This evaluation therefore focuses on components with a capacity of 5 kVA or more.

There is no electrical component with a capacity of more than 5 kVA in the control system of a product with more than 20 horsepower. To estimate the maximum risk, an electrical component with a capacity of 5 kVA or more is assumed to always be an ignition source following its first startup/shutdown. Assuming that the maximum number of startup/shutdown cycles per day is 6/h (screw chiller) or 2/h (centrifugal chiller) and that the time that the electromagnetic contactor is present is 1 s, the probability of the existence of an ignition source, is estimated to be of the order of 10^{-4} . Compared to the flame from a match, this probability is large and therefore a further detailed study will be conducted.

8.3.10 The relationship between the RA and GL

To determine the probability of the presence of a flammable space, the ignition probability at each life stage was calculated (assuming there was no ventilation and that ignition sources always ignite). The results are shown in Table 8.3.10. The sum of the probability of occurrence of fires and burns is more than 10^{-6} . Therefore, it is necessary to take measures to reduce the probability to a level that is considered acceptable by society. This represents the standard for ventilation and the system of holding by it.

Table 8.3.10 Risk assessment results

Accident scenario	Life stage probability	Probability (cases/units per year) Time × Volume	Assessment
Logistics	0.0564	$3.22 \times 10^{-7} X$ Time × Volume	Safe
Installation	0.0564	$5.01 \times 10^{-7} X$ Time × Volume	Safe
Usage	0.7809	$3.82 \times 10^{-6} X$ Time × Volume	Nearly safe
Repair	0.2523	$2.73 \times 10^{-6} X$ Time × Volume	Nearly safe
Disposal	0.0565	$1.38 \times 10^{-6} X$ Time × Volume	Safe

The items to be added are as follows:

- There is a wide-range of equipment conditions (such as transfer, storage, etc.) in the distribution process. Large warning stickers should be used, indicating that a slightly combustible gas is present and detailing its handling procedure.
- It is necessary to clarify installation conditions for outdoor applications because of the airflow.
- An electromagnetic contactor (< 5 kVA), which is within the scope of IEC60335-2-40⁷⁾ is not regarded as an ignition source on the basis of the results of the mini-split SWG.
- There is no technical standard specifying a chiller unit with a structure in which a refrigerant gas may accumulate due to a decorative panel or other design features. The requirement for an opening space, which does not have enclosed structure, is described in the GL as an intrinsically safe design.
- With regard to disposal, a risk assessment should be undertaken focusing on refrigerant recovery.

8.3.11 Guideline planning taking IEC60079-10-1 into consideration

8.3.11.1 Principle of IEC60079-10-1

The following principle from IEC60079-10-1 is crucial: “Installations in which flammable materials are handled or stored should be designed, operated and maintained so that any releases of flammable material, and consequently the extent of hazardous areas, are kept to a minimum, whether in normal operation or otherwise, with regard to frequency, duration and quantity.”

The classification of hazardous areas in which a danger may arise due to a flammable gas is defined in IEC60079-10-1¹⁶⁾. Areas can be categorized into one of three hazardous and non-hazardous areas based on their grade of release and two indexes of the ventilation condition: “degree of ventilation” and “availability of ventilation” (Table 8.3.11). In Japan, the classification of hazardous areas is established in JISC60079-10⁴⁾, which is the same as that established in IEC60079-10-1¹⁶⁾. In the chiller SWG, a study was conducted using JISC60079-10.

Table 8.3.11 Influence of independent ventilation on the type of zone

Grade of release	Ventilation						
	Degree						
	High			Medium			Low
	Availability						
	Good	Fair	Poor	Good	Fair	Poor	Good, fair or poor
Continuous	Non-hazardous	Zone 2	Zone 1	Zone 0	Zone 0 + Zone 2	Zone 0 + Zone 2	Zone 0
Primary	Non-hazardous	Zone 2	Zone 2	Zone 1	Zone 1 + Zone 2	Zone 1 + Zone 2	Zone 1 or Zone 0
Secondary	Non-hazardous	Non-hazardous	Zone 2	Zone 2	Zone 2	Zone 2	Zone 1 and even Zone 0

8.3.11.2 Guideline planning taking IEC60079-10-1 into consideration

In Japan, when a flammable gas is used in a chiller, the technical standard, JISC60079s⁴⁾, and the Refrigeration Safety Regulations (Article 7, item 14) must be complied with, and the use of explosion-proof electric equipment is necessary. However, the relationship between the equipment installation standard to be referenced (KHK0302-3⁵⁾ or ISO5149⁶⁾) and JISC60079s⁴⁾ is not specified. Although JISC60079s⁴⁾ specifies that explosion-proof equipment is not required in a non-hazardous area as determined by the availability-of-ventilation, this seems to be consistent with the fact that a mildly flammable refrigerant is not considered to be a flammable gas in the Refrigeration Safety Regulations.

Therefore, the conditions for implementing an RA, the techniques used, and the results obtained will be reported in the SWG. In addition, these will be applied to the requirements for the intrinsically safe design of the equipment in the GL, which is being established incorporating equipment installation requirements that do not require the setting of hazardous areas, in accordance with the principle of JISC60079s⁴⁾. The basic policy adopted and tasks required in the preparation of the GL are as follows.

8.3.11.3 Basic policy adopted in the guideline

The GL is being prepared by suggesting measures to take against risks identified by the RA to KHK0302-3 and incorporating the necessary sections of ISO 5149-1, 3. The basic policy adopted in the GL is as follows:

- Only one slightly combustible refrigerant (A2L) is referred to as the target refrigerant and descriptions of the applications of other refrigerants will be deleted.
- The following measures should be adopted with reference to IEC60079 so that a machine room does not become a hazardous area, even if a refrigerant leaks.
 - (1) Installation and inspection of ventilation devices (including backup with multiple devices as required).
 - (2) Refrigerant detector (including UPS and periodical inspection).

Note: The following is under debate in the SWG.

- Outdoor installation should be considered to be a non-hazardous area following an analysis.
- Electrical equipment should have a non-explosion-proof specification and conform to IEC/ISO.
- Specific values (twice or more/h ventilation, scope of a hazardous area) must be determined on the basis of the results of the analysis.
- Firearms are classified as either work firearms or other firearms (conforming to ISO) and must be considered in the risk assessment, with the exception of the construction period.

8.3.11.4 Tasks for establishing a guideline

The following are the tasks required to establish the GL. The GL is described as a means for reducing the risk and will be established within 2014.

1) Rule of recovery after long-term suspension

- An evaluation at the time of restart if a refrigerant leaks during long-term suspension is under consideration.

2) Rule of outdoor installation in consideration of IEC60079.

3) A method to consider spontaneous ignition temperature

- The spontaneous ignition temperature is being considered with regard to the limits of an open fire in a machine room according to ISO5149 and the limitations of the equipment surface temperature.

4) Rule to establish a refrigerant detector

- A comparison of ISO/GL-13 to determine adequate regulations is under consideration.

(1) **Power supply (alarm, detector):** Installing an independent power supply and UPS is desirable.

(2) **Target to detect:** This should be refrigerant concentration rather than the oxygen concentration (RCL standard).

(3) **Setting values:** To conform to ISO and GL-13.

(4) **Interlock:** Although the adoption of an interlock is under consideration with reference to IEC60079, if the risk is low, an interlock will not be adopted.

5) Control of refrigerant concentration (regulation of the amount of refrigerant filling)

- Although KHKS demands the control of the volume of a machine room and the amount of refrigerant filling so that the refrigerant concentration is equal to or lower than the limiting concentration, the easing of regulations is under consideration because ventilation is presupposed in the GL.

- As a result of the stationary analysis, a regulation to specify the minimum amount of refrigerant filling in a machine room system is under consideration (no filling amount regulation).

Acknowledgments

This report was written by the author and Mr. Yosuke Mukai by compiling the research results of 10 Committee members, as well as Mr. Masayuki Aiyama, Mr. Mikio Ito, Mr. Isao Iba, Mr. Tetsuji Saikusa, Mr. Yoshihiro Sumida, Mr. Mamoru Senda, Mr. Takuho Hirahara, Mr. Syuji Fukano, Mr. Koichi Yamaguchi, and Mr. Tomokazu Tashimo. Sincere appreciation is extended to the members concerned.

References

- 1) Report on the Result of Risk Assessment Consideration of Room Air-Conditioner with R290 Refrigerant: The Japan Refrigeration and Air Conditioning Industry Association Environment Committee Refrigerant Global Warming Response Commission: Summary of the Non-FC Refrigerant Consideration Session Meeting (1999).
- 2) "Risk Assessment of HFC-32 and HFC-32/134a (30/70wt%)," Split System Residential Heat Pump, Arthur D Little Inc., United States (1998).
- 3) Ministry of Economy, Trade, and Industry: Risk Assessment Handbook Practice Edition (2011).
- 4) JISC60079-10(2008): Electric Machinery and Instruments Used in Explosive Atmospheres - Chapter 10: Classification of Hazardous Areas.
- 5) KHKS0302-3: Standards of Refrigeration and Air-Conditioning Equipment Facilities [Facilities with Flammable Gases (including low-flammable Gases)], (2011).
- 6) ISO5149: Refrigerating Systems and Heat Pumps – Safety and Environmental Requirements, (1993)
Part 1) Definitions, classification and selection criteria
Part 2) Design, construction, testing, marking and documentation
Part 3) Installation site
Part 4) Operation, maintenance, repair and recovery.
- 7) IEC60335-2-40: Household and Similar Electrical Appliances -Safety-, (2005)
Part 2-40) Particular requirements for electrical heat pumps, air conditioners and dehumidifiers.
- 8) JRA GL-13: Guideline for Ensuring Safety in the Event of a Refrigerant Leak from a Multi-Unit Air Conditioning System, (2011).
- 9) ASHRAE15: Proposed Addendum to Standard 15-2010, Safety Standard for Refrigeration Systems, (2010).
- 10) Assessment of flammability of R-1234yf and R-1234ze(E): The 49th Combustion Symposium (2011/12).
- 11) T. Toyonaka: "Refrigeration," 70 (811), 5 (1995).
- 12) T. Imamura: Evaluation of Fire Hazards of A2L Class Refrigerants, The International Symposium on New Refrigerants and Environmental Technology 2012, pp. 65-68, Kobe (2012).
- 13) T. Saburi: Combustion Characteristics of Flammable Refrigerant Gases, International Symposium on New Refrigerants and Environmental Technology 2012, pp. 69-72, Kobe (2012).
- 14) K. Takizawa: Flammability Property of 2L Refrigerants, International Symposium on New Refrigerants and Environmental Technology 2012, pp. 73-79, Kobe (2012).
- 15) JT website: http://www.jti.co.jp/investors/press_releases/2012/0730_01_appendix_02.html, (2013).

16) IEC60079-10-1: Explosive
Atmospheres - Part 10-1: Classification of Areas - Explosive Gas Atmospheres.

9. Deregulation Activities in Japan for the Introduction of Mobile Air Conditioning Refrigerant R1234yf

9.1 Background to R1234yf Introduction in Japan

Worldwide efforts to reduce greenhouse gases (GHGs) have resulted in a growing demand for mobile air conditioning refrigerants with low global warming potential (GWP). Since 2011, the European Union (EU) has banned the use of refrigerants with a GWP of greater than 150 in new-model vehicles (from 2017 onwards, the ban will apply to all new vehicles). Japanese automakers are taking the necessary steps for vehicles destined for the EU market.

Preparations for the introduction of low-GWP refrigerants are also underway in North America. The United States (U.S.)-based international Society of Automotive Engineers (SAE International) has completed a risk assessment study on R1234yf, and the American Society of Heating, Refrigerating and Air-Conditioning Engineers (ASHRAE) has classified R1234yf as a mildly flammable gas. In addition, on April 1, 2010 the U.S. Environmental Protection Agency (EPA) issued GHG regulations allowing vehicles that use a low-GWP refrigerant to be provided with credits.

In Japan, the Global Warming Prevention Measures Subcommittee under the Industrial Structure Council's Chemicals and Bio-industry Committee approved, on February 17, 2011, the interim course outlined during its discussions on substitute refrigerants. Specifically, the Subcommittee acknowledged the urgent need to promote refrigerant replacement through collaboration among automakers, government agencies, research institutes, and equipment manufacturers and recommended the resolution of various existing obstacles by 2014.

In response, the Japan Automobile Manufacturers Association, Inc. (JAMA), in concert with research institutes and the manufacturers of refrigerant retrieval/recharging equipment, launched a risk assessment study aimed at ensuring the safe and easy handling of R1234yf by automotive maintenance shops throughout Japan by the target year of 2014.

9.2 Obstacles to R1234yf Introduction

Table 9.1 summarizes existing obstacles to the introduction of R1234yf from the perspective of a vehicle's life cycle and indicates the need (or not) for measures to address them.

A special ministerial approval scheme is currently in place in Japan to facilitate the approval of factory lines producing R1234yf-equipped vehicles based on the explosion-prevention measures taken. Because the number of these production lines is projected to increase in step with the growing number of vehicle models incorporating R1234yf, further deregulation of R1234yf is necessary.

With regard to after-sales servicing, operators of varying types and scale—including auto maintenance shop operators, auto body repair shop operators, and electrical equipment repair shop operators—are engaged in the retrieval/recharging of refrigerants for vehicles in need of repair or that were in accidents. For many of these operators, making the large investment necessitated by regulations governing R1234yf is difficult.

JAMA’s Vehicle Maintenance Subcommittee has singled out requirements concerning mandatory safe distances from gas cylinders as the top-priority deregulation target (see item 4 in Table 9.1 above). Regarding the handling of R1234yf that may be generated from the dismantling of end-of-life vehicles, the Subcommittee decided not to address this matter in the present project because regulations on the retrieval of R1234yf at the vehicle dismantling stage have yet to be established.

Table 9.1 Obstacles and measures required

1) Vehicle production	Current flammable-gas explosion prevention requirements (government ministry-approved)	Deregulatory measures required
2) Charging gas (after-sales servicing)	No obstacles if: -Compliant with Announcement No. 139 -Charging gas pressure does not exceed 0.8 MPa at 35 °C and satisfies terms of Art. 4-3 in Announcement No. 139	No deregulatory measures required
3) Storage of charging gas	[As per High-Pressure Gas Safety Law] Current requirements on mandatory safe distance from fire/flammables	Deregulatory measures required
4) Retrieval/recharging (after-sales servicing)	[As per High-Pressure Gas Safety Law] Current requirements on: -Mandatory safe distances from gas cylinders (hospitals, schools: at least 15 m; homes: at least 10 m) -Removal of static electricity, etc. -Mandatory licensing by prefectural governments of auto maintenance shops	Deregulatory measures required

9.3 Activities of JAMA’s Vehicle Maintenance Subcommittee

In collaboration with the manufacturers of refrigerant retrieval/recharging equipment, refrigerant suppliers, auto maintenance shop associations and other stakeholders, JAMA has been carrying out activities aimed at resolving existing obstacles to the widespread use of R1234yf by 2014. One such activity was a study that used the risk assessment mapping method to assess risk by combining the “probability of injury” and “severity of injury” in a 6 × 5 matrix. Supported by the risk assessment mapping data, JAMA will petition the government to review its safety regulations in order to more accurately reflect the actual risks of R1234yf.

As a first step in its risk assessment study, JAMA conducted hearings with refrigerant retrieval/recharging equipment manufacturers and a survey of retrieval/recharging operators to more clearly identify the risks at maintenance work sites. In cooperation with the Japan Automobile Service Promotion Association, Japan Auto Body Repair Association, and Japan Automotive Electrical Equipment Service Association, the survey questionnaire was distributed to a representative selection of auto maintenance shops, in terms of business scale and services offered, across Japan.

Completed questionnaires were received from a total of 756 auto maintenance shops. The information provided by the 533 shops that performed their own retrieval/recharging operations was compiled into basic data on auto maintenance shops (number of workers, number of vehicles repaired, shop layout information, etc.) and workers’ on-the-job observations (on refrigerant leakage occurrence, ventilation conditions, the presence of ignition sources, etc.).

Based on the data obtained from the questionnaires on leakage-prone points, leakage amounts, and ignition source specifications, JAMA conducted an ignition test and leak simulation test; in both instances, worst-case R1234yf leakage conditions were assumed. The data obtained in these tests were used to calculate the probability and severity of injury caused by R1234yf leakage and map them for risk assessment. Based on the results of its risk assessment study, JAMA is now preparing to propose to the regulatory authorities a package of

measures that would allow R1234yf to be treated as an inert gas (Table 9.2).

Table 9.2 JAMA’s R1234yf-related activities

Conduct of risk assessment study (NEDO* project including questionnaire-based survey; data compilation commissioned from JARI) *New Energy and Industrial Technology Development Organization	Apr. 2011– Mar. 2013
Discussion of measures for regulatory exemption of R1234yf (Participation in METI-sponsored KHK project)	Oct. 2012– Mar. 2013
Submission of proposal for review by METI* *Ministry of Economy, Trade and Industry	Apr. 2013–

9.4 Ignition Test

9.4.1 Test method

The ignition test was carried out by Tokyo University of Science, Suwa, in the Hy-SEF explosive fire resistance test facility at the Japan Automobile Research Institute’s Shirosato Test Center (Fig. 9.1).



Fig. 9.1 Overview of the Hy-SEF test facility

Based on data obtained from the survey questionnaire described above, the identified risks were classified into four categories, as shown in Table 9.3, and prioritized according to the probability and severity of injury caused by R1234yf leakage. The two leading risks—namely, hose rupture and leakage from inside retrieval/recharging equipment—were examined to determine the answers to the following questions:

- In the event of refrigerant leakage from a pinhole in the hose, to what extent does flammable gas escape and aggregate? Does it cause ignition?
- In the event of refrigerant leakage inside the retrieval/recharging equipment, is there a risk of ignition owing to sparks from the electrical relay or other similar parts of the equipment?

Table 9.3 Risk Classification by JAMA’s Vehicle Maintenance Subcommittee

	Risk Description	Leak Speed (amount/time)	Remarks
1)	Slow leak from a junction	1 kg/24 h (gas)	Ignition potential: Low
2)	Hose rupture (including hose pinhole)	1 kg/60 s (gas)	Inner diameter of hose: 4 mm Internal pressure of hose: 0.5 MPa (at normal temperature)
3)	Cylinder safety valve activation (fusible plug)	24 kg/1 h (gas)	Activation possibility: Low
4)	Leakage from (safety valve, etc.) inside retrieval/ recharging equipment	300 g/60 s (liquid) (initially 100 g/0.5 s)	Activation possibility: Low

A testing space of 8 m × 8 m was secured within the test facility, and a testing apparatus (specifically, a 1 m × 1 m acrylic box) to simulate retrieval/recharging equipment was installed inside the testing space. The testing apparatus featured a 20 mm-wide slit on two opposing sides that could be closed or opened for ventilation (Fig. 9.3).

In the hose pinhole ignition test, which was conducted in the open testing space, the refrigerant was made to leak continuously from a pinhole in the hose, and refrigerant concentrations were measured at various locations from the pinhole. The potential for ignition was then examined by applying electric sparks (both a single spark and repeated sparks) or a naked flame near the pinhole. In the retrieval/recharging equipment ignition test, a single spark was discharged to examine the potential for ignition when the ventilation slits were open and when they were closed.



Fig. 9.2 Testing space simulating a work site

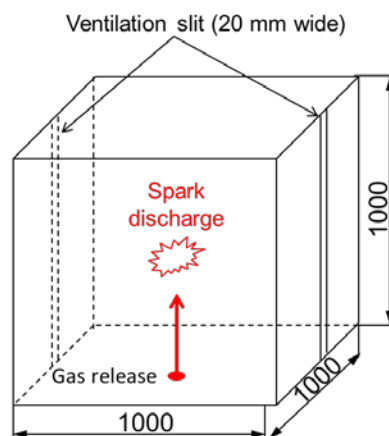


Fig. 9.3 Apparatus simulating retrieval/recharging equipment

9.4.2 Test results

As shown in Table 9.4, the results of the hose pinhole ignition test confirmed that the area within a 10-cm radius from the pinhole was flammable. Nevertheless, despite the application of an ignition energy of 10 J or more, which far exceeded the maximum ignition energy existing inside the equipment (1.07 J at the relay contact), ignition could not be induced anywhere near or away from the pinhole. Similarly, in the retrieval/recharging equipment ignition test and despite the application of a large ignition energy of 16 J, ignition did not occur; this was presumably because of the exchange of air between outside and inside the testing apparatus through the opened slits. As previously reported, combustion and flame propagation occurred when the slits were kept closed; however, no blast pressures were generated.

Table 9.4 Ignition test results

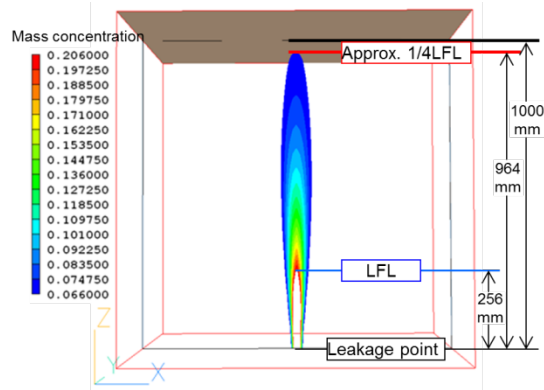
Priority Risk	Test Objective and Outline	Results
Hose rupture (including hose pinhole)	Leakage from $\Phi 4$ mm hose; observation of concentration distribution and potential ignition <ul style="list-style-type: none"> ▪ Leak speed: 470 g/min (cylinder heated to 50 °C) ▪ Ignition source: Repeated electric sparks 	<ul style="list-style-type: none"> ▪ Flammable area extending to a 10-cm radius from pinhole ▪ No ignition
Leakage inside retrieval/recharging equipment	Leakage inside closed 1 m ³ space (acrylic box) with vertical slits on two opposing sides <ul style="list-style-type: none"> ▪ Leak speed: 380 g/min ▪ Ignition source: Electric sparks (16 J, 6 Hz) ▪ Temp./humidity: 25 °C, 75% 	<ul style="list-style-type: none"> ▪ Generation of flammable area after leakage ▪ No ignition

9.5 R1234yf Leak Simulation Test

As stated in the preceding section with regard to retrieval/recharging equipment ignition testing, leaked R1234yf would not ignite when the slits on the testing apparatus were kept open for ventilation, even when electric sparks of a sufficiently large ignition energy were applied. An R1234yf leak simulation test was subsequently conducted to examine this phenomenon in greater detail through analysis of the refrigerant concentrations and flow velocity inside the simulated retrieval/recharging equipment. The analytical conditions were established as follows:

- Analysis code: PHOENICS (thermal fluid analysis code)
- Analysis model: 1 m × 1 m × 1 m cube with slits (each 20 mm wide and 1 m high) on two opposing sides
- Gas discharge speed: 500 g/min (from bottom of equipment)
- Model size: 500,000 elements (100 × 100, 50 vertical partitions)
- Calculation method: 0.5 s steps, 50 repetitions

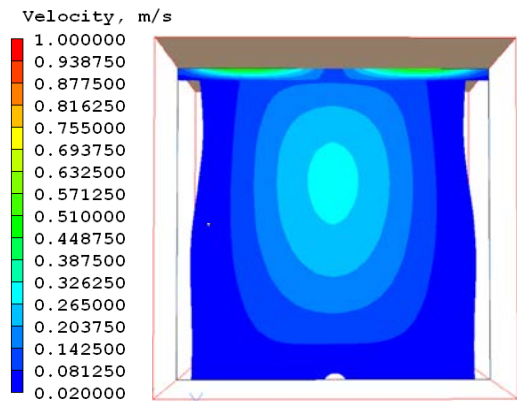
Fig. 9.4 shows an analytical image of R1234yf concentrations during discharge. Given the known lower flammable limit (LFL) of 6.2 vol% (JFMA, 2012), the distances of LFL and 1/4LFL from the leakage point proved to be 256 and 964 mm, respectively. Assuming that these distances hold true in the real world, the LFL distance of about 10 cm determined in the ignition test under review here signifies a 1/4LFL distance of approximately 38 cm.



Note: Figures on the left denote mass concentration values.

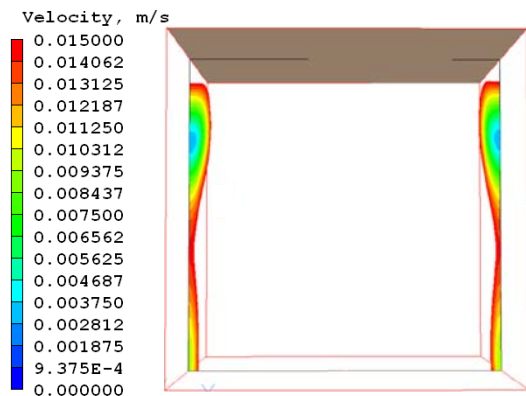
Fig. 9.4 R1234yf concentrations during discharge

Figs. 9.5 and 9.6 show R1234yf's flow velocity 30 s after the cessation of leakage. Areas of low flow velocity were found along the slits, where air flow velocity was moderated by the simultaneous entry and exit of air through the slits. In most of the other areas, the flow velocity was 2 cm/s or faster and thus exceeded R1234yf's maximum combustion speed of 1.5 cm/s (Takizawa, 2012). This clearly demonstrates that R1234yf cannot ignite inside a ventilated container when an air flow is present.



(Velocity display range: 0.02–1 m/s)

Fig. 9.5 R1234yf flow velocity 30 s after leakage Cessation



(Velocity display range: 0–0.015 m/s)

Fig. 9.6 R1234yf flow velocity 30 s after leakage cessation

9.6 Risk Assessment and Mapping

9.6.1 Probability of injury

The probability of injury was calculated based on fault tree analysis (FTA). First, unfavorable events (top events) were identified. The routes leading to a fault or accident, as well as probability values, were then established in a fault tree diagram to analyze the probability of top-event occurrence on the basis of lower-level

events that caused the top events. A report on fault tree analysis of ignition risks at automotive maintenance shops having already been published by the SAE (Gradient Corporation, 2008; 2009), JAMA conducted its own fault tree analysis based on actual conditions in auto maintenance shops in Japan taking into account the SAE’s findings.

Fig. 9.7 shows the fault tree diagram used in the risk assessment. “Ignition” was identified as the top event. For ignition to take place, the following three events would have to occur simultaneously: (i) the presence of refrigerant concentrations at flammable levels or between the lower and upper flammable limits; (ii) the execution of maintenance work under unsatisfactory ventilation conditions; and (iii) the presence of a flame source having an amount of energy exceeding the minimum ignition energy. These three events were applied to each of three possible leakage locations—hose junction, hose rupture, and cylinder—and their leakage probabilities were determined on the basis of data obtained from the survey questionnaire and the ignition and leak simulation tests.

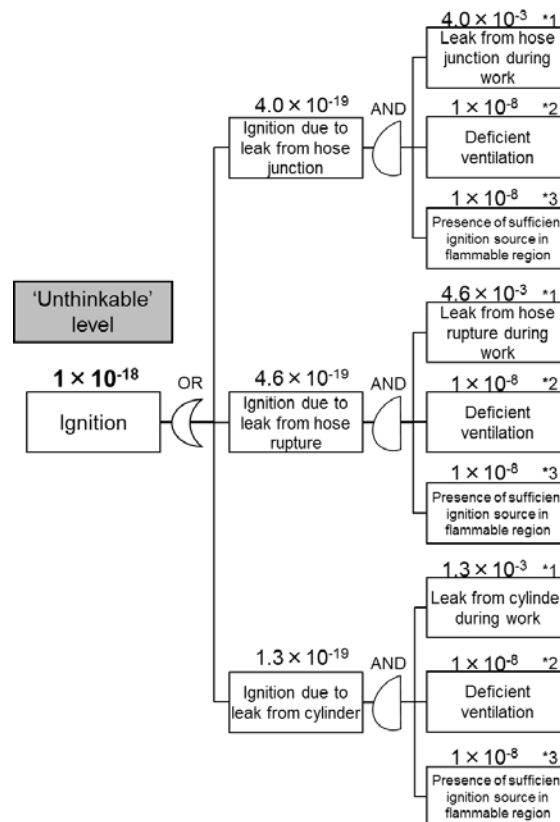


Fig. 9.7 Fault tree diagram

Refrigerant leakage (*1 in Fig. 9.7)

Probabilities of refrigerant leakage were calculated from the leakage frequency data obtained from the survey questionnaire.

(b) Deficient ventilation (*2 in Fig. 9.7)

Fact 1: Presumably because ventilation is required by law, no survey questionnaire respondents answered that they had handled refrigerants in the absence of ventilation. Fact 2: The results of the ignition and leak

simulation tests confirmed that, because the flow velocity of the leaked refrigerant exceeded its maximum combustion speed in the presence of ventilation, no stable flames would be generated inside an indoor facility or a container with slits. In light of these facts and the impracticality of assuming that there is no air flow at auto maintenance shop work sites in Japan, the probability of deficient ventilation was rated at 10^{-8} .

(c) Ignition source inside flammable area (*3 in Fig. 9.7)

In the ignition test, no stable flames were generated by 16-J sparks even in the flammable area within a 10-cm radius from the pinhole. This was presumably because air was stirred by convection in the indoor test facility. Moreover, it is hard to conceive that trained maintenance technicians would handle a heater, welding machine, or other similar ignition source within 10 cm of a flammable refrigerant. In the case of retrieval/recharging equipment, the compressor-driven relay contact was the ignition source with the greatest ignition energy. Because most of the relay body was sealed from the atmosphere by a cover and the quenching diameter (i.e., maximum diameter of a hole through which flames do not pass) for R1234yf is 7–8 mm, it is unlikely that flames would propagate even if ignition occurred at the relay contact. Thus, the probability of the presence of a significant ignition source (to enable combustion) was rated at 10^{-8} .

(d) Ignition

Based on the observations and calculations described above, the probability of ignition was considered to be 1×10^{-18} for refrigerant retrieval/recharging equipment. This probability is unthinkable low compared to the standard probability of 10^{-8} assigned to relays in the guidelines introduced by the Union of Japanese Scientists and Engineers' R-Map study group.



Fig. 9.8 Retrieval/recharging equipment relay configuration (general-purpose model)

9.6.2 Severity of injury

The severity of injury was derived from the ignition test results related to physical criteria (i.e., heat- and pressure-related factors including flame temperature, radiant heat, and sound pressure) and chemical criteria (i.e., hydrogen fluoride concentration, which is a toxic factor). Because ignition did not occur in the test setups simulating a maintenance work site and the inside of retrieval/recharging equipment, no heat, pressure, or toxicity was generated. Consequently, the severity of injury was rated at zero—i.e., no injury (Table 9.5).

Table 9.5 Injury at work site

Item Measured		Value Measured	Injury
Heat	Flame temperature	No temperature rise	None
	Radiant heat	None	None
Pressure	Sound (blast) pressure	None	None
Toxicity	HF concentration	None (0.0 ppm by densitometer)	None

A worst-case test was also conducted assuming the occurrence of combustion in a closed space. The test results are summarized in Table 9.6. According to video analysis, the flame spread to a vinyl chloride side sheet 50 cm away 1.25 s after ignition; this resulted in an estimated flame temperature of 400 °C or higher. Nevertheless, the combustion was moderate rather than explosive and was short-lived (lasting no more than several seconds); any injury incurred would therefore be only a slight burn, even if the flame were to come into contact with a human body. Because the hydrogen fluoride concentration exceeded the maximum permissible limit, a worker exposed to it would feel a skin irritation. However, the hydrogen fluoride quickly dispersed, which would enable the worker to evacuate safely. For these reasons, the worst-case injury severity was rated at I (slight).

Table 9.6 Injury in worst-case (closed space) ignition testing

Item Measured		Value Measured	Injury
Heat	Flame temperature	Not measured (video analysis: ≥ 400 °C)	Slight
	Radiant heat	Not measured	
Pressure	Sound (blast) pressure	None (video analysis)	None
Toxicity	HF concentration	Exceeding maximum limit of 3 ppm	Slight

9.6.3 Risk mapping

Based on the probability and severity of injury derived in the tests described above, the ignition risk of R1234yf during retrieval/recharging was plotted in Region C of the risk assessment map, even for the worst case (Fig. 9.9). The ignition risk of R1234yf can therefore be considered socially acceptable.

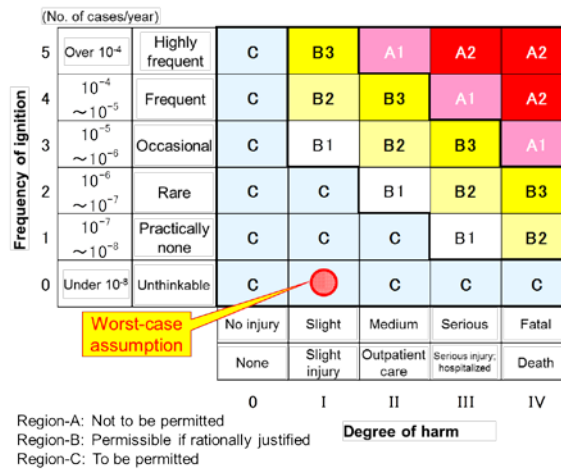


Fig. 9.9 Risk assessment map

9.7 Progress towards Deregulation

9.7.1 Risk reduction measures

The results of the risk assessment activity described above were submitted in a report (KHK, 2013) to the Committee for the Study of R1234yf Retrieval/Recharging Equipment Standards and Implementation (chair: Professor Eiji Hihara of the University of Tokyo's Graduate School of Frontier Sciences) by the High-Pressure Gas Safety Institute of Japan as part of its research work commissioned by Japan's Ministry of Economy, Trade and Industry (METI).

The committee reviewed the assessment results with respect to the ignition risk of R1234yf and confirmed that the risk is within socially acceptable parameters. In addition, for deregulation purposes, the committee examined the risk reduction potential of double-layer safety measures such as the application of a well-ventilated structure to the retrieval/recharging equipment mainframe (with a fan and ventilation openings in two directions), elimination of static electricity, restricted refrigerant storage container capacity, and the introduction of user warning labels concerning R1234yf flammability.

The committee subsequently submitted to METI a report on R1234yf; this was then released to the public by METI in June 2013 with the comment that, given the proposed safety measures, the R1234yf retrieval/recharging equipment can be regarded as equally safe as the existing inert fluorocarbon retrieval/recharging equipment which has been exempted from the High-Pressure Gas Safety Law.

9.7.2 Industrial Structure Council activity

In response to METI's action, Japan's Industrial Structure Council is scheduled to start discussing in March 2014 the possible exemption of R1234yf retrieval/recharging equipment from the High-Pressure Gas Safety Law.

9.8 Conclusion

As reported above, Japan has made great strides towards the deregulation of R1234yf retrieval/recharging equipment and the promotion of a low-GWP refrigerant beginning in 2014.

Acknowledgments

JAMA expresses its gratitude to the Japan Automobile Service Promotion Association, Japan Auto Body Repair Association, and Japan Automotive Electrical Equipment Service Association for their assistance in the distribution of the survey questionnaire; to auto maintenance shop personnel for completing the questionnaire; to Researcher Tetsuya Suzuki of the Japan Automobile Research Institute and Mr. Yoshisuke Kusakari of Yamada Corporation for their advice on the risk assessment study; and to Professor Osami Sugawa and Junior

Associate Professor Tomohiko Imamura of Tokyo University of Science, Suwa, for their cooperation with the ignition test.

References

- Japan Fluorocarbon Manufacturers Association (JFMA) ed., 2012, List of CFCs, HCFCs and fluorocarbons' environmental and safety data, JFMA, <http://www.jfma.org/atabase/table.html> (in Japanese)
- Takizawa, K., 2012. Flammability properties of 2L refrigerants, Proceedings of the International Symposium on New Refrigerants and Environmental Technology 2012, Kobe, Japan.
- Gradient Corporation, 2008. Risk Assessment for Alternative Refrigerant HFO-1234yf.
- Gradient Corporation, 2009. Risk Assessment for Alternative Refrigerants HFO-1234yf and R744 (CO₂)-Phase III.
- High-Pressure Gas Safety Institute of Japan (KHK), 2013. Report to the Committee for the Study of R1234yf Retrieval/Recharging Equipment Standards and Implementation (prepared as part of the 2012 high-pressure gas safety project commissioned by the Ministry of Economy, Trade and Industry for the drafting of a high-pressure safety standard and an implementation method).

Member List

Chair

Eiji HIHARA, Professor

- Graduate School of Frontier Sciences, The University of Tokyo.

Associate Chair

Satoru FUJIMOTO

- The Japan Refrigeration and Air Conditioning Industry Association. (JRAIA)
(Daikin Industries, Ltd.)

Committee Members

Sigeru KOYAMA, Professor

- Interdisciplinary Graduate School of Engineering Sciences, Kyushu University.

Osami SUGAWA, Professor

Tomohiko IMAMURA, Junior Associate Professor

- Department of Mechanical Engineering, Faculty of Engineering, Tokyo University of Science, Suwa.

Chaobin DANG, Associate Professor

- Graduate School of Frontier Sciences, The University of Tokyo.

Masanori TAMURA

Kenji TAKIZAWA, Senior Researcher

- Research Institute for Innovation in Sustainable Chemistry, National Institute of Advanced Industrial Science and Technology. (AIST)

Masayuki SAGISAKA, Principal Research Manager

Tei SABURI, Senior Researcher

Hiroumi SHINA, Senior Researcher

Yuji WADA, Group Leader

- Research Institute of Science for Safety and Sustainability, National Institute of Advanced Industrial Science and Technology. (AIST)

Kenji MATSUDA, Senior Manager of Engineering Department

Kazuhiro HASEGAWA, Section Manager of Engineering Department

- The Japan Refrigeration and Air Conditioning Industry Association. (JRAIA)

Kenji TAKAICHI, Staff Engineer

- The Japan Refrigeration and Air Conditioning Industry Association. (JRAIA)
(Appliances Company Corporation Engineering Division, Panasonic Corporation.)

Ryuzaburo YAJIMA

- The Japan Refrigeration and Air Conditioning Industry Association. (JRAIA)
(Daikin Industries, Ltd.)

Kenji UEDA

- The Japan Refrigeration and Air Conditioning Industry Association. (JRAIA)
(Machinery, Equipment & Infrastructure Air-Conditioning & Refrigeration Division Chiller & Heat Pump Engineering Department, Mitsubishi Heavy Industries, Ltd.)

Takeshi ICHINOSE, Group Leader

- Business Affairs Department, Japan Automobile Manufacturers Association, Inc. (JAMA)

Atsushi OOKI, Group Manager

- Japan Automobile Manufacturers Association, Inc. (JAMA)
(Toyota Motor Corporation.)

Tetsuya SUZUKI, Researcher

- Japan Automobile Manufacturers Association, Inc. (JAMA)
(Japan Automobile Research Institute.)

Jun ICHIOKA

- Safety Committee, Japan Society of Refrigeration and Air Conditioning Engineers. (JSRAE)
(Toyo Engineering Works, Ltd.)

Kenji TSUJI

- Safety Committee, Japan Society of Refrigeration and Air Conditioning Engineers. (JSRAE)
(Daikin Industries, Ltd.)

Observers

Shinichi OIKAWA, Senior Analyst

Shinzo KATAGIRI, Deputy Director

Yoichi MIYASHITA, Technical Specialist

- Fluoride Gases Management Office, Chemical Management Policy Division, Ministry of Economy, Trade and Industry

Shinji KAKUNO, Deputy Director General

Masayoshi TAKANO, Director

Masamichi ABE, Project Coordinator

- Environment Department, New Energy and Industrial Technology Development Organization. (NEDO)

Moriaki IINUMA, Manager

- Refrigeration Safety Division, High Pressure Gas Safety Department, The High Pressure Gas Safety Institute of Japan

Yasuhisa NAKASO, Manager (Energy Utilization Research)

- Sales Department, The Kansai Electric Power Co, Inc.

Hiroaki OKAMOTO, Project Researcher

Makoto ITO, Student

- Graduate School of Frontier Sciences, The University of Tokyo.